UNIVERSITÉ DE REIMS CHAMPAGNE-ARDENNE

THÈSE DE DOCTORAT

Spécialité Biochimie

Bases cytologiques et moléculaires de la dégradation enzymatique du son de blé tendre

par

Johnny BEAUGRAND

Soutenue le 7 Septembre 2004

Jury de soutenance:

Mr J.A. DELCOUR, Professeur Université Catholique de Louvain, Belgique	**Rapporteur**
Mr L. SAULNIER, Directeur de Recherche INRA, Nantes	**Rapporteur**
Mr C. CLEMENT, Professeur Université de Reims magne-Ardenne	**Président**
Mme D. REIS, Marre de Conférences Université de Paris VI	**Examinateur**
Mr F. MARTEL, Recherche et Développement, ARD	**Examinateur**
Mme B. CHABBERT, Chargée de Recherche INRA, Reims	**Co-directrice de Thèse**
Mr P. DEBEIRE, Directeur de Recherche INRA, Reims	**Co-directeur de Thèse**

Laboratoire INRA, UNIR-614 Fractionnement des AgroRessources et Emballages, Reims

Je souhaite exprimer dans cet avant-propos ma reconnaissance envers les personnes et organismes qui ont participé au déroulement et à la valorisation de cette thèse.

Je tiens tout d'abord à remercier Brigitte Chabbert et Philippe Debeire, chercheurs de l'UMR-FARE qui ont co-encadré les recherches engagées au cours de cette thèse.
Merci à vous deux pour m'avoir accepté sur ce projet, et pour la confiance que vous m'avez accordée au cours de ces trois années. Grâce à vous, j'ai eu l'opportunité de pouvoir à la fois découvrir et conjuguer la biochimie des parois végétales et l'outil enzymatique.

En particulier, c'est avec enthousiasme que j'ai travaillé au quotidien avec Brigitte Chabbert. Son professionnalisme et son discernement, sa modestie et finalement le soutien qu'elle m'a témoigné ont renforcé ma motivation durant cette formation de chercheur.

Je remercie sincèrement les membres de ce jury pour avoir accepté le travail d'analyse qu'implique ce statut.
Merci à Messieurs Luc Saulnier et Jan Delcour, de l'INRA de Nantes et de l'Université Catholique de Louvain, scientifiques réputés notamment pour leurs compétences dans le domaine des arabinoxylanes et de leurs enzymes associées. Merci d'avoir spontanément accepté d'être rapporteurs de ce travail, et d'avoir pris la charge de travail liée à cette fonction.
Merci à Danièle Reis, membre examinateur de ce jury, microscopiste et botaniste renommée de l'Université Paris VI qui m'a reçu dans son laboratoire, et avec qui j'ai pris plaisir à travailler et à discuter ardûment dans la bonne humeur.
Merci à Frédéric Martel, membre examinateur de ce jury, scientifique opérant en recherche et développement, qui m'a amicalement accueilli puis concrètement éclairé sur le potentiel et les attentes d'un substrat tel que le son de blé en industrie.
Merci à Christophe Clément, membre examinateur de ce jury, microscopiste et botaniste de l'Université de Reims, pour son excellence scientifique mise à profit dans l'évaluation de ce travail. Merci également de m'avoir recommandé à mes co-directeurs de thèse.

Je remercie chacun des coauteurs et leurs collaborateurs pour leur participation active à ces recherches. Ils sont nombreux, et je renonce volontairement à présenter une «liste de noms» qui ne pourrait être exhaustive. Je souligne de nouveau le rôle important des collaborations menées avec ces spécialistes sur l'issue de ce projet. Certains m'ont accueilli dans leur laboratoire, me conseillant et partageant une partie de leur savoir. Je vous remercie pour ces échanges amicaux et formateurs.

Je tiens à remercier l'ensemble des personnes de l'unité INRA de Reims: merci pour l'accueil chaleureux que vous m'avez témoigné, ainsi que pour les avis et les connaissances pluridisciplinaires que vous m'avez transmis.

J'ai une pensée pour mes amis de la confrérie des non-titulaires, de France ou d'ailleurs, j'ai passé d'excellents moments «cosmopolites» grâce à eux.

Je remercie mes mécènes, d'abord le gouvernement Français pour les bourses d'études qui m'ont été octroyées, et plus récemment l'INRA et la Région **Champagne-Ardenne** qui ont conjointement financé ce projet.

Merci à ma mère pour avoir encouragé ses enfants à persévérer dans leurs choix. Enfin, il y a Sandrine, ma moitié, à qui je dois d'avoir travaillé sereinement grâce à sa compréhension et ses encouragements.

En plus des publications présentées dans ce manuscrit, l'ensemble de ces travaux a donné lieu aux communications suivantes:

Communications orales

J. Beaugrand, D. Reis, F. Guillon, B. Chabbert, P. Debeire. Localisation *in situ* d'une xylanase au cours de l'hydrolyse du son de blé. *Journées du Réseau Français des Parois (RFP), Le Croisic, 6-7 Novembre 2003.*

J. Beaugrand, D. Reis, F. Guillon, P. Debeire, B. Chabbert. *In situ* visualization of xylanase-mediated hydrolysis of wheat bran tissues. *RSC Carbohydrate Group spring Meeting, Huddersfield UK, 9-11 April 2003.*

J. Beaugrand, D. Reis, F. Guillon, B. Chabbert, P. Debeire. Etude par techniques immunocytochimiques d'une xylanase au cours de la cinétique d'hydrolyse du son de blé. *Prix jeunes chercheurs de la SBR, Reims, 21 Mai 2003.*

Communications par affiches

J. Beaugrand, D. Reis, G. Paës, F. Guillon, P. Debeire, M. O'Donohue and B. Chabbert. *In situ* visualization of xylanase-mediated hydrolysis of wheat bran: further insights using inactive enzyme. Accepted for the *10`h International Cell Wall meeting, Sorento, Italy 29 August-3 September 2004.*

S. Benamrouche, J. Beaugrand, G. Chambat, B. Chabbert, M. O'Donohue, P. Debeire. Dégradation enzymatique des hémicelluloses du son de blé. *Journées du Réseau Français des Parois, Reims, 29-30 Mai 2002.*

D. Cronier, B. Chabbert, J. Beaugrand, S. Benamrouche, P. Debeire. Structural and tissular heterogeneity of cell walls in wheat layers. *9th International Cell Wall meeting, Toulouse, 2-7 September 2001.*

Figures des travaux antérieurs

Figure 1 : Coupe longitudinale d'un grain de blé (Pomeranz et al. 1987) et vue agrandie du son de blé mature sur coupe colorée au bleu de toluidine. 3

Figure 2 : Alcools précurseurs des lignines. 12

Figure 3 : Modèle de structure de lignine de monocotylédones (d'après Sun et al. 1997). 12

Figure 4: Les deux principaux acides hydroxycinnamiques rencontrés chez les monocotylédones. 14

Figure 5 : Les différents déhydrodimères d'acide férulique isolés de monocotylédones. 14

Figure 6 : Un exemple de liaison inter polymère via la dimérisation des acides féruliques pariétaux (d'après Jung et al. 1993). 16

Figure 7 : Structure des alkylrésorcinols. 18

Figure 8 : Schématisation de la structure des arabinoxylanes des sons de blé et des sites de coupure des enzymes impliquées dans leur dépolymerisation. 21

Figure 9 : Structure tridimensionnelle des xylanases de faible masse moléculaire (famille 11) d'après Harris 1997. 24

Figure 10 Représentation schématique de l'action des xylanases des familles 10 et 11 sur des arabinoxylanes (Adapté de Biely et al. 1997). 29

Sommaire

Travaux antérieurs 1

1 Le son de blé 1

1.1 Le blé 1

1.2 Le grain de blé 2

1.3 Anatomie du son de blé 2

1.3.1 Le péricarpe externe 4

1.3.2 Le péricarpe interne 5

1.3.3 La testa 5

1.3.4 La couche nucellaire 6

1.3.5 La couche à aleurone 6

2 Les composants du son 8

2.1 Les arabinoxylanes 8

2.2 La cellulose 10

2.3 Les pectines 10

2.4 Les (3-glucanes 11

2.5 Les lignines 11

2.6 Les acides phénoliques 13

2.7 Les lipides 17

2.8 Les protéines 17

2.9 Les alkylrésorcinols 17

3 Dégradation enzymatique des parois: une catalyse en phase hétérogène 18

3.1 Les principales étapes de la catalyse enzymatique 18

3.2 L'accessibilité des composés pariétaux aux enzymes 19

3.3 Ligand et adsorption de l'enzyme sur le substrat insoluble 20

4 Hydrolyse enzymatique des arabinoxylanes pariétaux 21

4.1 Les endo-(3-1,4-xylanases (EC 3.2.1.8) 22

4.1.1 Classification des endoxylanases 22

4.1.2 Structure des endoxylanases, spécificité de leurs inhibiteurs protéiques 23

4.1.3 Les domaines structuraux des xylanases 24

4.1.4 Réaction catalysée par les xylanases 26

4.1.4.1 Mécanisme de la réaction 26

4.1.4.2 Les acides aminés impliqués dans la catalyse 26

4.1.4.3 Sites actifs et sous sites de fixation des xylanases 27
4.1.4.4 Action des xylanases sur les arabinoxylanes 28
4.2 Les J3-xylosidases et enzymes accessoires 30
Présentation du sujet 32
Chapitre I Relations entre variabilité biochimique des sons industriels – dégradabilité à la xylanase 37
Abstract 37
Introduction 38
Experimental 39
Results and discussion 41
Conclusion 45
Abbreviations 46
References 46
Tables 51
Figure 55
Chapitre II Relations entre mise en place des parois – dégradabilité desarabinoxylanes à la xylanase
Abstract
Intoduction
Material and methods
Results and discussion
Abbreviations
References
Tables
Figures
Chapitre III Relations entre nature des substrats – efficacité enzymatique
Abstract
Introduction
Results
Discussion
Experimental
Abbreviations
References
Tables

Les sons de blé sont des produits technologiques résultant de la mouture des grains de blé afin d'en obtenir des farines ou semoules. Ils représentent les enveloppes du grain plus une couche de cellule de l'albumen du grain, la couche à aleurone, et ne sont pas les constituants au coeur de la transformation des grains en meunerie. Le principal objectif est de fragmenter et séparer l'albumen amylacé qui contient l'amidon. Les sons de blé peuvent donc être considérés comme des co-produits de la filière blé, constituant une abondante biomasse renouvelable (plusieurs millions de tonnes uniquement pour la France). Cette biomasse, encore insuffisamment utilisée, représente théoriquement un potentiel considérable. Outre l'utilisation d'une partie des sons en alimentation animale et de façon plus anecdotique en alimentation humaine, l'exploitation ciblée de certains composés à forte valeur ajoutée contenue dans les sons de blé semble prometteuse dans des domaines touchant la cosmétique (crème solaire etc...), les détergents industriels (tensioactif), l'agroalimentaire (xylo-oligosaccharide, xylitol, Kabel 2002), les biocarburants etc.... Néanmoins, si l'on connaît assez bien la liste des composés présents dans les sons de blé, leur extraction reste une étape limitante et un verrou économique à l'exploitation complète des sons de blé. Les voies chimiques sont actuellement les plus employées, cependant la mise en oeuvre de biocatalyseurs spécifiques devient une alternative réaliste. Théoriquement très prometteuses, ces voies «bis» n'ont pas totalement convaincu et révolutionné les modes de transformation à l'échelle industrielle. Les causes sont nombreuses, une des restrictions à l'utilisation des enzymes hydrolytiques est un rendement de conversion souvent inférieur à celui de l'action de produits acides/alcalins avec au final un coût financier accru. Toutefois de nouvelles enzymes possédant des propriétés catalytiques et/ou une stabilité physicochimique plus élevées ont été isolées d'organismes vivants dans des «milieux extrêmes». Leurs caractéristiques ainsi que les améliorations apportées par le génie génétique participent au regain d'intérêt porté à ces enzymes.

C'est dans ce contexte que s'inscrit cette étude dont le thème majeur est la dégradation des arabinoxylanes des sons de blé tendre *(Triticum aestivum)* par des endoxylanases thermostables. Le lecteur trouvera dans les travaux antérieurs des précisions concernant les principaux composés abordés dans l'ensemble du mémoire.

1 Le son de blé

1.1 Le blé

C'est une plante annuelle de la classe des monocotylédones, famille des Graminées, genre *Triticum*. En fonction du degré de diploïdie, on différencie les blés diploïdes *Triticum monococcum* (presque plus cultivés) (2n = 14), les blés durs tétraploïdes *Triticum durum* (2n = 28) et enfin les blés tendres hexaploïdes *Triticum aestivum* (2n = 48).

1.2 Le grain de blé

Appelé caryopse, il est le fruit sec et indéhiscent contenant la graine. Il est de forme ovoïde, traversé d'un sillon qui longe la longueur du grain. Il possède un pôle apical où se trouve une « brosse » et un pôle basal où se situe le germe du grain. De l'extérieur vers l'intérieur du grain on trouvera le manteau du fruit, issu de la paroi ovarienne après fécondation, puis intiment soudé le manteau de la graine issue de la croissance de l'ovule, et enfin l'albumen qui est lui même constitué d'une couche de cellules dites «aleurone» puis de cellules de réserves appelées albumen amylacé contenant l'amidon et le gluten (Figure 1).

1.3 Anatomie du son de blé

Les sons sont des produits technologiques dont la composition est en partie liée au mode de fractionnement, laissant des quantités d'amidons résiduels plus ou moins grandes. De plus, les variabilités génétiques et écophysiologiques rencontrées chez les grains de blé influenceront certainement la composition des sons. Il conviendrait donc d'évoquer « les sons ». Dans la suite de ce document, nous parlerons de son de blé, omettant de préciser pour des raisons de clarté qu'il s'agit de sons issues de blé tendre *Triticum aestivum*. Par ailleurs, c'est volontairement qu'un tableau proposant une composition chimique des sons n'a pas été inséré. En effet, les valeurs obtenues pour différents composés varient grandement selon les auteurs, en raison de la variabilité propre des sons mais aussi de l'importance du taux d'amidon résiduel dans les sons après mouture. Autrement dit, les compositions exprimées en pourcentage de matière sèche seront influencées par les teneurs variables des sons en amidon (jusqu'à 25%).

Histologiquement, le son de blé est un empilement de couches cellulaires (Figure 1) très différentes du point de vue botanique, cytologique et biochimique. Il comprend succinctement:

-Le manteau (tégument) du fruit, constitué de l'épiderme, de l'hypoderme formant le péricarpe externe, puis viennent les cellules croisées (perpendiculaires à l'axe long du grain,

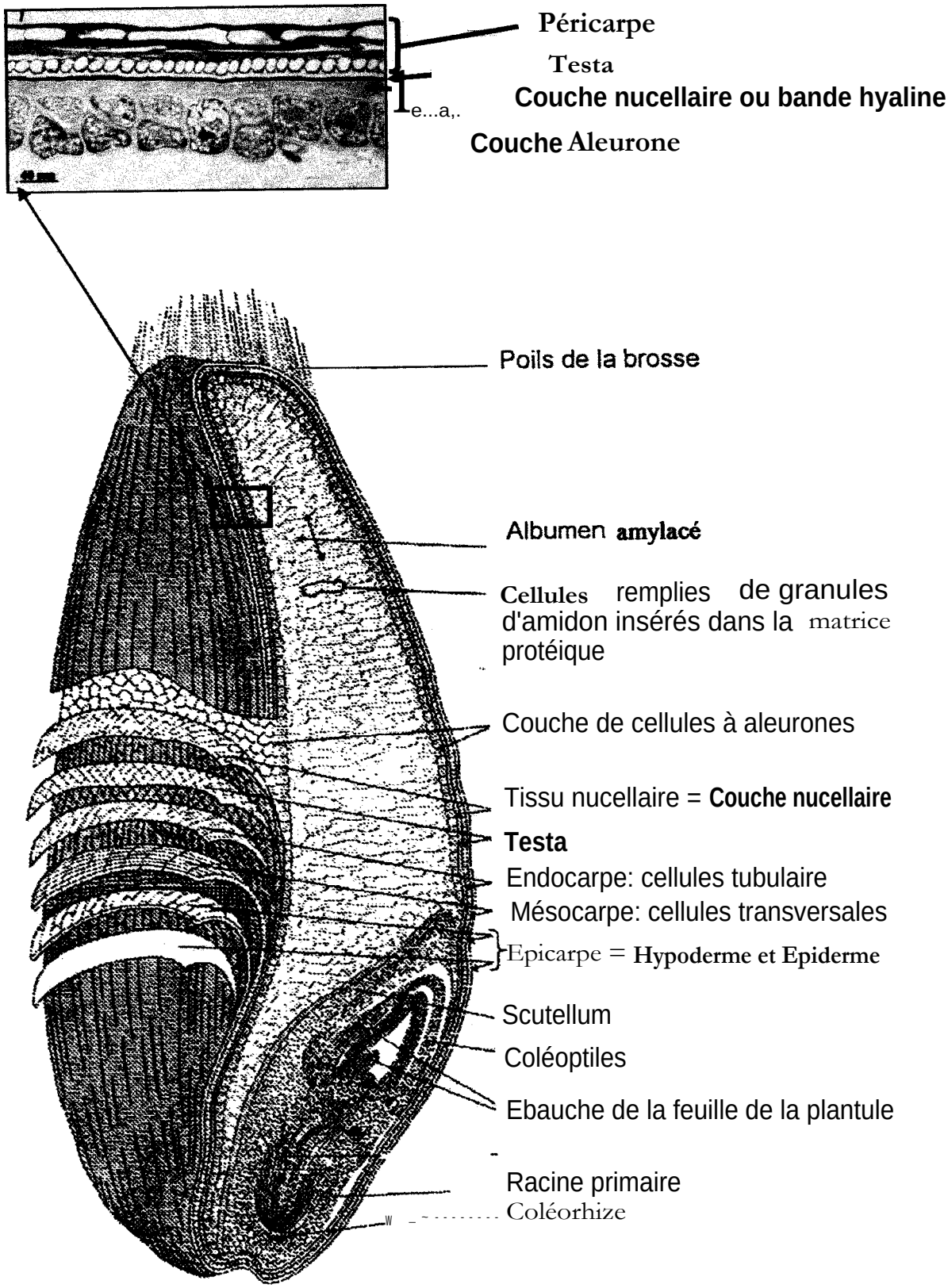

Figure 1 : Coupe longitudinale d'un grain de blé (Pomeranz et al. 1987) et vue agrandie du son de blé mature sur coupe colorée au bleu de toluidine.

Percival 1921) et les cellules tubulaires (parallèles à l'axe long du grain) formant le péricarpe interne. Le péricarpe a un rôle de protection mécanique mais intervient aussi dans la régulation de l'absorption de l'eau (Radley et al. 1976).

-le manteau de la graine, constitué de la testa et d'un film pigmentaire interpénétré. En pratique il est difficile de distinguer ces deux tissus tant ils sont combinés l'un à l'autre. Pour cette raison, nous parlerons dans la suite du manuscrit de testa, globalisant ces deux couches sans conséquence préjudiciable pour la compréhension du propos. Cette testa a un rôle important dans la circulation de l'eau entre l'extérieur et la graine, et participe à la régulation de la germination.

-La couche nucellaire ou bande hyaline, monocouche cellulaire complètement écrasée et vidée de son contenu lors de l'expansion de l'albumen amylacé au cours du remplissage du grain. Entre cette couche nucellaire et la couche cellulaire adjacente (aleurone) s'intercale une couche «amorphe» (Evers et Reed 1988), le lysat nucellaire, qui correspond vraisemblablement aux vestiges du contenu cytoplasmique de la couche nucellaire.

-La couche à aleurone, qui entoure complètement l'albumen et en fait partie. C'est la seule couche de cellules vivantes du son, ses rôles physiologiques sont nombreux, en particulier au cours de la germination de la graine.

Une description plus détaillée des tissus constitutifs des sons de blé, et centrée sur les parois, vous est proposée ci dessous.

1.3.1 Le péricarpe externe

Ce tissu mort comprend l'épiderme, formé d'une monocouche cellulaire de 20µm d'épaisseur sur 100 à 300µm de longueur (Percival 1921, Bradbury et al. 1956) recouverte sur la surface externe d'une très fine couche apparentée à une cuticule (Matzke et Riederer 1990). L'épiderme induit une certaine résistance à la pénétration de l'eau et de solutés (Hinton 1955). L'hypoderme solidaire de l'épiderme est constitué d'une ou deux couches cellulaires (Bradbury et al. 1956) moins épaisses (environ 61am, Percival 1921) qui présentent rarement un espace intercellulaire. Parfois, sous l'hypoderme des vestiges de cellules parenchymateuses écrasées (tissu nourricier) sont encore visibles, le détachement mécanique possible du péricarpe externe du péricarpe interne leur est sans doute dû.
A maturité physiologique du grain, le péricarpe externe est donc un assemblage de cellules mortes, à parois épaisses fortement compressées. Ces parois sont composées d'un grand

nombre de composés: cellulose, arabinoxylanes fortement ramifiés (groupement acétyle, acides hydroxycinnamiques) (Brillouet et Joseleau 1987), lignine, protéine, composés phénoliques (ramifiés aux arabinoxylanes) notamment acides di féruliques (Antoine et al. 2003), polyesters et autres composés mineurs (en masse) (Pomeranz 1982, 1987, Fincher et Stone 1986).
De par sa structure, sa composition et sa localisation dans le grain, l'implication du péricarpe externe dans la protection mécanique et la résistance aux agents pathogènes est désormais bien établie.

1.3.2 Le péricarpe interne

Il comprend les cellules croisées et les cellules tubulaires. Ces cellules, à maturité du grain, sont des cellules mortes. Les plus éloignées du centre du grain sont les cellules croisées, ou encore cellules transversales, de forme cylindrique et arrangées sans espace intercellulaire. De taille variable (environ 150µm sur 20µm), elles sont beaucoup moins épaisses au niveau des flancs du grain, en raison d'une pression accentuée liée au remplissage hétérogène de l'albumen amylacé (Bradbury 1956).
Vers l'intérieur du grain, viennent ensuite les cellules tubulaires dont la structure rappelle celles des cellules croisées. Néanmoins, des différences existent, leur présence est incomplète autour du grain, parfois espacée par de larges intervalles au niveau de l'arête dorsale du grain. Ainsi en fonction de la partie du son (du grain) examinée en microscopie, ces cellules peuvent être normalement absentes. Comme les cellules croisées, les cellules tubulaires possèdent une capacité photosynthétique lors de la phase de maturation, qui disparaît à maturité (Morrison et al. 1976). Les composés chimiques constitutifs du péricarpe interne sont aussi nombreux et en quantités comparables à ceux du péricarpe externe.

1.3.3 La testa

La testa est un assemblage pluristratifié décrit comme un ciment très hydrophobe dont la composition biochimique est complexe. A l'intérieur de la testa, une ou deux couches de cellules très compressées riches en lipides (Miyamoto et Everson 1958) d'environ 5 à 8 gm d'épaisseur (Bradbury et al. 1956, Evers et al. 1999) fusionnent avec le film pigmentaire lui même constitué de cellules déstructurées. Celles ci sont riches en lipides (Barlow et al. 1980), incrustations phénoliques et pigmentaires.

Cet assemblage conduit à un maillage très dense, lui même recouvert sur ses deux faces d'une couche apparentée à la cutine (Matzke et Riederer 1990).

Tout comme le péricarpe externe, la testa a un rôle physiologique dans le contrôle de la maturation et de la germination du grain, en agissant comme une barrière à la circulation d'eau, de nutriments et de gaz.

1.3.4 La couche nucellaire

Encore appelée bande hyaline ou épiderme du nucelle, cette couche est composée d'une assise cellulaire dont l'écrasement progressif lié au remplissage de l'albumen amylacé, ne laisse place qu'aux parois cellulaires (à maturité) (Fulcher et Wong 1980). D'environ 20µm d'épaisseur, mais très variable en fonction de la région du grain observée, l'aspect et la composition de ces parois tranchent avec celles précédemment décrites. Celles ci sont plus hydratées, et une étude suggère que les arabinoxylanes présents sont globalement faiblement substitués, en particulier par des groupements arabinose (Benamrouche et al. 2002).

Fortement adhérente à la testa par une couche cutinisée, on trouve sur sa face opposée une couche de faible épaisseur, inégale dans sa forme et dans son épaisseur, liant la couche nucellaire et la couche à aleurone. Evers et Reed (1988) la décrivent comme une structure vestige du contenu des cellules de la couche nucellaire. Pour cette raison, on la nomme couche du lysat nucellaire ou simplement lysat nucellaire. Cette structure serait hydrophobe et participerait au contrôle du passage de l'eau et de solutés provenant de l'extérieur du grain. A ce jour, peu d'informations sont disponibles sur sa composition biochimique.

1.3.5 La couche à aleurone

Les cellules de l'aleurone sont disposées sous forme d'une couche unique. Ces cellules volumineuses (proches de 40µm de diamètre) et de forme polygonale sont les seules cellules vivantes du son et probablement les plus étudiées. Elles présentent une proportion importante de parois (environ 35% du volume) et un contenu cytoplasmique dense avec un large noyau (Percival 1921; Evers et Witley 1989).

Le cytoplasme est très vacuolisé, beaucoup de ces vacuoles contiennent des enzymes hydrolytiques qui favoriseront l'amorce de la germination du grain, ou au contraire des antagonistes protéiques (inhibiteurs de ces mêmes enzymes). Les réserves intra cytoplasmiques de l'aleurone suscitent un grand intérêt en tant que sources nutritionnelles

(Antoine et al. 2002) ou produits de base destinés à diverses applications: phytates, lipides, minéraux, protéines (McMasters et al. 1971, Fincher et Stone 1986) etc....

Globalement, la paroi de l'aleurone est très riche en arabinoxylanes (environ 60%) et en (3-(1,3), 13-(1,4) glucanes (environ 25%) (Fincher et Stone 1986) mais ne contient que peu de cellulose. La chaîne principale des arabinoxylanes est moins substituée que dans le péricarpe, mais en revanche renferme de nombreux esters d'acides féruliques, expliquant la fluorescence émise par la paroi après excitation dans l'ultra violet (Fulcher et al. 1972, Harris et Hartley 1976). De plus, des études menées par microspectrofluorimétrie ou par spectroscopie Raman, soulignent une distribution hétérogène de l'acide férulique entre paroi périclinale/anticlinale et enfin jonction cellulaire (Akin 1995, Piot et al. 2000). La structure des arabinoxylanes de l'aleurone est plus proche de celle retrouvée dans les parois de l'albumen amylacé (environ 70% d'arabinoxylanes) que celle du péricarpe (Fincher et Stone 1986).

Les parois des cellules aleurones sont épaisses (jusqu'à 8µm d'épaisseur) et hétérogènes. Nous parlerons de paroi périclinale, se referant à la paroi mitoyenne de deux cellules aleurones, par opposition à la paroi anticlinale qui elle se situe aux deux pôles de la cellule (et donc en contact avec le lysat nucellaire ou avec l'albumen amylacé). Dans les deux cas, deux couches pariétales sont distinguées en microscopie électronique (Fulcher et al. 1972), l'une dite «interne» à proximité du contenu cytoplasmique et dont l'épaisseur se situe aux environs de 0,5µm, et une couche de paroi «externe» plus épaisse (Bacic et Stone 198la).

Les différences observées entre les deux couches pariétales des cellules aleurones ont pour origine la nature chimique de leurs constituants. La paroi interne contiendrait plus de f3 glucanes (Bacic et Stone 1981 b, Meikle et al. 1994) et renfermerait une proportion importante en dimères d'acide férulique (Rhodes et al. 2002). Un plus grand nombre de groupements acétyles liés aux xyloses de la chaîne principale est également proposé.

De nombreux plasmodesmes sont retrouvés dans les parois de l'aleurone (Morrison et al. 1975). Ces structures participeraient au transport des enzymes de l'aleurone vers la paroi externe, qui est dégradée au cours de l'initiation de la germination. Gubler et ses collaborateurs (1987) suggèrent que la résistance relative de la paroi interne aux hydrolases permettrait d'éviter l'effondrement complet de la paroi d'aleurone sur le contenu

cytoplasmique, autorisant la libération vers l'albumen amylacé des sacs contenant les médiateurs nécessaires à la germination.

Un dernier point concernant l'amidon résiduel contenu dans les sons doit être explicité. La couche à aleurone fait botaniquement partie de l'albumen, mais ne contient pas d'amidon contrairement aux cellules de réserves de l'albumen amylacé. Dans le son, il subsiste des parties plus ou moins importantes de cet albumen amylacé, et des vestiges des parois des cellules sub-aleuroniques, accolées aux parois périclinales des cellules aleurones. Dans l'albumen amylacé, l'amidon est distribué sous forme de granules plus ou moins grands qui sont en fait «déposés» en surface des cellules aleurones (Raynal-Ioualalen 1996). Le taux d'amidon résiduel retrouvé dans les sons va alors dépendre de différents facteurs comme l'espèce, le procédé de mouture, ou la présence ou non d'une étape de «brossage» des sons. Il en résulte une grande disparité du taux d'amidon résiduel des sons.

2 Les composants du son

Nous décrirons principalement les constituants associés aux parois du son. Leur répartition dans les différentes couches du son se traduit par une grande hétérogénéité qualitative et quantitative.

2.1 Les arabinoxylanes

Les arabinoxylanes sont les polysaccharides (hémicellulosiques) les plus représentés dans les sons de blé (environ 30 à 40% de la matière sèche) et plus généralement chez les monocotylédones (Dey et al. 1984). Ce sont des polymères qui doivent leur nom au fait qu'ils sont constitués d'une chaîne principale de (3-D-xylopyranose (xylose) liée en P (1–4) (ou xylane). Ils sont substitués par un certain nombre de chaînes latérales (Smith et Hartley 1983), dont les a-L-arabinofuranose (arabinose) sont les ramifications prépondérantes (Fincher et Stone 1986, Bacic et al. 1988). La chaîne principale de xylane est plus longue dans les parois de l'aleurone que celle du péricarpe. Les substituants arabinoses sont en position a-(0-2) et/ou a-(O-3) des résidus xyloses, un résidu xylose pouvant être di-substitué par l'arabinose sur ces deux carbones (Bacic et Stone 1981b, Brillouet et Joseleau 1987). De courtes chaînes d'arabinose (deux et exceptionnellement trois résidus) peuvent également ramifier les xyloses de la chaîne principale (Brillouet et al. 1982).

Le taux de substitution du squelette de xylane par l'arabinose (rapport arabinose/xylose ou AIX) reflète une valeur moyenne qui ne prend pas en compte la longueur de la chaîne principale, ni la nature des liaisons (mono ou disubstituées) du xylose par l'arabinose. La fréquence et le type de liaison par l'arabinose n'est pas aléatoire au sein des arabinoxylanes (Dervilly-Pinel 2001). Une relation inverse est généralement obtenue entre les proportions de disubstitution et monosubstitution par l'arabinose. Les disubstitutions seraient fréquemment rencontrées en amas (cluster), laissant libres des séquences de xylose non substitué dans le squelette principal et ce même lorsque le rapport arabinose/xylose est proche de 1 (Chanliaud et al. 1995, Adams et al. 2004). De même, dans le cas des arabinoxylanes d'albumen de céréales, la fréquence de distribution des résidus arabinoses, en blocs ou contigus, ne semble également pas aléatoire (Viëtor et al. 1992, Gruppen et al. 1993). Le taux de substitution arabinose/xylose augmente du centre vers la périphérie du grain de blé (Lempereur et al. 1997), le taux maximal étant retrouvé chez les arabinoxylanes du péricarpe où en moyenne un xylose porte un arabinose. L'augmentation de ce ratio est la conséquence conjointe de l'accroissement du nombre de xyloses disubstitués, et de la moindre proportion en xyloses non substitués (Delcour et al. 1999, Dervilly-Pinel 2001). Les arabinoxylanes présentent une diversité structurale à l'échelle tissulaire, cellulaire et subcellulaire.

En plus de l'arabinose, le squelette de xylose peut être ramifié par un certain nombre de chaînes dont la fréquence et la nature varient. Les glucurono-arabinoxylanes sont des arabinoxylanes (arabinoses majoritaires) qui sont substitués par des unités d'acide a-D-glucuronopyranosique (acide glucuronique) ou son dérivé 4-O méthyle (environ 50%), en position O-2 du résidu xylose (Ring et Selvendran 1980, Brillouet et Mercier 1981, Shiiba et al. 1993). Ces acides glucuroniques appartiennent à la famille des acides uroniques, et contribueraient, via des liaisons esters, à la réticulation intra ou inter chaine et inter polymère (lignine) (Hatfield 1993, Iiyama et al. 1994). Ces structures complexes sont majoritairement trouvées dans le péricarpe plutôt que dans l'aleurone (Aspinall, 1959, Benamrouche et al. 2002, Antoine et al. 2003).

Les arabinoxylanes portent également des ramifications d'acide galacturonique, en quantité moins importante que les acides glucuroniques, ce qui augmente encore la complexité structurale et chimique des arabinoxylanes. Des traces de galactopyranose lié en a sont également détectées au niveau des arabinoxylanes du péricarpe (Brillouet et Joseleau, 1987), ainsi que de faibles proportions de xyloglucanes (Brillouet et al. 1982, Du Pont et Selvendran 1987).

Les unités de xylose peuvent être estérifiées en position O-2 ou O-3 par des groupements O-acétyles (Chesson et al. 1983, Brillouet and Joseleau 1987, Ring et Selvandran 1980). Ces substituants interviendraient également en position O-2 des résidus latéraux des arabinoxylanes comme cela a été démontré dans le riz (Ishii 1991). Bacon et ses collaborateurs (1975) rapportent chez les graminées des teneurs en acétyle proches de 1% de la matière sèche des parois. Ces groupements contribueraient à la protection des polysaccharides face à de nombreuses hydrolases, leur présence serait plus importante dans les tissus externes du grain. Il a été proposé qu'une teneur accrue en groupements acétyles au niveau de la paroi interne de l'aleurone contribuerait à la plus grande résistance observée localement à de nombreuses hydrolases (Rhodes et Stone 2002).
Des acides hydroxycinnamiques sont associés aux arabinoxylanes. En majorité, il s'agit d'acide férulique (FA) estérifié à l'arabinose (Geissman et Neukon 1973).

2.2 La cellulose

C'est un homopolymère formé de longues chaînes linéaires d'unités D-glucose, reliées par des liaisons (3-(1-*4), principalement retrouvé dans le pericarpe mais absent (ou très faiblement représenté) des parois des cellules aleurones (Fincher et Stone, 1986). L'orientation des unités de glucose (rotation de 180 degrés autour de l'axe du polymère) permet des liaisons hydrogènes intermoléculaires entre l'O-5 et l'O-3 conférant une grande stabilité au polymère. Les chaînes de cellulose s'associent entre elles pour former des microfibrilles dont le diamètre varie en fonction de l'espèce végétale (Chanzy et al. 1990) et qui vont conférer aux parois une grande résistance aussi bien chimique que physique. Les microfibrilles ou faisceaux de fibrilles servent de trame rigide organisée pour la paroi. Des associations par liaisons non covalentes faibles mais parfois nombreuses peuvent se créer entre cellulose et hémicelluloses, parmi elles les arabinoxylanes, et contribuent à une grande cohésion des polymères pariétaux.

2.3 Les pectines

Ces hétéropolymères complexes formés par une chaîne linéaire de résidus d'acide galacturonique liés par des liaisons a (1-+4) ou a (1-+2) avec des composés L-Rhamnose.

Les pectines existent sous trois formes, les rhamnogalacturonanes de type I, les rhamnogalacturonanes de type II et les homogalacturonanes (ONeil et al. 1990). Selon la nature des substituants, les pectines sont minoritaires dans les parois de graminées et plus nombreuses chez les dicotylédones (Aman 1993). Dans le son, elles pourraient gainer les nombreux plasmodesmes (Roy et al. 1997) rencontrés dans les parois de l'aleurone.

2.4 Les (3-glucanes

Ce sont de longues chaînes de polyosides linéaires constitués d'unités de D-glucopyranoses liées par des liaisons 13-(1--*3) et f3-(1-*4). Le rapport entre ces types de liaisons est variable en fonction de l'origine de la céréale. Dans les sons, les P-glucanes sont localisés dans les cellules aleurones (environ 3% de la matière sèche, Bacic et al. 1981b), ce qui est une caractéristique des graminées. Dans une certaine mesure, au sein de la paroi, ces polymères prendraient le rôle de la cellulose. Leur structure mixte, liaisons f3-(1-->4) et f3-(1--->3), confère néanmoins une rigidité moins élevée que celle de la cellulose. Comme pour la cellulose, des interactions non covalentes ont été mises en évidence entre les R-glucanes et d'autres polymères, par exemple les arabinoxylanes (Izydorczyk et MacGregor 2000).

2.5 Les lignines

Les lignines résultent de la polymérisation de trois unités phénylpropanes: alcools p-coumarylique, l'acide conifér ylique et l'acide sinapylique, qui sont les précurseurs respectifs des unités p-hydroxyphenyle (H), gaïacyle (G) et syringyle (S) (Figure 2). Ces monomères diffèrent par leur degré de méthoxylation (Sarkanen et al. 1971) et établissent des liaisons de diverses natures, le mode de polymérisation étant responsable de la conformation tridimensionnelle des lignines (Monties 1980) (Figure 3). On désigne par liaisons condensées les liaisons carbone-carbone et diaryl éther car résistantes aux méthodes de dégradation chimique usuelles par opposition aux liaisons non condensées qui correspondent aux liaisons éther labiles ((3-0-4 et a-O-4 essentiellement).

Les lignines ont pour fonction le soutien mécanique des tissus et l'imperméabilisation des tissus conducteurs. Elles sont connues pour former une barrière physique bloquant la pénétration des agents pathogènes et pour limiter la dégradation des arabinoxylanes pariétaux

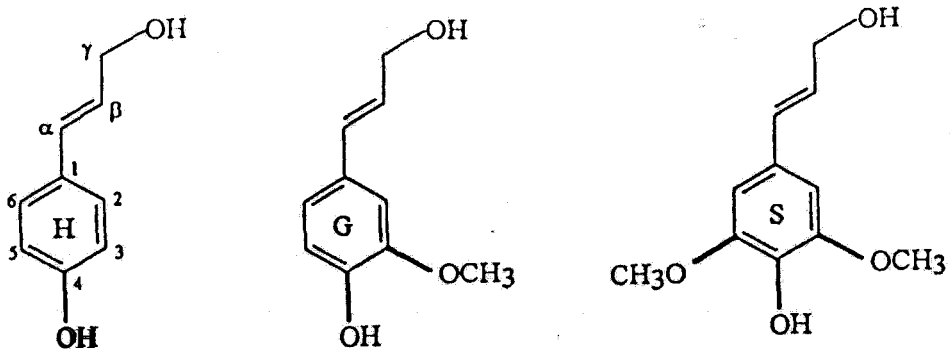

Alcool coumarylique | Alcool coniféryliquc | Alcool sinapylique

Unité p-hydroxyphénylpropane **H** | Unité Gaïacylpropane **G** | Unité Syringylpropane S

Figure 2 : Alcools précurseurs des lignines.

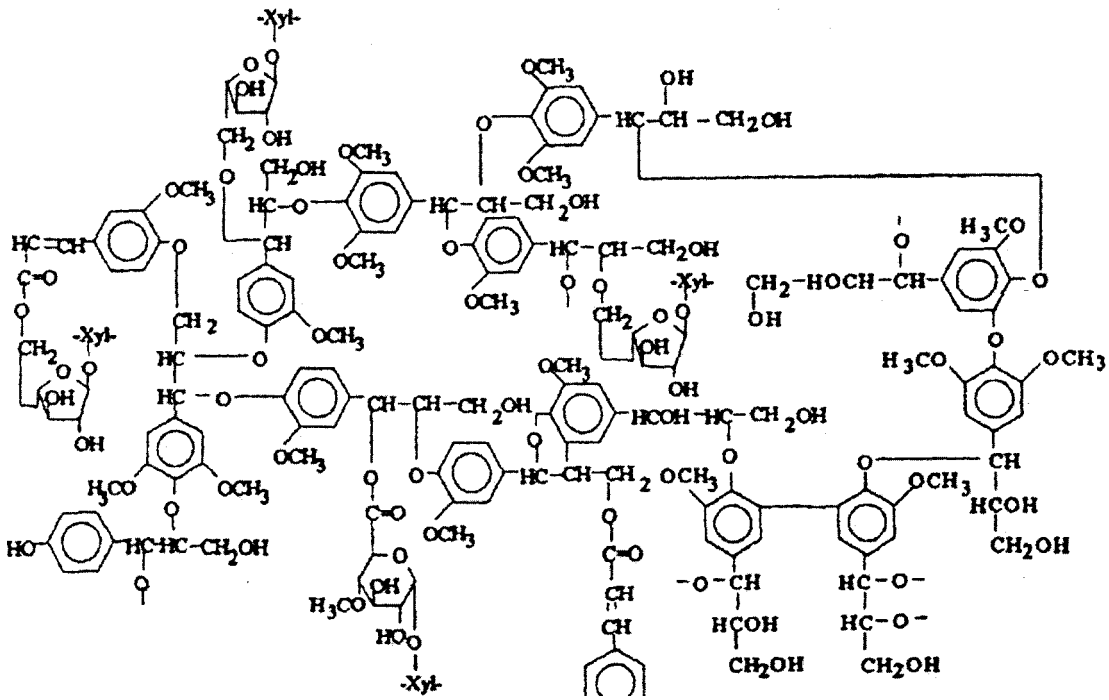

Figure 3 : Modèle de structure de lignine de monocotylédones (d'après Sun et al. 1997).

par des xylanases (Zilliox et Debeire 1998, Lequart et al. 1999). Les parois cellulaires des sons sont très peu lignifiées (–4% de la matière sèche). Les cellules aleurones en sont dépourvues (Shetlar et al. 1947, Antoine et al. 2003). Les concentrations locales les plus fortes sont retrouvées dans les cellules croisées, le péricarpe externe étant partiellement lignifié. Des localisations similaires ont été rapportées à propos de son de blé dur (Schwarz et al. 1988, 1989). Les arabinoxylanes, peuvent former des liaisons covalentes avec les lignines, par l'intermédiaire de liaisons chimiques type ester ou éther via les acides férulique ou p-coumarique ou encore par liaison ester par l'intermédiaire d'acides uroniques (Erikson et Goring 1980).

2.6 Les acides phénoliques

Quantitativement, ces molécules sont peu représentées dans les sons et principalement associées aux parois. L'acide férulique (FA), et dans une moindre proportion l'acide p-coumarique (pCA), sont les deux composés prédominants (Figure 4) mais d'autres acides hydroxycinnamiques ont été mis en évidence dans le grain de blé: acides sinapique, syringique, caféique et vanillique (Fincher et Stone 1986, McCallum et Walker, 1991).
FA et pCA peuvent se trouver sous les deux formes *cis* et *trans*, mais ils sont majoritairement présents sous la forme stable *trans*. Cette forme peut s'isomériser de la forme *trans* en *cis* sous l'action de l'énergie lumineuse. *In situ*, les acides hydroxycinnamiques sont détectables grâce à leur autofluorescence bleue après excitation sous rayons ultraviolets. Fulcher et al. (1972) ont ainsi suggéré que l'accumulation de composés phénoliques, essentiellement FA, dans les parois des cellules aleurones (Fulcher et al. 1980). Depuis cette hypothèse a été confirmée (Bacic et al. 1981, Lempereur et al. 1998, Peyron et al. 2001, Antoine et al. 2003).
Ces acides hydroxycinnamiques sont des molécules «bifonctionnelles» car elles peuvent engager leur fonction carboxylique dans des liaisons esters et leur groupement hydroxy-phénol dans des liaisons éthers (Scalbert et al. 1985). Les acides hydroxycinnamiques ont un rôle important dans la réticulation covalente des polymères pariétaux, le FA étant majoritairement estérifié aux arabinoxylanes alors que le pCA serait associé préférentiellement sous forme éthérifiée aux lignines (Ralph et al. 1995, Jacquet 1997).
L'oxydation des esters de FA au sein de la paroi aboutit à la formation de composés acides diféruliques (DiFA) ou encore appelés déhydrodimères (DHD). Il y a alors formation d'un pont covalent entre les structures porteuses de ces FA dimérisés. Ralph et al. (1994) ont principalement identifié dans les sons de blé les formes 8-0-4, 8-5' et 5-5 (Figure 5).

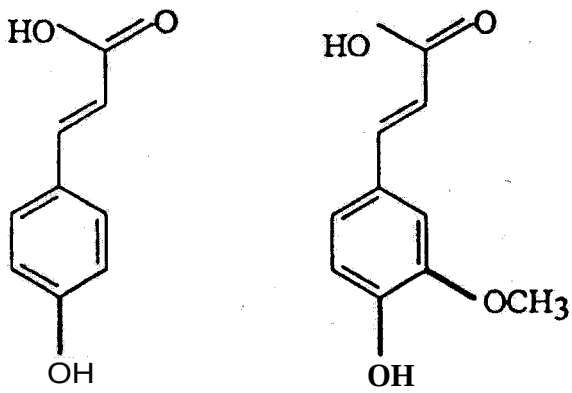

Acide p-coumarique **Acide féruliquc**

Figure 4 : Les deux principaux acides hydroxycinnamiques rencontrés chez les monocotylédones.

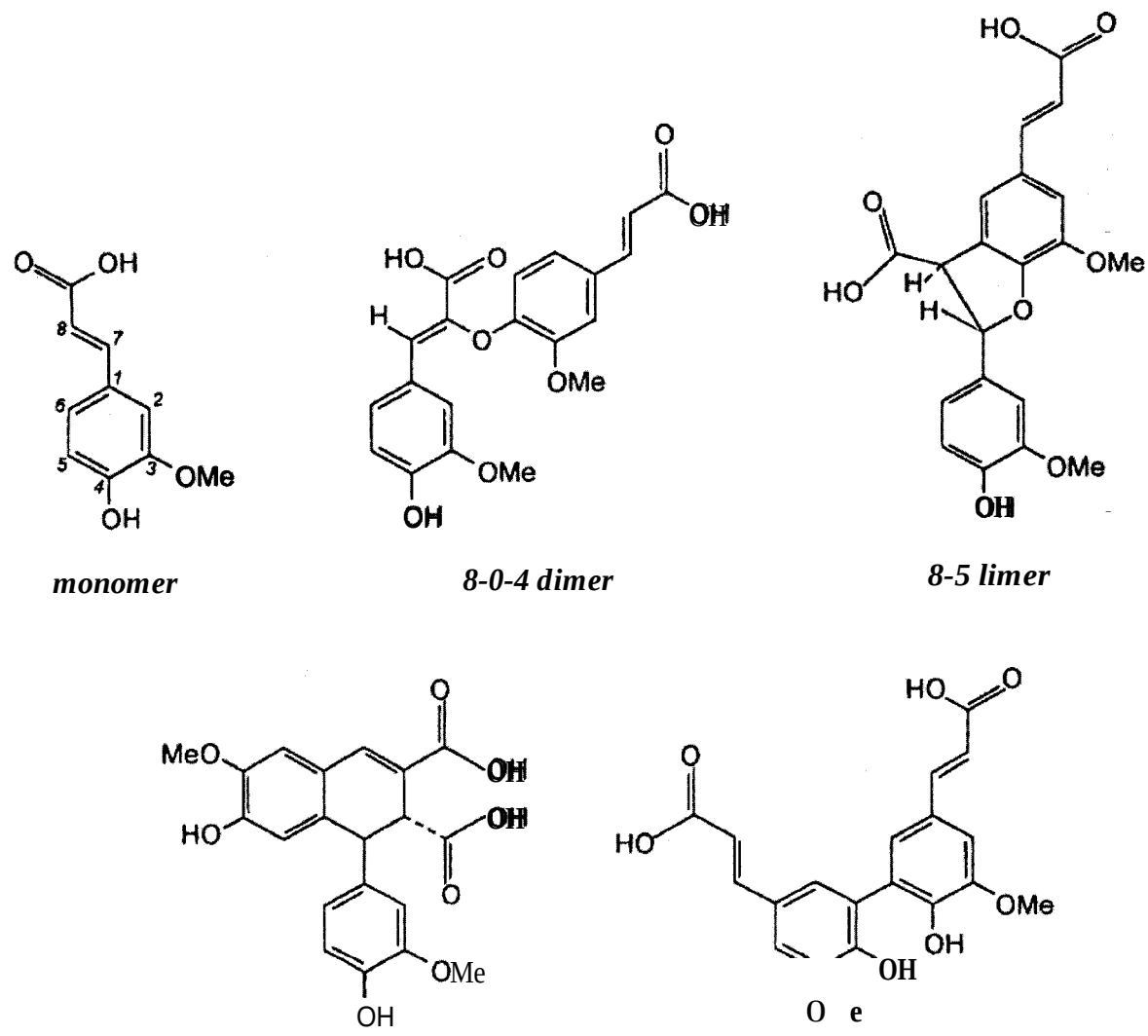

monomer ***8-0-4 dimer*** ***8-5 limer***

8-8 dimer ***5-5 dîmer***

Figure 5 : Les différents déhydrodimères d'acide férulique isolés de monocotylédones.

Monomères et dimères féruliques représentent plus de 90% des acides phénoliques pariétaux des sons, et comptent pour approximativement 0,5% du poids sec des sons. De façon remarquable, si les acides féruliques sont surtout monomériques et concentrés dans 1'aleurone (environ 10% dimérisé), il n'en va pas de même dans le péricarpe où plus de 50% de l'acide férulique est sous forme dimérisé (Antoine et al. 2003).
A noter qu'il existe en plus des DiFA formés par couplage oxydatif des cyclodimères ou photodimères, qui eux sont formés consécutivement à un apport énergétique sous forme de photons. Il s'agit des stéréoisomères: acides truxilliques et truxiniques (Morrison et al. 1992).

Les acides hydroxycinnamiques participent à la morphogenèse des cellules, en particulier par leur capacité à se dimériser dans les parois (Fry 1986, McCann et Roberts 1994). Ils engendrent par leur pontage des associations étroites entre les polysaccharides tels que les arabinoxylanes, et d'autres polymères non osidiques comme les lignines (Iiyama et al. 1994) (Figure 6). De telles interactions pourraient contribuer à «compacter» le réseau par un maillage resserré au niveau des parois du péricarpe (Chesson et al. 1997). De plus, les DiFA seraient impliqués dans l'adhésion des cellules entre elles (Waldron et al. 1997) et entre les couches cellulaires (Peyron 2002). Selon Ralph et al. (1995), monomères et dimères pourraient être des points d'initiation de la lignification dans les parois des graminées. On peut ainsi évaluer l'implication significative de ces composés dans la cohésion pariétale -et la résistance physique des végétaux.

Par ailleurs, monomères et dimères protégeraient les polyosides pariétaux de l'hydrolyse enzymatique et limiteraient la dégradation des parois par les insectes, phytopathogènes et bactéries (Hartley 1972, Hartley et al. 1977, Arnason et al. 1992, Jung et Sahlu 1986). Le rôle protecteur des parois semble étroitement lié à la physicochimie et à la structure tridimensionnelle du réseau pariétal résultant de leurs propriétés chimiques. Une synergie défensive pourrait également intervenir par le biais des produits libérés lors de la dégradation microbienne des parois. Certains de ces composés (féruloyl tétrasaccharide, féruloyl pentasaccharide) isolés de son de blé après l'action d'une endoxylanase purifiée (Lequart et al. 1999) montrent un potentiel anti-microbien (Christakopoulos et al. 2003).

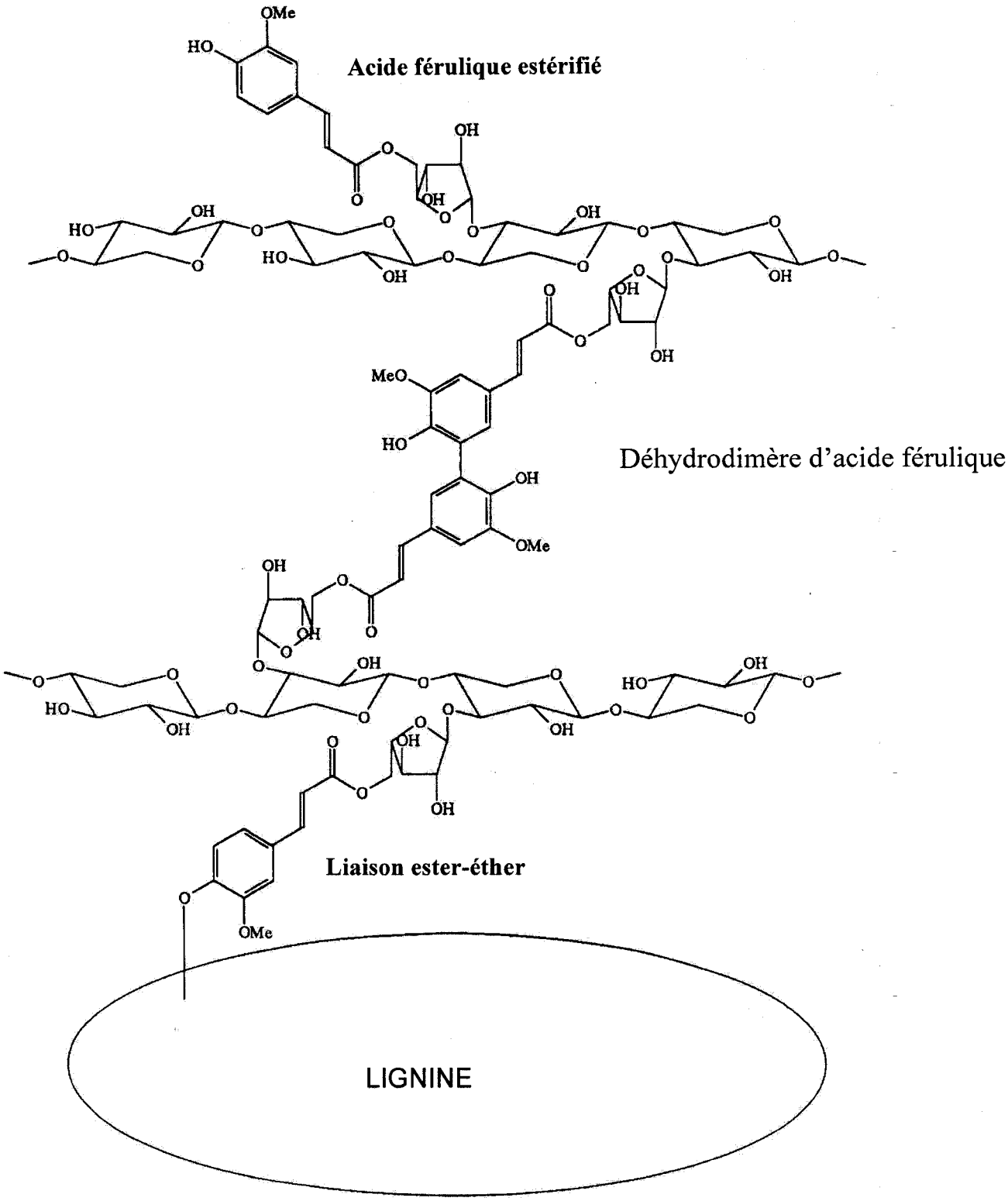

Figure 6 : Un exemple de liaison inter polymère via la dimérisation des acides féruliques pariétaux (d'après Jung et al. 1993).

2.7 Les lipides

Les lipides représentent environ 4 % de la matière sèche du son. Ils sont principalement déposés sous forme d'assises cuticulaires diverses, une fine couche au dessus de l'épiderme, et deux autres plus épaisses qui cloisonnent la testa. La cutine est constituée de polyesters d'acides gras hydroxy ou epoxy-substitués esterifiés (surtout acides gras C18 hydroxylés oléate-linoléate), et ils sont principalement retrouvés dans la testa (Kolattukudy 1981, 2001). On parle également d'assise cuticulaire, définie comme un assemblage de polyesters hydrophobes (Matzke et Riederer 1990). Ces couches participent à la résistance aux stress biotiques (microorganismes, insectes, virus, enzyme) ou abiotiques (température) et représentent une barrière physico chimique sélective au passage de nombreux composés comme les enzymes.

2.8 Les protéines

Dans les sons de blé, elles constituent environ de 10 à 20% de la matière sèche, mais sont essentiellement intracellulaires et localisées dans le cytoplasme des cellules aleurones. En faibles quantités dans les parois des différents tissus du son de blé (Morrison et al. 1975), les protéines pariétales participent à la mise en place ainsi qu'à la structure des parois, notamment dans le péricarpe (exemple du maïs, Saulnier et al. 1995). Des liaisons via les acides aminés aromatiques et les arabinoxylanes sont suspectées. Selon une étude récente (Rhodes et Stone, 2002), les protéines pariétales de l'aleurone contiennent un grand nombre d'hydroxy-prolines et cette particularité pourrait en partie expliquer, conjointement à leur localisation, la résistance constatée de la paroi interne de l'aleurone à diverses enzymes lors de l'initiation de la germination du grain.

2.9 Les alkylrésorcinols

Ces composés sont présents en faible quantité dans les sons (inférieur à lmg/g de son), mais leurs teneurs sont environ 5 fois supérieures à celle de la totalité du grain.
Essentiellement retrouvés dans le péricarpe (Evers et al. 1999), ils jouent un rôle important dans la germination du grain. Les alkylrésorcinols possèdent une structure de type phényl-C_nH_{2n+1}, avec n = 17, 19, 21, 23 et 25 (Figure 7). L'alkylrésorcinol en C21 est majoritaire dans le son de blé. Chaque homologue peut se trouver également sous forme saturée, mono-

insaturée ou di-insaturée (Kozubek 1985, Kozubek et Tyman 1995), ces formes participeraient à la protection des acides gras et des phospholipides par leur pouvoir anti-oxydant (Struski et Kozubec 1992, Nienartowicz et Kozubec 1993).

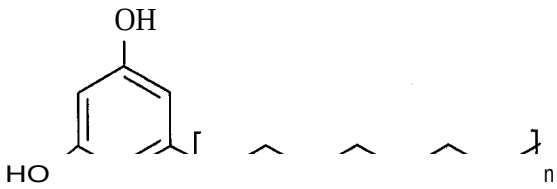

n= 17, 19, 21, 23 et 25

Figure 7 : Structure des alkylrésorcinols.

3 Dégradation enzymatique des parois: une catalyse en phase hétérogène

Les parois végétales présentent une diversité telle qu'il n'est pas possible d'envisager un modèle unique de dégradation enzymatique. La majorité des études sur le sujet s'appuie sur des modèles de parois type «bois», ou encore sur des parois riches en lignine. Ces structures sont assez éloignées des parois retrouvées dans les sons de blé. Malgré leurs différences, les parois végétales ont en commun une complexité structurale, reposant sur un ensemble de macromolécules et de molécules simples, intimement associées par différentes liaisons covalentes ou non. L'assemblage de ces polymères conduit à un réseau dense, autorisant le passage de certaines molécules. L'ensemble confère à la paroi sa rigidité et bien d'autres propriétés, en particulier une certaine résistance à la dégradation enzymatique.

3.1 Les principales étapes de la catalyse enzymatique

La plupart des études sur la catalyse enzymatique en milieu solide concernent essentiellement la dégradation de la cellulose par les cellulases; peu d'études s'adressent aux arabinoxylanes des parois. Le modèle généraliste proposé par Lee et Fan (1982) étudiant des cellulases peut néanmoins s'appliquer à d'autres couples enzymes-parois.
La décomposition du mécanisme conduisant à la dégradation par une enzyme d'un composé (substrat) appartenant à une paroi végétale peut s'établir en 5 étapes:

1 -Le transfert de l'enzyme du milieu aqueux vers le substrat
2 -L'adsorption de l'enzyme sur le substrat et la formation du complexe enzyme-substrat
3 -L'hydrolyse du substrat
4 -Le transfert des produits de réaction du substrat vers le milieu aqueux
5 -L'hydrolyse complémentaire des produits libérés dans le milieu aqueux

La formation du complexe enzyme-substrat (étape 2) est le point majeur de l'hydrolyse *in situ* des parois végétales (Lee et Fan 1982). Contrairement aux polymères isolés des parois, la liaison entre les enzymes solubles et le substrat insoluble dépend de nombreux paramètres. L'agencement des composés pariétaux et leurs interactions peuvent être visualisés par une sorte de trame dont l'accès est potentiellement difficile pour une enzyme de volume donné. La paroi peut également interagir chimiquement avec les enzymes (hydrophobie des lignines, Rémond-Zilliox et al. 1997). L'ensemble confère au substrat un degré d'accessibilité moindre aux enzymes par rapport à l'accessibilité de chacun des polymères pariétaux isolés.

3.2 L'accessibilité des composés pariétaux aux enzymes

Précédant l'établissement de la liaison enzyme-substrat, le transfert de l'enzyme du milieu aqueux au substrat doit s'opérer, au moins en partie, au travers de la paroi. Celle ci est un matériel «poreux» qui permet de nombreux échanges entre les cellules. Le volume accessible aux molécules circulantes est souvent défini par la porosité. Cette notion n'envisage pas la porosité comme constituée de pores sous forme de tunnels uniformes et de diamètre régulier, mais plutôt comme la résultante de cavités sans forme précise reliées entre elles. A ce sujet, et dans le but de définir les volumes accessibles d'une paroi, divers travaux ont été réalisés. Toutefois les résultats obtenus varient parfois de façon importante selon la méthodologie employée. La plupart ont fait appel à des dextranes, des polyéthylène glycols ou des protéines de masses moléculaires connues. D'autres ont fait appel à des méthodes utilisant la microscopie électronique afin d'observer des répliques de parois obtenues par cryofracture. La porosité des parois varie en fonction de la nature des polymères constitutifs du type de liaisons intra et inter moléculaires, ainsi que de la fréquence et de la répartition de ces liaisons au sein du réseau (Jung et al. 2000).
De l'ensemble de différentes études (Carpita et al. 1979, Grethlein 1985, Chesson et al. 1995) il ressort que la taille des pores varie considérablement, d'environ 3 à 5 nm, ce qui théoriquement permet la diffusion de protéines de masse moléculaire jusqu'à 20 kDa. La diffusion d'une molécule va être fonction de sa taille et de la porosité de la paroi. Pour une enzyme, sa masse moléculaire et sa structure tertiaire sont des facteurs determinants de sa capacité à diffuser; la porosité influence cette diffusion au travers de la paroi, comme démontré dans le cas de cellulases (Tanaka et al. 1987). L'incapacité de certaines enzymes à pénétrer dans certains types de parois a été également montrée par immunomarquage. En l'absence de volume accessible adapté, une enzyme ne pénètre pas en profondeur dans la

paroi son action reste limitée à l'attaque de zones externes (Engels 1989, Srebotnik et al. 1988).

L'accessibilité dans la paroi peut également être restreinte par des interactions non spécifiques entre l'enzyme et certains composés. La lignine a clairement été définie comme limitant la dégradation enzymatique des parois. Ces polymères très hydrophobes peuvent interagir et finalement «retenir» les enzymes pénétrant dans les parois. La lignine serait responsable de l'adsorption non spécifique d'endoxylanase dans les parois de paille de blé (Zilliox et Debeire 1998). Un rôle similaire pourrait être attribué aux polymères aliphatiques.

3.3 Ligand et adsorption de l'enzyme sur le substrat insoluble

Dans le cas d'une paroi, la vitesse et le degré d'hydrolyse seront en partie fonction de la quantité d'enzyme capable de pénétrer dans la paroi, puis dans un second temps de se fixer au substrat. Les études *in situ* des associations enzyme-substrat sont rendues difficiles du fait de la grande complexité architecturale des parois, les interactions entre les différents composés pariétaux rendent les interprétations délicates. On peut néanmoins considérer un certain nombre de faits avérés en relation avec la fixation enzyme-substrat dans la paroi. Il y a évidement la nature même du substrat. Dans le cas de polymères comme les arabinoxylanes, de nombreuses chaînes latérales peuvent empêcher la fixation de l'enzyme directement ou indirectement par leurs interactions (covalentes ou non) avec d'autres composés pariétaux. L'association covalente entre les arabinoxylanes pariétaux et les lignines par l'intermédiaire d'acides hydroxycinnamiques (liaisons esters, éthers et dimères féruliques) affecte la dégradation enzymatique (Hartley et al. 1977, 1989, Chesson et al. 1993, Jung et al. 1993). White et al. (1993) ont montré grâce à l'utilisation d'une endoxylanase et de glucurono-arabinoxylanes, que les nombreux substituants arabinoses et acides glucuroniques perturbent la reconnaissance de certains sites de coupure le long de la chaîne de xyloses.

En plus du substrat, le microenvironnement physicochimique (pH,...) de la phase hétérogène dans lequel a lieu la rencontre enzyme-substrat peut influencer le processus d'adsorption de l'enzyme sur le substrat (Reese 1977, Ricard 1987).

En conclusion intermédiaire de ce paragraphe, nous noterons que la dégradation efficace des composés de la paroi végétale par voie enzymatique nécessite l'action d'enzymes capables de contourner les limitations posées par ce substrat hétérogène. Schématiquement, l'enzyme doit pénétrer dans le réseau pariétal pour accéder au substrat, mais le substrat doit aussi présenter

un environnement et une nature favorable à l'action de l'enzyme. Dans le cas d'une hydrolase, la coupure au sein d'un substrat ne se traduit pas forcement par sa solubilisation. En effet, la libération du produit implique une absence de lien au reste du réseau insoluble.

4 Hydrolyse enzymatique des arabinoxylanes pariétaux

En raison de la nature complexe des arabinoxylanes des parois du son, un véritable arsenal enzymatique est nécessaire pour aboutir à leur hydrolyse complète, et cela que ce soit après extraction ou au sein du réseau pariétal. Nous distinguerons les enzymes capables de couper la chaîne principale de xylose, les endoxylanases, à ce titre désignées comme enzymes principales, et les enzymes qui «débranchent» les substitutions ou ramifications portées par la chaîne principale. Ces enzymes sont dites «accessoires» ou parfois «secondaires». Elles augmentent l'accessibilité des endoxylanases aux xylanes en libérant l'espace nécessaire à leur action. Quand les enzymes accessoires sont capables de catalyse sur un substrat donné, alors elles agissent de façon synergique avec les endoxylanases.

Les principales enzymes nécessaires au passage polymère-->oligosaccharides des arabinoxylanes des sons de blé sont schématisées ci dessous.

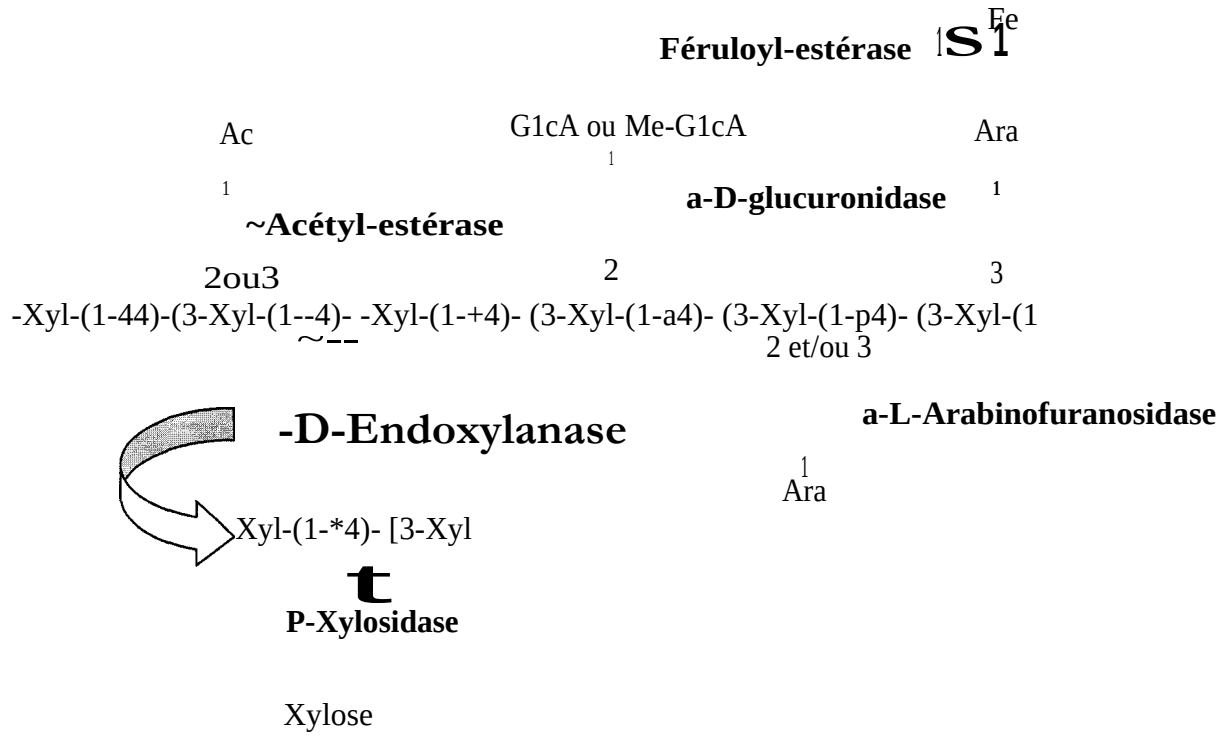

Figure 8 : Schématisation de la structure des arabinoxylanes des sons de blé et des sites de coupure des enzymes impliquées dans leur dépolymerisation.

4.1 Les endo-13-1,4-xylanases (EC 3.2.1.8)

Ces enzymes sont communément appelées «xylanases», elles catalysent la rupture de la liaison glycosidique reliant deux résidus xyloses de la chaîne principale des xylanes (arabinoxylanes dans les sons). Les endo-P-1,4-xylanases peuvent être d'origine fongique ou bactérienne. Les plus étudiées et les mieux caractérisées sont les endoxylanases d'origine fongique, parmi lesquelles celles *d'Aspergillus piger* (Poutanen 1988). Plusieurs espèces de *Trichoderma* produisent également des endoxylanases (Biely 1985, Hrmova et al. 1986, Wong et al. 1986, Wood et al. 1986). Des endo-P-1,4-xylanases bactériennes ont également été isolées et caractérisées, en particulier celles du genre *Bacillus* (Panbangred et al.1983, Debeire-Gosselin et al. 1992). Des levures produisent des xylanases extracellulaires, exemple des xylanases de *Cryptococcus* (Biely et al. 1980). Actuellement, la recherche et l'isolement de nouvelles xylanases sont menés conjointement à l'amélioration des propriétés physicochimiques des xylanases connues grâce aux techniques de biologie moléculaire.

4.1.1 Classification des endoxylanases

La comparaison des séquences d'acides aminés des domaines catalytiques, et l'analyse des zones hydrophobes (HCA pour Hydrophobic Cluster Analysis) des xylanases et des cellulases, a permis d'établir une ancienne classification de ces enzymes en 9 familles (A-I) (Henrissat et al. 1989). Les familles A, B, F et H contiennent les enzymes fongiques et bactériennes. La famille E inclut des enzymes bactériennes ainsi que des enzymes d'origine végétale. La famille C renfermerait uniquement des enzymes fongiques alors que les enzymes bactériennes sont rencontrées dans les familles D et G.

Récemment, Henrissat et Bairoch (1996) ont classé l'ensemble des glycosyles hydrolases en 58 familles où les anciennes xylanases des familles F et G appartiennent respectivement aux glycosyles hydrolases 10, (GH10) et glycosyles hydrolases 11 (GH11). La famille G/11 est constituée par les endoxylanases de faible masse moléculaire (< 30 kDa) et de pl basique, et la famille F/10 inclut des endoxylanases de masse moléculaire élevée (>30 kDa) et de pI acide (Biely et al. 1997).

Les endoxylanases catalysent la même réaction mais peuvent montrer des masses moléculaires et des propriétés physicochimiques très variables. Les xylanases bactériennes et fongiques sont représentées par des protéines dont la masse moléculaire varie très largement (Sunna et Antranikian 1997). La température optimale d'activité est également variable,

d'environ 40 à 60°C. Les xylanases bactériennes sont généralement plus thermostables que les enzymes fongiques; celles de bactéries thermophiles telles *Bacillus stearothermophilus* (Khasin et al. 1993) ont des températures optimales d'activité variant de 65 à 80°C. Autre exemple, la xylanase A produite par *Clostridium sterconarium* a une température optimale de 70°C et un temps de demie vie à 80°C de 90 minutes. Certaines possèdent des propriétés surprenantes, comme cette xylanase produite par *Thermotoga sp.* ayant une température optimale de 105°C et un temps de demie vie à 95°C de 90 minutes (Simpson et al. 1991).
La gamme de pH recouvrant une activité maximale comprend des valeurs situées entre 4 et 7, mais beaucoup de ces enzymes restent stables dans une gamme plus étendue, de pH 3 à pH 10 ce qui constitue un véritable intérêt biotechnologique.

4.1.2 Structure des endoxylanases, spécificité de leurs inhibiteurs protéiques

La structure cristalline de plusieurs endoxylanases de faible masse moléculaire (famille G ou GH11) a été déterminée. Elle comporte trois feuillets 13 anti-parallèles et une hélice a qui forment une main droite partiellement fermée, laissant apparaître une large crevasse sur l'un des côtés de la molécule (Figure 9) ainsi que le «pouce» de l'enzyme. Ce dernier est suspecté de contribuer à la spécificité du substrat pouvant entrer dans la crevasse catalytique, et d'être de surcroît la cible d'inhibiteurs protéiques (Tahir et al. 2002). Parmi les inhibiteurs spécifiques des xylanases, il existe des familles d'inhibiteurs thermolabiles rencontrés dans les blés (Rouau et Surget 1998). Ces inhibiteurs ont été identifiés récemment, et ciblent spécifiquement certaines structures des xylanases, leur fixation rendant les enzymes inactives. Ce sont les TAXI *(Triticum aestivum* xylanase inhibitor), premiers inhibiteurs caractérisés sous une forme monomérique de 40 kDA (TAXI-I) «mature» et une seconde (TAXI-II) dimérique de 30+10 kDA «non mature» (Debyser et al. 1997, Debyser et al. 1999, Gebruers et al. 2004). D'autres inhibiteurs, les XIP (ylanase inhibiting protein), protéines monomériques de 30 kDA ont également été décrits (McLauchlan et al. 1999, Juge et al. 2004), et très récemment caractérisée un nouveau type d'inhibiteur; TL-XI pour thaumatin-like xylanase inhibitor de 18 kDA (Fierens et al. 2004). Il est intéressant de remarquer que si les XIP de blé inhibent les xylanases fongiques de la famille 10 et certaines de la famille 11 *(Aspergillus, Penicillium),* les TAXI et les TL-XI n'ont pas d'activité inhibitrice face aux xylanases de la famille 10 (Goesaert et al. 2004). Cette spécificité d'action des inhibiteurs est à relier aux différences structurales entre les familles de xylanase.

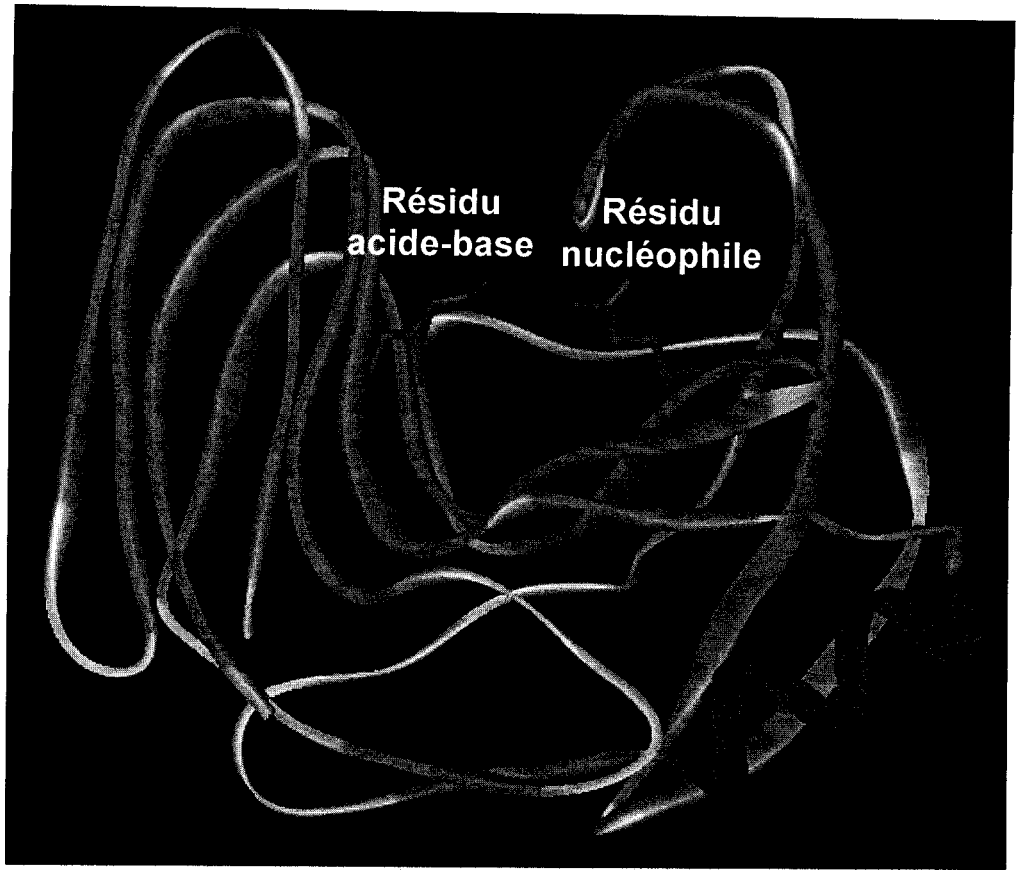

Figure 9 : Structure tridimensionnelle des xylanases de faible masse moléculaire (famille G ou xylanase 11) d'après Harris, 1997.

4.1.3 Les domaines structuraux des xylanases

Les xylanases sont constituées de domaines dits fonctionnels et d'autres dits non fonctionnels reliés par des régions fortement enrichies en acides aminés hydroxylés. Tous les domaines ne sont pas retrouvés au sein d'une même famille, les xylanases de la famille 10, généralement plus volumineuses, possèdent souvent un nombre plus élevé de domaines (fonctionnels ou non) que celles de la famille 11. Parmi ces domaines, nous citerons:

- Les domaines catalytiques (DC),

La grande majorité des xylanases est constituée d'un seul domaine catalytique (DC), au minimum celui qui permet la coupure de la liaison glycosidique reliant deux xyloses liés en $_{R}$ (1-+4). Des xylanases possèdent deux DC, généralement le cas d'un plus grand nombre

de xylanase de la famille 10. Pour exemple, la xylanase de *Ruminococcus flavefaciens* possède deux domaines catalytiques (Durand et al. 1996). Les séquences d'acides aminés des DC de xylanases appartenant à la même famille ont des taux d'homologie importants, proches de 50 % (Tôrrônen et al. 1992).

- Les domaines de liaison aux polysaccharides (Carbohydrate Binding Module)

Ils regroupent des domaines de liaison plus ou moins spécifiques d'une nature de ligand. Dans le cas des xylanases, on peut citer les CBD et XBD.

-Les CBD (Cellulose Binding Domains) sont des domaines de liaison à la cellulose. Initialement mis en évidence chez certaines cellulases, les CBD ont été découverts chez d'autres espèces enzymatiques telles que les xylanases et les arabinofuranosidases. Les CBD sont composés d'une centaine d'acides aminés chez les enzymes bactériennes et d'environ une trentaine chez les enzymes fongiques. Localisés en position N-terminale ou C-terminale, la majorité des CBD peut être classée en cinq familles principales (I, II, III, IV et V) selon l'homologie de structure primaire. La présence d'un nombre important d'acides aminés aromatiques conservés a été montrée, un exemple le CBD de la glucanase-xylanase Cex de *Cellulomonas fimi* contient 5 résidus tryptophane. Deux d'entre eux sont localisés entre les tonneaux a et F3, et les trois autres sont exposés à la surface de la protéine. Les résidus aromatiques exposés ont un rôle dans la fixation réversible de la cellulose (Bray et al. 1996). Les xylanases possédant un CBD ont la capacité de se lier à la cellulose, mais sont incapables de l'hydrolyser. On peut citer les cas de *Pseudomonas fluorescens* et *Clostridium thermocellum* (Gilkes et al. 1991). Les CBD conféreraient aux xylanases la capacité de se fixer à de nombreux sites dans les parois végétales et augmenteraient les chances de rencontre entre xylanases et leurs substrats.

- Les XBD (Xylan Binding Domains) sont des domaines de liaisons aux xylanes. La définition de ces domaines est sujette à controverse. En effet, les XBD fixent la xylanase sur les xylanes. Toutefois une étude réalisée sur la xylanase A de *Thermomonospora fusca* (Irwin et al. 1994) révèle que le domaine identifié comme étant un XBD montre également de l'affinité pour la cellulose. De plus, le domaine catalytique de l'enzyme peut également se lier aux xylanes. Toutes les xylanases ne possèdent pas ces domaines XBD. La présence d'un XBD apporterait des propriétés intéressantes pour l'enzyme, Black et al. (1995) ont étudié les CBD et les XBD de la xylanase D de *Cellulomonas fimi.* Ils ont montré que la délétion du CBD conduisait à l'incapacité de la xylanase à se fixer à la cellulose, sans affecter la capacité

de l'enzyme à fixer les xylanes. Cependant, le Km de la xylanase tronquée du CBD pour les xylanes insolubles est augmenté. Bien que le CBD n'affecte pas directement l'activité catalytique de la xylanase, il agit sur l'affinité de l'enzyme, ici en l'augmentant.

Enfin, on peut citer l'existence de séquences de liaison. Elles relient les différents domaines de la protéine, mais n'interviennent directement ni dans l'activité catalytique de la xylanase ni même dans la liaison avec le substrat (Ferreira et al. 1990). Ce sont en général de courtes séquences (de 10 à 60), riches en acides aminés hydroxylés, et souvent 0-glycosylés.

4.1.4 Réaction catalysée par les xylanases

4.1.4.1 Mécanisme de la réaction

Les xylanases catalysent l'hydrolyse des xylanes grâce à un mécanisme acide/base impliquant deux résidus catalytiques (mécanisme identique chez les cellulases). Le premier résidu catalytique protonne l'oxygène de la liaison glycosidique. Le second intervient comme nucléophile. La grande majorité des xylanases agissent selon un mécanisme de double déplacement permettant la formation d'un intermédiaire glycosyl-enzyme qui est ensuite hydrolysé par l'ion oxocarbonium. La réaction se poursuit par la formation d'un groupe hydroxyle à partir d'une molécule d'eau sur l'intermédiaire carbonium, et d'un proton sur le nucléophile. Cette réaction de double déplacement provoque la rétention de configuration alors qu'en revanche, la réaction de simple déplacement provoque une inversion de configuration anomérique. Cette réaction implique la participation d'un acide ou d'une base dans la catalyse avec l'attaque d'une molécule nucléophile d'eau (McCleary et Matheson 1983).

4.1.4.2 Les acides aminés impliqués dans la catalyse

Wakarchuk et al. (1994) ont proposé que les résidus Glu 78 et Glu 172 étaient respectivement les résidus nucléophiles et acide-base de la xylanase de *Bacillus circulans* grace à une étude cristallographique du complexe enzyme-substrat. Ces deux résidus d'acide glutamique, fortement conservés, sont localisés à l'opposé l'un de l'autre dans le site actif de l'enzyme, dans la crevasse ou sillon catalytique, et la mutation de ces résidus diminue fortement l'activité de l'enzyme. Ceci suggère qu'ils constituent les résidus catalytiques essentiels. De

même, la xylanase A de *Streptomyces commune* possède un couple Glu 87 et Glu 184 dans son site actif.

Le site actif de la xylanase de *Bacillus circulans* contient également trois résidus tryptophane (Wakarchuk et al. 1994). Le tryptophane a lui aussi un rôle important dans le site actif, ceci ayant été démontré chez des xylanases de *Chainia* (Deshpande et al. 1990) et de *Streptomyces* (Keskar et al. 1989). Ces mêmes auteurs ont également montré que la présence dans le site actif de certaines xylanases de résidus cystéine participe au repliement et à la conformation de la protéine, essentielle à l'activité xylanolytique. La modification de ces résidus entraînant la perte de toute activité, ils interviendraient dans la formation du complexe intermédiaire glycosyl-enzyme.

D'autres acides aminés très conservés, les résidus Proline 98, Asparagine 124 et Thréonine 133, pourraient participer à la fixation du substrat mais n'agiraient pas directement dans la réaction d'hydrolyse de la chaîne de xylane.

4.1.4.3 Sites actifs et sous sites de fixation des xylanases

Il existe plusieurs sous sites de fixation encadrant de part et d'autre la diade catalytique formée par les acides glutamiques. Ces sous sites participent à l'affinité des xylanases pour les différents substrats. En effet, c'est à leur niveau que les xyloses des chaînes adjacentes vont être positionnés, et la présence d'un éventuel substituant va être différemment acceptée en fonction de la nature de l'enzyme, du type de substituant (arabinose, acide glucuronique...) et du sous site impliqué.

Les sous sites de l'endoxylanase *d'Aspergillus Piger,* incapables d'hydrolyser le xylobiose, présentent en revanche une haute affinité pour les xylo-oligosaccharides de taille croissante. En fait, le site de fixation de cette xylanase est constitué de 5 sous sites (A à E), le site catalytique étant localisé au milieu, entre le troisième et le quatrième, a partir de l'extrémité non réductrice (Meagher et al.1988).

Debeire et al. (1990) ont déterminé les 5 sous sites (A-E) de la xylanase de *Clostridium thermolacticum* (famille 11), fixant cinq résidus xyloses (a à e). Le site catalytique est localisé entre les résidus xyloses b et c, et les sous sites (D) et (E) sont capables de fixer des résidus xyloses substitués contrairement aux sous sites A, B et C. En cas de substitution portée par le xylose, les contraintes liées à l'encombrement stérique occasionné dans la cavité du sous site

sont déterminantes pour l'issue de la réaction. Plus de 5 sous sites peuvent exister, 6 ou 7 sous sites ont par ailleurs été montrés chez d'autres xylanases microbiennes (Biely et al. 1981).

4.1.4.4 Action des xylanases sur les arabinoxylanes

Le nombre potentiel de sites de coupure d'une endoxylanase sur un substrat est fonction de la longueur et du niveau de substitution de ce dernier (Reilly *et* al. 1981). Par leur action, les endoxylanases diminuent le degré de polymérisation du substrat en libérant des xylo-oligomères dont les degrés de polymérisation et de substitution varient, selon l'enzyme et le substrat. Les endoxylanases des familles 10 et 11 coupent les chaînes de xylanes et lorsqu'une substitution (essentiellement arabinose et moins fréquemment acide glucuronique dans les sons de blé) se présente à elles, les deux familles d'enzymes vont se distinguer de la façon suivante:

-Les endoxylanases de la famille 10 coupent la liaison glycosidique à proximité d'un résidu de xylose substitué (Biely et al.1997) alors qu'au contraire

-Les endoxylanases de la famille 11 ne coupent la liaison glycosidique qu'entre deux résidus xylose adjacents non substitués (Biely et al. 1997) (Figure 10).

Des comportements très variables même au sein d'une famille de xylanase, pouvant provenir du même organisme, sont connus. Certaines xylanases n'agissent uniquement que sur des chaînes de xylanes non substitués. Une xylanase de *Trichoderma reesei* n'est active sur des acétylglucuronoxylanes qu'après action d'autres enzymes (accessoires) capables de libérer les groupements acétyles et acides glucuroniques (Poutanen et Puis 1989). De même, l'endoxylanase *d'Aspergillus Piger* est inactive sur les arabinoxylanes insolubles (Frederick et al. 1981) et son activité est augmentée lorsque les substitutions arabinoses sont débranchées sous l'action d'arabinofuranosidases.

Parmi les xylo-oligosaccharides non substitués issus de l'action des endoxylanases, le xylobiose et le xylotriose sont majoritaires. Certaines xylanases sont également capables de libérer du xylose sous forme monomérique *(Aspergillus Piger, Talaromyces byssochlamydoides...).* Le xylose libéré proviendrait de l'action de l'endoxylanase sur les xylo-oligosaccharides libérés (solubilisés) (Kanda et al. 1985). De très nombreuses études ont été publiées sur la nature des produits (xylo-oligosaccharides) libérés par diverses xylanases agissant sur une grande variété d'arabinoxylanes. Parmi celles ci, en lien avec le sujet de notre

Exemples de produits de réactions libérés par l'action des xylanases de la famille Il

Fe

GlcA ou Me-G1cA

Ait

Xyl-1:3-(1-+4)-Xyl

Xyl- -(1-A)-Xy - 3-(1--+4)

Xyl-13-(1-+4)-X. -g-(1--+4)-Xyl

-Xyl-β-(1→4)-Xyl-β-(1→4)-Xyl

Famille 11 GlcA ou Me.Glcp, 1

Ara

1.

-Xyl-13-(1--+4)-Xylie-(1--+4) Xyl-13-(1-94),Xyl- -(1- ►4)-Xyl-E341-+4)-Xy1-0-(1-34>.Xy1-13-(1

Ara

Famille 10

Exemples de produits de réactions libérés par l'action des xylanases de la famille IO

Fe

G1cA ou Me-G1cA

Xy1-P-(1-+4 -Xyl

àa

-Xyl-β-(1→4)-Xyl-β-(1→4)-Xyl

FigurelO : Représentation schématique de l'action des xylanases des familles 10 et 11 sur des arabinoxylanes (Adapté de Biely et al. 1997)

étude, nous citerons l'endoxylanase de 39 Kda produite par *Clostridium thermolacticum* (Debeire et al. 1990) qui libère des xylo-oligosaccharides obtenus à partir des glucuronoxylanes de mélèze. De degrés de polymérisation variables, ils sont substitués par un acide 4-0-méthyl-glucuronique. Des produits de réaction encore plus complexes sont libérés, pour exemple le cas d'une endoxylanase purifiée de *Thermobacillus xylanilyticus* qui en plus du xylobiose et du xylotriose à partir de la paille de blé, produit aussi des arabinoxylo-oligosacharides de degré de polymérisation supérieur à 2, substitués ou non par l'acide férulique (Lequart et al. 1999).

Les propriétés physicochimiques des arabinoxylanes, telles que la solubilité, peuvent également influencer l'efficacité des endoxylanases. Il existe une corrélation positive entre le degré de substitution et la solubilité dans l'eau. En effet, plus les xylanes sont substitués, plus ils seront solubles car capables grâce à leurs substituants, d'établir des liaisons faibles avec les molécules d'eau.

4.2 Les Ji-xylosidases et enzymes accessoires

Les enzymes nécessaires à la dégradation complète du polymère d'arabinoxylane du son de blé en monomère ou petits oligomères sont succinctement décrites ci dessous.

-Les (3-xylosidases (EC 3.2.1.37) sont, à la différence des endoxylanases, des exoglycosidases. Elles hydrolysent les xylo-oligosaccharides de faible degré de polymérisation à partir de leur extrémité réductrice et de manière générale, n'attaquent pas les polymères de xylanes. Cependant, de rares exemples montrent l'aptitude de certaines 13-xylosidases à libérer très lentement du xylose à partir de xylanes (Dekker et Richards 1976).

-Les a-L-arabinofuranosidases (EC 3.2.2.55)

Ce sont des exo-enzymes capables d'hydrolyser les liaisons a reliant les L-arabino-furanosyles de la chaîne latérale des arabinanes, des arabinogalactanes et des arabinoxylanes (Kaji 1984). Agissent principalement sur des oligosaccharides de faible degré de polymérisation, plus rarement sur des polymères (Poutanen 1988b), Greve et al. (1984) ont observé que l'arabinose serait une restriction à la dégradation des arabinoxylanes par les endoxylanases. Son action dénude la chaîne principale et permet la création de nouveaux sites

pour l'action des xylanases. Néanmoins, actuellement peu de données existent sur des arabinofuranosidases capables d'agir efficacement sur les disubstitutions d'arabinose portées par les xyloses de la chaîne principale.

-Les a-D-glucuronosidases (EC 3.2.1.139)

Ce sont des exo-enzymes, capables de couper les liaisons entre l'acide glucuronique (ou son dérivé 4-0-méthylé) et le xylose de la chaîne principale qui le porte. Principalement actives sur des glucuronoxylo-oligomères de faible degré de polymérisation (Johnson et al.1989) elles peuvent néanmoins libérer lentement de l'acide 4-O méthylglucuronique à partir de glucuronoxylanes.

-Les acétyle estérases (EC 3.1.1.6)

Ces enzymes libèrent des groupements acétyles liés en position C-2 ou C-3 d'un xylose, et comme pour beaucoup d'autres enzymes accessoires, sont souvent peu actives sur de longues chaînes de xylose, mais plus efficaces sur des xylo-oligosaccharides. De nombreuses acétyle estérases nécessitent donc l'action préalable d'endoxylanases afin d'obtenir une diminution de la taille du substrat. L'action des endoxylanases interviendraient dans des régions faiblement acétylées libérant des xylo-oligossacharides acétylés qui seront alors des substrats des acétyle estérases. Ce type d'enzyme associé à une endoxylanase conduit parfois à une action synergique (Blum et al. 1999).

-Les féruloyle estérases (EC 3.1.12)

Elles sont capables de libérer l'acide férulique estérifié à l'arabinose ramifiant les arabinoxylanes. Comme la plupart des enzymes accessoires de la dégradation des arabinoxylanes, les féruloyles estérases agissent préférentiellement sur des substrats de petite taille (oligomère) (Mac Kenzie et Bilous 1988), mais peuvent parfois agir sur des substrats polymériques (Tenkanen et al. 1991, Bartolomé et al. 1997). Récemment, il a été montré qu'en combinaison avec des xylanases provenant de familles et de microorganismes différents, les féruloyles estérases pouvaient solubiliser des taux variables d'acides féruliques pariétaux (Faulds et al. 2003)

Les sons de blé sont des co-produits de la transformation des grains de blé en farines et semoules. Fraction technologique de la mouture des grains, ils sont constitués des enveloppes du grain, ainsi que d'une couche de cellule provenant de l'albumen amylacé de ces fruits qui ne s'ouvrent pas à maturité (indéhiscents). Les sons constituant 15 à 20% de la masse du grain, et la production mondiale en blé avoisinant le milliard de tonnes par an, la transformation de cette céréale génère par conséquent des quantités considérables de ces co-produits.

Leur valorisation énergétique et financière est actuellement incomplète. Aujourd'hui, elle s'appuie essentiellement sur deux stratégies. La première utilise le son en tant que produit alimentaire, principalement destiné à l'alimentation animale en raison de son potentiel nutritionnel important (fibres et micronutriments). La deuxième stratégie repose sur l'extraction des composés constitutifs du son avant transformation pour des utilisations multiples en industrie agroalimentaire ou non alimentaire.

La région Champagne–Ardenne est un site de production du blé de tout premier ordre au niveau européen, produisant surtout des farines panifiables issues de blé «tendre» *Triticum aestivum*. En raison de la réduction des marges bénéficiaires, la valorisation des co-produits que sont les pailles et les sons est devenue une nécessité économique impérieuse. Cette étude s'inscrit dans ce contexte, auquel s'ajoute la prise en compte de transformations «non-polluantes», exigence sociale fortement exprimée depuis les dernières décennies. Au moins une partie du développement des biotechnologies en découle, les techniques chimiques dites polluantes utilisées jusqu'ici sont contraintes de chercher des substitutions plus «respectueuses» de l'environnement. Le laboratoire où j'ai effectué ces travaux travaille à l'élaboration de stratégies de bioconversion enzymatique de la biomasse, en particulier la dégradation enzymatique des sons de blé, *Triticum aestivum*. Ce cadre général a guidé mes travaux, co-financés par la Région Champagne–Ardenne et l'Institut National de la Recherche Agronomique (INRA).

Les objectifs majeurs de ces travaux sont la compréhension/amélioration de la dégradation des arabinoxylanes des sons de blé tendre par des endoxylanases. Une clé essentielle requise pour la bioconversion rationnelle du végétal est de mieux cerner les limitations de l'hydrolyse enzymatique et la disponibilité physicochimique des substrats. Paradoxalement, ces

limitations résultent de la richesse et de la diversité des interactions entre constituants pariétaux, ceux là même que l'on tente de valoriser.

Les recherches effectuées dans le cadre de ce projet s'appuient sur de précédents travaux (Benamrouche-Stitou, 2002), où les bases chimiques et histologiques de la dégradation des sons par une endoxylanase ont été établies. La démarche entreprise ici se situe essentiellement sur un plan cognitif, portant à la fois sur l'état des composés pariétaux natifs, puis post-hydrolytiques et leurs rendements de solubilisation. Les paramètres d'accessibilité des enzymes aux substrats dans les différents types de parois des sons matures ou lors du développement du grain ont été considérés. Afin de mieux maîtriser les applications pouvant résulter du désassemblage des composés pariétaux des sons, l'analyse biochimique des composants connus comme influençant l'organisation des parois, et par conséquent l'action des enzymes a été suivie au cours de la maturation des parois. Cette stratégie visait à définir temporellement certaines des limitations vis à vis de l'hydrolyse enzymatique.
Cette étude repose sur une approche multi disciplinaire où microscopie et biochimie se côtoient. La complémentarité des techniques mises en oeuvre permet d'explorer plusieurs niveaux d'organisation: histologique, cytologique et moléculaire.
L'architecture de ce manuscrit est organisée en quatre chapitres qui comportent chacun une introduction, le matériel et méthode, les résultats, la discussion ainsi que les références bibliographiques. Cette présentation repose sur un découpage des travaux en cinq articles scientifiques soumis pour publication dans des revues internationales à comité de lecture. Les principaux résultats sont regroupés et commentés dans une discussion générale, incluant les perspectives possibles à ce travail. Enfin, l'ensemble des références bibliographiques utilisées sont regroupées à la fin de ce mémoire.

Chapitre I Relations entre variabilité biochimique des sons industriels - dégradabilité à la xylanase

Publication 1: Teneurs en arabinoxylanes et acides hydroxycinnamiques des sons de blé *(Triticum aestivum)* en relation avec la dégradabilité à un type d' endoxylanase

> *Actuellement, lorsque l'on envisage la valorisation de la biomasse, on néglige sa diversité essentielle. Etant donné la variabilité naturelle des produits végétaux, il faut donc s'attendre à ce que des problèmes qualitatifs de*

valorisation des biomasses prennent le relais de celui de la valorisation de «la» biomasse. Bernard Monties -1980, Les polymères végétaux.

Tenant compte du contenu de cette citation, la disparité des composés tels que les arabinoxylanes des sons de blé tendre, mais aussi des acides hydroxycinnamiques connus pour réticuler les polymères au sein des parois végétales a été étudiée. La variabilité de ces composés dans les sons industriels de blé tendre *(Triticum aestivum)* a été évaluée, de même qu'une possible incidence de la diversité génétique et éco-physiologique sur la dégradation des sons par une endoxylanase de la famille 11 des glycosyles hydrolases. L'adéquation "teneur en arabinoxylane des sons/dégradabilité par voie enzymatique" pourrait conduire au choix de variétés de blé particulièrement adaptées pour cette application.

Chapitre II Relations entre mise en place des parois – dégradabilité des arabinoxylanes à la xylanase

Publication 2: Structure, composition chimique et dégradabilité à une endoxylanase des couches externes isolées de grain en maturation

L'action de la xylanase ne permettant pas la solubilisation de tous les arabinoxylanes des parois des sons de blé, nous avons testé l'effet de cette enzyme sur des enveloppes isolées manuellement à partir de grain en cours de maturation. Ces assises tissulaires correspondent aux cellules du son technologique. L'objectif est de mettre en relief les composés ou les structures susceptibles de limiter l'action de l'enzyme sur les sons de grain a maturité.

Dans un premier temps, nous avons suivi l'évolution de certains constituants dans les enveloppes externes de grain de blé à différents stades de maturation. Puis dans un deuxième temps, nous avons évalué l'impact de ces événements chimiques sur la dégradabilité des arabinoxylanes à une endoxylanase de la famille 11 des glycosyles hydrolases. Les approches chimiques en lien avec l'immunocytochimie nous permettrons alors de discuter les contributions d'ordre structural et physicochimique limitant l'action de l'enzyme.

Chapitre III Relations entre nature des substrats – efficacité enzymatique

Publication 3: Comparaison de l'efficacité de deux familles d'endoxylanases (10 et 11) sur le son de blé et des fractions d'arabinoxylanes extraites

Cette démarche visait à comparer l'action des enzymes dans la dégradation des arabinoxylanes pariétaux. Les différences de comportement, en lien avec les caractéristiques connues des enzymes (taille, mode d'action...), ont permis de proposer les points importants qui influencent le rendement global de dégradation.

Pour cela, deux endoxylanases thermostables appartenant aux familles 10 et 11 des glycosyles hydrolases, possédant des propriétés catalytiques différentes, ont été testées. L'analyse comparée de leur efficacité est fondée sur la caractérisation des produits solubilisés par les enzymes à partir de sons et d'une gamme d'arabinoxylanes en solution. La caractérisation des substrats et des produits d'hydrolyse a contribué à préciser les causes de l'efficacité variable des enzymes. En particulier, l'orientation du profil des produits obtenus a été abordée par combinaison des enzymes et analyse des oligosaccharides libérés par technique PACE.
De plus, l'étude des dérivés phénoliques co-solubilisés a permis d'appréhender les cibles pariétales.

Chapitre IV Relations entre distribution – accessibilité des substrats

Après avoir examiné l'importance de la variabilité des sons et l'incidence de la mise en place des tissus constitutifs dans la dégradation des arabinoxylanes par les xylanases, nous avons tenté de déterminer les modifications ultrastructurales des parois. A l'échelle microscopique, la séquence des événements liés à l'action de l'endoxylanase a été explorée afin de préciser la nature des barrières structurales et cytochimiques vis à vis de l'hydrolyse enzymatique. Ce chapitre a été scindé en deux parties.

Publication 4: Suivi de l'action d'une endoxylanase lors de l'hydrolyse de son de blé. Mise en évidence d'une hétérogénéité et de micro domaines pariétaux

Les modalités de l'action *in situ* de l'enzyme sur les arabinoxylanes ont été visualisées à l'aide d'outils immunocytochimiques au cours de la dégradation du son par une endoxylanase de la famille 11 des glycosyles hydrolases. Parallèlement à l'utilisation d'anticorps anti-

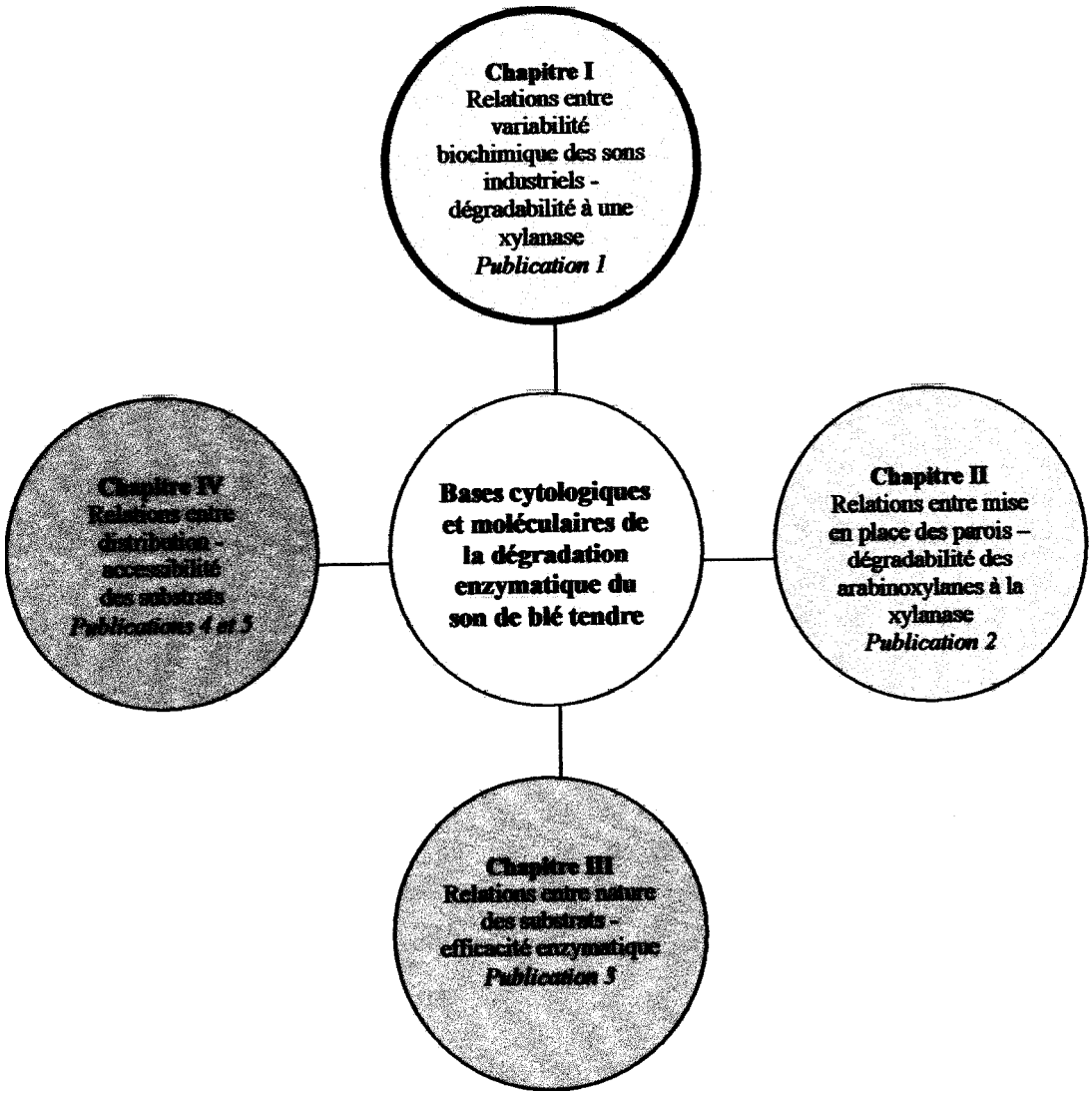
Chapitre I
Relations entre variabilité biochimique des sons industriels - dégradabilité à une xylanase
Publication 1
Chapitre IV
Relations entre distribution - accessibilité des substrats
Publications 4 et 5
Bases cytologiques et moléculaires de la dégradation enzymatique du son de blé tendre
Chapitre II
Relations entre mise en place des parois – dégradabilité des arabinoxylanes à la xylanase
Publication 2
Chapitre III
Relations entre nature des substrats – efficacité enzymatique
Publication 3

xylanase, un anticorps polyclonal dirigé contre des séquences d'arabinoxylanes peu substitués fournissent des informations sur la dégradabilité des parois à l'enzyme. Conjointement, un suivi topocytochimique renseigne également sur les structures des parois affectées. La dégradation des arabinoxylanes met ainsi en relief l'hétérogénéité tissulaire et cellulaire. Les observations microscopiques sont discutées en relation avec les données structurales et biochimiques des sons de blé.

Publication 5: Micro-hétérogénéité des parois de couches cellulaires isolées des sons: apport d'une xylanase mutante inactive

S'appuyant sur les résultats de la 4ème publication où l'évolution spatiale de l'enzyme a été précisée en relation avec la distribution des arabinoxylanes, une démarche similaire a été envisagée dans le but de comparer les effets obtenus sur du son ou sur des couches cellulaires isolées. Les effets de l'augmentation de la surface accessible à l'enzyme par ouverture du composite tissulaire sont discutés. L'immunolocalisation d'une endoxylanase mutante dépourvue de capacité hydrolytique est précisée au regard de la sauvage.

Afin de placer spécifiquement chacun des chapitres par rapport à la globalité des travaux, un organigramme placé au début de chacun des quatre chapitres permet de situer le lecteur.

J. Cereal Sci. XX (2004) 1-8

Arabinoxylan and hydroxycinnamate content of wheat bran in relation to endoxylanase susceptibility

J. Beaugrand, D. Crônier, P. Debeire and B. Chabbert

Institut National de la Recherche Agronomique, UMR FARE-614, Centre de Recherche Agronomique, 2 esplanade Roland Garros, BP 224, 51686 Reims Cedex 02, France

Abstract

Hydroxycinnamate and protein contents and monosaccharides composition were determined for 11 industrial wheat *(Triticum aestivum)* brans and related to their susceptibility of arabinoxylans (AX) to enzymatic degradation. There was significant variation in carbohydrate, A/X ratio, protein, hydroxycinnamic acid (HCA) and di ferulic acid (DiFA) content among the wheat brans. In addition, a strong correlation was found between AX and ferulic acid (FA) contents. Brans were extracted with water followed by a dry-thermal treatment to remove -90% starch and to inactivate endogenous enzymes and proteinaceous inhibitors. Treated brans were compared with respect to AX degradation by a family 11 xylanase. Digestion with xylanase had a strong impact on the chemical composition of the residual bran. The A/X ratio changed from 0.60 to 1.07. The solublised AX had an A/X ratio of 0.32. The A/X ratio of enzyme-depleted bran was negatively correlated with the loss of AX. Total DiFA in destarched brans was negatively correlated with the amount of soluble AX. There relationships indicate that structural features of AX and the extent of its cross-linking in the cell walls of the bran tissues influence its susceptibility to xylanase treatment. Thus the amount of enzyme-solublised AX was not directly related to the content of AX in the destarched bran. However, brans differed in their susceptibility to xylanase attack.

Keywords: Wheat bran, Xylanase, Arabinoxylans, Esterified hydroxycinnamates

1. Introduction

Wheat bran is a major milling by-product and represents an abundant but under-exploited renewable resource. Starch-depleted bran from wheat *(Triticum aestivum)* is rich in arabinoxylans (AX). Enzymatic upgrading of bran is an attractive alternative to environmentally-damaging chemical methods currently used for lignocellulose saccharification. Bran comprises the outer tissues of the wheat kernel and includes botanically distinct tissues of the pericarp (fruit coat), testa (seed coat), the hyaline layer and the aleurone layer, which is part of the endosperm (Evers and Millar, 2002). Wheat bran arabinoxylans are composed of a main (1÷4)-linked (3-D-xylopyranose backbone to which are attached side chains of variable nature and frequency of occurrence. a-L-Arabinofuranose and its feruloylated derivatives are the major substituents; a-D-glucuronic acid or its 4-methyl ether derivative, and acetyl groups are also present.

(1—+4)-(3-Endoxylanases (EC 3.2.1.8) depolymerise AX releasing xylo-oligosaccharides of varying composition and degree of polymerisation. The action pattern of xylanases has been documented using a large variety of AX sources (Biely et al., 1997; Li et al., 2000) and has been studied in relation to their uses in food and fibre biotechnology (Ebringerovâ and Hromâdkovâ, 1999). Based on the structural and sequence-classification of glycosyl hydrolases (Boume and Henrissat, 2001; Henrissat and Davies, 1997) two xylanase families, 10 and 11, are distinguishable in relation to specificity, size and their sensitivity to proteinaceous xylanase inhibitors found in cereal grains (Goesaert et al., 2004). Xylanases from the same family may show different activities against similar substrates (Biely et al., 1997; Faulds et al., 2003; Frederix et al., 2003). The impact of the association of AX with lignin in walls of cells in cereal brans on their susceptibility to xylanase treatment has not been studied in detail. Previous work showed that a thermostable, family 11 (1–*4)-(3-endoxylanase-treatment of wheat bran led to the release of 50% of the AX (Benamrouche et al., 2002). Since bran is histologically and chemically heterogeneous the susceptibility towards xylanase will depend on the individual tissues. For example, in addition to specific structural features of AX such as the degree of branching, cell-wall polysaccharides covalently bound to one another or to lignin through hydroxycinnamic acid (HCA) cross-links to form a cohesive wall network may limit enzyme access. Ferulic acid (FA) and diferulic acids (DiFA) represent the major cross-linking phenolic acids in cell walls of grasses (Chesson, 1988; Hartley et al., 1990; Iiyama et al., 1990). High concentrations are reported in cereal bran and could limit enzymatic digestibility (Andreasen et al., 2000; Hatfield et al., 1999; Lam et al., 2003; Saulnier et al., 1999). In particular, the pericarp

contains a high proportion of DiFA compared to the aleurone which has extremely low concentrations (Antoine et al., 2003; Rhodes et al., 2002). Genetic and environmental variability among wheat grains and their milling factions have been recorded in detail (Dupont and Altenbach, 2003; Kim et al., 2003; Lempereur et al., 1997, 1998). However, variation in the chemical composition of wheat bran has not been well documented although any structural diversity would be of technological interest.

The purpose of the present study was to examine the extent of variability in the content of protein, AX and HCA of brans obtained from common soft wheat cultivars grown in France and to assess their diversity in relation to xylanase susceptibility. Brans were standardized by removing starch using a water treatment prior to xylanase digestion.

2. **Experimental**

2.1 Wheat bran samples

Eleven industrial wheat bran samples were obtained from ten common soft wheat *(Triticum aestivum)* cultivars grown in France for flour production. The brans were supplied by SOUFFLET (Nogent-sur-Seine, France). The wheats were grown in 2000 (Baroudeur Scipion, Shango, Aztec), in 2001 (Courtot, Soissons, Aztec) and in 2002 (Apache, Cadenza, Lona, Renan). The brans contained 15-25% starch (dry matter). Samples were stored at -20°C.

2.2 Chemical analysis

Except for the native wheat-bran and soluble fractions (control and xylanase essays), samples were freeze-dried before analysis. The moisture content was determined using a moisture balance (Mettler Toledo, HR 73, Switzerland); all the analytical data were expressed on a dry matter basis.

2.3 Destarching

Ten grams of bran were suspended in 100 mL of water at 40°C with stil-ring for 10 min. The bran was recovered by filtration through a glass filter (40-100 µm porosity) and the water treatment was repeated twice. For the Apache 2002 bran, filtrates containing starch were pooled and dried before analysis for protein and soluble carbohydrate. Destarched brans were dried then autoclaved for 20 min at 121°C to inactivate any endogenous enzymes and proteinaceous inhibitors and stored at -20°C.

Starch content was determined spectroscopically using an enzyme kit (Boeringer/Mannheim).

2.4. Xylanase assay

Purified thermostable (1>4)-(3-endoxylanase (Debeire-Gosselin et al., 1992) (EC 3.2.1.8) activity was determined as previously described (Benamrouche et al., 2002). One Unit corresponds to the amount of xylanase required to release 1 µmol. min $^{-1}$ of reducing equivalent as xylose from birchwood xylan (Sigma) at 60°C.

2.5 Xylanase treatment of destarched bran

Destarched bran (30 g/1) was incubated at 60 °C with constant stirring in water (control) or xylanase (10 Units/ml), which allows maximal rate of hydrolysis (Benamrouche-Stitou, 2002). After incubation for 24 h the mixture was heated at 100 °C for 10 min. The supernatants were filtered through a glass filter (40-100 nm porosity), centrifuged at 6050g for 15 min and the supernatants containing the soluble hydrolysis products retained for analysis. Destarched residues were freeze-dried and ground using a bail crusher (Retsh, MM 2000).

2.6 Determination of monosaccharide, protein, and ester-linked hydroxycinnamic acids

The neutral monosaccharide composition was determined in triplicate after acid hydrolysis by HPAEC as previously described (Benamrouche et al., 2002), using a CarboPac PA1 anion-exchange column (4x250 mm, Dionex), and expressed as mean value with a coefficient of variation of 5%. Protein contents (N*5.7) were determined from total N contents using an elemental analyser (NA 1500, Carlo Erba) coupled to a mass spectrometer (Fisons Isochrom). Experiments were run in duplicate with a calculated experimental error of less than 5%.

HCA and DiFA were released by incubating 40 mg destarched bran, with NaOH (10 mL, 2 M) for 2 h at 35°C with constant stirring under nitrogen. After 10 min cooling, the reaction was stopped by adjusting the pH to 1 with HCL 6 M prior to the addition of 3,4,5 trimethoxy-trans-cinnamic acid as internal standard. HCA were extracted with ether (30 ml) three times. Ether fractions were pooled and evaporated to dryness under reduced pressure (800 mbar). The dried extract was dissolved in 1.5 ml of methanol/water (1:1, v/v) and filtered (0.45µm) prior injection on a Spherisorb S5 ODS2 (Waters, RP-18, 250 mm*2.6 mm) column. The elution gradient used solvant A (acetonitril, orthophosphoric acid 15 mM in Milli-Q water, 10:90, v/v), solvant B

(methanol, orthophosphoric acid 15 mM in Milli-Q water, 80:20, v/v), solvant C (acetonitril, orthophosphoric acid 15 mM in Milli-Q water, 80:20, v/v). The elution was convex gradient from 100% A to 92.5% A, 5% B and 2.5% C between 0 to 6 min; changed to 85 % A, 10% B and 5% C between 6 to 13.5 min with linear gradient; changed to 60% A, 20 % B and C between 13.5 to 27.5 min with concave gradient and stabilised during 2.5 min; changed to 50 % B and C between 30 to 35 min with concave gradient; changed to 100% A between 35 to 50 min with concave gradient and stabilised during 5 min.

HCA in the eluates were detected using a Waters photodiode array UV detector. HCA monomers were quantified at 302 nm using commercial standards. DiFA were identified and quantified from UV spectra of 8-0-4', 5-5'and 8-5' —benzofuran dimers and retention times. The 8-5' — benzofuran was a gift from X. Rouau (INRA, Montpellier, France); 8-0-4'and 5-5'dehydrodiferulic acids were obtained by de-esterifing 200 g wheat bran with 2M NaOH as described. The dehydrodiferulic acids were purified by preparative HPLC (Novaprep, Merck) using a Lichrospher (Merck, RP-18, 250 mm*25 mm) column. The products were separated using an isocratic gradient (water-methanol, 60:40,v/v) and a 40 ml/min flow rate. The ferulic dehydrodimers were detected at 320 nm and identified by UV spectrometry and GC/mass spectroscopy. Determinations of ester-linked HCA were performed in duplicate; with errors for monomers and DiFA of 4% and 5% respectively.

2.7 Statistical analysis of data

Multivariate analysis and mean comparison tests were used to study the variance (ANOVA) of a matrix including the chemical features analysed for the 11 wheat bran samples and treatments (water destarching and xylanase), with the SPSS software package, USA. Correlations were analysed by particular pairs with the Pearson's correlation test.

3. Results and discussion

3.1 Starch removal

The carbohydrate and protein contents of 11 wheat brans were analysed before and after water treatment. The water treatment dissociated starch granules from the bran allowing their removal by filtration. With the exception of AX discussed below, the results (Table I) show that there were significant differences in the monosaccharide profile and in the total neutral sugar content among the bran samples ($P<0.001$) and the

destarched bran (P<0.001) except for glucose and TCC (P<0,01). The untreated and destarched brans showed marked differences among the monosaccharides (P<0.001) except for galactose (P>0.05). Similarly, there were differences in protein content, ranging from 10.6 to 18.3%. The A/X ratio also showed a significant variation among bran samples (P<0.01), nevertheless there was no change that could be related to the destarching treatment (P = 0.926). A large and general decrease in glucose content (from 30.0 to 18.5%) was found for destarched brans with a concomitant enrichment in arabinoxylan (42.7 to 63.0%). The untreated bran showed large differences in AX expressed as a percentage of the total carbohydrate (Ara+Gal+Glc+Xyl) from 35.5 to 49.2%, but its range was quite narrow for the destarched bran (from 61.7 to 67.3%). The AX content, expressed on a dry matter basis, displayed significant variation among the untreated brans (P = 0.02), but after destarching, there was no significant variation in AX. The differences between destarched and untreated brans were presumably due to the loss of starch. Indeed, the water extracts from Apache 2002 contained 93% glucose found in the total neutral sugar, accounting for 53% of the dry malter. Besides glucose, arabinose, galactose and xylose were present at low levels, and proteins accounted for 17% of the material removed. These data suggest that in addition to starch granules, cellular compounds or small bran fragment were lost, as observed by microscopie observation (not shown). The extent of starch removal was close to 90%, as determined by enzymatic assay. The starch levels ranged from 1.5-2.5% of dry matter in destarched bran, indicating that water treatment effectively lowered the starch content. Subsequently, a thermal treatment that aimed at inactivating endogenous enzyme and xylanase inhibitors (Goesaert et al., 2004) was performed under dry conditions. The structural integrity of each bran was checked microscopically; some thin walls of sub-aleurone endosperm cells were visible but were present in very low amounts. The combined water and thermal treatments led to "standardised" samples that differed significantly (P<0.01) in chemical composition, notably in their A/X ratio.

3.2 Hydroxycinnamic acids in destarched bran

The contents of the ester-linked hydroxycinnamic acids, p-coumaric acid (pCA), sinapic acid (SA), ferulic acid (FA) and its dimeric forms (DiFA): 5,5'; 8-0-4' and 8,5' are shown in Table II. The most abundant HCA is FA, followed by pCA and SA. These values are similar to published data (Andreasen et al., 2001; Faulds et al., 2003) and clearly show a significant variation in HCA among the samples. The variation in content of DiFA amongst the brans was less pronounced (P<0.05, n = 22). Significant

differences in amounts of hydroxycinnamic acids in cereal grains in respect to agronomic and genetic factors have been recorded (Andreasen et al., 2000; Hernanz et al., 2001) there is, however, little information available about the variability among different brans. The content of FA in durum wheat grains shows marked genetic and agronomie variability whereas the concentration of DiFA is mostly influenced by genetic factors (Lempereur et al., 1997; 1998). The highest concentrations of dehydrodimers are found in the external layers of cereal grains, the 8-0-4' form being the predominant dimer (Hernanz et al., 2001; Lempereur et al., 1998). Differences in the proportion of dehydrodimers have been reported in durum wheat brans (Peyron et al., 2002). Moreover, Bily et al. (2003) showed that DiFA in maize bran are related to the resistance to *Fusarium* and are influenced by genetic variation.

The FA and AX content of destarched brans were highly correlated ($r = 0.731$, $P<0.01$), a trend consistent with the data for different milling fractions of durum wheat *(Triticum durum)* (Lempereur et al., 1997). Moreover, arabinose contents displayed a strong correlation with the proportion of 8-5' –benzofuran ($r = 0.63$, $P<0.01$) whereas weaker relationships were observed with other dimeric forms ($r = 0.51$ for 5-5' DiFA; $r = 0.45$ for 8-0-4' DiFA with $P<0.05$). The degree of arabinose substitution (A/X ratio) was related to the proportion of the 8-5' dimeric form ($r = 0.59$ with $P<0.01$). Finally, galactose contents were correlated with FA ($r = 0.58$), xylose ($r = 0.65$) and arabinose ($r = 0.58$) with $P<0.01$, a trend that is consistent with the high amount of galactose in the complex heteroxylans (Benamrouche et al., 2002; Brillouet and Joseleau, 1987) reported in wheat **pericarp.**

3.3 Xylanase treatment of destarched bran

The carbohydrate contents and composition of the soluble fractions released by the xylanase are shown in Table III. The average values were consistent with previous data for xylanase treated wheat bran that had been destarched on an industrial scale (Benamrouche et al., 2002). Xylose, arabinose, and glucose were the major monosaccharides recovered from acid hydrolysis of the soluble fraction and accounted for 20 % of the untreated bran dry matter. The significant amount of glucose in the soluble polysaccharide fraction may arise from glucans released from cell walls during AX degradation (Benamrouche et al., 2002). A very low proportion of galactose was also detected. The proportion of AX in the total carbohydrate released ranged from 14.3-18%. The A/X ratio (mean value 0.32) of the soluble xylo-oligosaccharides is significantly lower than the corresponding values for AX in untreated destarched bran

(mean value 0.60). This is consistent with the preferential degradation of low-substituted xylan by family 11 xylanases (Benamrouche et al., 2002; Brillouet and Joseleau, 1987). Control treatments without addition of xylanase released soluble-products that amounted to 4% of bran dry-matter and consisted mostly of AX. These small yields are in the range reported for water-extractable arabinoxylans from wheat bran (Cleemput et al., 1997; Frederix et al., 2003; Maes and Delcour, 2002).

Xylanase treatment led to an average 40% loss of dry matter from the destarched bran, nonetheless the bran residue displayed the same general characteristics in comparison with the untreated destarched bran (Table IV). The bran residue had a higher glucose content (–24% dry matter) and a lower AX concentration, due mainly to the release of xylo-oligosaccharides with low arabinose substitution (Table III). The glucose enrichment is most likely related to an enhanced cellulose content (Fincher and Stone, 1986). Xylanase treatment largely removed FA from the bran, in contrast the DiFA were at higher levels in bran residues as evidenced by the very significant increase in the DiFAIFA ratio. This is in agreement with previous microscopic observations showing degradation of the FA-rich walls of aleurone cells by xylanase (Lempereur et al., 1998; Pussayanawin et al., 1998; Rhodes et al., 2002) in contrast to the walls of cells in outer layer tissues where both ferulic acid and its dehydrodimers are abundant in wheat (Antoine et al., 2003; Benamrouche et al., 2002; Tervilâ-Wilo et al., 1996).

In contrast to the soluble xylanase products the residual arabinoxylans in the enzyme-treated bran had a high proportion of arabinose (mean A/X 1.07), due to the action pattern of the xylanase. The effect of arabinose substituents on the site of cleavage of arabinoxylans by xylanases has been discussed elsewhere (Benamrouche et al., 2002; Debeire et al., 1990; Faulds et al., 2003). Enzyme-treated bran exhibited significant differences in the ratio A/X at 99% confidence level. The A/X ratio of the bran residues was negatively correlated with the percentage of AX removed by xylanase treatment (r = -0.61; P<0.001, n = 33). This is not unexpected. Arabinoxylan conformation is partially determined by the degree of arabinosylation; besides the chain interactions, the backbone impresses minimum constraints strength (Atkins, 1992). The implications of the conformation of the substrate on the extent of cleavage by xylanases have been discussed (Dervilly et al., 2000; Faulds et al., 2003). However the correlation is moderate suggesting that the degree of arabinosylation is not the only factor limiting xylanase action. A negative correlation was also observed between xylanase-soluble AX and the total DiFA content of untreated destarched bran (r = -0.71, P = 0.001).

Together, these correlations suggest that the xylanase susceptibility of bran is related not only to the AX structure but also to its accessibility in the interconnected polymer network of the walls including cross-linking through ferulate dehydrodimers (Hatfield et al., 1999). Additionally, local arabinosylation and crosslinking may be different in the walls of cells of the different tissues that make up the bran, as suggested by Faulds et al. (2003). Following xylanase treatment, a general enrichment of protein was observed, and was correlated with the initial ranking ($r = 0.913$; $P<0.001$; $n = 22$). The protein content did not affect the xylanase efficiency since there was no correlation between AX release and protein content in the original brans. This data could be expected since the major part of bran protein is encountered in the intracellular aleurone. However, as recently evidenced for aleurone cell-wall (Rhodes and Stone, 2002), the protein characterisation and potential interaction within the wall components may need further investigation with respect to cell-wall hydrolytic process.

Mean comparison with the ANOVA way aims at comparing the impact of xylanase treatment against destarched wheat bran and the intra variability of these industrial brans (Table IV). Xylanase thus revealed strong influence on the levels of all components analyzed (Table IV), except arabinose whose extent of removal approximately corresponded to the dry matter loss (Table III). Xylose, AIX ratio and FA were particularly associated to the xylanase treatment. Although the extent of variability related to FA was high in residual bran, it did not exceed the difference linked to the xylanase treatment. In contrast, the high variability in protein contents was again evidenced and appeared much stronger than the effect of xylanase.

Xylanase efficiency was determined as the proportion of arabinoxylans removed (expressed as a percentage of the initial content of AX) and significantly varied ($P<0.001$) from 40 to 55%. However, the AX contents of wheat bran were not correlated with the xylanase efficiency (Figure 1). In other words, enzyme-release of xylo-oligosaccharides would reach similar yields irrespective of the potential variability of bran AX contents. This data suggests that xylanase fractionation aiming at oligosaccharide production could be applied to a large range of common wheat bran, but some varieties could be more suitable owing to both their high AX content and xylanase susceptibility.

4. Conclusion

We showed that destarched wheat bran display significant chemical differences regarding ester linked HCA, carbohydrates and protein contents. Chemical variations

were still observed in the xylanase-treated wheat bran, the enzyme treatment led to the decrease in AX and FA levels. The statistical evaluation of the data enabled to highlight important factors for xylanase efficiency that significantly varied according the type of bran. Therefore further insights into the genetic and agronomical basis of wheat bran diversity would be needed when addressing new enzyme-technologies.

Abbreviations

AX = arabinoxylan; A/X = arabinose/xylose ratio; DiFA = diferulic acid; FA = ferulic acid; GC, gas chromatography; HCA = hydroxycinnamic acid; HPAEC = high-pressure anion-exchange chromatography; pCA = p-coumaric acid; Prot = protein; SA = sinapic acid; TCC = total carbohydrate content; UV = ultraviolet.

Acknowledgements

We thank Marthe Carlier for her skilful technical assistance and Dr. B. Kurek for his helpful discussion concerning statistical analysis. The authors gratefully acknowledge Dr. X. Rouau for providing 8-5' –benzofuran and SOUFFLET for supplying bran samples. This work was supported by a grant from the Région Champagne-Ardenne.

References

Andreasen, M.F., Christensen, L.P., Meyer, A.S., Ansen, A., 2000. Content of phenolic acids and ferulic acid dehydrodimers in 17 rye *(Secale cereale)* cultivars. Journal of Agricultural and Food Chemistry 48, 2837-2842.

Andreasen, M.F., Kroon, P.A., Williamson, G., Garcia-Conesa, M.T., 2001. Esterase activity able to hydrolyse dietary antioxydant hydroxycinnamates is distributed along the intestine of mammals. Journal of Agricultural and Food Chemistry 49, 5679-5684.

Antoine, C., Peyron, S., Mabille, F., Lapierre, C., Bouchet, B., Abecassis, J., Rouau, X., 2003. Individual contribution of grain outer layers and their cell wall structure to the mechanical properties of wheat bran. Journal of Agricultural and Food Chemistry 51, 2026-2033.

Atkins, E.D.T., 1992. Three-dimensional structure, interactions and properties of xylans, in : Xylans and Xylanases (Visser, J., Beldman, G., Kusters-van Someren, M. A., and Voragen, A.G.J., Eds). Elsevier Science Publishers, 39-50.

Benamrouche, S., Crônier, D., Debeire, P., Chabbert B., 2002. A chemical and histological study on the effect of (1–>4)-(3-endo-xylanase treatment on wheat bran. Journal of Cereal Science 36, 253-260.

Benamrouche-Stitou, S., 2002. Biochimie et histologie de la dégradation enzymatique du son de blé par une endoxylanase. Ph.D Reims, Université Champagne-Ardenne, France.

Biely, P., Vrsanska, M., Tenkanen, M., Kluepfel, D., 1997. Endo-P-1,4-xylanase families: differences in catalytic properties. Journal of Biotechnology 57, 151-166.

Bily, A.C., Reid, L.M., Taylor, J.H., Johnston, D., Malouin, C., Burt, A.J., Bakan, B., Regnault-Roger, C., Pauls, K.P., Arnason, J.T., Philogène, B.J.R., 2003. Dehydrodimers of ferulic acid in maize grain pericarp and aleurone: resistance to *Fusarium graminearum*. Phytopathology 93, 712-719.

Boume, Y., Henrissat, B., 2001. Glycoside hydrolases and glycosyltransferases: families and functional modules. Current Opinion in Structural Biology 11, 593-600.

Brillouet, J.M., Joseleau, J.P., 1987. Investigation of the structure of a heteroxylan from the outer pericarp (beeswing bran) of wheat kernel. Carbohydrate Research 159, 109-126.

Chesson, A., 1988. Lignin-polysaccharide complexes of the plant tell wall and their effect on microbial degradation in the rumen. Animal Feed Science and Technology 21, 219-228.

Cleemput, G., Booij, C., Hessing, M., Gruppen, H., Delcour, J.A., 1997. Solubilisation and changes in molecular weight distribution of arabinoxylans and protein in wheat flours during bread-making, and the effects of endogenous arabinoxylan hydrolysing enzymes. Journal of Cereal Science 26, 55-66.

Debeire, P., Prim, D., Strecker, G:, Vignon, M., 1990. Purification and properties of an endo-1,4-xylanase excreted by a hydrolytic thermophilic anaerobe, *Clostridium thermolacticum*. *A* proposal for its action mechanism on larchwood 4-0-methylglucuronoxylan. European Journal of Biochemistry 187, 573-580.

Debeire-Gosselin, M., Loonis, M., Samain, E., Debeire, P., 1992. Purification and properties of 22 kDa endoxylanase excreted by a new strain of thermophilic *Bacillus,* in : Xylans and Xylanases (Visser, J., Beldman, G., Kusters-van Someren, M. A., and Voragen, A.G.J., Eds). Elsevier Science Publishers, 463-466.

Dervilly, G., Saulnier, L., Roger, P., Thibault, J.-F., 2000. Isolation of homogeneous fractions from wheat water-soluble arabinoxylans. Influence of the structure on their macromolecular characteristics. Journal of Agricultural and Food Chemistry 48, 270-278.

Dupont, F.M., Altenbach, S.B., 2003. Molecular and biochemical impacts of environmental factors on wheat grain development and protein synthesis. Journal of Cereal Science 38, 133-146.

Ebringerovâ, A., Hromâdkovâ, Z., 1999. Xylans of industrial and biomedical importance. Biotechnology and genetic Engineering Reviews 16, 325-341.

Evers, T., Millar, S., 2002. Cereal grain structure and development: some implication for quality. Journal of Cereal Science 36, 261-284.

Faulds, C.B., Zanichelli, D., Crepin, V.F., Connerton, I.F., Juge, N., Bhat, M.K., Waldron, K.W., 2003. Specificity of feruloyl esterases for water-extractable and water-unextractable feruloylated polysaccharides: influence of xylanase. Journal of Cereal Science 38, 281-288.

Fincher, G.B., and Stone, B.A., 1986. Cell walls their components in cereal grain technology. Advances in Cereal Science and Technology 8, 207-295.

Frederix, S.A., Courtin, C., Delcour, J.A., 2003. Impact of xylanases with different substrate selectivity on gluten-starch separation of wheat flour. Journal of Agricultural and Food Chemistry 51, 7338-7345.

Goesaert, H., Elliot, G., Kroon, P.A, Gebruers, K., Courtin, C.M., Robben, J., Delcour, J.A., Juge, N., 2004. Occurence of proteinaceous endoxylanase inhibitors in cereals. Biochimica et Biophysica Acta 1696, 193-202.

Hartley, R.D., Morrisson, W.H., Himmelsbach, D.S., Borneman, W.S., 1990. Cross-linking of cell wall phenolic arabinoxylans in graminaceous plants. Phytochemistry 29, 3705-3709.

Hatfield, R.D., Ralph, J., Grabber, J.H., 1999. Cell wall cross-linking by ferulates in grasses. Journal of the Science of Food and Agriculture 79, 403-407.

Henrissat, B., Davies, G., 1997. Structural and sequence-based classification of glycoside hydrolases. Current Opinion in Structural Biology 7, 637-644.

Hernanz, D., Nuisez, V., Sancho, A.I., Faulds, C.B., Williamson, G., Bartolomé, B., Gbmez-Cordovés, C., 2001. Hydroxycinnamic acids and ferulic acid dehydrodimers in barley and processed barley. Journal of Agricultural and Food Chemistry 49, 4884-4888.

Iiyama, K., Lam, T. B.T., Stone, B.A., 1990. Phenolic acid bridges between polysaccharides and lignin in wheat internodes. Phytochemistry 29, 733-737.

Kim, J.C., Mullan, B.P., Simmins, P.H., Pluske, J.R., 2003. Variation in the chemical composition of wheats grown in western Australia as influenced by variety, growing region, season, and post-harvest storage. Australian Journal of Agricultural Research 54, 541-550.

Lam, T.B.T., Iiyama, K., Stone, B.A., 2003. Hot alkali-labile linkages in the walls of the forage grass *Phalaris aquatica* and *Lolium perenne* and their relation to in vitro wall digestibility. Phytochemistry 64, 603-607.

Lempereur, I., Rouau, X., Abecassis, J., 1997. Genetic and agronomic variation in arabinoxylan and ferulic acid contents of durum wheat (Triticum durum L.) grain and its milling fractions. Journal of Cereal Science 25, 1-8.

Lempereur, I., Surget, A., Rouau, X., 1998. Variability in dehydrodiferulic acid composition of durum wheat *(Triticum durum)* and distribution in milling fractions. Journal of Cereal Science 28, 251-258.

Li, K., Azadi, P., Collins, R., Tolan, J., Kim, J.S., Eriksson, K.E., 2000. Relationships between activities of xylanases and xylan structures. Enzyme and Microbial Technology 27, 89-94.

Maes, C., Delcour, J.A., 2002. Structural characterisation of water-extractable and water-unextractable arabinoxylans in wheat bran. Journal of Cereal Science 35, 315-326.

Peyron, S., Chaurand, M., Rouau, X., Abecassis, J., 2002. Relationship between bran mechanical properties and milling behaviour of durum wheat *(Triticum durum* Desf.). Influence of tissue thickness and cell wall structure. Journal of Cereal Science 36, 377-386.

Pussayanawin, V., Wetzel, D.L., Fulcher, R.G., 1998. Fluorescence detection and mesurement of ferulic acid in wheat milling fractions by microscopy and HPLC. Journal of Agricultural and Food Chemistry 36, 515-520.

Rhodes, D.I., Sadek, M., Stone, B.A., 2002. Hydroxycinnamic acids in walls of wheat aleurone cells. Journal of Cereal Science 36, 67-81.

Rhodes, D.I., Stone, B.A., 2002. Proteins in walls of wheat aleurone cells. Journal of Cereal Science 36, 83-101

Saulnier, L., Crépeau, M.J., Lahaye, M., Thibault, J.F., Garcia-Conesa, M.T., Kroon, P.A., Williamson, G., 1997. Isolation and structural determination of two 5,5'-

Table I : Partial composition of wheat bran and water destarched wheat bran.

		Weight percentage of dry matter[a]							
		Carbohydrate							
		Protein	Ara	Gal	Glc	Xyl	AX[b]	A/X	TCC
Wheat bran	Aztec 2000	15.8	9.0	1.1	31.1	15.6	43.3	0.58	56.8
	Baroudeur 2000	nm	9.9	1.5	25.7	13.9	**46.6**	0.71	51.0
	Scipion 2000	nm	9.3	1.2	24.4	15.5	49.2	0.60	50.4
	Shango 2000	15.1	8.4	1.1	27.5	15.0	45.0	0.56	52.0
	Aztec 2001	nm	8.5	1.0	35.7	14.1	38.1	0.60	59.3
	Courtot 2001	18.4	9.6	1.1	31.9	16.2	43.8	0.59	**58.8**
	Soissons 2001	14.1	9.1	1.1	33.2	16.6	42.9	0.54	59.8
	Apache 2002	12.7	7.9	1.4	29.4	13.5	41.1	0.59	52.3
	Cadenza 2002	11.2	7.1	1.2	31.5	10.8	35.5	0.53	50.6
	Lona 2002	nm	9.9	1.4	31.8	15.2	43.0	0.64	58.3
	Renan 2002	nm	8.3	1.8	26.9	13.4	42.9	0.63	50.7
Destarched Wheat bran	Aztec 2000	15.9	14.5	1.3	18.9	24.3	65.7	0.59	59.0
	Baroudeur 2000	10.6	18.1	1.4	22.2	26.3	65.2	0.68	68.0
	Scipion 2000	12.5	16.8	1.5	20.8	29.1	67.3	0.58	68.2
	Shango 2000	15.6	15.9	1.4	20.6	27.4	66.3	0.58	65.3
	Aztec 2001	18.3	14.0	1.3	21.1	23.4	62.5	0.59	59.8
	Courtot 2001	17.9	13.3	1.1	18.4	23.4	65.3	0.57	56.2
	Soissons 2001	14.0	13.8	1.3	22.8	25.1	61.7	0.55	63.0
	Apache 2002	11.8	15.2	1.3	21.2	27.3	65.3	0.55	65.0
	Cadenza 2002	11.5	13.6	1.2	19.2	23.2	64.3	0.58	57.2
	Lona 2002	14.1	16.7	1.4	21.7	24.3	63.9	0.68	64.1
	Renan 2002	10.9	16.5	1.7	21.8	25.2	64.0	0.65	65.2

Contents are expressed as percentage of dry-matter mass, except AX.

Abbreviations: Prot, proteins; Ara, arabinose; Gal, galactose; Glc, glucose; Xyl, xylose; AX, % Ara + % Xyl; A/X, arabinose to xylose ratio; nm, not measured; TCC, total carbohydrate content. [b] Expressed as a percentage of the total neutral carbohydrate content (Ara+Gal+Glc+Xyl).

Table II : Distribution of ester-linked hydroxycinnamates and ferulic acid dehydrodimers in destarched wheat bran.

	p-Coumaric acid	Sinapic acid	Ferulic acid	DiFA [a]		
				5,5'	8-O-4'	8,5'
Aztec 2000	145	141	5719	139	302	118
Baroudeur 2000	158	254	5920	141	303	171
Scipion 2000	116	120	6592	189	385	151
Shango 2000	143	219	5673	117	282	102
Aztec 2001	126	197	5232	84	211	95
Courtot 2001	122	93	4277	74	225	71
Soissons 2001	128	166	4067	106	288	115
Apache 2002	215	242	5530	119	243	105
Cadenza 2002	141	209	4391	73	171	52
Lona 2002	182	217	4931	182	458	191
Renan 2002	224	193	5212	119	265	122

[a] DiFA = diferulic acid. Data are expressed as µg per g of dry matter.

TableIII : Monosaccharide composition of the soluble-products released by xylanase or water (control) from destarched wheat bran.

		Weight percentage of initial dry matter [a]						
		Carbohydrate						
		Ara	Gal	Glc	Xyl	AX [b]	A/X	TCC
Soluble endoxylanase products	Aztec 2000	3.38	0.19	4.20	10.9	76.4	0.31	18.7
	Baroudeur 2000	4.24	0.19	3.70	13.6	82.1	0.31	21.8
	Scipion 2000	3.33	0.14	3.05	13.1	83.9	0.25	19.7
	Shango 2000	3.11	0.14	2.73	12.2	84.2	0.25	18.2
	Aztec 2001	**3.68**	0.21	3.40	11.1	80.3	0.33	18.4
	Courtot 2001	3.24	0.16	2.67	11.8	84.2	0.27	17.9
	Soissons 2001	3.45	0.16	3.16	13.1	83.3	0.26	19.9
	Apache 2002	4.35	0.19	4.90	13.7	78.1	0.31	23.1
	Cadenza 2002	4.16	0.20	4.19	12.7	79.3	0.33	21.2
	Lona 2002	3.70	0.21	3.59	10.5	**78.8**	0.31	18.0
	Renan 2002	3.17	0.15	3.23	11.4	81.1	0.29	18.0
Soluble water control products	Aztec 2000	0.82	0.07	1.12	1.39	65.0	0.59	3.40
	Baroudeur 2000	0.41	0.03	0.46	0.72	70.0	0.57	1.62
	Scipion 2000	0.48	0.04	0.40	0.72	73.1	0.66	1.63
	Shango 2000	0.42	0.03	0.43	0.64	69.6	0.66	1.52
	Aztec 2001	0.58	0.08	0.82	1.09	64.9	0.53	2.57
	Courtot 2001	0.83	0.06	0.53	1.75	81.4	0.47	3.17
	Soissons 2001	0.35	0.10	**0.88**	0.59	49.0	0.59	1.93
	Apache 2002	0.77	0.08	0.90	1.48	69.4	0.52	3.23
	Cadenza 2002	**0.68**	0.11	1.43	1.23	55.0	0.55	3.45
	Lona 2002	0.67	0.05	0.62	1.39	75.4	0.49	2.74
	Renan 2002	0.49	0.06	0.43	0.85	72.9	0.57	1.84

The proportion of each monosaccharide is expressed as a percentage of the initial dry-matter mass of starch-depleted wheat bran, except AX. [a] Abbreviations: Ara, arabinose; Gal, galactose; Glc, glucose; Xyl, xylose; AX, % ara + % xyl; A/X, arabinose to xylose ratio; TCC, total carbohydrate content. [b] Expressed as a percentage of the total neutral carbohydrate content (Ara+Gal+Glc+Xyl).

Table IV : Partial composition of destarched wheat bran residual fractions from xylanase action.

	Weight percentage of dry malter[a]									
		Carbohydrate								
	Protein	Ara	Gal	Glc	Xyl	AX[b]	A/X	TCC	FA[a,0]	DiFA/ FA'
Aztec 2000	19.7	14.1	1.51	21.9	13.6	54.1	1.04	51.1	2168	0.29
Baroudeur 2000	11.4	17.1	1.44	24.9	16.3	55.9	1.05	59.7	2164	0.33
Scipion 2000	15.8	15.2	1.64	21.5	14.0	55.7	1.09	52.3	2903	0.12
Shango 2000	17.2	15.2	1.56	21.7	14.0	55.7	1.09	52.5	3055	0.30
Aztec 2001	21.8	13.1	1.50	22.1	12.9	54.4	1.01	49.6	2060	0.21
Courtot 2001	23.7	17.2	1.54	23.6	11.8	50.6	1.16	50.5	1852	0.17
Soissons 2001	15.0	14.8	1.45	24.9	13.4	51.7	1.10	54.6	2545	0.33
Apache 2002	13.7	14.9	1.58	24.8	15.8	53.7	0.94	57.1	2276	0.19
Cadenza 2002	14.5	15.6	1.58	25.4	15.4	53.4	1.16	58.0	2721	0.25
Lona 2002	15.8	15.6	1.47	25.4	16.7	54.6	1.08	59.2	2466	0.37
Renan 2002	12.5	17.2	1.54	25.6	15.8	54.8	1.09	60.1	2665	0.36
X	6.5 (e)	(ns)	12.0 ([f])	11.4 ([f])	530 ([g])	145 ([g])	253 ([g])	37 ([g])	240 ([g])	109 ([g])
S	112 ([g])	(ns)	(ns)	(ns)	3.5 ([f])	(ns)	3.4 ([f])	(ns)	150 ([g])	3.6 (e)

Contents are expressed as percentage of residual dry-matter mass, except AX.

Abbreviations: Ara, arabinose; Gal, galactose; Glc, glucose; Xyl, xylose; AX, % Ara + % Xyl; A/X, arabinose to xylose ratio; TCC, total carbohydrate content; FA, ferulic acid; DiFA, di ferulic acid. [b] Expressed as a percentage of the total neutral carbohydrate content (Ara+Gal+Glc+Xyl). ° Expressed as µg per g of dry-malter mass

X, Analysis of the xylanase contribution

S, Analysis of the samples variability contribution

(ns) not significant P<95%

(e) P<0.05

(f) P<0.01

(g) P<0.001

J. Agric. Food Chem. Accepted

Structure, Chemical Composition and Xylanase Degradation of External Layers Isolated from Developing Wheat Grain

Johnny Beaugrand [1], David Crônier [1], Pascal Thiebeau [2], Lucas Schreiber [3], Philippe Debeire [1] and Brigitte Chabbert [1]

[1] Equipe Parois Végétales et Matériaux Fibreux, UMR FARE-614, Institut National de la Recherche Agronomique, 2 Esplanade Roland Garros, 51686 Reims Cedex 02, France. [2] Unité d'Agronomie Laon-Reims-Mons, Institut National de la Recherche Agronomique, 2 Esplanade Roland Garros, 51686 Reims Cedex 02, France. Ecophysiology of Plants, IZMB - Institute of Cellular and Molecular Botany, University of Bonn, Kirschallee 1, D-53115 Bonn, Germany

ABSTRACT

The external layers of wheat grain were investigated during maturation with respect to chemical and structural features and xylanase degradability. Cytochemical changes were observed in the isolated peripheral tissues of the wheat grain at 4 defined stages following anthesis. Marked chemical changes were highlighted at 11 days after anthesis, for which protein and lipid contents varied weakly. The profile of esterified ferulic acid showed large variation in the maturing peripheral layers of grain in contrast to the deposition of ferulate dimers, p-coumaric and sinapic acids. Lignin was monitored at the latest stages of ripening, which corresponds to the cessation of reserve accumulation in the grain. Arabinoxylans reached a maximum at 20 days and did not display any significant change in arabinosyl substitution proportion until ripeness. When submitted to xylanase, all outer layers were similarly altered in the proportion of soluble AX except for the peripheral tissues of the 11 day-aged wheat grain that had very little AX. Aleurone and nucellar layers were mostly degraded whereas pericarp stayed intact at all stages of maturation. This degradation pattern was connected with the preferential immunolocalisation of xylanase in aleurone and nucellar layers irrespective of the developmental stages. Further chemical examination of the enzyme-digested peripheral tissues of the grain supports the facts that ferulic ester is not a limiting factor in enzyme efficiency. Arabinose branching, ferulic dimers and ether linked monomers that are early deposited in the external layers would have more relevance to the *in situ* degradability of AX.

KEYWORDS: Peripheral tissues of the wheat grain *(Triticum aestivum);* maturation; cell wall; arabinoxylans; xylanase; immunolocalisation; phenolic acids; lignin; aleurone; cutin, alkylresorcinol

INTRODUCTION

Wheat bran is a hemicellulose-rich milling products that may be processed besides its main use in animal feeding. Wheat bran thus constitutes an industrial product obtained from grain dry-milling and represents a heterogeneous laminate of several kinds of cells having distinct botanical origins and structural compositions. These layers are the peripheral tissues of the grain including from the inside to the outside, the aleurone layer (al), the nucellar lysate, nucellar layer (nl) *(1,* 2), the testa (t) and the pericarp *(3,* 4). Both nl and testa have a cuticle of lipophilic material (5). Pericarp consists of tube cells (tc), cross cells (cc), hypodermis and finally the epidermis. Wheat bran thus mainly consists of cell walls but also contains noticeable amounts of micronutrients such as vitamins, phytosterols, etc...mainly due to presence of the aleurone (4, 6).

Considering the great importance of cereal in human nutrition, some basic knowledge has been provided regarding arabinoxylans (AX) in the scope of cereal processing that aims at food and non-food uses (7). Indeed, arabinoxylans are the main hemicelluloses encountered in wheat brans and account for approximately 40% of the dry matter of de-starched wheat bran (8). More specifically, wheat bran AX consist of a (1--+4)-(3-D xylopyranose backbone which have substitution side-chains including a-L-arabinofuranose groups and to a much lower extent glucuronic acid or its methyl-derivative, and acetyl groups. Phenolic acids are the main interconnecting agents between polymers in graminaceous cell walls. Ferulic acid (FA) is reported to mainly cross-link polysaccharides whereas p-coumaric acid (pCA) would also cross-link lignin (9-15). Ferulic acid and its dehydrodimer forms (DHD) both link to the O-5 arabinofuranosyl residue and are the major phenolic acids in bran cell walls (10). The p-coumaric acid and sinapic acid (SA) are found in much lower amount. The potential role of structural protein in cross-linking AX was recently highlighted (16). Other wall components, such as 13-glucan and cellulose may also interact with AX through non covalent interactions (17). The resulting cohesive wall-network provides the grain with a strong mechanical and biological resistance. Likewise, xylanase degradation of wheat brans was shown to be tissue-specific, meanwhile the outermost bran layers were enzyme-recalcitrant in spite of their low lignin contents (18).

The present investigation aimed at evaluating the impact of outer-layer changes across grain ripening on the *in situ* degradation of the AX of the grain peripheral tissues with an endo-13-1,4-xylanase (EC 3.2.1.8) from family 11 of the glycoside hydrolase classification system, commonly named family 11 xylanase. This enzyme cleaves the internai R-1,4-xylosidic

linkages in the xylan backbone. Considering the maturation of wheat grains, little information is available on the chemical aspects of the external layers when compared to the whole grain. Most studies have thus focused on the cytological events that accompany development of the grain outer coverings (19, 20). Therefore, the purpose of this study was to provide some chemical insights of the peripheral layers during grain development. To reach this goal, the peripheral tissues of developing wheat grains were obtained at defined ripening stages of the grain and submitted to xylanase hydrolysis. Light microscopy and immunolocalisation of the enzyme was used to microscopically explore the maturing peripheral layers and the impact of xylanase. In addition, chemical characterization was undertaken in order to investigate structural components of peripheral tissues of the wheat grain, in particular arabinoxylans and the wall phenolics that would potentially limit substrate accessibility (cross-linked hydroxycinnamates and lignin). The protein and lipid fractions were also monitored in relation to the developmental stages.

MATERIAL AND METHODS

Development of Peripheral Tissues of the Wheat Grain.

The soft wheat *(Triticum aestivum)* cv.Cadenza was Brown in 2002 at Prunay (Reims, northeastern France, 49°14'N, 4°10'E). Plants for which anthesis (21) occurred simultaneously were ringed, this stage corresponds to the onset of grain development. Temperature was measured every hour from anthesis until complete maturity of the grains. Daily mean values were expressed in degree Celsius per 24 h (°C/day), where only positive temperature were considered. In order to evaluate the process of grain maturation, the median part of five spikes was collected daily from the principal stem. The corresponding grains were carefully released from spikelets, glumes and paleae were removed using tweezers. The fresh-matter weight of one grain was estimated as the weight mean value of 60 grains; subsequent dehydration of the grains (48 h at 80 °C) allowed determining the dry matter. The water contents were calculated from the difference between fresh and dry matter. The main stages of grain development were evidenced from the change in these characteristics on a growing-temperature sum basis.

Isolation of Peripheral Layers from the Wheat Grain.

Median parts of the spikes were hand-collected between 8 a.m and 9 a.m at specific post-anthesis stages, namely A (183 °C/day), B (384 °C/day), C (672 °C/day) and D (884 °C/day).

Spikes were placed in liquid nitrogen then samples were stored at -20 °C. Spikes were allowed to thaw overnight at 4 °C before removal of the grains as described above. The grain-ends (brush plus embryo) were discarded with a razor blade; the median part were soaked in distilled water at 4 °C during 2 h for stages B, C and D in order to soften endosperm. This softening step was not required for grains at stage A. An incision in the crease followed by an additional hour of soaking in cold distilled water permitted the removal of the endosperm by scrapping the bran under a stereomicroscope. Purity of the endosperm-depleted bran was checked microscopically prior to resin embedding or freeze-drying for biochemical analysis.

Endoxylanase Preparation.

A purified (1—>4)-f3-endo-xylanase (EC 3.2.1.8) of the glycosylhydrolase family 11 from *Thermobacillus xylanilyticus* culture was used as previously (22). Activity of the (1—*4)43-endo-xylanase was determined following incubation with birchwood xylan (0.5% w/v) for 10 min in 50 mM sodium acetate, pH 5.8 at 60 °C and determination of the reducing sugar using a ferricyanide-based method (23). Specific activity of the enzyme was 2000 Units/mg protein. One unit is the amount of xylanase required to release 1 'mol. min^{-1} of reducing equivalent as xylose from birchwood xylan at 60 °C.

Xylanase and Water Treatment of Peripheral Tissues of the Wheat Grain.

Xylanase hydrolysis of the peripheral layers isolated at stage A, B, C and D was performed in duplicate. Dry samples were hydrated into distillated water (3%, w/v) for 16 h at 60 °C, 10 Units/mL of (1—4)-(3-endo-xylanase were then added, and the reaction proceeded at 60 °C with constant stirring. After 1 and 2 h (one experiment) and 24h of incubation, the soluble fractions were retained for analysis, and heated at 100 °C (10 min) to stop the reaction. After 10 min of centrifugation at 13000 rpm, supernatants were submitted to acid hydrolysis before sugar analysis. The residual bran were washed twice with water and freeze dried. Control water-incubations of external layers were also performed without xylanase using a similar procedure.

In order to microscopically examine the effect of the xylanase treatment, grain external layers were incubated (3%, w/v) with a lower amount of enzyme 0.5 Unit/mL under gentle agitation (Polymax 1040, Heidolph). These conditions allowed the examination of the cytochemical features of the initial steps of the bran degradation although an optimal yield of arabinoxylan

solubilization could have been reached for longer periods i.e. 24 h (24). Samples were taken before enzyme addition (t 0) and after 75 min or 24 h of incubation.

Embedding of the Peripheral Tissues of the Wheat Grain.

Samples were cut into small pieces under a solution of 2% glutaraldehyde in phosphate buffer (0.1 M, pH 7.4) and fixed in the same reagent for 1 h at room temperature under vacuum. After several washes in phosphate buffer and in distilled water (15 min each), samples were dehydrated in an ethanol series over 48 h, then infiltrated (72 h) and embedded in LR White resin (Sigma) at 60 °C for 24 h. Specimens were cut into semi-thin sections (0.5 µm thick) using a diamond knife and a HM 360 (Microm, France) microtome, and deposited on glass multiwell slides.

Immunolabeling of the Xylanase.

The polyclonal antixylanase antiserum was made by New Zealand white rabbits and produced by Eurogentec, Belgium. A usual procedure and appropriate buffer were used for xylanase immunolabeling on semi-thin sections (2). Silver enhancement reagents (Amersham life science) were applied at room temperature for 7 min. Sections were covered with Eukitt mounting medium (Electron Microscopy Sciences, USA). Immunolabeling controls were carried out in the absence of the primary antibody or the secondary antibody; another control was obtained using water-treated samples in order to check that labeling specifically corresponded to the tested enzyme. The absence of unspecific binding of silver particles was also checked using unlabeled specimens.

Cytochemistry and Microscopic Observations.

Cytochemical staining of semi-thin sections was achieved using toluidine blue (1% w/v) for 5 min. All observations were performed using an Axioskop microscope (Zeiss, Germany) plus a AxioCam MRc digital camera, either with bright light (immunogold and toluidine blue staining) or mercury lamp (UV excitation for phenolic autofluorescence, $^{x}_{excitation}$ = 340 nm, $_{4mission}$ = 430 nm).

Carbohydrate Analysis.

Acid hydrolysis of peripheral tissues (stage A, B, C and D) was performed on 5 mg samples previously ground with a bail crusher (Retsh, MM 2000) using 12 M H_2SO_4 (2 h at room

temperature) then 1.5 M H_2SO_4 for 2 h at 100 °C. Analysis of solid samples was performed in triplicate, experimental error was 5%. Soluble fractions recovered from water or xylanase treatment (500 µL) were hydrolyzed for 2 h at 100 °C in the presence of 1 M H_2SO_4. Acid-soluble samples were filtered and injected into a CarboPac PA1 anion exchange column (4*250 mm, Dionex). Detection was performed by pulsed amperometry (PAD 2, Dionex). A post-column addition of 300 mM NaOH was used. Monosaccharide composition was determined using fucose as the internai standard. Calibration was performed with standard solutions of neutral carbohydrate; arabinose, glucose, xylose, galactose and acidic carbohydrate; galacturonic and glucuronic. The content of arabinoxylan was the sum of the amounts of xylose and arabinose.

Protein Contents.

Proteins contents were determined in duplicate by the total N contents (N*5.7 as an average value of the correcting factor) of 3 mg of ball-milled samples using an elemental analyser (NA 1500, Carlo Erba) coupled to a mass spectrometer (Fisons Isochrom). The experimental error was less than 5%.

Phenol Composition of the Peripheral Tissues of the Wheat Grain.

Samples were extracted three times with 80% ethanol, The residual peripheral tissues of wheat grain was recovered by filtration then freeze-dried. Olivetol (Aldrich) was added to the combined ethanol fractions prior to evaporation under reduced pressure. The dried extract was dissolved in 2 mL of acetone/methanol (1.4/0.6) and filtered (0.45 µm) prior injection on a Kromasil 5µ (RP-18, 250 mm*4.6 mm) A.I.T Chromato column. Alkylresorcinols were eluted using a methanol gradient and identified using a photodiode array detector by comparison of reference spectra and elution time (25), and were quantified at 280 nm. Data were mean value obtained from duplicate experiment and expressed as equivalent olivetol with 5% experimental error under the conditions used.

Ester-linked hydroxycinnamates were analysed alter 2 M NaOH treatment (10 mL) of 20 mg extractive-free peripheral tissues of wheat grain, for 2 h at 35 °C with constant stirring under nitrogen flow. Aikali-residues were recovered by centrifugation (13000 rpm, 10 min) and further treated by 4 M NaOH (10 mL) at 170 °C for 2 h in order to extract ether-linked phenolic acids. Each alkali filtrate was acidified to pH 1, mixed with 3,4,5 trimethoxy-trans-

cinnamic acid as an internai standard and extracted three times with 30 mL ether. The organic phase was dried under reduced pressure and analyzed by HPLC with an elution gradient using a combination of acetonitrile, methanol and 15 mM orthophosphoric acid in distilled water as previously described (8, 24). Ester- and ether-linked phenolic acids were quantified at 302 nm using commercial standards. Identification and quantification of esterified dehydrodimers were carried out according to UV spectra and retention time in respect to the spectra of 8-0-4', 5-5'and 8-5' –benzofuran dimers. The 8-5' –benzofuran was a gift from X. Rouau (INRA, Montpellier, France); 8-0-4'and 5-5'forms were formerly purified from an alkali filtrate of wheat bran using preparative HPLC (Novaprep, Merck) and a Lichrospher (Merck, RP-18, 250 mm*25 mm) column. Determination of ester-linked phenolic compounds was performed in triplicate; variation in experimental error of monomer and dimer reached 10% owing to the low amount of sample available.

Lignin detection was performed using thioacidolysis that specifically disrupts the non-condensed intermonomer linkages. The reaction was performed in triplicate on 10 mg extractive-free peripheral tissues of wheat grain samples at 100 °C using ethanethiol/BF_3etherate/dioxane reagent as detailed previously (26). Alter a 4 h reaction, the mixture was diluted with water containing tetracosane as an internal standard and extracted with dichloromethane. Guaiacyl (G) and syringyl (S) thioethylated monomers were analyzed as their trimethylsilyl derivatives using gas chromatograph equipped with a fused silica capillary DB1 column (30 m * 0.3 mm) and flame ionisation detector. The temperature gradient was 160-200 °C at 3 °C min (26). Due to the low amount of lignin analyzed, the experimental error (< 10%) was higher than usually obtained on highly lignified samples (26).

lipidAlysis

Aliphatic compounds were released as methyl ester of fatty acids by transesterification using 10% BF_3 in dry methanol (27). The reaction was performed in triplicate, samples (3 mg) were left to react in 3 mL reagent for 24 h at 70 °C. The methanol extract was removed and the residue washed three times in chloroform. The combined organic phase was washed in a NaCl saturated solution and dried over Na_2SO_4. Monomers were converted to their trimethyl silyl ethers prior to analysis by gas chromatography as above using a temperature gradient kept at 120 °C for 8 min then elevated to 300 °C at 2 °C min. Aliphatic monomers were identified using GC-MS with respect to reference spectra reported elsewhere and to fragmentation pattern (27-29). The analytical measurement of aliphatic compounds was 5%.

RESULTS AND DISCUSSION

Microscopic View of Peripheral Tissues of Maturing Wheat Grain.

Fresh and dry matters of the grain were determined daily over a period of approximately 50 days. These values are plotted in **Figure 1** on a growing-temperature sum basis. The experimental data allowed the selection of pertinent stages of grain development with respect to the physiological and cytological events of grain maturation (4, *30).*

The micrographs of stage Aure shown in **Figure 2 (a** and **b).** At this stage (183 °C/day or 11 day post-anthesis) the grains were very small and green; the external layers were clearly distinguished. All the cells had a large cytoplasm, which considerably contrasts with the crushed aspect of mature peripheral tissues of wheat grain. Cell walls occurred as thin and floppy layers, especially at the aleurone layer. This stage corresponds to an active proliferation of endosperm cell and to aleurone differentiation (4, *31).* The testa (in a) and the pericarp (in **b)** were distinguishable which agrees with previous studies (18, 32). At stage B (384 °C/day, 20 days after anthesis), water uptake has stopped **(Figure 1)** indicating reserve accumulation in the green grains. All peripheral tissues of the wheat grain could be observed. The testa cellular layer was not yet crushed **(Figure 2 c)** since the partially filled endosperm cannot exert a strong pressure on the external layers. The nucellar layer (nl) was fully expanded as some space between the two walls was easily seen **(Figure** 2 **d).** At this stage, the cuticles of both testa and nucellar layer as well as cross cells and tube celas (the last ones being not visible on the microphotographs) were fully differentiated as previously reported (33). The cytoplasm of cross cens began to degenerate in the vicinity of some persisting thin-walled cells (arrow in **Figure 2 c).** The stage C (627 °C/day, 37 days after anthesis) corresponds to the cessation of starch and water accumulation in endosperm. Grains got brown and reached their maximal weight; external layers appeared quite similar to peripheral tissues of mature wheat grain **(Figure 2 e).** The nucellar layer was now crushed and cross cells had lost their photosynthetic activity as previously described (19), the only living cells were the aleuronic ones. At stage D (884 °C/day, 49 days after anthesis) the water contents had substantially decreased; the grains were completely brown and the volume had declined. The grain was considered as mature and the section shown in **Figure 2** f was equivalent to earlier published microphotographs of mature wheat bran (two among numerous ones, 2 and 30).

Chemical Aspect of Peripheral Tissues of Maturing Wheat Grain.

Chemical composition of the peripheral layers of the maturing grain was assessed on three distinct samples. A significant reduction in the protein contents was noticed between stage A and B **(Table 1),** and could result from a much weaker metabolic activity at stage B. Thereafter, the protein levels slightly increased until stage D; these proteins are presumably part of the aleurone cells (4). The levels of aliphatic components in the extracted peripheral tissues of wheat grain showed a marked rise between stage A and later stages. This trend could correspond to the differentiation of the polyester-rich cuticular layers at stage B as observed microscopically. From stage B to grain ripeness, the percentage of aliphatics slightly decreased **(Table 1).** Moreover, alkane monomer composition that was attained by depolymerisation through transesterification displayed dramatic changes between stage A and B. Hydroxylated derivatives were prevalent in the external layers at stage A whereas at later stages, fatty acids accounted for nearly 80% of the transesterification products. The C16-, C 18-fatty acids and hydroxylated derivatives were the main monomers as previously reported in mature wheat bran (5). The 9,10-epoxy-C18 hydroxyoctadecanoic acid, usually encountered in cutin, was found in rather low proportions (7% of total aliphatic). However, epoxy derivatives might be unstable during transesterification and could be underestimated in our study (28). The dicarboxylic derivatives and long chain hydroxylated acids (>C20), which are reported as diagnostic features of suberin (29), were only found at trace level in agreement with aliphatic composition of wheat bran. Cereal alkylresorcinols are phenolic lipids containing 17 to 25 carbons in the aliphatic chains. The C19 and C21 alkyresorcinols were the major homologs in the peripheral tissues of maturing wheat grain **(Table 1)** as for mature grain (34). The contents of alkylresorcinol strongly increased from 20 day-aged grains. The proportions then significantly declined during maturation in accordance to previous report on the whole cereal grains (25). The aliphatic fraction and alkylresorcinols of peripheral tissues of wheat grain thus displayed similar profiles across ripening of the grain. These quantitative variations might indicate that the outer layers should undergo some rearrangements until the grain matured.

Carbohydrate analysis of the peripheral tissues of wheat grain led to similar amounts of total neutral sugar irrespective of their maturation stage **(Table** 2). However, the arabinoxylan (AX) contents at stage A was about 3 fold less than those measured at latest stages. Indeed, glucose accounted for nearly 74% of the neutral sugar at stage A, consistent with the observation of many granules in the pericarp parenchymatous cells **(Figure** 2 **b).** The carbohydrate contents determined at stage A should mostly reflect intracellular compounds

such as starch granules. In contrast, the glucose proportion strongly decreased at stages B-D and may have originated from cellulose and (3-(1-4,1-3) glucans; arabinoxylans represented approximately 65 % of the neutral sugar. The A/X ratio was close to 0.60, indicating a high substitution degree. This feature remained constant from stage B as well as the contents and composition of neutral sugars. Uronic acids are minor components of graminaceous cell-walls and accounted for only 1.5 % of the wheat bran at physiological maturity stage. A slight reduction in the galacturonic acid contents (14 %) was observed over the grain maturation **(Table** 2). Apart from stage A, the carbohydrate contents and the composition of the grain peripheral tissues were quite similar during grain maturation and provided values consistent with literature data on industrial bran (4, *18).*

Wall-bound phenolic acids were predominant in the grain external layers since the ethanol-soluble hydroxycinnamates represented less than 0.08% of the peripheral tissues of wheat grain (data not shown). Following successive alkaline hydrolyses of the extractive-free peripheral tissues of wheat grain, we estimated the contents in ester and ether-linked phenolic acids **(Table 3).** The data presented herein only concerns the *trans* form, trace levels of *cis*-isomers were found as previously described *(35, 36).* FA was the major phenolic monomer in the peripheral tissues of wheat grain at all development stages, pCA and SA occurred in much lower proportions. Particularly, SA was only quantified as its ether derivative. Except for the esterified FA, hydroxycinnamate monomer profiles exhibited similarities throughout wheat grain development. Indeed, their contents were in the same range and got increasing values from stage B to stage C when grains reached their maximal weight. At mature stage (D), slightly lower proportions were recovered after alkaline hydrolysis. These data were consistent with previous studies on phenolic changes in the whole maturing grain of *Triticum aestivum (35-38).* On the contrary, esterified FA was largely predominant and reached highest levels at stage B, at which lime the proportion of esterified FA then decreased until the maturity stage (D). Several hypotheses have been suggested to explain the great variation in FA concentrations. The rise in ferulic acid synthesis has been associated to significant levels of phenylalanine ammonia lyase at the early stage of grain formation after which peroxydase that occurs in the outer coverings would induce the formation of covalent cross-links between wall polymers *(36, 37).* Therefore, ferulate could be involved in other structures such as diferulic dehydrodimers (36). We thus checked whether changes in FA levels were connected to DHD and lignin accumulation *(39, 40).* Many kinds of DHD occur in graminaceous cell walls, 5,5', 8-0-4' and 8,5' derivatives being the most frequent ones in industrial bran (41). At stage A, DHD were found at trace levels **(Table 3)** but noticeable amounts were quantified

at the latest stages in agreement with literature data. However, the DHD contents were identical from the onset of the hydrical step up to the latest stage. Compensation for the loss of esterified FA would thus hardly rely on the formation in the three dehydrodimers presented here. Nevertheless, it should be pointed out that owing to the prevalent contribution of ferulate in cross-linking lignin and polysaccharide in graminaceous (12), part of the ferulate monomer and DHD cannot be measured by current solvolytic methods. Indeed, several studies have reported that ferulates and diferulates act in graminaceous cell-walls as nucleation or initiation sites for lignification. As an example, DHD accumulation in wheat bran did not compensate for the decrease in FA contents following UV irradiation, suggesting formation of new cross-linkage between lignin and hemicellulose (42). Due to limited quantities of microdissected-peripheral tissues of wheat grain samples, lignin contents were not determined by typical procedures. However, lignin could be monitored in the peripheral tissues samples of maturing grains at stage C and D using thioacidolysis that liberates syringyl (S) and guaiacyl (G) lignin monomers involved in [3-0-4 labile-ether linkages **(Table 3).** Earlier cytochemical studies already suggested late lignin deposition in the pericarp during grain maturation, although chemical diagnostic features were not provided. Thioacidolysis cleaves the labile aryl-alkyl-ether linkages thereby allowing the characterization of the so-called uncondensed lignin fraction (43). Total yields (S+G) were very low due to the weak proportion of lignin as previously reported (44), and did not show a significant variation between the developmental stages C and D. The proportion of labile-ether-linked lignin structures within the total lignin can be estimated assuming that thioacidolysis disrupts nearly 100% of the [3-O-4-bonds, the average molar mass of the lignin monomers is 200 and a 4% maximum lignin contents can be estimated from the data obtained in our laboratory on industrial bran (24). The uncondensed lignin fraction would thus represent less than 10 % of the polymer, suggesting the deposition of a highly condensed lignin in peripheral tissues of wheat grain. The weak S/G ratio further argued for a condensed lignin type which is often described as guaiacyl-enriched polymer (45). Altogether, the data on the bound phenolic-fraction suggest that progressive bonding patterns should operate in the cell-walls during grain maturation.

Microscopic View of Peripheral Tissues of Wheat Grain Degradation.

A pure thermostable xylanase was used to explore potential changes in the cell wall network of the external layers isolated from developing grain. For this, microscopie and chemical data

of xylanase-depleted peripheral tissues of wheat grain were compared to untreated and water-treated samples.

Peripheral tissues of wheat grain samples were microscopically assessed following short (75 min) and longer incubation time (24 h) however the most relevant changes that already occurred after a 75 min enzyme-treatment were illustrated. In addition, owing to the marked brittleness of the enzyme-treated samples at stage A, this study mainly informed on histological events occurring in samples collected at stages B-D. Cytochemical alterations were investigated using toluidine blue staining and UV-autofluorescence of hydroxycinnamates (46). In addition, xylanase immunolabeling enabled localization of the enzyme within the peripheral layers of wheat grain during hydrolysis. Immunocytochemical controls did not give detectable labeling of xylanase, indicating a specific xylanase labeling of cell-walls. Indeed, the antixylanase serum did not react with control peripheral layers as shown for instance, for the samples collected at stage B and D **(Figure 3, g-h).** Moreover, no xylanase labeling was detected using secondary antibodies alone or silver enhancement (picture not shown).

Toluidine blue staining of peripheral tissues of wheat grain at stage B showed collapsed aleurone and altered nl after 75 min of xylanase treatment **(Figure 3 a).** Nucellar layer that was partially detached and the aleurone cell-walls were heavily labeled with gold particles after silver enhancement **(Figure 3 b).** Therefore, xylanase had penetrated in these cellular layers inducing significant histological changes. In contrast, the other tissue layers did not react with xylanase antibodies and kept their cell integrity. Likewise, similar changes were obtained after 75 min xylanase treatment of peripheral tissues of wheat grain at stage C, where only the aleurone cell walls and nucellar layer were labeled. However, xylanase immunolabeling occurred in a more restricted area within the nl **(Figure 3 d).** At stage D, cytochemical alterations of the al layer and nl were similar as shown in **Figure 3 e;** the gap between external and inner pericarp observed in this photograph was not linked to the xylanase treatment. The immunolabeling of xylanase was encountered again only on the aleurone cell walls and nl **(Figure 3 f).**

The cell walls of remaining al displayed a weak blue autofluorescence in small domains when the specimen from the sample at stage C was exposed to UV light **(Figure 3 c).** For comparison, a strong blue fluorescence was observed in the 24 h water-treatment sample **(Figure 4 c)** indicating the widespread distribution of ferulate in peripheral tissues of wheat grain controls. Likewise, the blue fluorescence was present mainly in the al cell walls and remained so throughout grain maturation **(Figure 4, a-b, stage** B; c and **d** stages C and D).

Similar patterns of autofluorescence were observed in the untreated peripheral tissues of wheat grain indicating that water treatment did not induce any marked microscopic change for all the maturation stages (data not shown). In contrast, all samples had a weakened aleurone-fluorescence following xylanase treatment. Consistently, previous studies reported on the loss of UV blue autofluorescence from aleurone walls when degraded by hydrolytic enzyme (18, 47). The *in situ* xylanase location was even shown to be closely connected to AX degradation and autofluorescence disappearance of bran (2).

A 24 h enzyme-incubation did not induce visible change of the peripheral tissues of wheat grain other than aleurone cell walls or nl (data not shown), these layers were finally detached from the testa. No labeling of xylanase could be observed in the residual tissues. Overall, histological features did not outline a clear-cut effect of the grain development from 384 to 884 °C/day on the way xylanase degrades peripheral tissues of wheat grain. Aleurone and nucellar layer were target cells, and pericarp and testa remained recalcitrant as shown for industrial bran (18). Nevertheless, xylanase immunolabeling allowed pinpointing in the formation of nucellar lysate from stage B to later ones. Indeed, xylanase immunolabeling highlighted a dense layer at stage C that was not found on B (compare **b** and **d in Figure 3).** This thin amorphous layer interfaces with aleurone and nl and likely originates from the nucellus crushing (1). Interestingly, xylanase was previously shown to behave distinctively in the nucellar lysate of industrial bran (2).

Chemical Aspect of Xylanase Efficiency.

Chemical analysis was performed on the most relevant components regarding enzyme efficiency. At first, the yields of soluble carbohydrates, especially arabinoxylans products, were determined following water and xylanase treatments **(Tables 4 and 5).** The proportion of water-soluble carbohydrate was very high at stage A and should mainly corresponds to the release of glucose-rich components from intracellular components (see above). Also, a large variation in experimental results was obtained and likely arose from the heterogeneous and partial deposition of aleurone at stage A. Conversely, water control released small amounts of carbohydrates from the peripheral tissues of wheat grain isolated at later stages (about 2% of the initial dry matter) without any noticeable changes over 24 h **(Table 4).** The content of water-soluble carbohydrate was consistent with previous data on industrial bran, although the proportion of AX appeared low in D **(Table 5).**

When compared to the water incubation, a 24 h xylanase-treatment from stage A allowed the recovering of a slightly higher amount of soluble compounds. Longer incubation did not lead

to higher degradation (data not shown). In contrast, following addition of xylanase to samples collected at stages B to D, the proportion of soluble carbohydrates increased significantly, and reached maximum levels after 2 h of xylanase-incubation, indicating a rather fast enzymatic hydrolysis of the peripheral tissues of the wheat grain. No evidence of variation in the time course of the carbohydrate release was seen between samples **(Table 4).** Therefore, xylanase incubation was responsible for the release of nearly 20% carbohydrate of the initial dry matter. In contrast to stage A for which AX accounted for only 12% of the soluble fraction, AX represented nearly 80% of the carbohydrate released from the other samples **(Table 5),** which confirmed that AX were efficiently disrupted by xylanase. This degradation induced a dry matter loss that reached 40, 41 and 43% following enzymatic treatment of the peripheral tissues of wheat grain isolated at stage B, C and D respectively. Enzyme-soluble AX was characterized by low A/X ratio. These values agree well with previous data on the treatment of mature industrial wheat bran using similar enzyme (2, *18).* The A/X ratio reflected the substitution degree of the xylooligosaccharide and did not vary significantly during xylanase treatment. On average, grain peripheral tissues–released AX harbored 1 arabinose for 4 xylose and did not change depending on the grain maturation stage. This lack of variation suggests that rearrangement of the xylanase target-structures along maturation if any would not substantially impact on enzyme efficiency.

Enzyme-depleted peripheral tissues of wheat grain were further characterized regarding components that cross-link AX and potentially hinder substrate accessibility. In this respect, wall-bound phenolic compounds were mainly investigated. The relative proportions of hydroxycinnamates and of uncondensed monolignols are expressed as a percentage of their initial contents in the untreated samples **(Table 6).** No significant loss in the uncondensed lignin fraction was noticed following xylanase action, accordingly the molar ratio S/G stayed unchanged in the residual peripheral tissues of wheat grain (stage C or D). This trend is consistent with the preferential lignin distribution in pericarp (44), which did not show visible alteration under xylanase. On the whole, ether-linked hydroxycinnamates were less removed than the ester ones. Furthermore, the contents of residual esterified FA strongly decreased along development stage whereas sirnilar proportions of etherified FA were recovered in residual peripheral tissues of wheat grain. When compared to FA, the wall-bound pCA and SA were released in highest proportions irrespective of the kind of peripheral tissues of wheat grain. Variation in the yields of phenolic acid monomers remaining after enzyme degradation indicates that distribution and cross-linkage patterns may change according to peripheral layers and/or maturation stage. As a matter of fact, esterified FA decreased from stage B to D,

and appeared more extractable to enzyme treatment. In contrast to hydroxycinnamate monomers, DHD were concentrated in the xylanase residue from stage B to D and were even quantified in the degraded peripheral layers of wheat grain corresponding to stage A. Based on estimation of the dry matter loss induced by enzyme treatment and assuming that no DHD were released from the weak proportion of cell walls, DHD roughly represents 130 µgram per cell-wall gram. This means that bran DHD are deposited at very early stage of the grain formation. Considering that pericarp undergoes a very weak lignification at more advanced stages, DHD may significantly consolidate immature peripheral tissues of wheat grain cell-walls into mature ones prior to lignin deposition as previously suggested in wheat seedling (48).

Among peripheral tissues of wheat grain, xylanase led to the depletion of mostly aleurone and nl. The composition of enzymatic hydrolysates thus mostly reflected the degradation of these target structures that are rich in low-substituted AX (18). However, sub-cellular chemical heterogeneity cannot be excluded. Nucellar lysate was thus the latest altered layer. Additionally, the thin inner aleurone cell walls, which are not degraded by xylanase (2) contain structural proteins that can cross-link with DHD (49). Conversely, the chemical features of enzyme-depleted peripheral tissues of wheat grain largely account for the resistant outermost layers that are rich in lignin, cellulose, DHD and highly substituted AX. Altogether, chemical and cytochemical data argued for similar xylanase efficiency on the external layers isolated at various growing stages. Considering the preferential xylanase degradation of aleurone and nl, one can suggest that potentially hampering structures are deposited early in these target layers. Our results also showed that pericarp and testa layers are already enzyme-recalcitrant at stage B when uncondensed lignin was not detected. Therefore, the degree of xylan substitution and the pattern of cross-linkage pattern must be the main relevant factor in xylanase efficiency. In this respect, DHD are detected at the early stages of grain maturation and did not further vary. This could explain to some extent that maturing peripheral tissues of wheat grain are similarly degraded. The biodegradability of highly lignified graminaceous cell-walls was reported to decline during plant maturity. Several factors are involved, notably hydroxycinnamate interconnecting lignin and hemicelluloses and pCA linkage to lignin, which are key factors that impede wall disassembly. In comparison, neither high deposition of pCA, nor intense lignification accompanies maturation of the external layers of the grain, supporting the fact that DHD cross-linking would mainly contribute to the resistance of wheat grain against enzymatic degradation. In this respect, further studies are needed to get a better understanding of the various forms of hydroxycinnamates that occur in peripheral tissues of

grain, as recently illustrated by the isolation of a ferulate dehydrotrimer and sinapate dimers *(50, 51)*. In cereal bran, deposition of ferulate dimers could display tissue-specific patterns with respect to the high level of DHD in pericarp. Further studies are on the way in order to get a more comprehensive view of the chemical events related to maturation of the peripheral tissues of wheat grain using individual micro dissected layers. Moreover, it is noteworthy that results reported in this study concern only peripheral tissues from the central portion of the wheat grain, including a small proportion of crease material for which composition may differ from the rest of the grain surrounding layers. This material was distinguishable from milling bran fractions which comprises the poles of the grain; therefore comparison with the whole bran would need some care. In addition, studies on the early stage of grain formation would improve our understanding of the initial steps of the substitution pattern of arabinoxylans that must occur in the outer layers for a few days alter anthesis.

Our chemicals results provided significant insight regarding chemical evolution of the peripheral tissues of wheat grain with emphasis to xylanase degradation. Nevertheless, taking into account the significant chemical variability of wheat brans (8, *10)* this study that focused on one wheat cultivar would require further investigation regarding genetic and environmental effects on the development of the grain outer coverings.

ABBREVIATIONS USED

Al, aleurone; AX, arabinoxylans; DHD, dehydrodimers; FA, ferulic acid; G, guaiacyl; nl, nucellar layer; pCA, p-coumaric acid; SA, sinapic acid; S, syringyl; xylanase, (1—+4)-(3-endo-xylanase

ACKNOWLEDGEMENTS

This work was supported by a grant from the "Région Champagne-Ardenne", France. We thank Marthe Carlier for her skilful technical assistance, and Dr. X. Rouau for providing 8-5'—benzofuran.

LITERATURE CITED

(1) Evers, A.D.; Reed, M. Some novel observations by scanning electron microscopy on the seed coat and nucellar layer of the mature wheat grain. *Cereal Chem*. **1988,** 65, 81-85.

(2) Beaugrand, J.; Reis, D.; Guillon, F.; Debeire, P.; Chabbert, B. Xylanase-mediated hydrolysis of wheat bran. Evidence for subcellular heterogeneity of cell walls. *Int. 1 Plant Sci.* ***2004,*** in press.

(3) Shetlar, M.R. Chemical study of the mature wheat kernel by means of the microscope. *Cereal Chem*. **1948,** 25, 99-110.

(4) Evers, T.; Millar, S. Cereal grain structure and development: some implication for quality. *J. Cereal Sci.* ***2002,*** 36, 261-284.

(5) Matzke, K.; Riederer, M. The composition of the cutin of the caryopses and leaves of *Triticum aestivum* L. *Planta* ***1990,*** 182, 461-466.

(6) Fincher, G.B.; Stone, B.A. Cell walls and their components in cereal grain technology. In Advances in Cereal Sciences; Pomeranz, Y., Ed.; AACC: St. Paul, MN, 1986; Vol 8, pp 207-295.

(7) Ebringerovâ, A.; Hromâdkovâ, Z. Xylans of industrial and biomedical importance. *Biotechnol. Genet. Eng. Rev*. **1999,** 16, 325-341.

(8) Beaugrand, J.; Crônier, D.; Debeire, P.; Chabbert, B. Arabinoxylan and hydroxycinnamate content of wheat bran in relation to endoxylanase susceptibility. *J Cereal Sci* ***2004,*** **in press.**

(9) Hartley, R.D.; Morrisson, W.H.; Himmelsbach, D.S.; Borneman, W.S. Cross-linking of cell wall phenolic arabinoxylans in graminaceous plants. *Phytochemistry* ***1990,*** 29, 3705-3709.

(10) Lempereur, I.; Surget, A.; and Rouau, X. Variability in dehydrodiferulic acid composition of durum wheat *(Triticum durum)* and distribution in milling fractions. *J. Cereal Sci.* **1998,** 28, 251-258.

(11) Chesson, A. Lignin-polysaccharide complexes of the plant cell wall and their effect on microbial degradation in the rumen. *Anim. Feed Sci. Technol.* **1988,** 21, 219-228.

(12) Hatfield, R.D.; Ralph, J.; Grabber, J.H. Cell wall cross-linking by ferulates in grasses. J. *Sci. Food Agric.* **1999,** 79, 403-407.

(13) Lam, T.B.T.; Iiyama, K.; Stone, B.A. Hot alkali-labile linkages in the walls of the forage grass *Phalaris aquatica* and *Lolium perenne* and their relation to in vitro wall digestibility. *Phytochemistry* ***2003,*** 64, 603-607.

(14) Scalbert, A.; Monties, B.; Lallemand, J.-Y.; Guittet, E.; Rolando, C. Ether linkage between phenolic acids and lignin fractions from wheat straw. *Phytochemistry* **1985,** 24, 1359-1362.

(15) Lam, TB-T.; Iiyama, K.; Stone, B.A. Cinnamic acid bridges between cell wall polymers in wheat and phalaris internodes. *Phytochemistry* **1992,** 31, 1179-1183.

(16) Rhodes, D.I.; Sadek, M.; Stone B.A. Hydroxycinnamic acids in walls of wheat aleurone cells. *J. Cereal Sci.* **2002,** 36, 67-81.

(17) Izydorczyk, M.S.; MacGregor, A.W. Evidence of intermolecular interactions of f3-glucans and arabinoxylans. *Carbohydr. Polym*. ***2000,*** 41, 417-420.

(18) Benamrouche, S.; Crônier, D.; Debeire, P.; Chabbert B. A chemical and histological study on the effect of (1--*4)-f3-endo-xylanase treatment on wheat bran. *J. Cereal Sci.* **2002,** 36, 253-260.

(19) Cochrane, M.P.; Duffus, C.M. Morphology and ultrastructure of immature cereal grains in relation to transport. *Ann. Bot.* **1979,** 44, 67-72.

(20) Duffus, C.M.; Rosie, R. Some enzyme activities associated with the chlorophyll containing layers of the immature barley pericarp. *Planta* **1973,** 114, 219-226.

(21) Tottman, D.R.; Makepeace, R.J. An explanation of the decimal code for the growth stages of cereals, with illustrations. *Ann. appl. Biol.* **1979,** 93, 221-234.

(22) Debeire-Gosselin, M.; Loonis, M.; Samain, E.; Debeire, P. Purification and properties of 22 kDa endoxylanase excreted by a new strain of thermophilic Bacillus. *In Xylans and Xylanases,* Visser, J., Beldman, G., Kusters-van Someren, M. A., and Voragen, A.G.J., Eds.; *Elsevier Science Publishers,* 1992, pp 463-466.

(23) Kidby, D.K.; Davidson, D.J.A. Convenient ferricyanide estimation of reducing sugars in the nanomole range. *Anal. Biochem*. **1973,** 55, 321-325.

(24) Benamrouche-Stitou, S. Biochimie et histologie de la dégradation enzymatique du son de blé par une endoxylanase. Ph.D. Dissertation, Université Reims Champagne-Ardenne, France, 2002.

(25) Verdeal, K.; Lorenz, K. Alkylresorcinols in wheat, rye, and triticale. *Cereal Chem*. **1977,** 54, 475-483.

(26) Hamm, M.; Debeire, P.; Monties, B.; Chabbert, B. Changes in the cell wall network during the thermal dehydration of alfalfa stems. *J. Agric. Food Chem*. ***2002,*** 50, 1897-1903

(27) Zeier, J.; Schreiber, L. Comparative investigation of primary and tertiary endodermal cell walls isolated from the roots of five monocotyledoneous species: chemical composition in relation to fine structure. *Planta* ***1998,*** 206, 349-361.

(28) Riederer, M.; Schonherr, J. Quantitative gas chromatographic analysis of methyl esters of hydroxy acids derived from plant cutin. *J. Chromat.* **1986,** 360, 151-161.

(29) Kolattukudy, P. Biopolyester membranes of plants: cutin and suberin. *Science* **1980,** 208, 990-999.

(30) Mac Masters, M. M.; Hinton, J. J. C.; Bradbury, D. Microscopic structure and composition of the wheat kernel. In *Wheat Chemistry and technology;* Pomeranz, Y., Eds.; Pullman, Washington State University, 1978; pp 51-113.

(31) Briarty, L. G.; Hugues, C. E.; Evers, A. D. The developing endosperm of wheat. A stereological analysis. *Ann. Bot.* **1979,** 44, 641-658.

(32) Harlan, H.V. Daily development of kernels of hannchen barley from flowering to maturity at Aberdeen, Idaho. *J. Agr. Res.* **1920,** 9, 393-430.

(33) Morrisson, I. N.; Kuo, J.; O'Brien, T.P. Histochemistry and fine structure of developing wheat aleurone cells. *Planta.* **1975,** 123, 105-116.

(34) Hengtrakul, P.; Lorenz, K.; Mathias, M. Alkylresorcinol homologs in cereals grains. J. *Food Compos. Anal.* **1991,** 4, 52-57.

(35) McCallum, J.A.; Walker, J.R.L. Phenolic biosynthesis during grain development in wheat *(Triticum aestivum* L.) III. Changes in hydroxycinnamic acids during grain development. *J. Cereal Sci.* **1991,** 13, 161-172.

(36) Régnier, T.; Macheix, J.J. Changes in wall-bound phenolic acids, phenylalanine and tyrosine ammonia-lyases, and peroxidases in developing durum wheat grains *(Triticum turgidum* L. var. durum). *J. Agric. Food Chem*. **1996,** 44, 1727-1730.

(37) McKeehen, J.D.; Busch, R.H.; Fulcher, R.G. Evaluation of wheat *(Triticum aestivum* L.) phenolic acids during grain development and their contribution to *Fusarium* resistance. *J. Agric. Food Chem*. **1999,** 47, 1476-1482.

(38) Régnier, T. Les composés phénoliques du blé dur (Triticum turgidum L. var. durum): variations au cours du développement et de la maturation du grain. Relations avec

l'apparition de la moucheture. Ph.D. Dissertation, Université Montpellier II, France, 1994.

(39) Ring, S.G.; Selvendran, R.R. Isolation and analysis of cell wall material from beeswing wheat bran *(Triticum aestivum). Phytochemistry* **1980,** 19, 1723-1730.

(40) Ralph, J.; Quideau, S.; Grabber, J.H.; Hatfield, R.D. Identification and synthesis of new ferulic dehydrodymers present in grass cell walls. *J. Chem. Soc.* **1994,** 1, 3485-3498.

(41) Garcia-Conesa, M.T.; Plumb, G.W.; Waldron, K.W.; Ralph, J.; Williamson, G. Ferulic acid dehydrodimers from wheat bran: isolation, purification and antioxidant properties of 8-O-4-diferulic acid. *Redox Report.* **1997,** 3, 319-323.

(42) Péyron, S.; Abecassis, J.; Autran, J.C.; Rouau X. Influence of UV exposure on the phenolic acid content, the mechanical properties of the bran and the milling behaviour of durum wheat (Triticum durum desf.). *Cereal Chem.* ***2002,*** 79, 726-731.

(43) Lapierre, C.; Monties, B.; Rolando, R. Thioacidolysis of poplar lignins: identification of monomeric syringyl products and caracterizationet of guaiacyl-syringyl rich fractions. *Holzforschung* **1986,** 40, 113-119.

(44) Antoine, C.; Peyron, S.; Mabille, F.; Lapierre, C.; Bouchet, B.; Abecassis, J.; Rouau, X. Individual contribution of grain outer layers and their cell wall structure to the mechanical properties of wheat bran. *J. Agric. Food Chem.* ***2003,*** 51, 2026-2033.

(45) Terashima, N.; Fukushima, K.; He, L.-F.; Takabe, K. Comprehensive model of the lignified plant cell wall. In *Forage cell wall structure and digestibility;* Jung, H. G., Buxton, D. R., Hatfield, R. D., Ralph, J., Eds.; ASA, CSSA, SSSA: Madison, WI, 1993; pp. 247-270.

(46) Fulcher, R.G.; O'Brien, T.P.; Lee, J.W. Studies on the aleurone layer, conventional and fluorescence microscopy of the cell wall with emphasis on phenol-carbohydrate complexes in wheat. *Aust. J. Biol. Sci.* **1972,** 25, 23-34.

(47) Tervil i-Wilo, A.; Parkkonen, T.; Morgan, A.; Hopeakoski-Nurminen, M.; Poutanen, K.; Heikkinen, P.; Autio, K. *In vitro* digestion of wheat microstructure with xylanase and cellulase from *Trichoderma reesei. J. Cereal Sci.* ***1996,*** 24, 215-225.

(48) Obel, N; Porchia, A.C.; Scheller, H.V. Dynamic changes in cell wall polysaccharides during wheat seedling development. *Phytochemistry* ***2002,*** 60, 603-610.

(49) Rhodes, D.I.; Stone, B.A. Proteins in walls of wheat aleurone cells. *J. Cereal Sci.* ***2002,*** 36, 83-101.

TABLES

Table 1: Protein, aliphatic components and alkylresorcinol contents of peripheral tissues of developing wheat grain

Maturation stage	A	B	C	D
Protein [a]	12.0	9.2	10.0	11.3
Aliphatic components				
MePalmitate, C 16	nq	0.26	0.31	0.23
MeStearate,C 18	nq	0.28	0.22	0.21
McOleate, C18:1	0.19	2.90	1.75	1.43
MeLinoleate, C18:2	0.33	6.56	5.94	5.31
C 16 (OH)	0.51	0.48	0.33	0.39
C18:1 (OH)	0.69	0.97	0.92	0.68
C16 di OH	nq	nq	0.12	0.12
C18 tri OH	nq	nq	0.10	0.10
C18 di OH 9-époxy	0.42	0.85	0.81	0.66
Alkylresorcinols [b]				
C17	59	216	64	62
C19	nq	807	328	343
C21	21	966	348	467
C23	236	348	56	107
C25	nq	72	nq	42

Abbreviation: nq, not quantifiable. [a] Expressed as weigh percentage of dry matter. [b] Expressed as mol of equivalent olivetol/ g extractive-free peripheral tissues of wheat grain. Standard deviation averaged 5% for protein, aliphatic components and alkylresorcinols.

Table 2 : Carbohydrate composition of peripheral tissues of developing wheat grain.

Maturation stage	Neutral Carbohydrate				TNCC	AIX	AX [a]	Glc Ac	Gal Ac
	Ara	Gal	Glc	Xyl					
A	6.01	1.59	41.7	7.32	56.7	0.82	23.6	0.23	0.45
B	13.8	1.17	18.6	23.3	56.8	0.58	65.1	1.04	0.80
C	14.2	**1.11**	19.5	23.7	58.5	0.59	64.8	1.08	0.79
D	13.2	1.19	18.0	21.5	53.9	0.61	64.4	1.01	0.69

Contents are expressed in weight percentage of dry-matter, except for AX. Abbreviations: Ara, arabinose; Gal, galactose; Gal Ac, galacturonic acid; Glc, glucose; Glc Ac, glucuronic acid; Xyl, xylose; AX, % Ara + % Xyl; AIX, arabinose to xylose ratio; TNCC, total neutral carbohydrate contents. [a] Expressed as a percentage of the total neutral carbohydrate contents (Ara+Gal+Glc+Xyl). Standard deviation averaged 5%.

Table 3: Cell-wall phenolic components of peripheral tissues of developing wheat grain.

Maturation stage			B	C	D
Hydroxycinnamic acids					
Ester	Ferulic acid	4750	12590	9607	4519
	p-Coumaric acid	nq	205	249	180
Ether	Ferulic acid	128	113	401	333
	p-Coumaric acid	135	106	244	201
	Sinapic acid	106	80	132	93
Ester-DHD	5,5'	nq	58	62	71
	8-0-4'	nq	165	168	174
	8,5'	nq	57	60	53
Lignin [b]					
	Total S+G		nd	4.8	4.3
	S/G molar ratio	nd	nd	0.8	0.8

Abbreviations: DHD, dehydrodimer; nd, not detectable; nq: not quantifiable. [a] Expressed as µg/g extractive-free peripheral tissues of wheat grain. [b] Expressed as µmol/g extractive-free peripheral tissues of wheat grain. ° Total yields of labile-ether linked guaiacyl (G) and syringyl (S) derivatives released from extractive-free peripheral tissues of wheat grain. Standard deviation averaged 15% for lignin monomer and 10% for hydroxycinnamate.

Table 4: Yields of the neutral carbohydrate components released from peripheral tissues of developing wheat grain following water and xylanase treatments.

Maturation stage	Water incubation		Xylanase incubation		
	Oh'	24h [b]	1 h [c]	2h°	24h [b]
	35.2±3.60	35.7±5.31	nm	nm	40.8±2.69
B	1.71 ± 0.31	2.25 ± 0.10	19.8	22.2	22.9 ± 0.40
C	1.84 ± 0.29	1.96 ± 0.16	17.1	17.3	22.2±0.96
D	2.11 ± 0.17	2.16 ± 0.08	16.2	18.7	20.5 ± 1.72

Contents were expressed as a weight percentage of the initial peripheral tissues of wheat grain dry matter. Abbreviation: nm = not measured. Data are mean values ± SD. [a] n =-4; [b] n = 2; ° only one experiment.

Table 5: AX content and A/X ratio of the soluble products released from peripheral tissues of developing wheat grain following water and xylanase treatments.

Maturation Stage		Water incubation		Xylanase incubation		
		Oh'	24h [b]	1 h [e]	2h [c]	24h [b]
A	AX (%)	3.93 ± 1.78	5.03±1.01	nm	nm	12.0 ± 1.13
	A/X	0.46 ± 0.03	0.42 ± 0.07			0.44 ± 0.06
B	AX (%)	29.2 ± 6.12	30.0 ± 4.77	83.7	81.8	77.9 ± 2.69
	A/X	0.71 ± 0.08	0.67 ± 0.06	0.24	0.24	0.23 ± 0.01
C	AX (%)	49.5 ± 2.26	52.6 ± 2.90	88.8	88.4	85.6 ± 1.60
	AIX	0.54 ± 0.03	0.52 ± 0.02	0.28	0.27	0.27 ± 0.03
D	AX (%)	12.1 ± 1.07	12.3 ± 0.31	81.5	81.4	77.9±4.26
	A/X	0.57 ± 0.03	0.59 ±0.03	0.30	0.28	0.27 ± 0.03

Results were expressed as a percentage of the total soluble-neutral carbohydrate. Abbreviations: AX, % Ara + % Xyl; AIX, arabinose to xylose ratio; nm = not measured. Data are mean values ± SD. [a] n = 4; [b] n = 2; ° only one experiment.

Table 6: Recovery yield of phenolic components in the xylanase-residues of peripheral tissues of developing wheat grain.

Maturation stage		A	B	C	D
Hydroxycinnamates					
Ester	Ferulic acid	37	65	49	39
	p-Coumaric acid	nd	14	24	25
Ether	Ferulic acid	11	84	75	91
	p-Coumaric acid	19	57	45	49
	Sinapic acid	12	53	55	64
Ester-DHD	5,5'	nq	83	101	93
	8-0-4'	nq	116	111	120
	8,5'		94	108	83
Lignin [a]					
	Total S+G	nd	nd	95	114
	S/G molar ratio	nd	nd	0.8	0.9

Abbreviations: DHD, dehydrodimer; G, guaiacyl; S, syringyl; nq, not quantifiable; nm, not measured. [a] Recovery yield expressed in percentage of initial contents in untreated peripheral tissues of wheat grain.

FIGURES

Figure 1:

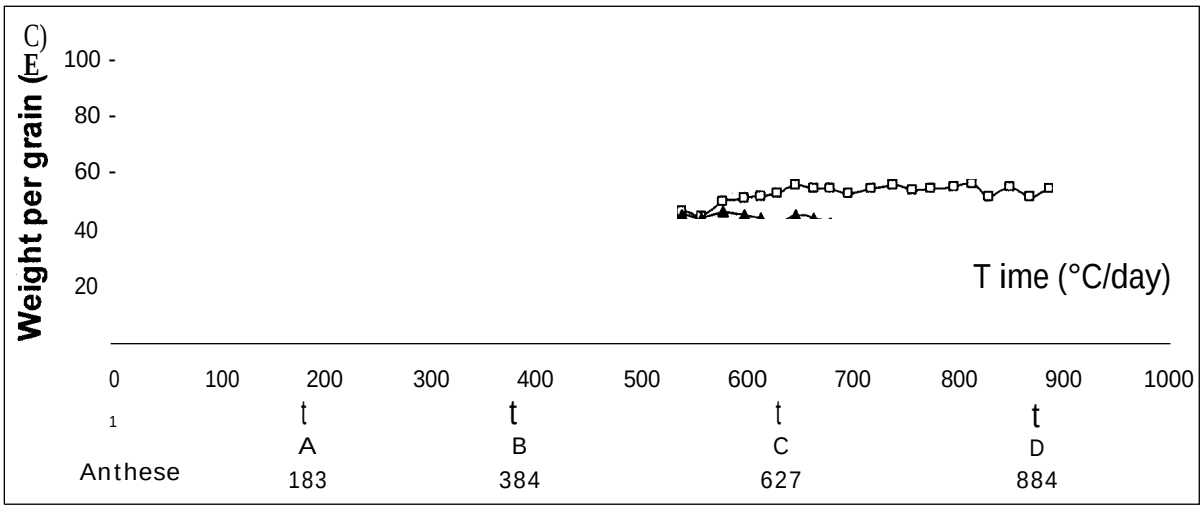

Chronological events of the Cadenza grain development: Change in the fresh weight (trapeze), dry weight (square) and water contents (triangle) of individual grain as a function of cumulative growing degrees since anthesis. Relevant harvesting-stages were labeled as A, B, C and D.

Figure2

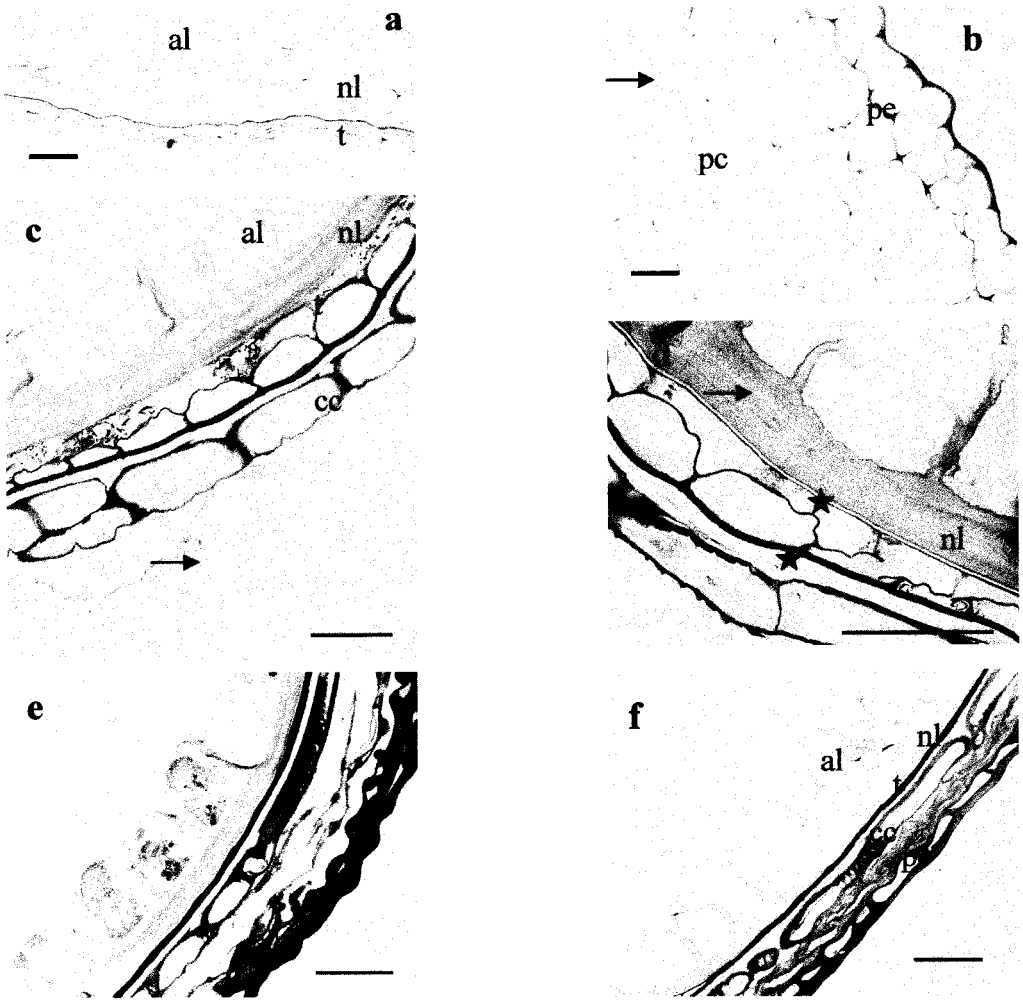

Micrographs of the peripheral tissues of wheat grain sections isolated at different development stages stained by toluidine blue. This topochemical reagent enlightens the histological features of peripheral tissues of wheat grain from stage A where the aleurone and nucellar layers can be observed as well as cells which prefigure the future testa **(a)** and pericarp is not yet crushed (b). The arrow in b spots the presumably starch granules accumulation in the pericarp parenchymatous cells. Toluidine blue staining of stage B (c and **d** at respectively t 0 and t 24 h water treatment) shows the complete (the tube cells are not visible) but immature structure of peripheral tissues of wheat grain. In c the arrow point some vestige of persisting thin cell wall. Additionally, these two pictures can be considered as a control, since no structural change was observable during the 24 h water incubation. On **d** the arrow points the space inside the nucellar walls, and the stars indicate the cuticles of both testa and nucellar layer. In e (stage C at t 0 h) and f (stage D at t 0 h) the mature aspect of peripheral wheat layers was distinguishable. al = aleurone layer; n1= nucellar layer; t = testa; cc = cross cells; pc = parenchymatous cells; pe = external pericarp. Scale bars = 40 µm.

Figure3

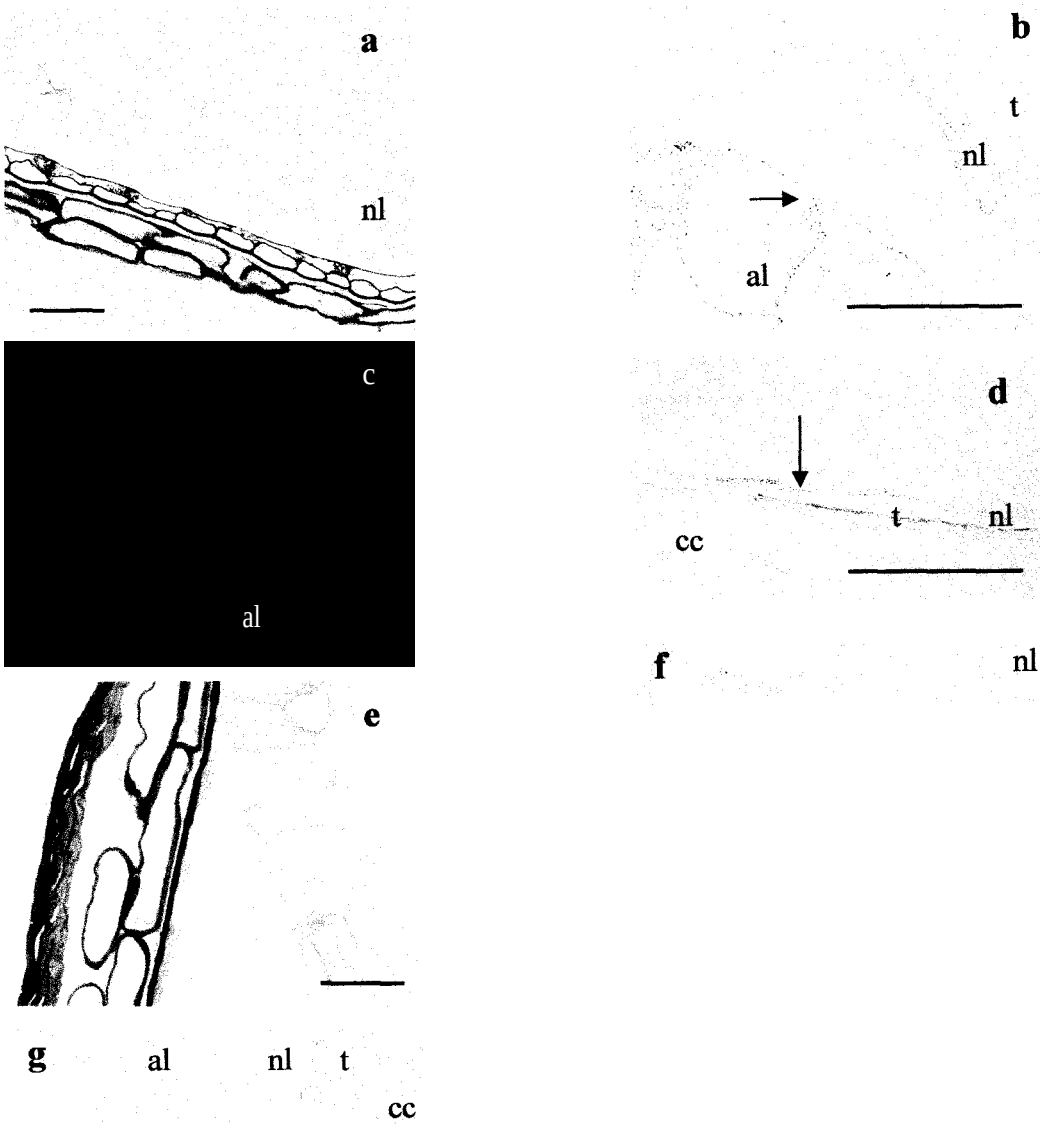

Micrographs of sections of 75 min xylanase-depleted peripheral tissues of wheat grain isolated at different development stages and xylanase immunolabeling controls. Pictures **a** and **b** are respectively toluidine blue staining and xylanase-immunolabeling of peripheral tissues of wheat grain at stage B. The arrow in **b** indicates the heavily xylanase immunolabeling as visualized by gold particles. In **d** the xylanase immunolabeling of peripheral layers of wheat grain at stage C (black arrow) show a wave of gold particles in the nl. In addition for the stage C, the picture c displays phenolic UV-autofluorescence in restricted cell-wall domains under UV light (white arrow). Picture e and f are stage D respectively stained by toluidine blue and labeled by xylanase antibodies. Xylanase-immunolabeling controls show the absence of gold particles when **(g)** peripheral tissues of wheat grain (stage B) is not incubated with xylanase, and **(h)** following omission of the primary antibody (stage D). al = aleurone layer; nl = nucellar layer; t = testa; cc = cross cells. Scale bars = 40 µm.

Figure 4

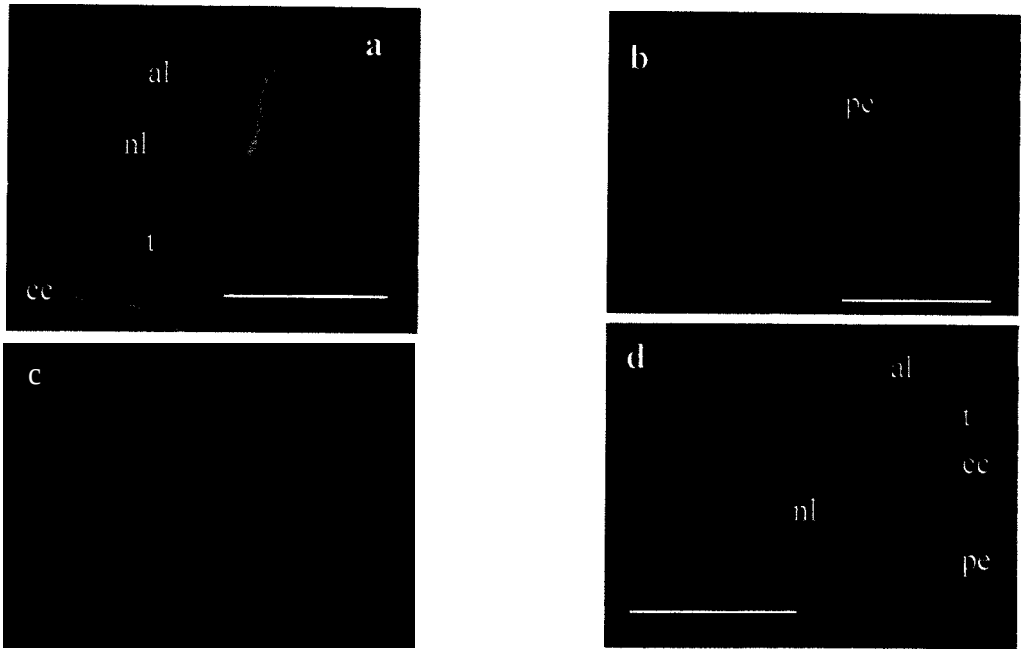

Micrographs of peripheral tissues of wheat grain sections isolated at different development stages under UV lamp. Examination of the wall phenol-linked autofluorescence with UV light exposure of peripheral layers of wheat grain obtained at stage B (a and **b),** C (c) and D (d). All the pictures present a blue fluorescence of tissues alter 24 h water treatment, especially in the aleurone cell walls. al = aleurone layer; n1= nucellar layer; t = testa; cc = cross cells; pe = external pericarp. Scale bars = 40 µm.

Carbohyd. Res. In press

Impact and efficiency of GH10 and GH11 thermostable endoxylanases on wheat bran and alkali-extractable arabinoxylans

Johnny Beaugrand [a], Gérard Chambat [b], Vicky W.K. Wong [c], Florence Goubet [c], Caroline Rémond [a], Gabriel Paës [a], Samina Benamrouche [a], Philippe Debeire [a], Michael O'Donohue [a], Brigitte Chabbert'

[a] Institut National de la Recherche Agronomique, UMR FARE-614, Centre de Recherche Agronomique, 2 esplanade Roland Garros, BP 224, 51686 Reims Cedex 02, France. [b] CERMAV-CNRS, Laboratoire associé à l'Université Joseph Fourier, BP 53, F-38041, Grenoble, France. ° Department of Biochemistry, Building O, Downing Site, University of Cambridge, Cambridge CB2 1 QW, UK

Abstract

The results of a comparative study of two thermostable (1—*4)-(3-xylan endoxylanases using a multi-technical approach indicate that a GH11 xylanase is more useful than a GH10 xylanase for the upgrading of wheat bran into soluble oligosaccharides. Both enzymes liberated complex mixtures of xylooligosaccharides. ^{13}C NMR analysis provided evidence that xylanases cause the co-solubilisation of (3-glucan, which is a result of cell-wall disassembly. The simultaneous use of bath xylanases did not result in a synergistic action on wheat bran arabinoxylans, but instead led to the production of a product mixture whose profile resembled that produced by the action of the GH10 xylanase alone. Upon treatment with either xylanase, the diferulic acid levels in residual bran were unaltered, whereas content in ferulic and p-coumaric acids were unequally decreased. With regard to the major differences between the enzymes, the products resulting from the action of the GH10 xylanase were smaller in size than those produced by the GH11 xylanase, indicating a higher proportion of cleavage sites for the GH10 xylanase. The comparison of the kinetic parameters of each xylanase using various alkali-extractable arabinoxylans indicated that the GH10 xylanase was most active on soluble arabinoxylans. In contrast, probably because GH11 xylanase can better penetrate the cell wall network, this enzyme was more efficient than the GH10 xylanase in the hydrolysis of wheat bran. Indeed the former enzyme displayed a nearly 2 fold higher affinity and a 6.8 fold higher turnover rate in the presence of this important by-product of the milling industry.

Keywords: Xylanases, wheat bran, cell wall, arabinoxylans, hydroxycinnamic acids

1. Introduction

Wheat bran is an abundant, xylan-rich by-product of the milling industry that is mainly used as feed for livestock. Bran is also a potential feedstock for the production of non-food products (bioenergy, bulk chemicals, etc.). To this end, previously developed transformation processes based on chemical hydrolysis using dilute or strong acid solutions are applicable to wheat bran. However, taking into account the high arabinoxylan (AX) content of wheat bran (40% dry weight of destarched wheat bran), enzymatic strategies for bran upgrading may constitute viable alternatives to such chemical methods.

The major prerequisite for the development of an enzymatic upgrading strategy is the identification of suitable enzymes. Enzyme suitability can be defined using multiple criteria that include appropriate specificity, high catalytic efficiency and good intrinsic stability. For the enzymatic hydrolysis of AX-rich substrates such as bran, the major enzyme requirement is that of a depolymerising xylanase capable of hydrolysing the (3-(1—*4)-linkages between xylopyranoside residues in xylans. [1]

Based on structural and sequence-classification [2,3] of glycoside hydrolases, two major xylanase (EC 3.2.1.8) families (GH10 and GH11) that differ both in structure and in catalytic properties have been distinguished. [4] The members of both families have been extensively studied and certain enzymes, most frequently from GH11, have been incorporated into industrial processes. [5,6,7] The GH10 family members all possess a catalytic domain which exhibits $(13/a)_8$ architecture and displays an average molecular mass of approximately 40 kDa. The GH11 members are generally smaller (approximately 20 kDa) and display a $_{P}$ jelly roll structure. The enzymes from both families hydrolyse (3-(1—4)-linkages between adjacent xylopyranoside residues which are accommodated within subsites (—1) and (+1). Additionally, the enzymes from both families display endo-action and thus exhibit extended active site clefts that are generally composed of three, five [8] or more subsites. [9] Endoxylanases may also harbour carbohydrate binding domains that would presumably facilitate enzyme fixation on insoluble substrate. [10] Although GH11 xylanases are most frequently chosen for industrial processes, an increasingly large amount of data reveal that GH10 enzymes display certain enzymological characteristics which could theoretically make them better candidates for enzymatic upgrading of lignocellulosic biomass. First, GH10 xylanases are more permissive in ternis of substrate specificity. Xylanases from GH11 do not tolerate the presence of arabinose decorations on either the O-2/0-3 positions of the xylose residues present in the (—1) and (+1) subsites or on the 0-2/0-3 of the xylose residue present in the (—2) subsite. [4,11] In contrast, enzymes from GH10 appear to tolerate arabinose-decorated xylose residues in either the (—3), (—2),

or (+1) subsites.[4,12] Likewise, Fujimoto et al.[13] suggested that some GH10 members might also accommodate arabinose-decorated xylose residues in the (+2) subsite. Secondly, unlike GH11 xylanases, GH10 xylanases have also been shown to be unaffected by the presence of TAXI-like proteinaceous inhibitors which occur in cereals.[14] However, importantly GH11 are most active against insoluble polymeric xylans, whereas GH10 xylanases are preferentially active against soluble substrates and can readily hydrolyse small xylooligosaccharides such as xylotriose.[4,i',I']

Previously, we have identified and characterized two thermostable xylanases (one from GH11 and one from GH10) from the thermophilic bacterium *Thermobacillus xylanilyticus*[17,18] (designated as XYL11 and XYL 10 respectively) that exhibit similar physicochemical characteristics. So far, studies mainly using the GH11 enzyme have shown that wheat bran is partially degraded, with the aleurone and nucellar layer being the main targets.[19] Furthermore, analysis of the residual fraction has revealed that the arabinoxylans therein are highly substituted with arabinose, indicating that, like other GH11 enzymes, XYL11 is unable to attack such substrates. Accordingly, in addition to cellulose and lignin, pericarp is known to contain AX which are highly substituted with glucuronic acid and phenolic acids, in addition to cellulose and lignin.[20] Moreover, hydroxycinnamic acids (HCA), notably ferulic acid (FA) and its diferulic form (DiFA) are known to play a significant role in covalently interconnecting cell wall polymers.[21] Non covalent interactions between xylans and polymers like 13-glucans or cellulose also contribute to the cohesiveness of the wall network.[22] The intimately interconnected cell-wall network would then possibly impair AX susceptibility to endoxylanase by limiting enzyme contact and mobility.[23,24]

Therefore, in this current study we have sought to address two major questions. The first concerns the role of arabinose substitution of arabinoxylans in limiting xylanase activity. The second concerns the limiting effects of cell-wall network encountered in wheat bran on the ability of xylanases to access and hydrolyse their appropriate substrates. Studies on both destarched wheat bran (DWB) and on various AX fractions isolated from DWB or XYL11 residual bran (RBW) were thus undertaken. Finally, these questions have been correlated to the type of xylanase used, in order to elucidate the relative usefulness of GH10 and GH11 xylanases for industrial processes.

2. Results

2.1. Impact of XYL10 and XYL11 on wheat bran carbohydrates

Alter a 24 h treatment, the action of XYL 11 upon DWB resulted in the release of 49 % of AX, whereas XYL 10 action released only half that amount (Table 1). Moreover, XYL 11 action was rapid since the yield of (Ara+Xyl) was near maximal after a 1 h incubation period, whereas XYL 10

action was more progressive. Additionally, in the water control experiments, a very few amount of AX was released (3.0 and 3.9 % of the initial content in DWB sample after 1 h and 24 h respectively), and accounted for nearly 60 and 80% of the soluble neutral carbohydrate at 1 h and 24 h incubation time; moreover, values of the Ara/Xyl ratio did not vary during incubation and were closed to 0.44. The Ara/Xyl ratio of carbohydrates solubilised by XYL 11 remained constant from 1 h to 24 h time period while that of carbohydrates released by XYL 10 decreased alter 1 h incubation. At the end of the 24 h period, carbohydrates solubilised by XYL 11 or XYL 10 exhibited an Ara/Xyl ratio of 1:4 and 1:2.5 respectively. When XYL10 and XYL11 were combined, the rate and extent of hydrolysis was similar to that observed when XYL11 was used alone. However, analysis of the fraction from 24 h hydrolyses involving XYL 11 or XYL 11 + XYL10 revealed that RWB showed a higher Ara/Xyl ratio (1.00) compared to that obtained from the XYL 10-derived RWB (0.71) or water-treated control bran (0.58).

AX represented the major part of the soluble fraction released by both xylanases from DWB, although an increasing co-solubilisation of other carbohydrates was noticeable after prolonged enzyme incubation (Table 1). These carbohydrates were mainly composed of glucose and, to a lesser extent, of galactose. To further investigate their nature, the XYL 11-solubilised (24 h treatment) wheat bran fraction was concentrated. During the volume reduction, some precipitation occurred; the precipitate was isolated by centrifugation and examined by ^{13}C NMR spectroscopy (Figure 1). Specific high intensity resonances at 103.7 ppm, C-1 (3-(1—>3); 87.2 ppm, C-3 (3-(1->3); 102.8 ppm, Cl R-(1--4) and 80.2 ppm, C4 (3-(1-*4) indicated the presence of (1-+3) (1—>4)-(3-glucan[22,25] After 24 h treatment by XYL11 and XYL10, non-AX carbohydrates accounted for approximately 10% and 15% (dry weight) respectively of the soluble fractions. Since XYL10 was an impure enzyme preparation, a control reaction using XYL 10-free *E. coli* lysate was performed in order to ascertain whether XYL10 action was directly responsible for the greater removal of glucose-containing carbohydrates. The results of this control revealed that a small amount of glucose monomer was obtained, but this could not account for the 5% difference described above.

Oligosaccharides released from DWB after treatment with XYL10 and/or XYL11 were studied by polysaccharide analysis using carbohydrate gel electrophoresis (PACE).[26] Two fluorophores, ANTS (8-aminonaphthalene-1,3,6-trisulfonic acid) and AMAC (2-aminoacridone) are used to study the oligosaccharides. ANTS (a charged compound) is used to study both uncharged and charged oligosaccharides (Figure 2A), whereas AMAC (an uncharged compound) is used to study charged oligosaccharides only (Figure 2B). Controls were performed using the same conditions as for the assays but with the absence of either xylanase(s) or polysaccharide in order to detect compounds present in the absence of enzyme (see arrows in Figure 2A). XYL10 and/or

XYL 11 action on DWB produced complex fingerprints with mainly small DP xylooligosaccharides being released (Figure 2A and 2B). XYL 10 produced mainly xylose monomer (Xyl) and xylobiose (Xyl_2), whereas XYL11 was also able to produce xylotriose (Xyl_3). Additionally, bands corresponding to higher DP components (> Xyl_6) were also observed; a higher intensity being displayed in the case of XYL11-soluble products. Other observed oligosaccharides migrated either between or above the xylooligosaccharide standards. When compared to the oligosaccharides generated by the same enzymes using commercial xylans (data not shown) and to results reported elsewhere,[27,28] some of the products released from DWB were oligo-glucuronoxylans or oligo-arabinoxylans indicated by either stars or circles (Figure 2A and 2B). The remaining unassigned bands might represent xylooligosaccharides containing varying degrees of substitution. Indeed, some charged species were observed using the AMAC fluorophore (Figure 2B), which constitute oligoxylans substituted with uronic acids and/or arabinose conjugated with phenolic acids.

Prolonged incubation (24 h versus 1 h) resulted in the decrease in bands intensity of very large DP along with the appearance of new bands with smaller DP species and increase in the bands intensity of small DP (Figure 2A). Using the ANTS conditions, the simultaneous hydrolysis of DWB by both enzymes produced a fingerprint which was highly similar to that produced by XYL 10 alone than XYL11. A few marked differences were observed such as the absence/presence of bands in the 1 h/24 h incubation times (respectively) when compared to the same times with XYL 10 alone (triangles in Figure 2A). Analysis of the same samples using the AMAC conditions clearly indicated that the simultaneous action of both enzymes on DWB resulted in a much simpler and different fingerprint of charged oligosaccharides when compared to those obtained with either enzyme alone (Figure 2B). As previously found with ANTS, differences in band occurrence were also observed (with AMAC). Likewise, the band indicated by a triangle in Figure 2B, which was only detected after 24 h incubation when XYL10 was used, was present after only 1 h incubation when both enzymes were employed.

2.2. Impact of XYL10 and XYL11 on wheat bran hydroxycinnamic acids

Ferulic acid (FA), p-coumaric acid (pCA) and diferulic acids (DiFA) were quantified both in the DWB and RWB samples (Table 2). Recovery yields of phenolic acids from RWB were calculated with respect to the extent of (Ara+Xyl) removal and were expressed as a percentage of the initial hydroxycinnamic acids (HCA) content in water treated-DWB (100%). In DWB, pCA was detected as a minor component when compared to FA; sinapic acid was only detected at trace levels. With regard to DiFA, three different forms were detected. The 8-0-4' form was the most abundant, followed by the 5-5' one and then the 8-5' form. In the both XYL 10- and XYL11-

generated RWB, both FA and pCA were decreased (Table 2). Indeed, nearly 40 and 30% of the initial pCA content and 50% and 36% of initial FA content were removed by XYL 11 and XYL 10. However, DiFA content in RWB samples remained unaltered compared to DWB, irrespective of the enzyme used (the maximal 9% variations in the amount of residual DiFA are very close to experimental error).

2.3. Extraction and partial characterization of AX fractions

The yield and composition of AX fractions arising from DWB and from XYL 11-RWB are shown in Table 3. Apart from WS-AX,50 for which (Ara+Xyl) content and recovery yields were feeble, all other fractions contained a high proportion of AX and were obtained in sufficient yields for further enzymatic assays. The DWB-derived fractions, each of which represented an approximately equal proportion of DWB, showed variability in Ara/Xyl ratio. WS-AX,-80 was highly substituted, WS-AX,-50 less so and WI-AX; was poorly substituted with approximately one arabinose for six xylose residues. In contrast, XYL11-RWB was essentially composed of one major fraction (WS-AX,80) that was highly substituted and a minor fraction (WI-AXr) that displayed Ara/Xyl ratio of 0.85. The various AX fractions contained differing amounts of protein, glucose, galactose and uronic acids, which together accounted for 15% to 43% of the total weight of the fraction. In spite of their small amount, uronic acids with glucuronic acid being dominant were found in higher proportions in the most arabinosyl- substituted fractions. Structural information of AXs in each fraction was provided by methylation analysis; arabinose and xylose were the only sugar considered herein. The major differences between samples concerned the relative molar percentage of: (i) arabinose di-substituted xylose (referred as "Xyl" in Table 4); (ii) terminal xylose (2,3,4-Me_3-Xyl) and; (iii) non substituted xylose (2,3-Me_2-Xyl). Based on chemical features and glycosyl linkage patterns, the AX fractions were distinguishable, with the exception of WS-AX,-80 and WS-AX,80 that both displayed high Ara/Xyl ratios and similar structural profiles.

2.4. Kinetic parameters of XYL10 and XYL11 on soluble AX fractions and DWB

The kinetic parameters Kn, $^{(app)}$, V. and $_{kcai}$ for hydrolyses of soluble AX fractions or DWB by XYL 10 and XYL11 are shown in Table 5. Several of the reactions described were complicated by the relative insolubility of the substrates. This was particularly true for birchwood glucuronoxylan and WI-AX_i. With these substrates the highest attainable concentration was never higher than 2 x Km. Therefore, the data presented here must be interpreted with prudence. Similarly, the poor affinity (high $Km^{(app)}$) of XYL11 for WS-AX_i-80 and WS-AX,80 precluded the determination of

kinetic parameters. Overall, when kinetic parameters could be determined, XYL 10 appeared to be a better enzyme for AX hydrolysis, although the $^{Km(aPP)}$ values for both enzymes increased and k_{cat} values decreased with increasing Ara/Xyl ratio of the AXs (Figure 3). In most cases XYL 10 displayed lower $^{Km(aPP)}$ values and higher k_{cat}/K_m values than XYL11. The major exception to this trend was XYL11 activity on DWB. In this case, when compared to XYL10, the XYL11 displayed an approximately 2-fold lower K_m value and a nearly 7-fold higher k_{cat} value. Therefore, on DWB XYL 11 was approximately 11 times more efficient than XYL 10 $(k_{cat}/K_m^{(aPP)}$ = 127 for XYL 11 and 11.5 for XYL 10). Likewise, when compared to XYL 10, XYL 11 displayed an approximately 2-fold higher k_{cat}/K_m on WI-AX, although the $^{Km(aPP)}$ value was also much higher. Finally, it is important to note that the use of an appropriate quantity of XYL10-free *E.coli* lysate as a control did not give rise to any detectable production of reducing sugars so the measures were specific of the xylanase actions.

3. Discussion

The aim of this study was to compare the activities of two similarly thermostable xylanases, belonging to two distinct enzyme families (GH 10 and GH11), on different substrates. The use of two enzymes, whose native forms are produced by the same thermophilic bacterium, was attractive since these enzymes share several common characteristics. Both enzymes are thermostable and exhibit very similar temperature (for thermoactivity) and pH optima, thus allowing reactions to be performed in identical conditions.

3.1. Influence of the substrate structure and solubility on xylanase activity

To study the impact of the arabinose substitution on the efficiency of thermostable xylanases, AX fractions having distinct Ara/Xyl ratio were used as substrates. To this end, AX fractions were isolated from both DWB and XYL 11-RWB using an alkaline extraction procedure; consequently, these fractions were almost free of esterified hydroxycinnamic acids and acetate moieties in contrast to DWB. Furthermore, the simple 3-step fractionation procedure efficiently gave rise to several distinct AX fractions whose cumulative extraction yields (approximately 35% of Ara+Xyl content in DWB or RWB) were comparable to those obtained from wheat bran using other procedures.[29,30]

Using the alkali-extractable AX fractions as substrates for the two xylanases revealed for both enzymes an inverse relationship between catalytic efficiency and arabinose substitution. In the case of XYL11 this relationship was very clear, whereas the behaviour of XYL10 did not

completely comply with this trend. The catalytic efficiency of XYL10 towards birchwood xylan, the least substituted was lower than that towards WI-AX;. However, in the recent study by Courtin and Delcour,[15] it was suggested that GH10 xylanases should be most active against AXs exhibiting an intermediate level of substitution, a suggestion that is coherent with the high activity of XYL10 towards $WI\text{-}AX_i$. Moreover, the chain length may have an impact on catalytic activity of xylanases.[31] The superiority of XYL10 upon isolated arabinoxylan fractions and birchwood xylans is certainly due to the preference exhibited by XYL10 for soluble substrates[18] which is coherent with the observations made by others using other GH10 xylanases and other substrates.[15,32] Similarly, the use of comparable amounts (IU) of XYL10 and XYL11 for the hydrolysis of DWB also revealed significant differences in catalytic efficiency. Only a 12-fold difference in efficiency $(k_{cat}/Km^{(aPP)})$ of XYL 11 on DWB and birchwood xylan was measured, whereas XYL 10 was 260-fold more efficient on birchwood xylan than DWB. In the presence of DWB, an intrinsically insoluble substrate, XYL11 solubilised approximately twice as much AX than XYL10. Furthermore, combining the two enzymes did not enhance AX solubilisation, indicating the absence of synergistic action on DWB. Once again, these findings highlight the superior efficiency of GH1 1 xylanases toward insoluble substrates and confirm their suitability for industrial applications that require the treatment of insoluble substrates.

Other factors may also determine enzyme efficiency towards complex substrates such as wheat bran. A heterogeneous distribution of arabinose substituents on xylans is one likely candidate. Such a phenomenon is partially illustrated by the fraction WI-AXr that was composed of almost as much arabinose as xylose. Upon this fraction, XYL11 activity was measurable. Taking into account the fact that GH11 enzymes cannot hydrolyse bonds adjacent to substituted xylose residues, this observation suggests that some regions of the substrate were devoid of substitution. Concordantly, structural analysis of WI-AXr revealed a high proportion of disubstituted xylose residues that must be clustered in such a way that several successive xylose residues are unsubstituted. Finally, although substrate solubility and structural features are important factors for enzyme activity, it is noteworthy to recall that WI-AXr is an alkaline-extracted fraction of RWB, which itself is the residue of XYL11 hydrolysis of intact bran. Therefore, within RWB, WI-AXr was not accessible to XYL11, indicating that the cell wall network is also a major determinant of enzyme activity.

3.2. Impact of the cell wall network on xylanase efficiency

Within the different tissues that constitute wheat bran, cell walls are composed of a complex interconnected network in which AXs, cellulose and lignin are closely associated. Among the key

elements that contribute to this network are the hydroxycinnamic acids. Compared to other graminaceous tissues, bran is particularly rich in cell wall-bound phenolics. The FA monomer represents the predominant phenolic species, the minority species being pCA and to a much lower level, sinapic acid. FA is one of the main actors involved in lignin and polysaccharide cross-linkage in graminaceous cell walls,[20] notably through the formation of dimers (DiFA). In wheat bran, these are mainly present as 5,5', 8-0-4' and 8,5' derivatives.[33] In maize, DiFA is known to be a major limiting factor for enzymatic hydrolysis.[34] In wheat bran, this has not been demonstrated, although such a role for DiFA has been recently suggested.[35] Analysis of the residual bran fractions has shown that both XYL 10 and XYL 11 are able to release HCA from bran cell-wall polysaccharides in the form of cinnamoyl-oligosaccharides.[36] XYL11 degraded DWB-AX and removed HCA to a greater extent than XYL10. Accordingly, higher proportions of FA and pCA were removed from DWB. However, taking into account the fact that XYL11 displayed a 2 fold higher activity on bran AX, the removal of HCA by this enzyme was not 2 fold greater than that of XYL10. Therefore, if one assumes that xylanases had provided a similar yield of AX degradation, one can calculate that XYL 10 would have presumably liberated approximately 40% more FA and pCA compounds than XYL11. In contrast, DiFA were not altered by treatment with either xylanase, suggesting that both XYL10 and XYL11 attacked similar cell walls. This is in agreement with the findings of Maes et al.[16] who speculated that GH10 and GH11 enzymes might use the same AX subpopulations in wheat bran. Moreover, in this context it is relevant to recall that in a previous study GH11 xylanases were found to be the preferred synergistic partners for feruloyl esterase action.[37] Concordantly, on the basis of our present data, we propose that GH11 xylanases are better partners because they hydrolyse more AXs, but GH10 xylanases degrade more substituted regions of AXs and produce a higher relative yield of FA substituted products. Finally, we can conclude that, while the poorer performance of XYL 10 on wheat bran cannot be correlated with the presence of phenolic compounds, DiFA would constitute a limiting factor for both types of xylanase.

To hydrolyse bran AXs, enzymes must be able to penetrate the cell wall network and thus gain access to their substrates. However, XYL 10 and XYL 11 should have distinct action patterns on DWB since the enzyme-solubilised AX fractions obtained in our study clearly exhibited different Ara/Xyl ratios. This supposition is supported by the results of the electrophoretic analysis of the xylooligosaccharides solubilised by XYL10 and XYL11 that showed distinct profiles for each type of hydrolysis. In this respect, PACE proved to be very suitable in providing size analysis of the heterogeneous populations, hence allowing tentative identification of certain species.[26] Consistent with the high efficiency of GH10 on soluble substrates, XYL10 produced smaller oligosaccharides than XYL 11, which is in agreement with the conclusions drawn from previous studies in which size

determination of xylanase-soluble was performed by high performance size exclusion chromatography.[15, 16,38] Indeed, after initially generating intermediate-size oligosaccharides, XYL10 action led to their progressive hydrolysis over a 24 h period.

In the case of XYL11, previously obtained data has revealed that this enzyme initially penetrates wheat bran from the subaleurone and then gradually progresses via aleurone cell-walls towards the nucellar layer, causing disintegration of the cell walls along its path.[24] In this work, we have shown that AX depletion by xylanases is accompanied by 13-glucan release, consistent with the degradation of the aleurone cell walls which are known to contain such polymers.[20] This finding also supports previous data which indicated the existence of intermolecular interactions between glucans and arabinoxylans.[22] Finally, the detection by PACE of oligosaccharides probably containing aldouronic acid[38] and/or hydroxycinnamic acid,[36] is also indicative of XYL 11-induced disassembly of the wall network. With regard to XYL10 action, taking into account the similarity of Ara/Xyl ratios displayed by the products released by either XYL10 or by the combined action of XYL11 + XYL10, like Maes et al.[16] we conclude that the GH10 enzyme does not act upon tissues other than those degraded by XYL11. Indeed, because (i) the extent of AX degradation by XYL 11 was not enhanced by the presence of XYL10 and (ii) the PACE profile of oligosaccharides generated by XYL10 was not dramatically changed upon the combined action of XYL 11 and XYL10, it is probable that when used with XYL11, the XYL10 acts preferentially upon the soluble products of XYL11. This finding, which is in agreement with previous data,[15] underlines the fact that XYL10 does not attack the more branched XYL11-resistant AX population present in the pericarp, even though the data for the XYL10-catalysed hydrolysis of a similarly-substituted, extracted AX population would suggest the contrary. Accordingly, preliminary microscopic observations of XYL10-treated bran appear to confirm this conclusion and show enzyme-induced disintegration of part of the aleurone (data not shown). Furthermore, during XYL 10 hydrolysis of DWB, the average Ara/Xyl ratio of soluble products was subject to a time-dependent decline that suggests that the initial target of hydrolysis was more substituted than the subsequent ones. Overall, it is clear that DWB cannot be equated to water-unextractable AXs. Instead, it must be considered as a heterogeneous, xylan-rich substrate.

Finally, with regard to the slower penetration of bran tissues by XYL 10 compared to XYL 11, which is evidenced by the slower kinetics of the former enzyme in the presence of bran, size might be an important factor. The pore radius in wheat cell walls ranges from 1.5 to 4 nm, with smaller pores being reported for the pericarp and larger ones in the aleurone.[39] Assuming that in solution both XYL10 and XYL11 are in a monomeric state, one can estimate that XYL11 (20 kDa) will have an approximate volume of 24 nm^3, whereas that of XYL10 (40 kDa) will be

approximately 40 nm^3, suggesting that XYL 10 protein would have more difficulty to penetrate the bran tissues.

In conclusion, we have compared the hydrolytic ability of two naturally thermostable xylanases towards an economically relevant agricultural by-product. Based on our analyses, although the GH10 xylanase is more efficient on alkaline-extractable AXs, it is probable that the smaller size and the higher efficiency of the GH11 xylanase towards insoluble substrates make it a better enzyme for wheat bran hydrolysis. Therefore, taken together with previous data, we conclude that GH11 xylanases should be better tools for the initial stage of processing. Nevertheless, GH10 xylanases, such as XYL 10, might constitute better candidates for further by-product refining. Indeed, XYL 10 displayed higher efficiency towards soluble AXs and produced smaller arabinoxylosaccharide products. Finally, despite the absence of synergy between the two enzymes on wheat bran, the simultaneous use of both GH10 and GH11 xylanases could be advantageous for the production of certain specific arabinoxylosaccharide products. Indeed, the growing interest in xylanases as tools for the processing of AX-rich materials is highlighted by a recent report by Palackal et al.[28] that described the use of sophisticated enzyme engineering technology for the improvement of thermostability in a GH11 xylanase.

4. Experimental

4.1. Specialist reagents

Birchwood xylan was purchased either from Sigma-Aldrich S.A.RL. (Saint-Quentin Fallavier, France) or from Carl Roth GmbH (Karlsruhe, Germany). Wheat arabinoxylan and xylooligosaccharides were purchased from Megazyme (Megazyme Corp. Wicklow, Ireland). The neutral monosaccharides L-arabinose, L-fucose, D-xylose and D-galactose were obtained from Sigma-Aldrich S.A.R.L. (Saint-Quentin Fallavier, France) and D-glucose was from Carl Roth GmbH (Karlsruhe, Germany). D-glucuronic and D-galacturonic acids were purchased from Sigma-Aldrich S.A.RL. (Saint-Quentin Fallavier, France). The fluorescent probes 2-aminoacridone (AMAC) and 8-aminonaphthalene-1,3,6-trisulfonic acid (ANTS) were purchased from Sigma-Aldrich S.A.R.L. (Saint-Quentin Fallavier, France) and Molecular Probes (Leiden, The Netherlands) respectively. Polyacrylamide for PACE containing a ratio of acrylamide/N,N'-methylenebisacrylamide (29:1) was obtained from Severn Biotech Ltd. (Worcs, UK).

4.2. Production of xylanases

The GH 11 xylanase (XYL 11) used in this study is a (3-(1--4)-endo-xylanase (EC 3.2.1.8) that was purified to homogeneity from *Thermobacillus xylanilyticus* culture medium using a previously established protocol.[40] The degree of purity of XYL11 was checked by SDS-PAGE. The GH10 xylanase (XYL10) is recombinant protein produced by the plasmid pBADXYL. Briefly, to construct pBADXYL the previously isolated xylanase encoding *T xylanilyticus* genomic DNA[41] was inserted between the Nco I and Hind III sites of the expression vector pBABMycHisC (Invitrogen, Amsterdam, Netherlands). For expression, precultured pBADXYL-harbouring *Escherichia coli* TOP 10 cells were diluted (1:1,000) in Erlenmeyer flasks containing LB broth and ampicillin (100 µg/mL). The cultures were incubated at 37 °C with shaking until an OD_{600nm} of approximately 0.5 was reached. To induce expression of recombinant xylanase, an aq soin of L-arabinose was added to achieve a final concentration of 0.2 % (wlv). Incubation was continued for 4 h, alter which the *E. coli* cells were harvested by centrifugation (6,000g, 15 min, 4 °C) and re-suspended in 1 mM EDTA, 1 mM DTT, 20 mM Tris-HC1, pH 7.5. Cell lysis was achieved by sonication and the xylanase-containing supernatant was recovered after centrifugation (12,000g, 20 min, 4 °C). Finally, to provide a crude purification of the xylanase, a 30 min heat treatment (60 °C) and centrifugation (12,000g, 20 min, 4 °C) were performed. To extend the shelf-life of the recombinant XYL10, ethylene glycol (10 % v/v final concentration) was added to the supernatant which was then stored at 4 °C. In addition, a control expression using pBADMycHisC-harbouring *E. coli* TOP 10 cells was also performed in order to provide a xylanase-free *E. coli* lysate which was used as an experimental control in certain assays. The specific activity values of XYL 11 and XYL10 were 2,000 and 960 IU/mg protein respectively.[8,40] One IU is the amount of xylanase required to release 1 µmol of xylose reducing equivalent from birchwood xylan per min at 60 °C.

4.3. Xylanase treatment of destarched wheat bran

Destarched wheat bran (DWB provided by ARD, Pomacle, France) was hydrated in distilled water (3% w/v) for 16 h at 60 °C. After, an aliquot of XYL10 or XYL11 (10 IU/mL) was added and incubation at 60 °C with constant stirring was continued. Experiments in which both xylanases were employed simultaneously were performed using equal amounts (5 IU/mL) of each enzyme. All experiments were performed in duplicate. Alter 1 h, 6 h or 24 h of incubation, the supernatant (soluble fraction) was separated from the solid, residual wheat bran (RWB) by centrifugation (4,000g for 15 min) and the enzymes were denatured by heating at 100 °C for 10 min. The supernatant and the residual RWB were retained for analysis; the supernatant was further centrifuged at 6,050g for 15 min prior to carbohydrate analysis by HPAEC. For XYL 10 hydrolyses, a control experiment using a xylanase-free E. *coli* TOP 10 lysate was included in order to evaluate

any cell-wall hydrolysis provoked by endogenous E. *colt* glycoside hydrolases. Before carbohydrate or phenol analyses, residual bran fractions were freeze-dried and ground using a bail crusher (MM 2000, Retsch GmbH, Haan Germany). Another control experiment consisted of incubating DWB in distilled water at 60 °C in the absence of xylanase. The supernatant and residue from this control were prepared and analysed as before. In a separate experiment, a larger amount of DWB was treated with XYL11 using the conditions described above and the RWB was then retained for alkali-extraction of three enzyme-resistant AX fractions, WI-AXr, WS-AXr 50 and WS-AX,80 (see section 4.4 "Extraction method for AX-enriched fraction").

4.4. Extraction method for AX-enriched fractions

Alkaline extraction of AX fractions from native DWB or RWB after a 24 h XYL11 treatment (see section Production of xylanases) was achieved according to Zinbo and Timell.[42] Samples (15 g) were immerged in 300 mL of $NaBH_4$ 1% (w/v)/ KOH 24% (w/v) for 3 h with agitation at room temperature. After centrifugation, EtOH (6 vol) 95% (v/v) was added to the supernatant. The pH was adjusted to neutral by the addition of AcOH. During overnight incubation at 4 °C, hemicellulose precipitation occurred. Hemicelluloses were then recovered by centrifugation (30 min, 9,000g, 4 °C) and washed vigorously in EtOH 80%. The hemicellulose-rich fractions were suspended in distilled water. After 12 h at 4 °C, the water-insoluble arabinoxylan (WI-AX) fraction was recovered by centrifugation and designated as either $WI\text{-}AX_i$ (initial water-insoluble arabinoxylan) or WI-AXr (residual water-insoluble arabinoxylan). Water soluble arabinoxylans (WS-AX) were further fractionated by a two step ethanol precipitation procedure. First the WS-AX was adjusted to 50% (v/v) EtOH and incubated at 4 °C for 12 h. The resulting precipitates were designated either WS-AX,-50 or WS-AX,-50. After the final EtOH concentration in the remaining supernatant was raised to 80% (v/v), incubation at 4 °C was repeated. This gave rise to a second precipitate which was designated either $WS\text{-}AX_i$-80 or WS-AX,80. All fractions were then freeze-dried prior to further analysis.

4.5. Activities of XYL10 and XYL11 on AXs and DWB

The activities of XYL 10 or XYL 11 towards isolated AX fractions were determined by the quantification of reducing sugar liberation using the ferricyanide-based method described by Kidby and Davidson.[43] The assay mixture (1 mL) consisted of various concentrations of substrate (0.05% to 3% w/v) in 50 mM sodium acetate, pH 5.8. Before the assay, both the alkali-extractable AXs and commercial birchwood xylan were stirred and vigorously homogenised before incubation at 60 °C in the presence of XYL 10 or XYL 11 (0.025 to 0.1 IU/mL final). Following enzyme addition,

aliquots were removed at 2 min intervals for reducing sugar quantification. Additionally, in order to ascertain the level of non-specific hydrolysis catalysed by *E. coli*-encoded glycoside hydrolases, a control experiment using xylanase-free *E. coli* lysate was performed for ail AXs tested. For such controls, each substrate was incubated with an aliquot of lysate whose volume was equivalent to that needed to obtain 0.1 IU/mL of XYL 10 in the other experiments.

To determine the kinetic parameters $K_{m(aPP)}$, V_{max} and k_{cat}, xylanase assays were also performed in initial rate conditions using DWB (0.05 to 20% w/v in distilled water). Reactions were performed at 60 °C with stirring in the presence of either XYL10 or XYL 11 at concentrations of 0.2 and 0.05 IU/mL respectively. Each experimental condition was reproduced in triplicate and the progression of hydrolysis was determined after 10 min by monitoring the liberation of reducing sugars. Data were analysed using the Enzyme Kinetics software (SPSS Science, Inc., USA). $K_{m(app)}$ and V_{max} were expressed ± standard error.

4.6. Chemical analysis

4.6.1. Carbohydrate analysis. The identification and quantification of neutral and acidic carbohydrates was carried using HPAEC. The various AX fractions (see section 4.4 "Xylanase treatment of destarched wheat bran") were hydrolysed (5 mg) using 12 M H_2SO_4 acid for 2 h at room temperature, then diluted at 1.5 M for again 2 h at 100 °C. The same procedure was used for the carbohydrate analysis of both DWB and RWB. Soluble fractions (500 µL) released by xylanase from DWB were hydrolyzed for 2 h at 100 °C in the presence of 1 M H_2SO_4. All samples were then filtered (PTFE, 0.22 µm) before injection onto a CarboPac PA-1 anion exchange column (4 x 250 mm, Dionex). Detection was performed by pulsed amperometry (PAD 2, Dionex) and samples were eluted using the following conditions: A (Milli-Q water) 95-0 % with B (0.1 M NaOH in Milli-Q water) 5-100 % for 19 min; then 100-0% B with C (0.3 M AcONa; 0.1 M NaOH in Milli-Q water) 0-100% until 49 min, and finally D 100 % (0.3 M NaOH in Milli-Q water) for 6 min. A post-column addition of 0.3 M NaOH was used. Monosaccharide composition was analysed and quantified using both L-fucose as the internai standard and standard solutions of neutral carbohydrates (L-arabinose, D-glucose, D-xylose, D-galactose) and uronic acids (D-galacturonic and D-glucuronic acids). AX content was expressed as the sum of the amounts of xylose and arabinose. Variation SD in the analytical measurements was < 5%.

4.6.2. Structural analysis of arabinoxylan-enriched fractions. All alkali-extracted AX fractions, except WS-AX,50, which was not obtained in sufficient quantities, were subjected to structural

analysis. Briefly, 4 mg of each AX were methylated twice (to ensure complete methylation) as previously described.[44] The dry extract of the methylated sample was then hydrolysed with formic acid (0.8 mL, 90% at 100 °C by mg of samples) for 1 h. After drying, further hydrolysis with trifluoroacetic acid (1 mL, 2 M, 100 °C) was performed for 3 h. Samples were then reduced with a $NaBH_4$ solution for 16 h at room temperature. Borate compounds were eliminated by MeOH/HC1 1% treatment. The reduced samples were acetylated with acetic anhydride/pyridine (v/v) at 100 °C for 1 h.[45] Alditol acetate derivatives were analysed using a Hewlett Packard 5890A gas chromatography system equipped with a flame-ionisation detector (GC/FID) and a SP2380 macrobore column (0,53 mm x 30 m) (Sigma-Aldrich Chimie S.A.R.L, Saint-Quentin Fallavier, France). Appropriate methylated alditol carbohydrates were used as standards. The carrier gas was high-purity nitrogen and the injector port and detector were heated at 260 and 280 °C respectively. For sample separation the following conditions were applied: 3 min at an initial temperature of 165 °C followed by an incremental increase (2.5 °C/min) to a final of 225 °C during 3 min. Complementary analyses were performed using a GC-MS system (Delsi GC coupled to a Nermag R10-10C mass analyser) using the chromatographic protocol described above.

4.6.3. Determination of bran hydroxycinnamic acids. Esterified ferulic acid (FA), p-coumaric (pCA) and diferulic acid (DiFA) were released from the bail crushed RWB (40mg) and the water treated DWB (control) (see section 4.3. "Xylanase treatment of destarched wheat bran") by alkali extraction using 2 M NaOH (10 mL) for 2 h at 35 °C. Phenolic acids were quantified by HPLC using a Kromasil 5µ (RP-18, 250 mm*4.6 mm) A.I.T Chromato column and an MeCN/MeOH/water gradient for elution as previously described.[35] Measurements were performed in triplicate and the variation was estimated to be 5%.

4.7. Protein estimation

The protein content in each of the extracted AX fractions was calculated by determining in duplicate the total N content (N x 5.7) using approximately 3 mg of freeze-dried sample and an elementary analyzer (NA 1500, Carlo Erba) coupled to a mass spectrometer (Fisons Isochrom). The experimental error was less than 5%.

4.8. Analysis of oligosaccharides by PACE

Prior to PACE analysis, enzyme-produced oligosaccharides (0.5 mg/mL^{-1}) and standard xylooligosaccharides and monosaccharides (20 µmol) were vacuum air-dried. Derivatizations using the ANTS or AMAC fluorophores and polyacrylamide gel electrophoresis were carried out as

described previously.[28] Under ANTS conditions used, arabinose migrates very close to xylose and its position was not annotated. Gels were scanned using a MasterImager CCD camera system (Amersham, Bucks, UK) equipped with an excitation and detection filters at 400 nm and 530 nm respectively. Captured gel images (resolution 100 microns) were exported in an 8 bit file to Microsoft PowerPoint.

4.9. ^{13}C NMR spectroscopy

The ^{13}C NMR spectrum of the glucose-rich fraction that was solubilised by the action of XYL11 on wheat bran was recorded in Me_2SO-d_6 (12 mg/0.5 mL) at 75 MHz using a Bruker AM 300 FT spectrometer operating at 323 K. The chemical shifts were referenced to Me_2SO-d_6 at 39.6 ppm and are reported relative to TMS.

Acknowledgements

This work was partially supported by grants from the "Région Champagne-Ardenne" (FR) and the Biotechnology and Biological Sciences Research Council (UK). The authors also express their gratitude to Dr Paul Dupree for his support and advice and N. Aubry, D. Crônier, B. Hermant and D. N'Diaye for their skillful technical assistance

Abbreviations

ANTS, 8-aminonaphthalene-1,3,6-trisulfonic acid; AMAC, 2-aminoacridone; AX, arabinoxylans; DiFA, diferulic acid; DP, degree of polymerisation; DWB, destarched wheat bran; FA, ferulic acid; GH, glycosyl hydrolase; HCA, hydroxycinnamic acid; HPAEC, high-pressure anion-exchange chromatography; PACE, polysaccharide analysis using carbohydrate gel electrophoresis; pCA, p-coumaric acid; RWB, residual wheat bran; XYL10, *Thermobacillus xylanilyticus* family 10 endo-1,443-xylanase; XYL11, *Thermobacillus xylanilyticus* family 11 endo-1,4-P-xylanase; WI-AX,, WI-AXr, water-insoluble arabinoxylan isolated from initial and XYL11 residual wheat bran; WS-AX; -50, WS-AX, -80, 50 %- and 80 %- ethanol precipitate of water soluble arabinoxylans isolated from initial wheat bran; WS-AX,50, WS-AX,-80, 50 %- and 80 %- ethanol precipitate of water soluble arabinoxylans isolated from XYL11 residual wheat bran.

References

1. Prade, R. A. *Biotechnol. Genet. Eng. Rev.*, **1996,** *13,* 101-131.
2. Henrissat, B. *Biochem. J,* **1991,** *280,* 309-316.
3. Henrissat, B.; Callebaut, I.; Fabrega, S.; Lehn, P.; Mornon, J. P.; Davies, G. J. *Proc. Nat. Acad. Sci. USA,* **1995,** 92, 7090-7094.

4. Biely, P., Vrsanska, M., Tenkanen, M., Kluepfel, D. J. *Biotechnol.,* ***1997,*** *57,* 151-166.

5. Beg, Q. K.; Kapoor, M.; Mahajan, L.; Hoondal, G. S. *Appl. Microbiol. Biotechnol.,* **2001,** *56,* 326-338.

6. Buchert, T.; Tenkanen, M.; Kantelinen, A.; Viikari, L. *Bioresource Technology*, **1994,** *50,* 65-72.

7. Clarke, J. H.; Rixon, J. E.; Ciruela, A.; Gilbert, H. J.; Hazlewood, G. P. *Appl. Microbiol. Biotechnol.,* **1997,** *48,* 177-183.

8. Tôrrônen, A.; Rouvinen, *J. Biochemistry*, ***1995,*** *34,* 847-856.

9. Bray, M. R.; Clarke, A. J. *A. Eur. J. Biochem.,* **1992,** *204,* 191-196.

10. Simpson, D. J.; Fincher, G. B.; Huang, A. H. C.; Cameron-Mills, V. J. *Cereal Sci.,* ***2003,*** *37,* 111-127.

11. Debeire, P.; Priem, B.; Strecker, G.; Vignon, M. *Eur. J. Biochem.,* ***1990,*** *187,* 573-580.

12. Pell, G.; Taylors, E. J.; Gloster, T. M.; Turkenburgs, J. P.; Fontes, C. M. G. A.; Ferreira, L. M. A.; Nagy, T.; Clark, S. J.; Davies, G. J.; Gilbert, H. J. *Biol. Chem.,* ***2004,*** *279,* 9597-9605.

13. Fujimoto, Z.; Kaneko, S.; Kuno, A.; Kobayashi, H.; Kusakabe, I.; Mizuno, H. J. *Biol. Chem.,* ***2004,*** *279,* 9606-9614.

14. Goesaert, H.; Elliot, G.; Kroon, P. A.; Gebruers, K.; Courtin, C. M.; Robben, J.; Delcour, J. A.; Juge, N. *Biochem. Biophys. Acta,* ***2004,*** *1696,* 193-202.

15. Courtin, C. M.; Delcour, J. A. *J. Cereal Sci.,* ***2001, 33,*** 301-312.

16. Maes, C.; Vangeneugden, B.; Delcour, J. A. *J. Cereal Sci.,* ***2004,*** 39, 181-186.

17. Harris, G. H.; Pickersgill, R. W.; Conneron, I.; Debeire, P.; Touzel, J.P.; Breton, C.; Pérez, S. *Protein. Struct. Funct. Genet.,* **1997,** *29,* 77-86.

18. Connerton, I.; Cummings, N.; Harris, G. W.; Debeire, P.; Breton, *C. Biochem. Biophys. Acta,* **1999,** 1433, 110-121.

19. Benamrouche, S.; Crônier, D.; Debeire, P.; Chabbert, B. J. *Cereal Sci.,* ***2002,*** *36,* 253-260.

20. Fincher, G. B.; Stone, B. A. *Advan. Cereal Sci. Technol.,* **1986,** *8,* 207-295.

21. Hatfield, R. D.; Ralph, J.; Grabber, J. H. J. *Sci. Food Agric.,* **1999,** *79,* 403-407.

22. Izydorczyk, M. S.; MacGregor, A. W. *Carbohydr. Polym.,* ***2000,*** *41,* 417-420.

23. Bily, A. C.; Reid, L. M.; Taylor, J. H.; Johnston, D.; Malouin, C.; Burt, A. J.; Bakan, B.; Regnault-Roger, C.; Pauls, K. P.; Arnason, J. T.; Philogène, B. J. *R. Phytopathology*, ***2003,*** *93,* 712-719.

24. Beaugrand, J.; Reis, D.; Guillon, F.; Debeire, P.; Chabbert, B. *Int. J Plant Sci.,* ***2004,*** in press.

25. Cui, W.; Wood, P. J.; Blackwell, B.; Nikiforuk, J. *Carbohydr. Polym.,* ***2000,*** *41,* 249-258.

26. Goubet, F.; Jackson, P.; Deery, M. J.; Dupree, *P. Anal. Biochem.,* ***2002,*** *300,* 53-68.

27. Breannan, Y.; Callen, W. N.; Christoffersen, L.; Dupree, P.; Goubet, F.; Healey, S.; Hernândez, M.; Keller, M.; Li, K.; Palackal, N.; Sittenfeld, A.; Tamayo, G.; Wells, S.; Hazlewood, G. P.; Mathur, E. J.; Short, J. M.; Robertson, D. E.; Steer, B. A. *Appl. Environ. Microbiol.,* ***2004,*** *70,* 3609-3617.

28. Palackal, N.; Brennan, Y.; Callen, W. N.; Dupree, P.; Frey, G; Goubet, F.; Hazlewood, G. P.; Healey, S.; Kang, Y. E.; Kretz, K. A.; Lee, E.; Tan, X.; Tomlinson, G. L.; Verruto, J.; Wong, V. W. K.; Mathur, E. J.; Short, J. M.; Robertson, D. E.; Steer, B. A. *Protein Sci.,* ***2004,*** *13,* 494-503.

29.Schooneveld-Bergmans, M. E. F.; Beldman, G.; Voragen, A. G. J. J. *Cereal Sci.,* **1999,** *29,* 63-75.

30 Maes, C.; Delcour, J. A. J. *Cereal* ***Sci., 2002, 35,*** 315-326.

31. Li, K.; Azadi, P.; Collins, R.; Tolan, J.; Kim, J. S.; Eriksson, K. E. *Enzyme Microb. Technol.,* ***2000,*** *27,* 89-94.

32. Vardakou, M.; Katapodis, P.; Samiotaki, M.; Kekos, D.; Panayotou, G.; Christakopoulos, P. *Int. J. Biol. Macromol.,* ***2003, 33,*** 129-134.

33. Garcia-Conesa, M. T.; Plumb, G. W.; Waldron, K. W.; Ralph, J.; Williamson, *G. Redox Report,* ***1997, 3,*** 319-323.

34. Grabber, J. H.; Ralph, J.; Hatfield, R. D. *J. Agric. Food Chem.,* ***1998,*** *46,* 2609-2614.

35. Beaugrand, J.; Crônier, D.; Debeire, P.; Chabbert, B. J. *Cereal Sci.,* ***2004,*** in press.

36. Lequart, C.; Nuzillard, J. M.; Kurek, B.; Debeire, P. *Carbohyd. Res.,* **1999,** *319,* 102-111.

37. Faulds, C. B.; Zanichelli, D.; Crepin, V. F.; Connerton, I. F; Juge, N.; Bhat, M. K.; Waldron, K. *W. J. Cereal Sci.,* ***2003,*** *38,* 281-288.

38. Christakopoulos, P.; Katapodis, P.; Kalogeris, E.; Kekos, D.; Macris, B.J.; Stamatis, H.; Skaltsa, H. *Int. J. Biol. Macromol.,* ***2003,*** 31, 171-175.

39. Chesson, A.; Gardner, P. T.; Wood, T. J. *J. Sci. Food Agric.,* ***1997,*** *75,* 289-295.

40. Debeire-Gosselin, M.; Loonis, M.; Samain, E.; Debeire, P. Purification and properties of 22 kDa endoxylanase excreted by a new strain of thermophilic Bacillus. In *Xylans and Xylanases* Visser, J.; Beldman, G.; Kusters-van Someren, M. A.; Voragen, A. G. J. Eds.; Elsevier Science Publishers, Amsterdam, 1992; pp. 463-466.

41. Debeche, T.; Cummings, N.; Connerton, I.; Debeire, P.; O 'Donohue, M. *Appl. Environ. Microbiol.,* ***2000,*** *66,* 1734-1736.

42. Zinbo, M.; Timell, T. E. *Svensk. Papperstidn.,* **1965,** *68,* 647-662.

43. Kidby, D. K.; Davidson, D. J *.A. Anal. Biochem.,* **1973,** ***55,*** 321-325.

44. Hakomori, S. J. *Biochem.,* **1964,** *55,* 205-208.

45. Sarwardeker, J. S.; Sloneker, J. H.; Jeans, *A. Anal. Chem.,* **1965,** *37,* 1602-1604.

Table 1 - Kinetics of the release of soluble arabinoxylans from DWB by XYL 10 and/or XYL 11 treatments

Treatment		Ara + Xyl (%) removed[a]	Ara/Xyl	Ara + Xyl (%) of solubilised sugar[b]
XYL 10	1 h	13.6 ± 0.5	0.49 ± 0.02	87.1 ± 2.7
	6h	23.5 ± 0.7	0.39 ± 0.02	88.7 ± 3.4
	24h	25.5±0.7	0.43±0.02	85.7± 1.0
XYL11	1 h	46.0±1.1	0.23 ± 0.01	97.4 ± 2.2
	6h	48.4±0.6	0.23±0.01	95.3±2.5
	24 h	49.0 ± 1.4	0.23 ± 0.01	90.2 ± 1.2
XYL 10 + XYL11	1 h	48.1 ± 1.4	0.23 ± 0.02	92.8 ± 2.2
	6h	49.4± 1.8	0.24±0.01	91.2±2.5
	24h	50.7± 1.5	0.24 ± 0.01	89.4 ± 1.3

[a] % of (Ara + Xyl) removed with respect to initial (Ara +Xyl) content of DWB sample

[b] (Ara + Xyl) content of the soluble fractions was expressed as a percentage of total neutral carbohydrate content (Gal + Glc + Xyl + Ara = 100%).

Table 3 - Composition and recovery yield of alkali-extractable arabinoxylans fractions from DWB and XYL 11-RWB

Extraction	Yield [a]	Protein [b]	TC [b]	UA °	Glc [c]	Gal °	Ara + Xyl	Ara/Xyl
WI-AX;	10.5	8.03	64.1	1.74	8.57	0.65	89.0	0.16
WS-AX;-50	8.26	15.1	59.3	2.09	44.6	0.89	52.3	0.40
WS-AX;-80	8.29	8.80	68.6	4.98	3.31	2.08	88.8	1.13
WI-AXr	4.44	22.5	69.6	2.27	19.5	3.97	74.1	0.85
WS-AXr 50	0.40	nd	66.5	4.13	89.2	4.16	5.50	1.25
WS-AXr80	17.1	17.3	61.9	6.54	7.53	4.56	81.3	1.12

Abbreviations used: TC, total carbohydrate (UA + Glc + Gal + Ara + Xyl); UA, Uronic Acids

[a] Expressed as weight percentage of native or residual wheat bran dry matter.

[b] Expressed as weight percentage of fraction..

Expressed as weight percentage of total carbohydrates of fraction.

Table 5 - Kinetic parameters of XYL 10 and XYL 11 related to soluble and insoluble AX sources

	XYL 10			XYL 11		
	Km(aPP) (-)	V_{max} (tmol/min/mL)	kcat (s^{-1})	$K_m^{(app)}$ (g/L)	Vmax (µmol/min/mL)	k_{cat} (s^{-1})
WI-AX;	0.4 ± 0.03	0.09 ± 0.002	2400	°0.8 ± 0.1	0.07 ± 0.003	520
WS-AX;-50	1.0 ± 0.1	0.23 ± 0.01	1550	1.1 ± 0.1	0.07 ± 0.004	500
WS-AX;-80	°5.3 ± 1.5	0.14 ± 0.02	930	nd	nd	nd
WI-AXr	3.4 ± 0.6	0.24 ± 0.01	1600	[b] 14 ± 2.9	0.45 ± 0.06	3180
WS-AX_C80	[b]5.5 ± 1.0	0.14 ± 0.01	940	nd	nd	nd
Birch xylan	°0.5 ± 0.06	0.05 ± 0.003	1470	[a] 1.6 ± 0.1	0.36 ± 0.003	2550
DWB	°40 ± 9	0.14 ± 0.01	470	[c]25 ± 8	0.22 ± 0.02	3170

Abbreviation used: nd = not determined

[a] Measured for only one Km(aPP) value

[b] Measured for only upper of two fold Km("P) value

Measured for only upper of three fold Km(aPP) value

$K_m^{(app)}$ and V_{max} are given f their respective standard error

Figure 2 - Fingerprints of oligosaccharide products released from DWB following treatment by XYL 10 and/or XYL 11.

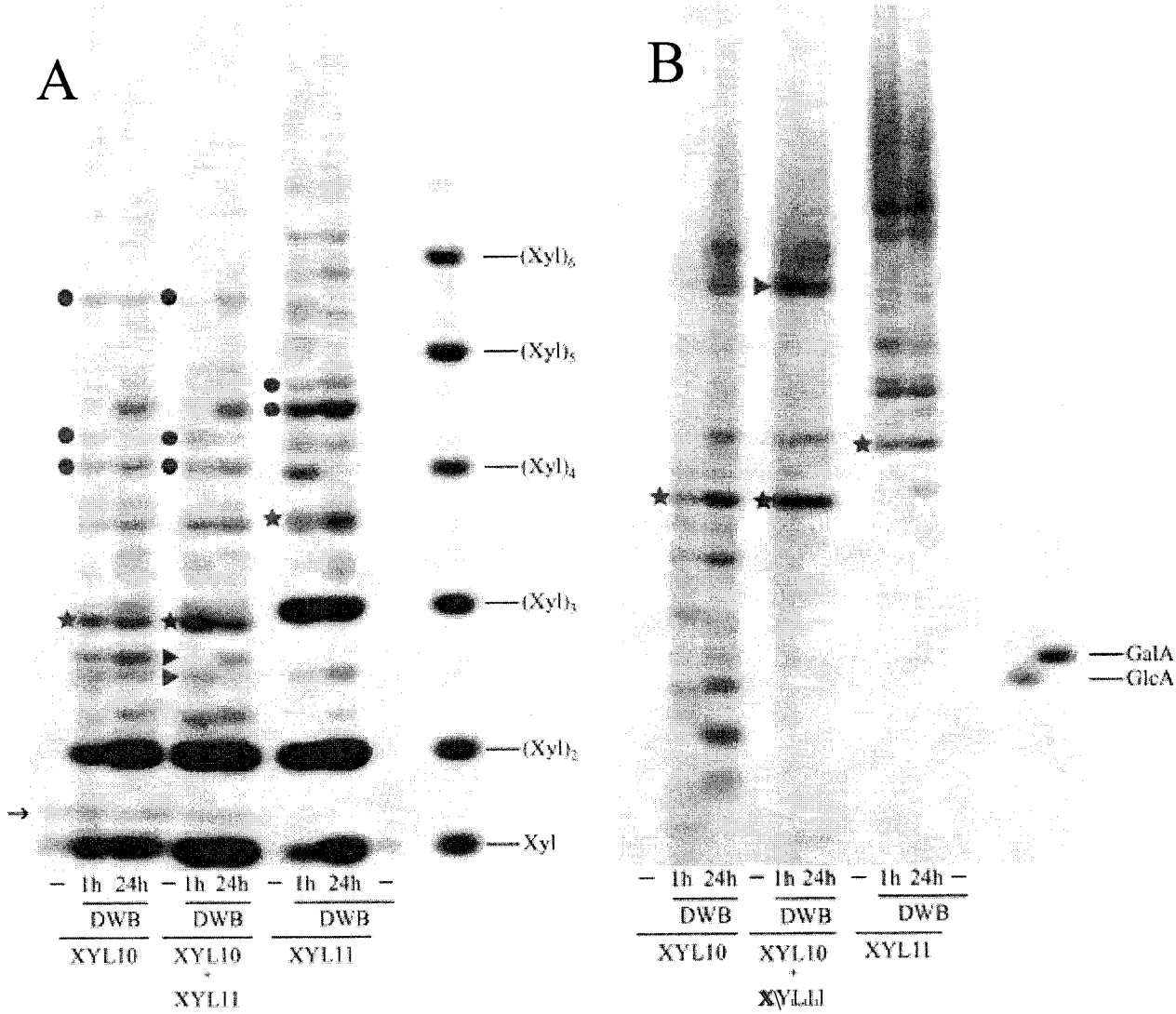

(A) Neutral and charged oligosaccharides observed following derivatization with ANTS.

(B) Charged oligosaccharides observed following derivatization with AMAC.

All reactions were performed at pH 7 and 60 °C for 1 h or 24 h. A standard xylo-oligosaccharides (DP 1 to 6) mixture was used to characterize the faster migrating species. Unspecific bands from the hydrolase and/or DWB controls are indicated by an arrow. DWB-hydrolysis products that co-migrated with those obtained from commercial xylan and arabinoxylan hydrolysed with the same enzyme(s) are indicated with stars or circles (glucuronoxylo- or arabinoxylo-oligosaccharides respectively). Specific DWB- hydrolysis products with differential occurrence are indicated with triangles.

Int. J. Plant Sci. 165(4):000-000. 2004

XYLANASE-MEDIATED HYDROLYSIS OF WHEAT BRAN. EVIDENCE FOR SUBCELLULAR HETEROGENEITY OF CELL WALLS

Johnny Beaugrand, [‡] Danièle Reis, [†] Fabienne Guillon, Philippe Debeire, [‡] and Brigitte Chabbert

[‡]Institut National de la Recherche Agronomique, UMR FARÉ-614, Centre de Recherche Agronomique, 2, esplanade Roland Garros, BP 224, 51686 Reims Cedex 02, France; [†]Laboratoire de Pathologie végetale INA-Paris-Grignon, 16, rue Claude Bernard, 75232 Paris Cedex 05, France; and INRA-URPOI, BP 71627, rue de la Geraudière, 44316 Nantes, France

Abstract

Previous work has shown that (1-÷4)-(3-D-endoxylanase-mediated hydrolysis of wheat bran leads to solubilization of 50% of arabinoxylans. However, xylanase efficiency on the individual bran tissues is unequal because of histological and chemical heterogeneity. We describe here the results of an immunocytochemical study which is aimed at a better understanding of *in situ* enzyme action on bran xylans, at different hydrolysis kinetic stages. Two polyclonal antibodies were used, one against xylanase and the other against (1—*4)-13-D-unsubstitued xylopyranosyl residues, to target poorly substituted arabinoxylans. These antibodies were used on optical microscopy or transmission electron microscopy sections of xylanase-treated and water treated wheat bran. After 30 min of xylanase treatment, xylanase distribution was found to be confined to the aleurone cell walls close to the endosperm and AX labeling had been lost. After 75 min, xylanase had progressed throughout the AL and had begun to attack the nucellar layer. Alter 24h, the aleurone layer was completely lost, while some remnants of the nucellar layer were still observable. In contrast, the morphology of the pericarp and the testa was unaltered and no xylanase labeling in these tissues was detected. Xylanase localization was correlated to the level of arabinoxylan substitution. That way, we showed that xylanase is preferentially localized and degrades poorly-substituted arabinoxylans, as shown by visible subcellular heterogeneity of aleurone and nucellus walls.

Keywords: wheat bran, cell wall, xylanase, arabinoxylans, immunolocalization, aleurone, nucellar layer.

Introduction

Wheat bran is a major agricultural by-product and represents an abundant but unexploited renewable carbon source. Indeed, starch-depleted wheat bran *(Triticum aestivum)* is rich in hemicelluloses, notably arabinoxylans (AX) which account for approximately 40% of dry weight. Enzymatic degradation of such lignocelluloses is a more suitable alternative to environmentally-damaging chemical methods which are presently employed for the saccharification of lignocelluloses.

The wheat bran surrounds the starchy endosperm and is the peripheral tegument of the kernel. It includes botanically distinct layers which are, starting from the albumen layer and going outwards: the aleurone layer (al), the nucellar layer (nl), the testa (t) or seed coat and the pericarp (pe) which corresponds to the fruit coat (Shetlar 1948). The aleurone layer is part of the endosperm, and is made of a single or double cell layer. It is bound to the starchy endosperm as well as to the first part of the nucellar layer. Aleurone is the only living cell in wheat bran and contains lipids, vitamins and much protein, notably hydrolytic enzymes that are involved in grain germination. The nucellar layer originates from the nucellar epidermis and includes crushed cells free of cell content. Nucellar layer is connected to the aleurone layer by a very thin amorphous layer. To this date, very little information is available about this nucellar lysate layer (Evers and Reed 1988). Testa is a pigmented layer derived from integument. The testa is covered by cuticle on both sides which are fused into one layer closely connected with the compressed integument. This layer is an essential actor of the water absorption (Stenvert and Kingswood 1976). Surrounding the testa, the pericarp acts as a protective coat for the caryopsis. This fruit coat comes into layers being from the inside: the tube cells (tc), elongated parallel with the long axis of the grain, the cross cells (cc) which are elongated transversely to the long axis of the grain, the hypodermis (hy) and the epidermis (ep). Finally, the outermost part of the pericarp is covered by a cuticle.

Except for the protein-rich aleurone layer, the tegument of mature grain is thus mostly composed of non-living cells with thick secondary cell walls. Plant cell-walls are usually described as a complex network of cellulosic fibers embedded in a matrix of non-cellulosic components including hemicelluloses, pectins, lignins and proteins. More specifically, cell walls of wheat bran contain arabinoxylans whose proportion and structure vary according to the tissular layer. In addition, occurrence of (1—>3; 1--*4)-(3-glucans and proteins have been reported in aleurone cell walls meanwhile pericarp contains large amount of cellulose (Brillouet and Joseleau 1987; Bacic and Stone 1981). Although they represent minor

components of the wheat bran, other non-carbohydrate polymers as lignin and cutin are located in the pericarp and in the testa respectively. Cell wall polymers are held together by covalent and non-covalent interactions (Aman and Nordkvist 1983; Iiyhama et al. 1990; Carpita and Gibeaut 1993). Notably, ferulic acid and dimeric forms are mainly responsible for cross-linking polysaccharides and/or lignin in grass cell walls (Hatfield et al. 1999; Chesson 1988; Andreasen et al. 2000; Saulnier et al. 1999). Uronic acid (1.5% of wheat bran dry matter) side group of arabinoxylans is also known to form covalent linkages (Erikson and Goring 1980).

On the whole, arabinoxylans are the major polysaccharide encountered in wheat bran. They consist of a main chain of (1—÷4)-linked (3-D xylopyranose residues, which harbors side chains whose nature and frequency vary. The a-L-arabinofuranose substituants and their feruloylated derivatives are the most frequent ones and are linked to the O-2 or O-3 of xylose residues. Although they are found in lower amounts, the a-D-glucuronic acid or its 4-0-methyl ether derivative at the O-2 position and acetyl groups at the O-2 or O-3 can also branch arabinoxylans (Brillouet and Joseleau 1987; Ring et Selvandran 1980; Schooneveld-Bergmans et al. 1999). A complete depolymerisation of the wheat bran AX thus requires many specific enzymes. The main one is the (1—*4)-(3-D-endoxylanase (EC 3.2.1.8), member of the family 11 glycosylhydrolase (Wong et al. 1988; Henrissat and Davies 1997), which degrades xylan by cutting between unsubstituted xylose residues. The products released from isolated arabinoxylans have decreased degree of polymerization along with the extent of xylanase degradation (Courtin and Delcour 2001).

Previous work using a purified thermostable (1—*4)-(3-D-endoxylanase belonging to the family 11 showed a 50% solubilization of wheat bran arabinoxylans (Benamrouche et al. 2002). The products released from AX degradation were mainly xylobiose, xylotriose and some arabinoxylosaccharides with a high xylose/ arabinose ratio (X/A), i.e. low substitution. Further studies using micro dissected tissular fractions showed a differential xylanase efficiency regarding the histochemical and chemical heterogeneity of the bran layers. Likewise, the aleurone and nucellar layers were the preferential targets for wheat bran degradation by endoxylanase. On the contrary, the outermost layers, as pericarp and testa appeared to resist enzymatic hydrolysis. Carbohydrate analysis of bran layers and the corresponding xylanase-released fraction further suggested that the degree of arabinose substitution is one of the major causes of the high resistance of these polymers to endoxylanase degradation. Indeed, X/A ratio ranged higher value in aleurone cells and nucella

as compared to pericarp. Additionally, arabinoxylan degradation could be hampered by uronic acid and diferulate moieties that show a higher content in the pericarp (Benamrouche et al. 2002; Antoine et al. 2003).

Besides structural limitations, degradation of arabinoxylans may be restricted due to the complex architecture of cell walls. As opposed to aleurone, interactions between arabinoxylans and other wall polymers should be strengthened in pericarp that contains not only highly substituted AX but also noticeable amount of cellulose, lignin and polyesters, thereby limiting xylanase access to the substrate. Enzymatic wall-disassembly can be addressed at ultrastructural levels in order to get a more comprehensive view of the impact of the wall network on the in situ enzyme-efficiency. In this respect, in situ visualization of xylanase and low-substituted AX was assessed at ultrastructural levels along the course of wheat bran degradation using immunocytochemical probes. The main aim was to understand the pattern of enzyme location throughout the bran tissues in relation to the distribution of its preferential substrate, by means of transmission electron microscopy and fluorescence microscopy. Concomitantly, changes in the overall cell wall network was investigated at different incubation times by staining the major wall polysaccharides (hemicelluloses, cellulose) with Periodic Acid-Thiocarbohydrazide-Silver proteinate reagent (PATAg). Ferulate distribution was further examined using UV-induced autofluorescence.

Material and methods

Wheat bran

The soft wheat *(Triticum aestivum)* cv.Isengrain was provided by Soufflet (Nogent-sur-Seine, France). Grains were soaked in distilled water overnight at 4°C, then were dissected under stereomicroscope. First, grain-ends were cut and discarded. Second, the remaining grains were soaked again for 1 hr in cold distilled water, and an incision in the crease permitted the removing of the endosperm by scrapping the bran. The purity of the endosperm-depleted bran was verified microscopically prior to endoxylanase or water control treatments. Starch-depleted wheat bran was provided by Soufflet (Nogent-sur-Seine, France).

Endoxylanase preparation

An (1--*4)-(3-endo-xylanase (EC 3.2.1.8) was purified from *Thermobacillus xylanilyticus* culture as previously described (Debeire-Gosselin et al. 1992). (1–*4)- (3-endo-xylanase activity was determined by incubating birchwood xylan (0.5% w/v) for 10 min in 50 mM

sodium acetate, pH 5.8 with an enzyme sample at 60 °C. The reducing sugar released was measured using a ferricyanide-based method of Kidby and Davidson (1973).

The specific activity of the enzyme was 2000 Units/mg protein, where 1 Unit corresponds to the amount of xylanase required to release 1 µmol. min^{-1} of reducing equivalent as xylose from birchwood xylan at 60°C (Pellerin et al. 1991).

Treatment of wheat bran

Enzymatic hydrolysis of the starch-depleted wheat bran (30 g/L) was performed for 15 min, 6 hrs and 24 hrs incubation periods at 60 °C, with constant stirring in the presence of 10 Units/mL of (1—>4)-(3-endo-xylanase. The supernatant containing the reaction products was retained for analysis, and the reaction was stopped by heating at 100 °C for 10 min then samples were centrifuged at 13000 rpm for 5 min.

For the microscopic study, (1—4)-f 3-endo-xylanase (0.5 Units/mL) or water incubation of wheat bran (30 g/L) were performed in distilled water at 60°C with constant stirring. Xylanase samples were taken after 30 min, 75 min and 24 hrs and water treated controls were done alter 0 min, 30 min and 24 hrs. Samples were then directly embedded for microscopy.

Wheat bran embedding

Xylanase treated wheat bran and control water samples were cut into small pieces under a solution of 2% glutaraldehyde in phosphate buffer (0.1 M, pH 7.4) and fixed in the same reagent for 45 min at room temperature. After several washes of 15 min in phosphate buffer then in distilled water, samples were dehydrated in an ethanol series, then infiltrated and embedded in LR White resin (Sigma) at 60°C for 24 hrs. LR White-embedded specimens were cut into semi thin (0.5 gm thick) and ultra thin sections (80-90 nm). Ultra thin sections were collected on nickel (for immunogold labeling) or gold grids (for PATAg staining), whereas semi thin sections were deposited on glass multiwell slides.

Topochemical and cytochemical staining

Semi thin sections (0.5 µm) of wheat bran samples were stained for 5 min with 1% toluidine blue and observed using a light microscope (LM). Periodic acid thiocarbohydrazide-silver proteinate staining (PATAg) was observed on thin bran specimen sections (80-90 nm) using a transmission electron microscope (TEM). The staining use was modified from Thiery (1967). Sections were floated on 1% periodic acid for 30 min; washed three times (for 10 min) with distilled water; then floated overnight at 4°C on 0.2% thiosemicarbazide in 20% acetic acid.

The sections were progressively washed with decreased concentrations of acetic acid (20%, 10%, 5%, 10 min each time) then distilled water (three times, 10 min each time) and treated with 1% silver proteinate for 30 min in darkness. Finally, sections were washed three times with water before being air-dried. PATAg reacts with vicinal diol moieties of polysaccharides (i.e. cellulose, hemicelluloses and pectin). Staining intensity is related to the density of silver deposits on reactive structures and allows the comparison of the richness of polysaccharides of bran cell wall before and after xylanase treatment.

Immunolabeling of the xylanase

The polyclonal antixylanase antiserum was raised in New Zealand White rabbits and produced by Eurogentec, Belgium following a standard protocol. Antibodies that can react with bran antigens may induce non-specific labeling during immunostaining of xylanase on wheat bran. Therefore, the antiserum was treated in order to remove the non-specific binding groups according to the protocol of Marlow and Lane (1988). Twenty grams of ball-milled de-starched wheat bran were suspended in 0.9% NaCl buffer, cooled on ice during 10 min, then 400 mL of cold acetone (-20°C) was added. Alter 30 min of vigorous mixing on ice, solvent-treated bran was recovered by centrifugation (10000g, 10min at 4°C) and dried. Antixylanase antiserum (60 mL) was incubated with the acetone-extracted bran for 30 min at 4°C. Subsequent centrifugation (13 min at 10000g, 4°C) provides a serum that is free of non-specific antibodies. For further immunolabeling of the xylanase by the antiserum, an optimal dilution of 1:320 was retained. Semi thin sections of wheat bran were incubated with 0.2 M Tris—buffered saline, pH 8.2, containing 1% normal goat serum (Sigma), 5% skimmed milk, 0.1% Tween 20 and 0.1% sodium azide (buffer A) for 30 min at room temperature. They were then incubated with the primary antibody (1:320 dilution) in 0.2 M Tris—buffered saline, pH 8.2, containing 1% normal goat serum, 1% skimmed milk, 0.1% Tween 20 and 0.1% sodium azide (buffer B), for 4 hrs 30 min in a moisture chamber. After thorough washings in buffer B, sections were incubated for 1 hr with a gold-labeled (5 nm) goat antirabbit immunoglobulin G conjugate (British Biocell International) diluted 1:40 in buffer B. For immunofluorescent labeling, the secondary antibody was Alexa Fluor 546 goat antirabbit immunoglobulin G conjugate (Interchim Molecular Probes) diluted 1:150 in buffer B, and incubated for lhr in darkness. The samples were then washed thoroughly in buffer A and in distilled water. Finally, the immunogoldlabeling of semi thin sections was enhanced with silver (Amersham life science) for 7 min at room temperature. Alter dehydration, **all**

specimens were covered with Eukitt mounting medium (Electron Microscopy Sciences, USA).

All observations were performed using an Axioskop microscope (Zeiss, Germany), either with bright light (immunogold and toluidine blue staining) or mercury light (green excitation for immunofluorescence and UV excitation for ferulate autofluorescence). For transmission electron microscopy, ultra thin sections were treated in the same way as semi thin sections. The size of gold particles bound to the secondary antibody was 10 nm. After immunolabeling, ultra thin sections were stained with uranyl acetate, and then examined with a Philips 201 electron microscope operating at 80kV.

All experiments were accompanied by the following controls: an immunolabeling performed without the primary antibody, an immunolabeling without the secondary antibody and an immunolabeling performed in the absence of xylanase hydrolysis in order to check that labeling corresponds only to the bacterial xylanase. For light microscopic observations, additional controls were performed by treating unlabeled specimens with the silver kit enhancer in order to verify that no unspecific binding of silver particles occurred.

Immunolabeling of the (1—>4)/-unsubstituted xylan

The anti (1-->4)-13-unsubstituted xylan antiserum was raised against a (1—*4)-f3-xylotetraose-bovine serum albumin conjugate in two New Zealand white rabbits. Further characterizations of the antiserum using indirect competitive ELISA were performed by Guillon et al. (2002), on a large variety of oligosaccharides inhibitors.

For further immunolabeling of the unsubstituted xylan by the antiserum, an optimal dilution of 1:500 was retained for subsequent experiments. Immunofluorescent and immunogoldlabeling of the (1-->4)-(3-unsubstituted xylan was performed on semi thin and ultra thin sections respectively, using the same procedure as for xylanase immunolabeling. All experiments were accompanied by the same controls as for xylanase (immunolabeling performed without the primary antibody or the secondary antibody) plus an immunolabeling performed with the preimmune (1—*4)-13-unsubstituted xylan serum in order to check that labeling corresponded only to the (1—>4)-(3-unsubstituted xylan.

Sugar analysis

Prior to analysis of monosaccharide composition by HPAEC, soluble fractions were hydrolyzed for 2 hrs at 100 °C in the presence of 1 M H_2SO_4. After hydrolysis, the samples were diluted 4 times, filtered and injected into a CarboPac PAl anion exchange column

(4*250 mm, Dionex). Neutral monosaccharides were separated in 5 mM NaOH for 12 min and for a further 7 min with a linear gradient up to 100 mM NaOH. The flow rate was 1 mL.min^{1} and detection was performed by pulsed amperometry (PAD 2, Dionex). A post-column addition of 300 mM NaOH (0.7 mL min^{-1}) was used. Monosaccharide composition was determined using fucose as the internai standard. Calibration was performed with standard solutions of arabinose, glucose, xylose and galactose.

Results

Sugar analysis

Xylanase treatment of starch-depleted wheat bran was evaluated throughout the time course release of total neutral carbohydrates and of arabinoxylan in the soluble fraction. After a 24 hour-incubation, ten units of xylanase approximately led to a 20% dry matter loss due to the release of neutral carbohydrates (fig. 1). Arabinose and xylose accounted for nearly 80% of the monosaccharides recovered from acid hydrolysis of the enzyme-solubilized carbohydrates, and represented 50% of the initial bran AX. The enzyme-released products were essentially composed of AX but also contained glucose and galactose (nearly 20%). Mannose that represents less than 0.3% of the bran dry matter and a very minor proportion in soluble fractions was not quantified. After 15 min, half of the maximum level of AX and total neutral carbohydrate degradation was attained. After a 6-hr-incubation, the percentage of degradation of the AX was close to the maximum, as was the total neutral sugar. The X/A ratio of the soluble products increased during the incubation time and averaged 3.3 after 24 hrs. These data show that 10 units of purified xylanase (0.33 U/mg bran) provided a quick and efficient degradation of wheat bran. For the microscopy study, a lower concentration of enzyme was chosen in order to visualize step-by step xylanase hydrolysis of the bran cell walls. Indeed, 0.5 Unit xylanase meant to lower degradation yields at the early stages of the bran hydrolysis whereas the extent of AX hydrolysis after a 24 hr-incubation (45% degradation, data not shown) was similar to the 10-unit-xylanase treatment.

Cytochemical observations of bran cell walls

Toluidine blue staining of longitudinal sections of the untreated bran (fig. 2A) underlined the histological heterogeneity of the bran layers. The aleurone layer occurred mainly as a single layer, and showed sometimes two layers depending on the location within the grain. Aleurone cell walls and nucella were less stained than pericarp layers. The testa displayed at least two

cellular structures (one highly and the other no stained). Tube cells were not visible here due to their irregular distribution around the grain. Except for the testa layer, bran cell walls gave a blue fluorescence under UV light (fig. 2B). Aleurone cell walls, which contain most of the bran ester-linked ferulic acid, had an intense blue fluorescence. Similar wheat bran structures were observed after 24 hrs of water treatment at 60°C.

Cell-wall polysaccharide distribution was examined using PATAg staining of wheat bran before and alter xylanase treatment. However, the present paper will focus on microphotographs of the aleurone and nucellar layers where subcellular changes were clearly evidenced. In the absence of xylanase treatment, a thin inner layer (iawl) of aleurone cell walls showed an intensive staining as compared to the thick outer layer (oawl) (fig. 2C). Plasmodesmata could also be distinguished.

Following a 30 min-incubation, xylanase action induced a loss of aleurone fluorescence in the cell wall close to the removed endosperm (fig. 3A); cell walls were still distinguishable. PATAg staining of the corresponding aleurone area showed that the polysaccharide distribution was strongly altered at the outer wall layer while the inner one remained intact (fig. 3B).

After 75 min of xylanase treatment, lateral cell wall in adjacent aleurone cells (namely anticlinal cell wall) swelled and collapsed, providing evidence for dramatic changes in the wall ultrastructure (fig. 3C). The weak and heterogeneous PATAg staining within the outer layer of aleurone cell wall suggests that some polysaccharides were removed. An even higher disorganization in this wall layer permitted the visualization of a parallel structure recalling cellulose microfibril arrangement. At this stage of degradation, unaltered polysaccharides were more concentrated at both junction areas between aleurone - endosperm wall pairs and between nucellar layer - aleurone as well as the inner aleurone-wall layer. Moreover, plasmodesmata were heavily stained with PATAg and displayed tubular or circular elements depending on the localization in the cell wall. In concordance to the polysaccharide distribution, the collapsed aleurone cell wall did not give UV-induced fluorescence (fig. 3D) except for some areas found at the junction of the nucellar layer. A thin layer surrounding the protoplast retained a faint blue fluorescence and could correspond to the inner aleurone wall layer. Increased incubation time with xylanase (24 hrs) led to the complete disappearance of the aleurone layer; nucellar layer was detached and partially disrupted (fig. 3E). Remnants of the nucellar layer were not fluorescent under UV light in contrast to water-treated bran (control) and cross cells appeared partially detached from hypoderma. However tissue dislocation could not specifically hold on xylanase treatment as similar observations were

obtained in the water–treated, control bran. On the contrary, control bran recovered after a 24 hr water- incubation displayed a normal distribution of the polysaccharides as illustrated for the aleurone layer (fig. 3F). Neither histological nor cytochemical changes were significantly observed in the case of bran after a 24 hr water-control.

Immunocytochemical controls

No significant labeling was obtained with the (1--*4)-(3-D-unsubstitued xylan preimmune sera. Nevertheless, a very little unspecific but non significant labeling was found at the testa-nucellar layer (fig. 4A). In addition, the antixylanase sera did not react with sections obtained from water-treated bran (control) (fig. 5A). No labeling was detected using secondary antibodies alone, and silver enhancement alone gave no visible particles under light microscopy. Similar observations were obtained using immunofluorescence detection (data not shown). The overall immunocytochemical controls thus show that both poorly substituted AX and xylanase labeling were specific.

Localization of poorly substituted AX

Immunolabeling of the poorly substituted arabinoxylans showed a heterogeneous distribution in the bran cell-walls. Only the aleurone cell-walls and the nucellar layer were strongly labeled (fig. 4B). No other structures were immunofluorescent. After 30 min of xylanase treatment, labeling of the aleurone cell-walls close to the removed endosperm disappeared (fig. 4C), which correlates with the aforementioned loss of UV-induced fluorescence. In the next step of xylanase treatment (75 min), the strong labeling of arabinoxylans had disappeared in all aleurone cell-walls (fig. 4F). On the other hand, immunolabeling labeling of low-branched arabinoxylans was abundant on the nucella and similar to control bran (fig. 4D, 4F). After 24 hrs of enzyme incubation, a very weak AX labeling was still detected in the nucellar layer (fig. 4E) and was similar to immunocytochemical control using preimmune sera (fig.4A). According to this, no more epitopes of the low-branched arabinoxylan was observed in the nucellar layer after 24 hrs of xylanase incubation. Finally, the intensity of arabinoxylan immunolabeling did not show visible change in the water-control incubation after being 24 hrs in water (60°C) when compared to the untreated bran (fig. 4B). We presented here a section corresponding to a minor part of the wheat bran where aleurone layer has two cells (fig. 4G).

Localization ofxylanase

After 30 min of xylanase treatment, xylanase immunogoldlabeling indicated that xylanase is only distributed within the aleurone cell walls close to the removed endosperm (fig. 5B). This localization was consistent with the loss of cell-wall autofluorescence and the distribution of the poorly substituted AX (fig. 3A and fig. 4C respectively). A zoom of the xylanase-labeled area indicated that xylanase occurred inside the wall as shown by the gold particles (fig. 5C). Notably, gold particles were numerous in the outer aleurone wall layer but not in the inner aleurone wall layer, which appeared brighter than oawl with uranyl acetate staining.

After 75 min of xylanase treatment, the enzyme progressed throughout the aleurone. The obtained red immunofluorescence further underlined the swollen and collapsed cell walls (fig. 5D). Xylanase started to penetrate the nucellar layer. In the aleurone layer, a higher intensity of xylanase immunogold-labeling was found at cell junctions of the anticlinal and periclinal (fig. 5F and 5G) cell walls when compared to anticlinal cell walls (fig. 5D and 5E). This observation indicates a heterogeneous localization of the enzyme within the cell walls. Xylanase also displayed a preferential accumulation at the nucellar lysate layer, in the same area where polysaccharides have been shown to stain with PATAg, (fig. 3C). This specific area gave positive AX labeling (fig. 4F) and blue UV-induced fluorescence (fig. 3D). In addition, a strong xylanase-labeling was obtained at the aleurone - endosperm junction of the anticlinal and periclinal wall areas where a positive staining of polysaccharide was shown. However, this junction area was no more fluorescent under UV light. Moreover, the disassembly of the cells walls could be evidenced as white area under electron beam.

Following a 24 hr-incubation, as for the lowly-substituted arabinoxylan epitopes (fig. 4E), xylanase antibodies could not be detected on the residual nucellar layer. The total degradation of aleurone layer did not allow further observation of the enzyme.

Discussion

Xylanase treatment led to a partial destruction of the wheat bran (mainly the aleurone layer). Consistent with a previous study, only 50% of the bran AX was depleted (Benamrouche-Stitou 2002). Xylanase action degraded 20% of the wheat bran dry matter into soluble neutral carbohydrates of which 18% represent nearly half of the total wheat bran arabinoxylans. Interestingly, this purified enzyme cosolubilized noticeable amounts of polysaccharides containing glucose and galactose. This data suggests that arabinoxylan degradation induces a cell wall disassembly this is due to disruption of the wall network. Many studies have reported that arabinoxylans are linked to other wall polymers through covalent and non

covalent bonds (Schooneveld-Bergmans et al. 1999, Izydorczyk and MacGregor 2000). Indeed, feruloylated oligosaccharides were previously isolated from the products released by xylanase from different kinds of cereal (Lequart et al. 1999, Saulnier et al. 1999). Mixed glucans were also identified among the xylanase-released carbohydrate from destarched wheat bran (Benamrouche-Stitou 2002). Xylooligosaccharides produced along the course of xylanase degradation of wheat bran were characterized by an increased X/A ratio. Therefore, xylanase may act sequentially on bran tissues whose arabinoxylans have distinct branching levels. This is supported by the findings of Benamrouche et al. (2002). They found a four-fold higher X/A ratio of xylooligosaccharides released from nucellus-rich fractions as compared to aleurone enzymatic products.

In this work, the chemical studies of xylanase-mediated degradation of wheat bran aimed at a high rate of arabinoxylan solubilization and clearly showed that 10-unit enzymes (0.33U/mg bran) were very efficient within a short period. However, investigation of the bran degradation at ultrastructural levels required intermediated incubation times (30 min and 75 min) and the use of a 20 fold less concentrated xylanase. These conditions allowed the examination of the cytochemical features of the initial steps of the bran degradation although an optimal yield of arabinoxylan solubilization could still be reached for longer periods i.e. 24 hrs (Benamrouche-Stitou 2002).

In addition to wet-chemistry, investigation of the plant cell-walls using non-destructive approaches such as immunocytochemistry can provide specific information about polysaccharide distribution at ultrastructural levels (Reis et al. 1993; Migné et al. 1994; Suzuki et al. 2000; Remond-Zilliox et al. 1997). Our probing study indicated that poorly-substituted arabinoxylans are not uniformly distributed within bran. This observation was consistent to chemical data of isolated tissular fractions (Bacic and Stone 1981; Benamrouche et al. 2002; Antoine et al. 2003). The poorly-substituted arabinoxylans were found in the aleurone layer and the nucellar layer. Accordingly, the localization of the xylanase in the enzyme-treated bran appeared closely related to the low-branched arabinoxylan distribution. The enzyme was not found in the external bran layers (testa and pericarp) even after 24 hr-incubation time. Antigenic sites may have been masked due to steric hindrance brought by interconnecting dimeric phenolic acids that occur mainly in the pericarp (Migné et al. 1994; Antoine et al. 2003). However, previous work using a similar enzyme already showed that the pericarp and the testa were recalcitrant to the enzymatic degradation. Indeed, in these layers, arabinoxylans are highly branched (X/A lower than 1) with arabinose, glucuronic and acetyl ramifications (Maes and Delcour 2002; Rhodes et al. 2002 a). The higher proportion of

ferulate dimers in pericarp as compared to aleurone could also contribute to the resistance of this layer towards xylanase degradation. Indeed, dimeric structures could be a more efficient limiting factor than ferulic ester linkage to enzymatic degradation of AX (Grabber et al. 1998). Accordingly, the ferulic ester-linked arabinoxylans are well depolymerized in the aleurone cell walls.

The *in situ* xylanase location seems closely connected to the AX degradation, which leads to major alteration of the cell wall network and to the loss of the UV-autofluorescence. In bran layers the blue autofluorescence under UV light is mainly related to the occurrence of ferulic acid which represents the major part of cell wall linked hydroxycinnamic acids (Fulcher et al. 1972). Therefore, ferulic acid related autofluorescence could be considered as an indicator of the extent of arabinoxylan breakdown in aleurone and nucellar layers. Xylanase penetration seems to proceed sequentially since the enzyme first degrades the periclinal walls facing endosperm then the anticlinal walls. Consistently, a loss of wall autofluorescence is primarily observed for the periclinal walls. This pattern may be related to the spatial inhomogeneity of hydroxycinnamic acids. Higher concentrations of ferulic derivatives were reported in anticlinal aleurone walls and at the junction of periclinal/anticlinal walls when compared to periclinal walls (Saadi et al. 1998). A "polarized nature" of aleurone-wall degradation was initially observed during the gibberellic acid induction of aleurone hydrolytic enzymes (Taiz and Jones 1970). However, the authors did not evidence any anticlinal /periclinal wall heterogeneity.

After 75 min xylanase treatment, xylanase is found throughout the aleurone cells as well as the connecting layer between nucellus and aleurone. This layer was first described as an amorphous layer by Evers and Reed (1988), and is a remnant of nucellar lysate. The authors suggested a relationship between its variation in thickness and the rate of water penetration into the grain. Our observations indicate that this layer could hinder xylanase penetration from the aleurone to the external layers. Moreover this nucellar lysate layer is strongly labeled by anti poorly substituted AX and is fluorescent under UV. Compared to the xylanase penetration in the aleurone wall, here the enzyme seems to proceed slowly and consequently to concentrate at this "delaying" layer. An additional incubation time between 75 min and 24 hrs and further observation would be required to elucidate the process of xylanase penetration through the nucellar layer up to the testa. The barrier effect of the nucellar lysate towards xylanase and water penetration could imply similar patterns whose mechanisms remain unknown.

Within aleurone cell walls, xylanase had opposite effects on the thin inner layer (iawl) and the thick outer layer (oawl) of aleurone cell walls. The PATAg density in these layers was not uniform, the thin iawl giving a stronger staining in contrast to the thick oawl. Moreover, the intensity of polysaccharide staining was not altered in iawl, and no antixylanase labeling was observed during the action of xylanase; a slight autofluorescence was also retained. In contrast, xylanase antibodies reacted with the oawl. In addition, the decreased PATAg staining of the oawl indicates that this layer was degraded due to polysaccharide disruption. Altogether, these observations argued for a marked variation in the composition of aleurone wall layers. Likewise, Rhodes and Stone (2002) proposed that the iawl could be richer in ferulate dimers compared to oawl. In addition, acetyl substituants and protein-polysaccharide cross-linkages through hydroxycinnamic dimerisation may be responsible for the relative resistance of the iawl to enzymatic degradation. In this respect, previous studies indicated a similar resistance pattern of this layer to the aleurone enzymes released during activation of non dormant barley therefore suggesting that the inner layer of aleurone cell wall play a physiological role during grain germination (Gubler et al. 1987).

Consistent with previous observations (Morrison et al 1975; Taiz and Jones 1973, Gubler et al. 1987), our study evidenced that aleurone cell walls are rich in plasmodesmata. These channel elements did not exhibit any visible wall alteration following bran incubation with xylanase. Meikle et al. (1994) have previously shown that specific labeling with monoclonal antibody against (1—>3)-f3-glucan is confined to areas that correspond to plasmodesmata. However, cell-wall architectures that accommodate plasmodesmata formation are not well documented. Recent studies described microdomains of pectin epitopes in the wall regions surrounding plasmodesmata (Roy et al. 1997). PATAg staining may thus originate from the occurrence of pectin in these areas. Plasmodesmata are also known to contain high glycoprotein content from the cell coat (Fisher 2000), which can react with PATAg.

Based on the ultrastructural examination of aleurone degradation by xylanase, one could argue that xylanase penetration is allowed by degradation of AX. Indeed, the subsequent disruption of the wall network may facilitate penetration of the enzyme. However, besides structural limitations, the size and distribution of the cell-wall pores are relevant factors of protein diffusion in the interwoven network. In this respect, the pore radius in wheat cell-walls ranges 1.5-4 nm (Chesson et al. 1997). In the case of our xylanase, the Stokes radius of this 20 Kdalton globular protein approximates 3-4 **nm.** This protein may have difficulty in free diffusion within the wall layer. Noteworthy, smaller pore sizes have been reported in pericarp than in aleurone (Chesson et al. 1997). The polyester rich layers (testa

and epidermis cuticle) can thus provide a tighter and hydrophobic network that can prevent enzyme penetration into the pericarp. Further studies are underway to get a more comprehensive view of the pattern of xylanase location in wheat bran. Particularly, immunocytochemical investigation of xylanase-treated pericarp and testa are in process using individual micro dissected layers. Examination of the spatial distribution of highly branched AX and of feruloylated derivatives will also provide relevant information regarding bran degradation by xylanase.

Conclusions

The changes in the wheat bran tissues, especially aleurone and nucellar layers, were examined at ultrastructural levels along the course of xylanase action. Both immuno and cytochemical observations evidenced that the AX degradation acts in a progressive way starting from the area close to the endosperm side and going outward to the nucellar layer. Xylanase location was highly connected to the distribution of low-substituted AX whose epitopes are preferentially encountered in aleurone and nucellar layers. However, apart from the enzyme-resistant pericarp, some subcellular areas appeared to be recalcitrant (inner aleurone wall layers, wall regions surrounding plasmodesmata) or partially resistant (remnant of nucellar lysate, aleurone cell wall junction). Further studies are needed to get a more comprehensive view of the specific diffusion of the xylanase throughout cell wall network.

Acknowledgements

We thank Dr Michael O'Donohue for critical view of the manuscript. This work was supported by a grant from the district of Champagne-Ardenne. Electron microscopy observations were performed at the Centre de microscopie électronique à transmission conventionnelle de l'université Paris VI, Paris, France.

Literature Cited

Aman P, E Nordkvist 1983 Chemical composition and in vitro degrability of botanical fractions of cereal straw. Journal of Agricultural Research 13:61-67.

Andreasen MF, LP Christensen, AS Meyer, A Ansen 2000 Content of phenolic acids and ferulic acid dehydrodimers in 17 rye *(Secale* cereal) varieties. Journal of Agricultural Food Chemistry 48:2837-2842.

Antoine C, S Peyron, F Mabille, C Lapierre, B Bouchet, J Abecassis, X Rouau 2003 Individual contribution of grain outer layers and their cell wall structure to the mechanical properties of wheat bran. Journal of Agricultural Food Chemistry 51:2026-2033.

Bacic A, BA Stone 1981 Chemistry and organization of aleurone cell wall components from wheat and barley. Australian Journal of Plant Physiology 8:475-495.

Benamrouche S, D Cronier, P Debeire, B Chabbert 2002 A chemical and histological study on the effect of (1-*4)-(3-endo-xylanase treatment on wheat bran. Journal of Cereal Science 36:253-260.

Benamrouche-Stitou S 2002 Biochimie et histologie de la dégradation enzymatique du son de blé par une endoxylanase. PhD diss.Université de Reims Champagne-Ardenne, Reims, France.

Brillouet JM, JP Joseleau 1987 Investigation of the structure of a heteroxylan from the outer pericarp (beeswing bran) of wheat kernel. Carbohydrate Research 159:109-126.

Carpita NC, DN Gibeaut 1993 Structural models of primary cell walls in flowering plants: consistency of molecular structure with the physical properties of the walls during growth. Plant Journal 3:1-30.

Chesson A 1988 Lignin-polysaccharide complexes of the plant cell wall and their effect on microbial degradation in the rumen. Animal Feed Science and Technology 21:219-228.

Chesson A, PT Gardner, TJ Wood 1997 Cell wall porosity and available surface area of wheat straw and wheat grain fractions. Journal of the Science of Food and Agriculture 75:289-295.

Courtin CM, JA Delcour 2001 Relative activity of endoxylanases towards water-extractable and water-unextractable arabinoxylan. Journal of Cereal Science 33:301-312.

Debeire-Gosselin M, M Loonis, E Samain, P Debeire 1992 Purification and properties of 22 kDa endoxylanase excreted by a new strain of thermophilic *Bacillus.* Pages 463-466 in J Visser, G Beldman, MA Kusters-van Somersen, AGJ Voragen, eds. Xylans and Xylanases. Elsevier Science, Amsterdam.

Erikson (J, AI Goring 1980 Structural studies on the chemical bonds between lignins and carbohydrates in spruce wood. Wood Science Technology 14:267-279.

Evers AD, M Reed 1988 Some novel observations by scanning electron microscopy on the seed coat and nucellar layer of the mature wheat grain. Cereal Chemistry 65(2):81-85.

Fisher DB 2000 Long-distance transport. Pages 748-758 in B Buchanan, W Gruissem, R Jones, eds. Biochemistry and Molecular Biology of Plants, American Society of Plant Physiologists.

Fulcher RG, TP O'Brien, JW Lee 1972 Studies on the aleurone layer, conventional and fluorescence microscopy of the cell wall with emphasis on phenol-carbohydrate complexes in wheat. Australian Journal of Biological Science 25:23-34.

Grabber JH, RD Hatfield, J Ralph 1998 Diferulate cross-links impede the enzymatic degradation of non-lignified maize walls. Journal of the Science of Food and Agriculture 77:193-200.

Gubler F, AE Ashford, JV Jacobsen 1987 The release of a-amylase through gibberellin-treated barley aleurone cell walls. Planta 172:155-161.

Guillon F, T Chevalier, JJ Ordaz Ortiz, L Quillien, JP Utille, B Bouchet, MF Devaux, L Saulnier 2002 A xylan polyclonal antibody and its use in immunocytochemical location of poorly substituted arabinoxylans in wheat grain', 3 `d European symposium Enzymes in Grain processing, September 25-27, Louvain, Belgium.

Hatfield RD, J Ralph, JH Grabber 1999 Cell wall cross-linking by ferulates in grasses. Journal of Science Food Agricultural 79:403-407.

Henrissat B, G Davies 1997 Structural and sequence-based classification of glycoside hydrolases. Current Opinion in Structural Biology 7:637-644.

Iiyama K, TBT Lam, BA Stone 1990 Phenolic acid bridges between polysaccharides and lignin in wheat internodes. Phytochemistry 29:733-737.

Izydorczyk MS, AW MacGregor 2000 Evidence of intermolecular interactions of f3-glucans and arabinoxylans. Carbohydrate Polymers 41:417-420.

Kidby DK, DJA Davidson 1973 Convenient ferricyanide estimation of reducing sugars in the nanomole range. Analysis Biochemistry 55:321-325

Lequart C, JM Nuzillard, B Kurek, P Debeire 1999 Hydrolysis of wheat bran and straw by an endoxylanase : production and structural characterization of cinnamoyl-oligosaccharides. Carbohydrate Research 319:102-111.

Maes C, JA. Delcour 2002 Structural characterisation of water-extractable and water-unextractable arabinoxylans in wheat bran. Journal of Cereal Science 35:315-326.

Marlow E, D Lane 1988 Adsorption to remove nonspecific binding. Pages 632-633 in Antibodies: A laboratory manual. Cold Spring Harbor Laboratory Press, New York.

Meikle PJ, NJ Hoogenraad, I Bonig, AE Clarke, BA Stone 1994 A (1-*3,1-*4)-f3-glucan-specific monoclonal antibody and its use in the quantification and immunocytochemical location of (1-*3,1-*4)-(3-glucans. The Plant Journal 5(1):1-9.

Migné C, G Prensier, E Grenet 1994 Immunogold labeling of xylans and arabinoxylans in the plant cell walls of maize stem. Biol Cell 81:267-276.

Morrison IN, J Kuo, TP O'Brien 1975 Histochemistry and fine structure of developing wheat aleurone cells. Planta 123:105-116.

Pellerin P, M Gosselin, JP Lepoutre, E Samain, P Debeire 1991 Enzymatic production of oligosaccharides from corncob xylan. Enzyme Microbiology Technology 13:617-621.

Reis D, B Vian, JC Roland 1993 Cellulose-glucuronoxylans and plant cell wall structure. Micron 25: 171-187

Rémond-Zilliox C, P Debeire, D Reis, B Vian 1997 Immunolocalization of a purified xylanase during hydrolysis of wheat straw stems. International Journal of Plant Sciences 158(6):769-777.

Rhodes DI, M Sadek, BA Stone 2002 Hydroxycinnamic acids in walls of wheat aleurone cells. Journal of Cereal Science 36:67-81.

Rhodes DI, BA Stone 2002 Proteins in walls of wheat aleurone cells. Journal of Cereal Science 36:83-101.

Ring SG, RR Selvendran 1980 Isolation and analysis of cell wall material from beeswing wheat bran *(Triticum aestivum).* Phytochemistry 19:1723-1730.

Roy S, AE Watada, WP Wergin 1997 Characterisation of the cell wall microdomain surrounding plasmodesmata in apple fruit. Plant Physiology 114:539-547.

Saadi A, I Lempereur, S sharonov, JC Autran, M Manfait 1998 Spatial distribution of phenolic materials in durum wheat grain as probed by confocal fluorescence spectral imaging. Journal of Cereal Science 28:107-114.

Saulnier L, MJ Crépeau, M Lahaye, JF Thibault, MT Garcia-Conesa, PA Kroon, G Williamson 1999 Isolation and structural determination of two 5,5'-diferuloyl oligosaccharides indicate that maize heteroxylans are covalently cross linked by oxidatively coupled ferulates. Carbohydrate Research 320:82-92.

Schooneveld-Bergmans MEF, MJW Dignum, JH Grabber, G Beldman, AGJ Voragen 1999 Studies on the oxidative cross-linking of feruloylated arabinoxylans from wheat flour and wheat bran. Carbohydrate Polymers 38:309-317.

Shetlar MR 1948 Chemical study of the mature wheat kernel by means of the microscope. Cereal Chemistry 25:99-110.

Stenvert NL, K Kingswood 1976 An autoradiographic demonstration of the penetration of water into wheat during tempering. Cereal Chemistry 53:141-149.

Suzuki K, S Kitamura, Y Kato, T Itoh 2000 Highly Substituted glucuronoarabinoxylans (hsGAXs) and low-branched xylans show a distinct localization pattern in the tissues of *Zea mays* L. Plant Cell Physiology 41(8):948-959.

Taiz L, RL Jones 1970 Gibberelic acid, (3-1,3-glucanase and the cell walls of barley aleurone layers. Planta 92:73-84

Taiz L, RL Jones 1973 Plasmodesmata and an associated cell wall component in barley aleurone tissue. American Journal of Botany 60(1):67-75.

Thiéry JP 1967 Mise en évidence des polysaccharides sur coupes fines en microscopie électronique. Journal de Microscopie 6:987-1018.

Wong KKY, LUL tan, JN Saddler 1988 Multiplicity of (3 (1,4) xylanase in microorganisms: functions and applications. Microbiology Review 52:305-317.

Fig. 1

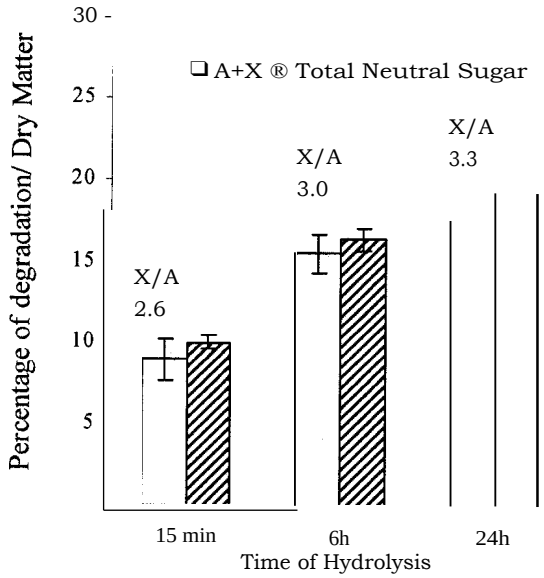

Change in the total neutral sugar (ara+gal+glc+xyl) and the total A+X (ara+xyl) recovered from acid hydrolysis of the soluble fraction released during the course of xylanase degradation of wheat bran. The percentage of degradation corresponds to the amount of neutral sugar or A+X expressed as percentage of initial bran dry matter. The X/A ratio informs us about the degree of substitution of the AX released during bran xylanase-mediated degradation. Experiments were performed in triplicates.

Fig. 2

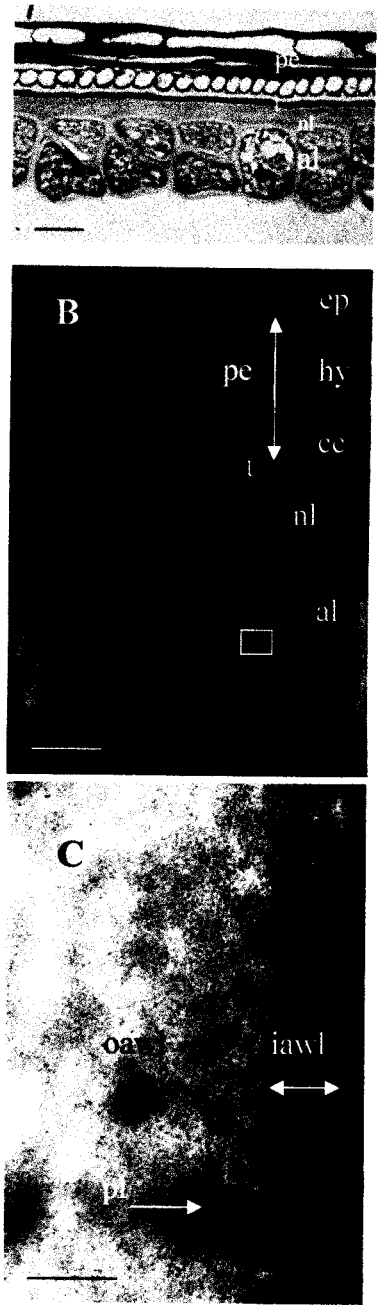

Longitudinal section of untreated wheat bran at tO (A, B, C). A, the histological features of intact wheat bran are shown by toluidine blue staining (LM). B, cell-wall phenolic autofluorescence is evidenced with exposure under UV light. Pericarp is composed of the epidermis, hypodermis, and cross cells. The frame marks the region shown in Fig. 2C. C, examination of PATAg stained aleurone (frame, Fig. 2B) shows a heterogeneous distribution of polysaccharides. The inner layer of aleurone cell walls gives an intensive staining as compared to the thick outer layer. Dark areas in the outer layer are probably plasmodesmata (TEM). al = aleurone layer; nl = nucellar layer; t = testa; cc = cross cells; hy = hypodermis; ep = epidermis; pe = pericarp; pl plasmodesmata; iawl = inner aleurone wall layer; oawl = outer aleurone wall layer. Scale bars = 40 μm in A, B; and 0.2 μm in C.

Fig. 3

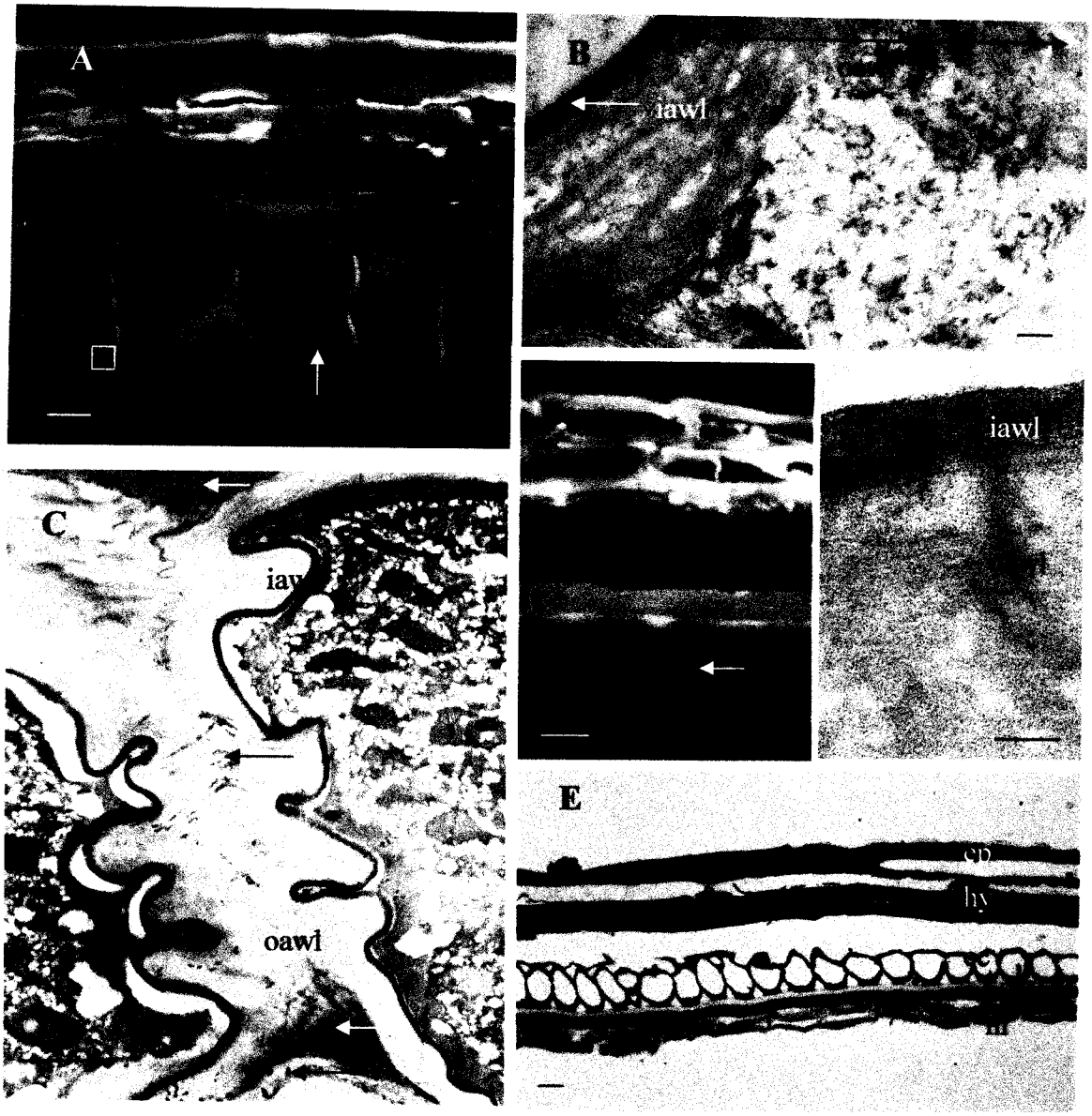

Longitudinal section of xylanase-treated wheat bran after: 30 min (A, B,), 75 min (C, D), and 24 hrs (E), or 24 hr water-treated bran (F). A, UV light microscope shows a loss of autofluorescence in the aleurone cell wall close to the endosperm (arrow). The frame marks the region shown in Fig.3B. B, PATAg staining of aleurone cell wall close to the endosperm (frame, fig. 3A), shows polysaccharide disorganization of the outer aleurone wall layer in contrast to the inner aleurone wall layer (TEM). C, PATAg staining of aleurone cell wall section of a pair of lateral aleurone cells evidences swollen cell wall, intense disorganization and loss of polysaccharides in the outer aleurone wall layer are, whereas inner aleurone wall layer keeps structural integrity. Polysaccharides are more concentrated at the junction area of the aleurone close to endosperm and in the aleurone (white arrows). Plasmodesmata (black arrows) are still present and heavily stained (TEM). D, UV-induced autofluorescence in the aleurone has disappeared, except for a thin layer surrounding the protoplast, that corresponds to the inner aleurone wall layer (arrow). E, toluidine blue staining shows that the aleurone layer is destroyed, nucellar layer is detached and partially disrupted after a 24 hr xylanase-treatment. F, PATAg of aleurone cell wall after 24 hrs of water incubation indicates no alteration of the polysaccharides within inner aleurone wall layer and outer aleurone wall layer (TEM). al = aleurone layer; cc = cross cells; ep = epidermis; hy = hypodermis; nl = nucellar layer; iawl = inner aleurone wall layer; oawl = outer aleurone wall layer; t = testa. Scale bars = 40 gin in A, D, E; 2µm in C; and 0.2 gm in B, F.

Fig. 4

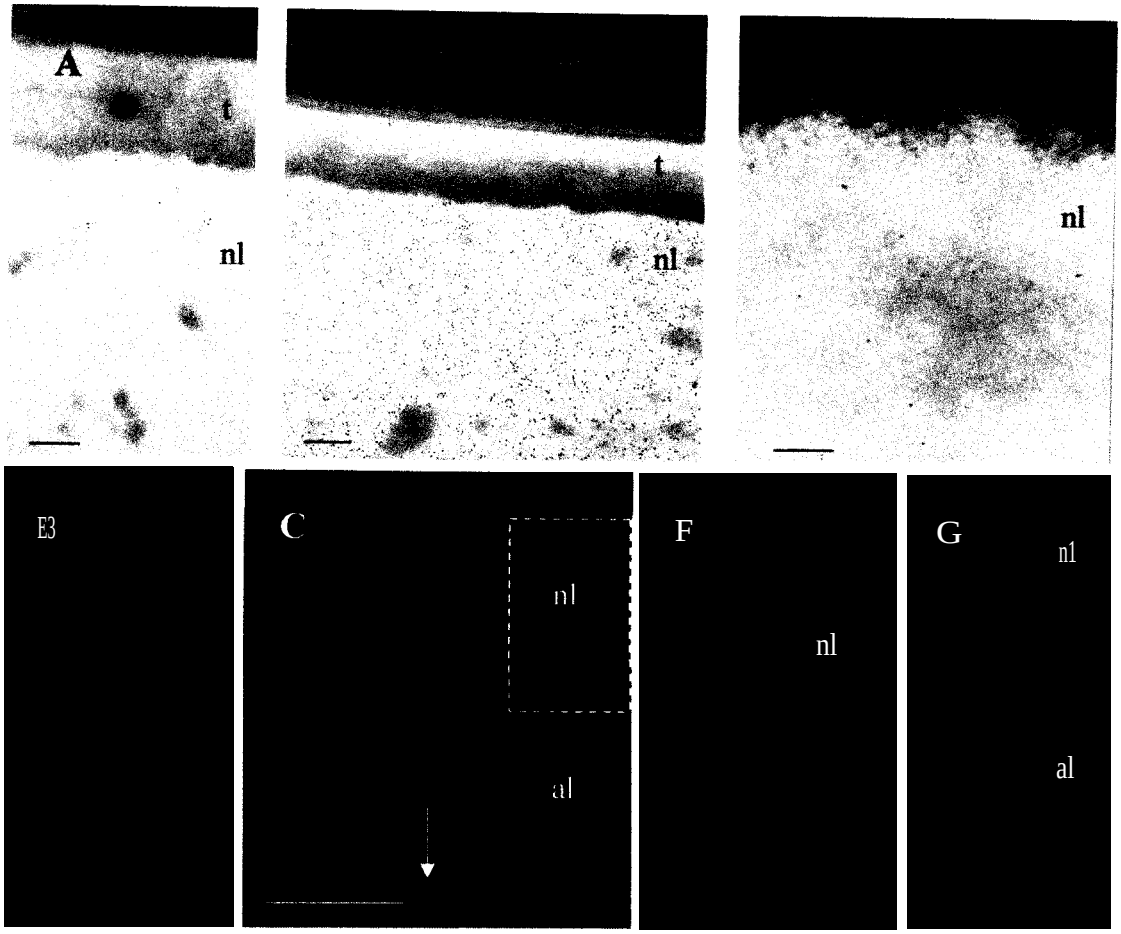

Immunolabeling of poorly substituted AX on water-treated wheat bran at: t0 (A, B), and t24 hrs (G), or xylanase-treated wheat bran after: 30 min (C), 75 min (D, F)), and 24 hrs (E). A, immunogold labeling control using the pre immune serum is not significant on wheat bran sections (TEM). B, shows immunofluorescent labeling of the wheat bran before xylanase hydrolysis. Only aleurone cell wall and nucellar layer are strongly labeled, whereas pericarp and testa structures give no reaction (LM). C, immunofluorescent labeling of an aleurone cell wall and the nucellar layer. Labeling has disappeared in the aleurone layer cell walls close to the endosperm (arrow). The frame marks the region shown in Fig. 4F (LM). D, gold particles are abundant on the nucellar layer (TEM). E, the density of gold particles is very weak in the nucellar layer (TEM). F, immunofluorescent labeling of an aleurone cell wall and the nucellar layer (frame Fig. 4C). Labeling has disappeared in the aleurone cell walls close to the nucellar layer (LM). G, immunofluorescence labeling of poorly AX in control bran. They are intact after a 24 hrs water incubation; here a two-layered aleurone cell is shown (LM). al = aleurone layer; nl = nucellar layer; pe = pericarp; t = testa. Scale bars = 40 µm in B, C, F, G; and 0.2 µm in A, D, E.

Fig. 5

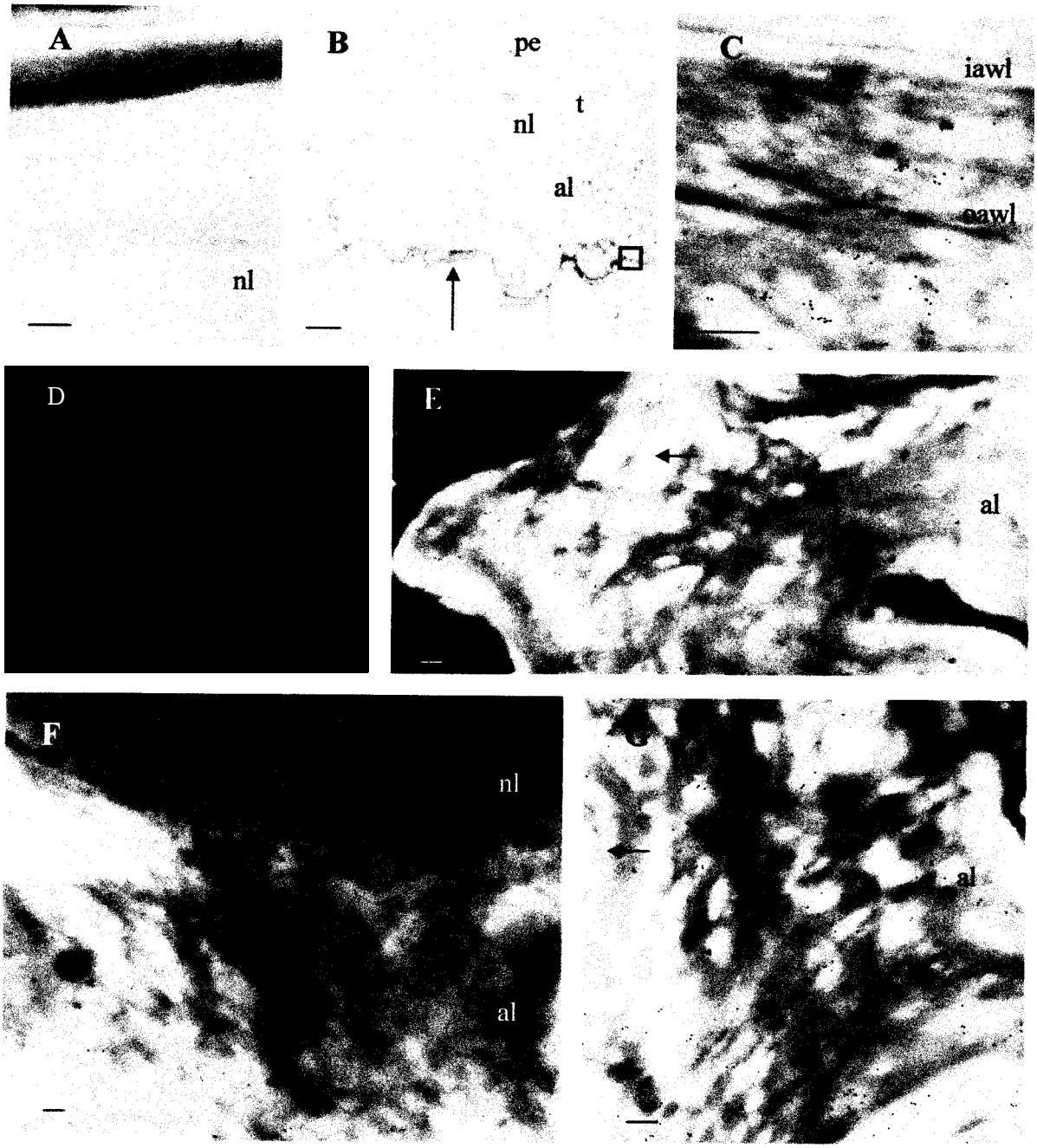

Immunolabeling of xylapase on water treated wheat bran at tO (A), and xylanase treated wheat bran after: 30 min (B, C), and 75 min (D, E, F, G). A, immunogoldlabeling control of xylanase using wheat bran without xylanase contact. No significant labeling is seen on control (TEM). B, immunogoldlabeling of xylanase after silver enhancement is abundant and located only at the aleurone cell walls close to the endosperm (arrow). The frame marks the region shown in Fig. 5C (LM). C, an enlarged view of aleurone (frame fig. 5B) shows gold particles through the outer aleurone wall layer but not on the inner aleurone wall layer (TEM). D, immunofluorescence localization indicated that xylanase is present throughout the whole aleurone layer with preferential location at junction. Aeeurone cell walls are swollen and collapsed. The upper frame marks the region shown in Fig. 5F, the middle frame marks the region shown in Fig. 5E and the

down frame shows the region in Fig. 5G (TEM). E, gold particles are less concentrated in the anticlinal aleurone wall (middle frame Fig. 5D) than at periclinal/anticlinal junctions, disassembly of the cell wall is evidenced by the presence of numerous brightened areas (black arrow) (TEM). F, immunogold labeling of the aleurone layer and the proximal part of the nucellar layer (upper frame Fig.5D) shows a non-uniform distribution of xylanase; the nucellar layer displays a heavy labeling (TEM). G, immunogold labeling of the junction wall close to the endosperm (down frame Fig. 5D) shows similar heterogeneous distribution of xylanase, as in Fig. 5F. There is more intense labeling at the junction area than in the anticlinal cell wall, Fig. 5E. The inner aleurone wall (arrow) is designable (TEM). al = aleurone layer; nl = nucellar layer; pe = pericarp; t = testa; iawl = inner aleurone wall layer; oawl = outer aleurone wall layer. Scale bars = 40 µm in B, D; and 0.2 µm in A, C, E, F, G iawl = inner aleurone wall layer; oawl = outer aleurone wall layer.

Planta, Submitted

Probing the cell-wall heterogeneity of micro-dissected wheat caryopsis using both native and inactive forms of a GH11 xylanase

Johnny Beaugrand[1], Gabriel Paës[1], Danièle Reis[2], Masayuki Takahashi[3], Philippe Debeire[1], Michael O'Donohue[1], Brigitte Chabbert[1]*

[1] Institut National de la Recherche Agronomique, UMR614 FARE, Centre de Recherche Agronomique, 2, esplanade Roland Garros, BP 224, 51686 Reims Cedex 02, France. [2] Laboratoire de Pathologie Végetale, Institut National Agronomique-Paris-Grignon, 16, rue Claude Bernard, 75232 Paris Cedex 05, France. [3] Centre National de la Recherche Scientifique, Université de Nantes, UMR6204, 2, rue de la Houssiniere, 44322, Nantes Cedex 03, France

Abstract The external envelope of wheat grain *(Triticum aestivum* L. *cv*. Isengrain) is a natural composite whose tissular and cellular heterogeneity constitute a significant barrier for enzymatic cell-wall disassembly. To better understand the way in which the cell-wall network and tissular organization hamper enzyme penetration, we have devised a strategy based on *in situ* visualisation of an active and an inactive form of a xylanase in whole-wheat bran and in three micro-dissected layers (the outer bran, the inner bran and the aleurone layer). The main aims of this study were to (i) evaluate the contribution of the cuticular layers in hampering enzyme diffusion (ii) assess the impact of the cell-wall network on xylanase penetration and (iii) to highlight cell-wall heterogeneity. To conduct this study, we created by *in vitro* mutagenesis a hydrolytically inactive xylanase that displayed full substrate binding ability, as demonstrated by the calculation of dissociation constants (Kd) using fluorescence titration. To examine enzyme penetration and action, immunocytochemical localization of the xylanases and of feebly substituted arabinoxylans was performed following incubation of the bran layers or whole bran with active and inactive enzyme for different time periods. The data obtained showed that the micro-dissected layers provided an increased accessible surface for xylanase and that the enzyme-targeted cell walls were penetrated more quickly than those in intact bran. Examination of immunolabelling of xylanase indicated that the cuticle layers constitute a barrier for enzyme penetration in bran. Moreover, our data indicate that the cell wall network itself physically restricts enzyme penetration. Inactive xylanase penetration was much lower than that of the active form, whose penetration was facilitated by the concomitant depletion of arabinoxylans in enzyme-sensitive cell walls.

Keywords: Wheat bran, Xylanase, Arabinoxylans, Cell wall, Accessibility, Mutagenesis

Introduction

Wheat bran *(Triticum aestivum)* is an arabinoxylan-rich by-product of the milling industry. Besides its main application as feed for livestock, wheat bran could be, of industrial interest for non-food products (bulk chemicals, bioenergy, etc.), notably through enzymatic bioconversion and upgrading. In addition, owing to its tissular and cellular complexity, wheat bran may be considered as an attractive model for the study of the organisational and chemical aspects of low-lignified fibrous material. Indeed, such complexity can be investigated with emphasis to glycoside hydrolase penetration and action.

Histologicaly, wheat bran is the peripheral part of the grain. From the exterior to the interior, bran is composed of the outer pericarp, comprised of epidermis (ep) and hypodermis (hy), the inner pericarp, containing cross and tube cells (cc and tc) (Shetlar 1948, Evers and Millar 2002), the testa (t), which is a complex heterogeneous layer of crushed cells (Morrisson et al. 1976), the nucellar layer (nl), a remnant of the nucellar epidermis, which is connected to the aleurone cells by an amorphous band known as the nucellar lysate (nly) (Evers and Reed 1988). The innermost aleurone layer (al) is composed of a single-cell layer that botanically covers and belongs to the starchy endosperm. The al contains the only living cells of the wheat caryopsis.

The cell walls encountered in the different tissular layers that comprise wheat bran display marked cytochemical heterogeneity. Cellulose and a small amount of lignins are found in the pericarp, whereas R-glucan is only present in aleurone wall (Fincher and Stone 1986, Brillouet and Joseleau 1987, Antoine et al. 2003). Lipophilic materials are essentially arranged as several polyester-rich cuticular layers (Matzke and Rieder 1990) that are encountered in the epidermis and the testa. Due to their composition, these layers could act as selective barriers in molecule transport (Kolattukudy 1980, Schreiber et al. 1999) and protect the grain against pathogenic aggression (Stenvert and Kingswood 1976). In cereal grains, the outer layers are generally characterized by a relatively high content in wall-bound hydroxycinnamic acids, ferulic acid (FA) and its diferulic derivative (DiFA) being the major acids in wheat bran. These phenolic species, along with traces of p-coumaric and sinapic acids, can be microscopically evidenced via their blue fluorescence that can be detected upon UV excitation (Funcher et al. 1972). In the wheat caryopsis, FA is more concentrated in aleurone, whereas the highest levels of DiFA are found in the pericarp cell-walls (Antoine et al. 2003). Hydroxycinnamic acids are known to cross-link cell-wall polymers in grasses (Hatfield et al. 1999), notably arabinoxylans (AXs) that represent approximately 40% of the dry matter in

destarched wheat bran (DWB) (Beaugrand et al. 2004a). These hemicelluloses consist of a (1–+4)-13-D xylopyranose backbone that displays a variable amount of substitution by a-L-arabinofuranose and, to a lesser extent, glucuronic acid (and its methyl-derivative) and acetyl groups (Schooneveld-Bergmans et al. 1999). Likewise, AXs are structurally variable and are heterogeneously distributed within bran layers (Brillouet and Joseleau 1987, Benamrouche et al. 2002).

For AX disruption in wheat bran, endo-(3-1,4-xylanases are the favoured enzymes as they cleave the internai (3-1,4-xylosidic linkages in the xylan backbone. In the glycoside hydrolase classification system (Henrissat 1991, Davies and Henrissat 1995), xylanases (EC 3.2.1.8) are mainly grouped in two families, GH10 and GH11. However, owing to their high efficiency towards insoluble lignocellulosic materials (Remond-Zilliox et al. 1997, Beaugrand et al. 2004b), GH11 family are better candidates for depolymerization of AX embedded in a complex composite such as the caryopsis outer-layers. In a recent study on the enzymatic degradation of wheat bran using a thermostable GH11 xylanase, we revealed differential tissue and cell-wall susceptibility to enzyme action which could be related to the distribution of the enzyme's substrate *(Le.* the poorly-substituted arabinoxylans). In contrast to the xylanase-resistant pericarp, AX depletion in both the al and nl led to a marked disassembly of the corresponding cell walls. Moreover, *in situ* visualization of the xylanase-treated bran layers revealed `micro-domains' within the cell walls that gave rise to uneven degradation patterns (Beaugrand et al. 2004c). In addition to AX structural variability, the cell wall network, which is maintained by a variety of covalent and non-covalent interactions, may also impede tissue penetration by xylanase and/or obstruct substrate accessibility. This may be particularly true in the case of the outer layers of the wheat caryopsis that display significant chemical and organizational heterogeneity.

In the present investigation we aimed to evaluate the extent to which the tissular and cellular architecture of wheat bran can act as physical barriers to xylanase action. In an attempt to circumvent the problem of the cuticular layers and to dissociate the histologically-coherent wheat bran tissues, microscope-assisted peeling of different layers was performed prior to enzymatic treatment. With regard to the enzymatic tools, we employed both the wild type (XYL 11-WT) and an engineering inactive (XYL 11-1NAC) forms of a xylanase GH11 from *Thermobacillus xylanilyticus,* which is thermostable at 60°C, and has a molecular mass of 20,692 Da (Samain et al. 1991). The time-dependant degradation of weakly substituted AX was monitored and correlated with xylanase localization using immunocytochemistry. In

parallel, the diffusion of xylanase within the targeted cell walls was assessed using XYL11-INAC that keeps high affinity for AX but did not induce wall disassembly.

Materials and methods

External layers of wheat grain

The grain-ends (brush plus germ) of mature wheat grain *(Triticum aestivum* L. cv. Isengrain) were removed using a razor blade and the remaining median parts were soaked in distilled water at 4°C during 2 h before layer isolation. A stereomicroscope was used to monitor the subsequent operations. Incisions in the crease, followed by one hour of soaking in cold distilled water permitted the removal of the endosperm by scraping the external layers. The resultant external layer of the grain, corresponding to industrial wheat bran, was designated WB. The outermost part of WB (outer bran, OB) was then carefully isolated using a scalpel and a needle. Finally, the inner bran (IB) was peeled away from the aleurone layer (AL) (Fig 1). Outer bran includes the external pericarp composed of hypodermis and epidermis, the latter being covered by a thin cuticular layer. Inner bran is made of the inner pericarp (cross and tubes cells), the testa (seed coat) and the nucellar layer. The aleurone layer is composed of single layer of aleurone cells.

Xylanase and (1—*4)-R-unsubstituted xylan antisera

The antixylanase sera was produced in New Zealand white rabbits by Eurogentec (Belgium) and prepared as described by Beaugrand et al. (2004c) following a standard protocol. An antiserum raised against a (1—>4)-P-xylotetraose-bovine serum albumin conjugate in New Zealand white rabbits was a gift from Dr F. Guillon. Indirect, competitive ELISA characterization using a large variety of oligosaccharides demonstrated that these polyclonal antibodies preferentially recognized xylotetraose and xylotetriose, indicating that *in muro* they can recognize weakly substituted xylan (Guillon et al. 2004).

Cloning and mutagenesis of the xylanase-encoding DNA sequence

The DNA encoding XYL11-WT was cloned into the *Nde I* et *Eco* RI (New England Biolabs, Ozyme, France) sites of the T7 promoter-based vector pRSETA (Invitrogen SARL, Cergy Pontoise, France). The resulting plasmid construction was then used to transform *Escherichia coli* JM109-DE3 cells. To inactivate the *T. xylanilyticus* xylanase, the catalytic nucleophile was first identified by comparison with previous work on GH11 xylanases (Tôrrônen et al.

1994, Wakarchuk et al. 1994) substitute the catalytic nucleophile, Glu [76], by a glutamine, site-directed mutagenesis was performed using a QuickChange kit (Stratagene, Amsterdam, The Netherlands) which was used according to manufacturer's instructions. To direct the mutation two complementary mutagenic primers were used:

Forward primer: 5'- CGCAACCCGCTCATCCAATACTACGTCGTCGAC-3'

After mutagenesis, the mutated plasmid was used to transform E. *coli* XL1-blue cells (Stratagene, Amsterdam, The Netherlands) that were grown on solid LB medium supplemented with ampicillin (100 µg/ml) at 37°C for 16 h. The correct introduction of the mutation was confirmed by DNA sequence analysis using a MegaBACE 1000 automated DNA sequencer (Amersham Biosciences Europe Gmbh, Orsay, France).

Xylanase production and purification

Thermobacillus xylanilyticus GH11 glycosyl hydrolase (XYL11-WT), which was isolated from the patented *Bacillus* strain D3 (Samain et al. 1991, Samain et al. 1992) was obtained and purified as previously described (Debeire-Gosselin et al. 1992). To produce XYL11-INAC, E. *coli* cells harbouring the appropriate mutated gene sequence were grown at 37°C in 1 litre of LB medium containing ampicillin (100 .tg/ml) until an absorbance (600 nm) of 0.50.6 was reached. At this stage, protein expression was induced by the addition of IPTG to a final concentration of 0.4 mM. Incubation was continued for 4–5 hours. After, cells were recovered by centrifugation at (6,000 x g, 30 min) and suspended in 100 ml buffer (20 mM Tris-HC1, 10 mM EDTA, 10 mM DTT, pH 8). Cell lysis was achieved by sonification (40 min) using a Vibra-cell 72412 (Bioblock Scientific, Illkirch, France). Cell debris was removed by centrifugation (10,000 x g, 15 min) and the protein-containing supernatant was recovered. Purification of XYL11-INAC was achieved using a chromatographic procedure identical to that used for the purification of XYL11-WT (Debeire-Gosselin et al. 1992). The degree of purity of both xylanases was verified using SDS-PAGE and the molecular weight of XYL 11-INAC was measured by MALDI-TOF mass spectrometry using a Voyager-DE spectrometer (Perseptive Biosystems, USA). For mass analysis, 4-hydroxy-3,5-dimethoxycinnamic acid matrix dissolved in 50% (v/v) acetonitrile and 0.1% (v/v) trifluoroacetic acid was used as the matrix. XYL 11-WT was used as a mass standard and spectral acquisitions were repeated ten times.

Xylanase characterisation

Xylanase activity was determined by monitoring the release of reducing sugars using a colorimetric method (Kidby and Davidson 1973). The substrate, birchwood xylan (Sigma-

Aldrich SARL, St. Quentin-Fallavier, France) was prepared at a concentration of 5 mg/ml in 50 mM sodium acetate, pH 5.8. Measurements were performed by incubating the substrate with xylanase for 10 min at 60°C in a final volume of 1 ml. Every two minutes, 150 µl were removed and mixed with 1.5 ml of Kidby solution (1% Na_2CO3 and 0.03% potassium hexacyanoferrate (III)) coloration was developed by heating in a water bath (100°C) for 10 min. Absorbance was measured at 420 nm. The amount of released sugar was estimated using a xylose calibration curve (0–400 µg/ml) and activity units (IU) were defined as the quantity of enzyme needed to release 1 'mol of equivalent xylose per minute.

To verify correct folding XYL11-INAC, a protein solution (5 µM in 50mM K_2HPO_4, pH 6.5) was examined by circular dichroism using a J-810 spectrometer (Jasco, Japan). Measurements were performed at 20°C using a quartz cell (1.0 cm path length). The buffer signal was subtracted and data were averaged from two acquisitions.

Substrate binding functionality of XYL11-INAC was compared to that of XYL11-WT using fluorescence spectroscopy. The substrates xylotetaose (X_4) and xylopentaose (X_5) were purchased from Megazyme (Co. Wicklow, Ireland). Freshly purified XYL11-WT and XYL11-INAC were exhaustively dialysed against 2 x 100 volumes of 50 mM sodium acetate, pH 5.8. Enzyme concentrations were estimated by measuring the absorbance at 280 nm using a molar extinction coefficient of 218 592 $M^{-1}cm^{-1}$. Fluorescence was measured at 5°C on a FP-6500 spectrofluorimeter (Jasco, Japan) equipped with a Peltier temperature controller using a 1.0 x 1.0 cm quartz cell under continuous stirring. Titration of (active site) tryptophan fluorescence using X_4 of X_5 was performed with 1.8 ml of protein solution (0.1 µM). Tryptophan excitation was achieved at 295 nm and emission spectra were collected in duplicate over the wavelength range 300-450 nm, using a band width of 3 nm for both excitation and emission (response time of 0.2 s and scan rate of 100 nm/min). Fluorescence spectra were corrected for buffer fluorescence and volume changes that were always inferior to 2% (v/v). To calculate the dissociation constant Kd, fluorescence intensity changes were recorded at 320 nm and 360 nm. Likewise, for each oligosaccharide concentration [L], the change in fluorescence $3,F = F_{360,,m} - F320»m$ was calculated and a plot of $MF(= AF_o - OF$, where AF_0 is fluorescence of unbound protein) versus [L] was plotted. To obtain Kd and MF_m, the resulting curve was fitted to the hyperbolic equation $MF = \frac{.àAFmax_{IL}}{Kd + [L]}$ using SigmaPlot 6.1 (SPSS, IL, USA). Gibb's free energy changes were calculated using the equation $-4G = RT \ln K$, where R is Boltzmann's constant, T is temperature in K and K is the calculated Kd.

Xylanase treatment of bran layers

Whole bran (WB), OB, IB and AL parts were hydrated in distilled water (3% w/v) for 16 h at 60 °C. After, 0.5 IU/ml of XYL11-WT or an equivalent amount of XYL11-INAC was added and incubation at 60°C was continued with gentle agitation (Polymax 1040, Heidolph). Water-incubation controls without enzyme were also performed. XYL11-WT or XYL11-INAC-treated bran layers were removed for microscopic examination after different incubation periods: 15 and 30 min for AL, 30 and 75 min for OB and IB, 30 min, 75 min and 24 h for WB. Water-treated controls were examined at 75 min (OB, IB, AL, and WB) and 24h (WB).

Sample embedding

Small hand-cut specimens were fixed using a glutaraldehyde solution (2%) in phosphate buffer (0.1 M, pH 7.4) for 1 h at room temperature under vacuum. Alter several washes of 15 min in phosphate buffer then in distilled water, samples were dehydrated in an ethanol series over 48 h and then gradually infiltrated (over 72 h) with increasing concentrations (up 100%) of LR White resin (Sigma-Aldrich SARL, St. Quentin-Fallavier, France). The samples were finally polymerised in fresh LR White resin at 60 °C for 24 h.

Microscopic observations

Immunolabelling was performed on semi-thin sections (0.5 .tm thick) deposited on glass multiwell slides for light microscopy (LM) and on ultra thin sections (80-90 nm) placed on nickel grids for electron microscopy (EM). Immunolabelling was performed by incubating samples (4 h at room temperature) with antixylanase serum (1/320 dilution) and anti (1— 4)-J3-unsubstituted xylan (1/500 dilution) and the corresponding pre-immune serum as described previously (Beaugrand et al. 2004c). Gold-labelled (5 nm for LM and 10 nm for EM) goat antirabbit immunoglobulin G conjugate (British Biocell International, Cardiff, UK) was used as secondary antibody at 1/40 dilution and incubated for 1 h. For LM observations, gold-labelling was silver enhanced (7 min at room temperature) using an appropriate reagents kit (Amersham Biosciences Gmbh, Orsay, France). Sections were then covered with Eukitt mounting medium (Electron Microscopy Sciences, PA, USA). Several immunolabelling controls were prepared as previously described (Beaugrand et al. 2004c) in order to ensure that labelling was specific. Cytochemical observations of the bran cell-walls were further investigated by monitoring the blue fluorescence of phenolic compounds upon excitation at 340 nm. LM observations were performed using an Axioskop microscope (Cari Zeiss AG, Oberkochen, Germany) equipped with an AxioCam MRc digital camera, under bright light or

mercury lamp (UV excitation and epipolarisation for immunogold labelling), EM examinations were obtained with a Philips 201 transmission electron microscope operating at 80 kV.

Results

Characterisation of the mutant xylanase, XYL 11-INAC

Site directed mutagenesis engineering was used to mutate one of the diade catalytic-residues in the way that modifications in volume occupation and substrate affinity would be minimized in the inactive xylanase. SDS-PAGE showed that XYL11-INAC was purified to homogeneity. Mass spectrometry revealed a molecular weight of 20,648 ± 2 Da, which is nearly identical to the theoretical mass of 20,649 Da. Comparison of the circular dichroism spectra obtained for wild type and XYL 11-WT and XYL 11-INAC were superimposable, indicating that the mutation $Glu^{76}Gln$ did not lead to major alterations of secondary structure (Fig 2). Coherent with the loss of an essential element of the catalytic machinery (Koshland 1953), the XYL11-INAC did not display any activity towards birchwood xylan, even after a prolonged (8 h) incubation period. To investigate substrate binding by XYL11-INAC, titration of tryptophan fluorescence was performed using X_4 and X_5. These experiments were performed at 5°C in order to reduce substrate hydrolysis by XYL11-WT. At this temperature XYL11-WT exhibited a specific activity of 10 IU/mg on birchwood xylan (i.e. 0.5% of its activity at 60°C). Therefore, we considered that the substrate remained approximately constant during the titration. The titration of tryptophan fluorescence in either xylanase produced a measurable quenching effect that was accompanied by a blue shift in the spectra (Fig 3). This difference is dependent on the substrate concentration according to the curve shown in Fig 4 for XYL11-INAC and X_5. Calculated dissociation constants are reported in Table 1. Both xylanases exhibited higher affinity for X_5 compared to that for X_4. However, compared to XYL11-WT, XYL11-INAC displayed higher affinity for both substrates, this difference being more pronounced in the case of X_5. Changes in free energy, $\Delta G°$, were also calculated (Table 1). The $\Delta G°$ values showed similarity for XYL 11 and XYL11-INAC and were very close to those computed by Hegde et al. (1998) for the interaction of X_4 and X_5 (– 20,2 and – 20,5 kJ mol^{-1} respectively) with another GH11 xylanase from *Chainia sp.*

Microscopic examination of wall-bound phenolic fluorescence during bran degradation

As in a previous study (Beaugrand et al. 2004c), the UV-induced autofluorescence of phenolic cell-wall compounds was exploited in order to monitor *in situ* bran layer degradation by

xylanase. Compared to water-treated control, no significant changes of WB were observed upon incubation with XYL11-INAC for 24 h (Fig 5a). Similarly, XYL11-INAC (24 h incubation) did not alter the blue autofluorescence associated with the WB and the three micro-dissected layers, IB, OB and AL. Interestingly, in IB (Fig 5b) some small, highly fluorescent, triangular-shaped zones were observed along the exposed side of the nucellar layer (nl), which presumably correspond to nucellar lysate (nly) (Evers and Reed 1988). Although less visible, these areas were also evidenced in WB. The OB displayed weaker fluorescence (Fig 5c), whereas AL (Fig 5d) was the most fluorescent, which is consistent with WB observations. Incubation with XYL11-WT did not induce any visible change in the OB-associated fluorescence even after 24 h (not shown). In contrast, XYL11-WT induced significant alteration of the autofluorescence and the structural integrity of IB and AL cell walls. After only 15 min, XYL11-WT had penetrated the AL and provoked therein the loss of autofluorescence within the two periclinal walls and their prolonged anticlinal walls (Fig 5e), in contrast to WB degradation where al destructuration proceeds from the periclinal walls closed to the starchy endosperm (Beaugrand et al. 2004c) After 30 min, the cell walls had collapsed and were structurally altered (Fig 5f). At this point, XYL11-WT penetration was complete and only a faint blue fluorescence was visible, corresponding to the inner aleurone wall layer. When IB was treated with XYL 11-WT, the loss of blue fluorescence was more progressive. Alter 30 min, a diminution of autofluorescence was observed at the exposed face of the nl, this effect became generalised throughout the nl after 75 min (data not shown).

Immunolabelling of XYL11-WT and XYL11-INAC on bran samples

The distribution of XYL11-WT or XYL11-INAC in AL, OB, IB and WB was examined after different incubation periods using polyclonal antibodies. LM observation of highly contrasted labelling was possible using epipolarisation system, with which gold particles are visualised as bright spots. Consistent with our previous report on WB treatment by XYL11-WT (Beaugrand et al. 2004c) neither of the two xylanases (WT or INAC) could be detected in the OB, even though the hy layer was in direct contact with the enzymes. Following a 30-min treatment with XYL 11-WT, antixylanase labelling of IB (Fig 6a) was localized in a thin layer on the external face of the nl, which presumably represents the amorphous layer which in WB constitutes the interface between AL and nl, the nucellar lysate (nly). After further incubation (75 min) (Fig 6b), XYL11-WT labelling was localized throughout the nl and nly was no longer visible. Inversely, no antixylanase labelling of XYL11-WT was observed in the inner pericarp (cross cells), even after a 75 min treatment. Immunolabelling of XYL11-INAC

revealed that after 75 min its distribution within IB was similar to the pattern observed with XYL11-WT after 30 min (Fig 6f), indicating that the lack of catalytic activity slows down xylanase penetration of the nly. Electron microscopic observation of XYL11-WT or XYL11-INAC-treated IB (after 75 min incubation), showed a heterogeneous distribution of XYL11-WT (Fig 6d) across the nl, with a graduat increase in labelling near the testa. In contrast, in intact nl, the XYL11-INAC was mainly found at the distal area from the testa (Fig 6e) and very little labelling was evidenced deeper in the wall. After 75 min in the presence of AL, XYL11-INAC was located in the periclinal wall layers (Fig 6c). In the case of WB, after 75 min only the exposed peripheral aleurone cell walls were labelled (Fig 6g). After an extended incubation period (24 h), XYL 11-INAC was more generalised within the aleurone cells, although labelling was progressively weaker towards the nl (6h). Importantly, the penetration of XYL11-INAC into the cell walls did not induce any visible alteration autofluorescence. In addition, it was noted that XYL11-INAC exhibited a high affinity for the residual endosperm cell walls (sew in Fig 7), which is consistent with the presence of poorty substituted AX in the endosperm (Tervila-Wito et al. 1996, Lempereur et al. 1997).

Immunolabelling of (1—*4)-(3-unsubstituted xylan in bran samples

Labelling of XYL 11-INAC-treated WB (24 h incubation) with arabinoxylan-specific polyclonal antibodies revealed that like water-treated WB (Beaugrand et al. 2004c) poorty substituted AX were distributed throughout the AL cell wall and were highly concentrated across the whole nl (Fig 8a). Treatment (75 min) of micro-dissected AL (Fig 8b) and IB (Fig 8c) with XYL11-INAC gave rise to similar tissue-specific labelling patterns of AX. Interestingly, AX immunolabelling also revealed a degree of cellular heterogeneity in nl and AL. In ni, AX labelling revealed three layers that were evidenced on the basis of distinct labelling density. This micro heterogeneity was clearly observed on IB, but less so in WB. In the micro-dissected AL strip intense, labelling was observed at the anticlinal-periclinal junctions. Finally, no AX labelling was detected in the micro-dissected OB strip (data not shown), coherent with similar observations made for WB.

Cytochemical and immunological controls

Immunological controls were performed for the two antibodies tested. As previously reported for WB (Beaugrand et al. 2004c), the controls performed for xylanase-specific immunolabelling did not reveal labelling when (i) bran strips were not treated with either XYL11-WT or XYL11-INAC and (ii) when the primary antibody was omitted. Similarly,

bran samples incubated with the (1–4)-(3-unsubstituted xylan pre-immune serum gave no significant labelling as illustrated with IB after 75-min enzyme treatment (Fig 8d). Therefore, one can conclude that all immunocytochemical probes were specific, thus allowing reliable data interpretation.

Discussion

Investigation of plant cell walls using non-invasive methods such as cytochemistry (especially blue fluorescence emission by cell wall-associated phenols), or immunocytochemistry provide specific chemical information at both cellular and subcellular levels (Willats et al. 2000). Such techniques have allowed significant advancements in knowledge, even though numerous artefacts related to sample preparation may complicate data interpretation (McCann et al. 1990, Thimm et al. 2000). More specifically, enzyme immunolabelling has been widely employed to investigate plant cell-wall biosynthesis and biodegradation (Daniel et al. 1989, Reis et al. 1993). More recently, the use of inactive enzymes seems promising as tools for probing substrates in their native form (Adams et al. 2004). However, in order for such tools to provide reliable data, rigorous analysis of mutated enzymes is necessary to ascertain whether the loss of catalytic properties is accompanied by a loss of substrate binding capacity. In this study, we took a variety of precautions before using a hydrolytically-impaired xylanase. In particular, circular dichroism provided confirmation of correct overall folding, while binding studies using fluorescence spectrophotometry allowed accurate determination of dissociation constants Kd for both the active and inactive xylanase forms. Importantly, titration with relevant substrates such as xylotetraose or xylopentaose unequivocally demonstrated that XYL11-WT and XYL11-INAC display similar substrate affinities. The apparent higher affinity of XYL 11-INAC over XYL 11-WT for $Xy1_5$ could be explained by the fact that the latter enzyme is weakly active at 5°C; consequently, substrate saturation is hardly obtained giving rise to an apparent weaker binding energy in contrast to XYL11-INAC. Moreover, calculation of AG ° values for binding indicated that the mode of substrate interaction for both enzymes was highly similar. Finally, the fact that (i) antixylanase antibodies recognize XYL11-INAC *in situ* in bran cell walls and (ii) XYL11-INAC did not induce any loss of UV fluorescence or degradation of the poorly substituted AX further confirmed the usefulness of this inactive enzyme probe.

Previously, we have shown that the poorly-substituted arabinoxylans are not uniformly distributed within bran tissues and that xylanase location appears closely connected to AX degradation (Beaugrand et al. 2004c). Upon xylanase treatment, drastic alterations in the cell

wall network occur and UV-induced blue autofluorescence is partially lost due to the release of phenolic acids from al and nl in the form of cinnamoyl-xylooligosaccharides (Lequart et al. 1999). Furthermore, xylanase-induced AX depletion in bran was shown to proceed in a sequential manner. The enzyme begins with the periclinal walls, which are normally in direct contact with the starchy endosperm, then degrades the anticlinal walls and finally invades the nl. Ultra structural examination of xylanase-degraded cell walls suggested that xylanase penetration would be enhanced by AX degradation.

In this work we showed that both OB and IB, with the exception of nl, were recalcitrant to any labelling. In contrast, the micro-dissected AL treated by XYL11-WT was clearly penetrated in a bipolar manner, certainly due to the fact that AL isolation provided a second exposed surface for enzyme action. Indeed in WB where only the endosperm side of AL is exposed, this phenomenon is not observed. Despite this difference, the final cytological alterations were similar: the inner cell walls of aleurone seem not altered. Significantly, in IB, exposure of the two tissular interfaces did not provide suitable access for bidirectional enzyme penetration. Therefore, it is likely that xylanase cannot traverse the lipophilic layers present in IB. Moreover, it is important to note that although the cuticular layers in the enzyme-insensitive pericarp are commonly thought to be obstacles for enzyme action on WB, this consideration is irrelevant with regard to the micro-dissected OB and IB layers. Here, our data clearly show that xylanase did not induce any alterations in the hypoderma cells in OB or the cross cells in IB. Chemical analysis of the different bran layers (Benamrouche et al. 2002) has already revealed another potentially major obstacle for pericarp degradation. Pericarp-associated AXs are highly ramified by arabinose, making them theoretically unsuitable substrates for XYL11-WT action. However, it is well known that arabinosyl substitutions can be unevenly distributed along the xylose backbone (Chanliaud et al. 1995, Dervilly et al. 2000, Adams et al. 2004, Dervilly-Pinel et al. 2004). In the case of pericarp AX, this would appear to be true because the use of alkaline-extracted pericarp AX as substrate for XYL 11-WT has revealed weak but detectable activity (Beaugrand et al. 2004b). Likewise, one might expect limited enzyme-specific of zones on pericarp AX devoid of arabinose labelling in the pericarp when using XYL 11-INAC and/or local detection using the AX-specific antibody. This was not the case, suggesting that (i) the low activity of xylanase towards extracted pericarp AX is not sufficient to allow significant binding of the same AX by the enzyme when it is localized *in situ* in a structured cell wall context and (ii) that the AX-specific antibodies cannot recognize its infrequently-occurring xylo-oligosaccharide epitope within the same complex, structured context.

In al and nl cell-walls that were shown to be sensitive to XYL11-WT action, XYL11-INAC penetration was drastically reduced. Hence, one can conclude that xylanase penetration is intrinsically linked to AX degradation, with progressive cell wall disassembly facilitating cell wall penetration. Therefore, physical constraints associated both with enzyme size and structure and with the interwoven cell wall network must be considered as relevant factors for determining enzyme diffusion. Likewise, the partial penetration of al by XYL11-INAC after a 24 h-incubation period could be partially attributed the prolonged exposure of the bran tissue to water treatment at 60°C. It is possible that such treatment induced a loosening of the cell wall network, thus facilitating diffusion of XYL11-INAC. In the case of the pericarp and testa, little or no relevant substrate (poorly substituted arabinoxylans) appeared to be available for XYL11-WT action. Therefore, xylanase penetration of these tissues is probably solely dependant on the ability of the xylanase to diffuse (Srebotnik et al. 1988) that rely on possible unspecific interaction with the wall polymers and steric hindrance of the wall network. Since no apparent penetration was observed, we can conclude that, consistent with data obtained by Chesson et al. (1997), the narrow pores that occur in pericarp cell walls exclude the xylanase based on its size (20 kDa). Overall, these findings have important implications for the *in situ* probing of plant cell wall components. Clearly, in the absence of a degrading ability many of the largest protein probes would encounter penetration/diffusion problems linked to the cell wall network/pore size besides potential interaction with the wall components.

Finally, it is noteworthy that AX immunolabelling in IB revealed three distinct layers within the nl, whereas only two are usually visible in DWB. This phenomenon is likely to be due to grain compression. Within nl, both inactive and active forms of the xylanase appeared to be trapped within the nly, even though some disintegration of this strata did occur using active enzyme. Therefore, a detailed analysis of chemical composition and cell wall arrangement of nly should provide further insight into the nature of obstacles that limit xylanase action.

In conclusion, we have shown that the combination micro-dissection techniques and use of active and inactive forms of a xylanase is a useful strategy for the study of histologically complex plant structures such as wheat bran. Likewise, it is possible to probe tissular resistance to enzyme treatment and investigate the impact of organized cell wall architecture on substrate accessibility. In particular, our data highlight the fact that enzyme penetration/diffusion is a key parameter when the substrate is contained within intact cell walls. Our work thus confirms the usefulness of mutated enzymes as tools for the study of enzyme diffusion in plants cell-wall networks. More generally, the results of this work provide some important indicators for the future use of protein probes for the *in muro*

investigation of the cell-wall composition and architecture. Further enzyme engineering aimed at optimising enzyme size and modulating enzyme activity will provide a variety of tools that can be coupled to appropriate microscopic analyses to get in-depth knowledge at the organizational heterogeneity of plant cell-walls.

Abbreviations

AL micro-dissected aleurone layer, al aleurone cell, cc cross cell, DiFA diferulic acid, EM electon microscopy, ep epiderm, FA ferulic acid, hy hypoderm, IB inner bran, LM light microscopy, nl nucellar layer, nly nucellar lysate, sew starchy endosperm wall, t testa, tc tube cell, OB outer bran, UV ultraviolet, WB wheat bran, XYL11-WT (1--►4)-J3-endoxylanase (EC 3.2.1.8), XYL 11-INAC inactive catalytic mutant of XYL 11-WT.

Acknowledgements

We gratefully thanks Dr Fabienne Guillon (URPOI, INRA, Nantes) for the gift of anti (1--44)-(3-unsubstituted xylan antiserum. This work was supported by a grant from the district of Champagne-Ardenne. Electron microscopy observations were performed at the Centre de microscopie électronique à transmission conventionnelle de l'Université ParisVl, Paris, France.

References

Adams EL, Kroon PA, Williamson G, Gilbert HJ, Morris VJ (2004) Inactiveted enzymes as probes of the structure of arabinoxylans as observed by atomic force microscopy. Carbohyd Res 339:579-590

Antoine C, Peyron S, Mabille F, Lapierre C, Bouchet B, Abecassis J, Rouau X (2003) Individual contribution of grain outer layers and their cell wall structure to the mechanical properties of wheat bran. J Agric Food Chem 51:2026-2033

Beaugrand J, Crônier D, Debeire P, Chabbert B (2004a) Arabinoxylan and hydroxycinnamate content of wheat bran in relation to endoxylanase susceptibility. J Cereal Sci In press

Beaugrand J, Chambat G, Wong V, Goubet F, Rémond C, Paës G, Benamrouche S, Debeire P, O'Donohue M, Chabbert B (2004b) Impact and efficiency of GH10 and GH11 thermostable endoxylanases on wheat bran and alkali-extractable arabinoxylans. Carbohyd Research In press

Beaugrand J, Reis D, Guillon F, Debeire P, Chabbert B (2004c) Xylanase-mediated hydrolysis of wheat bran. Evidence for subcellular heterogeneity of cell walls. Int J Plant Sci In press

Benamrouche S, Crônier D, Debeire P, Chabbert B (2002) A chemical and histological study on the effect of (1—*4)-(3-endo-xylanase treatment on wheat bran. J Cereal Sci 36:253-260

Biely P, Vrsanskà M, Tenkanen M, Kluepfel D (1997) Endo-P-1,4-xylanases families: differences in catalytic properties. J Biotech 57:151-166

Brillouet JM, Joseleau JP (1987) Investigation of the structure of a heteroxylan from the outer pericarp (beeswing bran) of wheat kernel. Carbohyd Res 159:109-126

Chanliaud E, Saulnier L, Thibault J-F (1995) Alkaline extraction and characterisation of heteroxylans from maize bran. J Cereal Sci 21:195-203

Chesson A, Gardner PT, Wood TJ (1997) Cell wall porosity and available surface area of wheat straw and wheat grain fractions. J Sci Food Agr 75:289-295

Daniel G, Nilsson T, Pettersson B (1989) Intra- and extracellular localization of lignin peroxidase during the degradation of solid wood and wood fragments by *Phanerochaete chrysosporium* by using transmission electron microscopy and immuno-gold labeling. Appl Environ Microbiol 54:871-881

Davies GJ, Henrissat B (1995) Structures and mechanisms of glycosyl hydrolases. Structure 3:853-859

Debeire-Gosselin M, Loonis M, Samain E, Debeire P (1992) Purification and properties of a 22kDa endoxylanase excreted by a new strain of thermophilic *Bacillus.* In Visser J, Beldman G, Kusters- van Someren MA, Voragen AGJ (eds) Xylans and Xylanases. Elsevier Science Publishers BV, Amsterdam, pp 463-466

Dervilly G, Saulnier L, Roger P, Thibault J-F (2000) Isolation of homogeneous fractions from wheat water-soluble arabinoxylans. Influence of the structure on their macromolecular characteristics. J Agr Food Chem 48:270-278

Dervilly-Pinel G, Tran V, Saulnier L (2004) Investigation of the distribution of arabinose residues on the xylan backbone of water-soluble arabinoxylans from wheat flour. Carbohyd Polym 55:171-177

Evers AD, Reed M (1988) Some novel observations by scanning electron microscopy on the seed coat and nucellar layer of the mature wheat grain. Cereal Chem 65:81-85

Evers T, Millar S (2002) Cereal grain structure and development: some implication for quality. J Cereal Sci 36:261-284

Fincher GB, Stone BA (1986) Cell walls and their components in cereal grain technology. In Advances in Cereal Sciences, Pomeranz Y (eds), AACC: St Paul; MN, Vol 8 pp207-295

Fulcher RG, O'Brien TP, Lee JW (1972) Studies on the aleurone layer, conventional and fluorescence microscopy of the cell wall with emphasis on phenol-carbohydrate complexes in wheat. Aust J Biol Sci 25:23-34

Guillon F, Tranquet O, Quillien L, Utille JP, Ordaz Ortiz JJ, Saulnier L (2004) Generation of polyclonal and monoclonal antibodies against arabinoxylans and their use for immunocytochemical localization of arabinoxylans in cell walls of the wheat grain endosperm. J Cereal Sci (in press)

Hatfield RD, Ralph J, Grabber JH (1999) Cell wall cross-linking by ferulates in grasses. J Sci Food Agric 79:403-407

Hegde SS, Kumar AR, Ganesh KN, Swaminathan CP, Khan MI (1998) Thermodynamics of ligand (substrate/end product) binding to endoxylanase from *Chainia* sp. (NCL-82-5-1): isothermal calorimetry and fluorescence titration studies. Biochim Biophys Acta 1388:93-100

Henrissat B (1991) A classification of glycosyl hydrolases based on amino acid sequence similarities. Biochem J 280:309-316

Hildèn L, Daniel G, Johansson G. (2003) Use of a fluorescent, carbohydrate-binding module from Phanerochaete chrysosporium Ce17D for studying wood cell wall ultrastructure. Biotchnol Lett 25: 553-558

Kidby DK, Davidson DJ (1973) A convenient ferricyanide estimation of reducing sugars in the nanomole range. Anal Biochem 55:321-325

Kolattukudy P (1980) Biopolyester membranes of plants: cutin and suberin. Science 208:990-999

Koshland DE (1953) Stereochemistry and the mechanism of enzymatic reactions. Biol Rev 28:416-436

Lempereur I, Rouau X, Abecassis J (1997) Genetic and agronomic variation in arabinoxylan and ferulic acid contents of durum wheat *(Triticum durum L.)* grain and its milling fractions. J Cereal Sci 25:1-8

Lequart C, Nuzillard J, Kurek B, Debeire P (1999) Hydrolysis of wheat bran and straw by an endoxylanase : production and structural characterization of cinnamoyl-oligosaccharides. Carbohyd Res 319: 102-111

Matzke K, Riederer M (1990) The composition of the cutin of the caryopses and leaves of *Triticum aestivum* L. Planta 182:461-466

McCann MC, Wells B, Roberts K (1990) Direct visualisation of cross-links in the primary cell wall. J Cell Sci 96:323-334

Morrisson IN, Kuo J, O'Brien TP (1976) Histochemistry and fine structure of developing wheat aleurone cells. Planta 123:105-116

Reis D, Vian B, Roland JC (1993) Cellulose-glucuronoxylans and plant cell wall structure. Micron 25:171-187

Rémond-Zilliox C, Debeire P, Reis D, Vian B (1997) Immunolocalization of a purified xylanase during hydrolysis of wheat straw stems. Int J Plant Sci 158:769-777

Samain E, Debeire P, Debeire-Gosselin M, Touzel J-P (1991) Xylanase, souches de Bacillus productrices de xylanases et leurs utilisations. Patent FR-9101191

Samain E, Touzel J-P, Brodel B, Debeire P (1992) Isolation of a thermophilic bacterium producing high levels of xylanase. In Visser J, Beldman G, Kusters- van Someren MA, Voragen AGJ (eds) Xylans and Xylanases. Elsevier Science Publishers BV, Amsterdam, pp 467-470

Schooneveld-Bergmans MEF, Beldman G, Voragen AGJ (1999) Structural features of (Glucurono)arabinoxylans extracted from wheat bran by barium hydroxide. J Cereal Sci 29:63-75

Schreiber L, Hartmann K, Skrabs M, Zeier J (1999) Apoplastic barriers in roots: chemical composition of endodermal and hypodermal cell walls. J Exp Bot 50:1267-1280

Shetlar MR (1948) Chemical study of the mature wheat kernel by means of the microscope. Cereal Chem 25:99-110

Srebotnik E, Messner K, Foisner R (1988) Penetrability of white rot-degraded pine wood by the lignin peroxydase of *Phanerochaete chrysosporium*. Appl Environ Microbiol 54:2608-2614

Stenvert NL, Kingswood K (1976) An autoradiographic demonstration of the penetration of water into wheat during tempering. Cereal Chem 53:141-149

Tervilit-Wilo A, Parkkonen T, Morgan A, Hopeakoski-Nurminen M, Poutanen K, Heikkinen P, Autio K (1996) *In vitro* digestion of wheat microstructure with xylanase and cellulase from *Trichoderma reesei.* J Cereal Sci 24:215-225

Thimm JC, Burritt DJ, Ducker WA, Melton LD (2000) Celery *(Apium graveolens* L.) parenchyma cell walls examined by atomic force microscopy: effect of dehydration on cellulose microfibrils. Planta 212:25-32

Figures

Figure 1 – Schematic representation of a cross-section of wheat bran *(Triticum aestivum)* and its three constituent layers obtained by micro dissection.

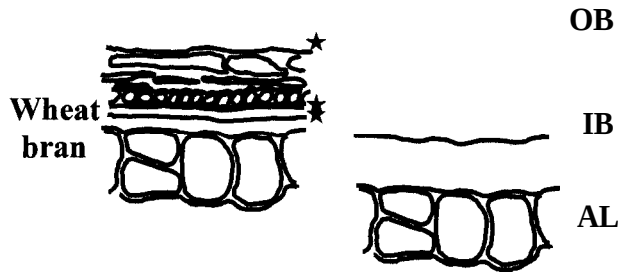

OB represents the outer bran layers constituted by the epidermis and hypoderm. IB (inner bran) is composed of the tube cells and cross cells, the testa and the nucellar layer. AL is a homogenous single cell layer. Stars indicate the location of cuticular layers.

Figure 2 – Circular dichroism spectra of XYL 11-WT (black line) and XYL 11-INAC (grey line).

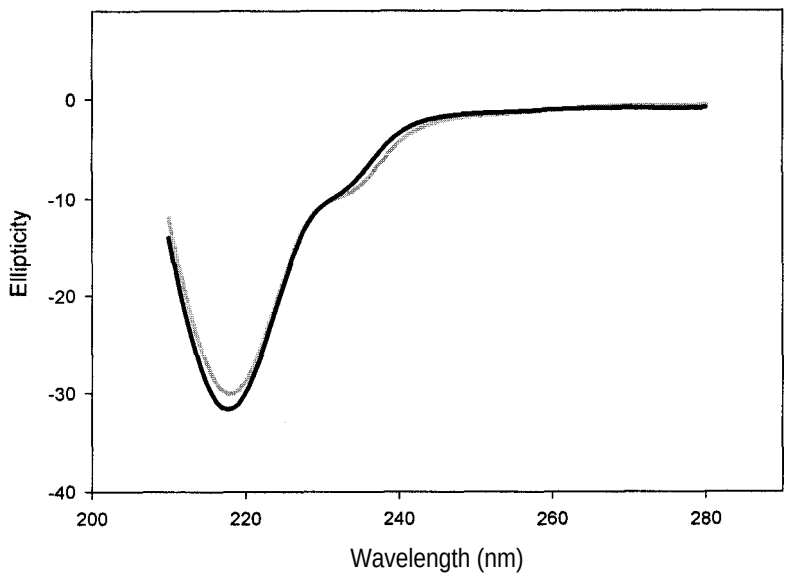

Figure 3 – Titration of XYL 11-INAC with xylopentaose X_5.

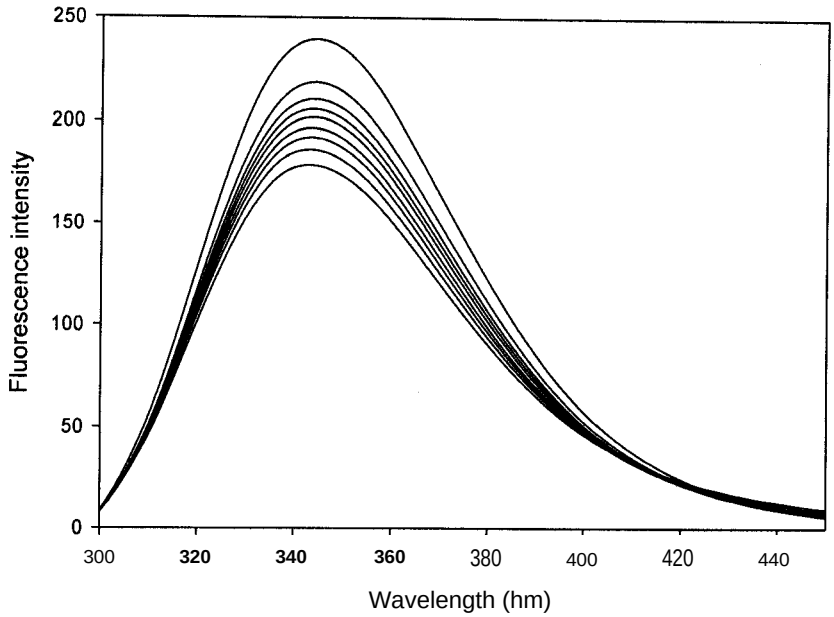

Figure 4 – Hyperbola of saturation of XYL 11-INAC with xylopentaose X_5.

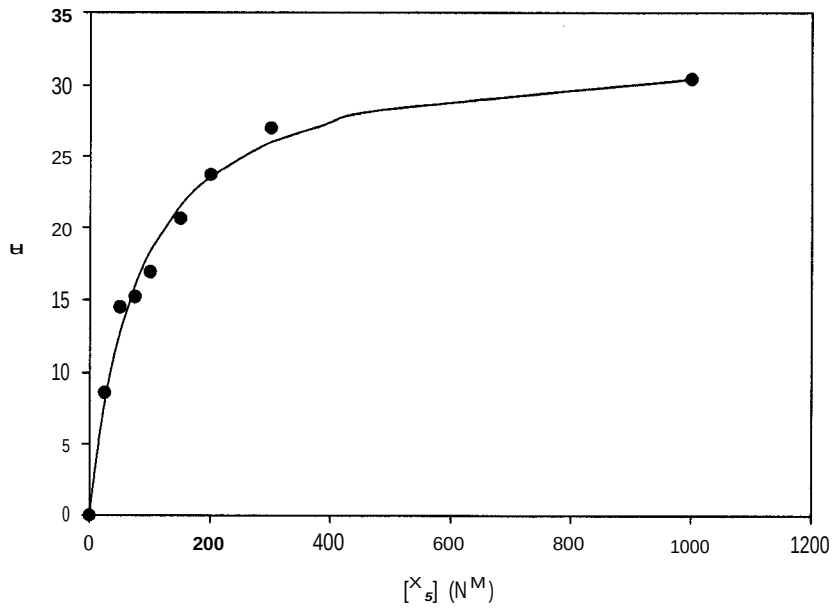

The form of the curve is described by the equation $OAF = \frac{DOF'm\ [L]}{Kd + [L]}$, where

$OOF = AF_0 - AF$ and $AF = F_{360,,,n} - F_{320»,n}$. The x-axis is the oligosaccharide concentration $[L]$.

Figure 5 – Micrographs of wheat-bran sections observed under UV exposure.

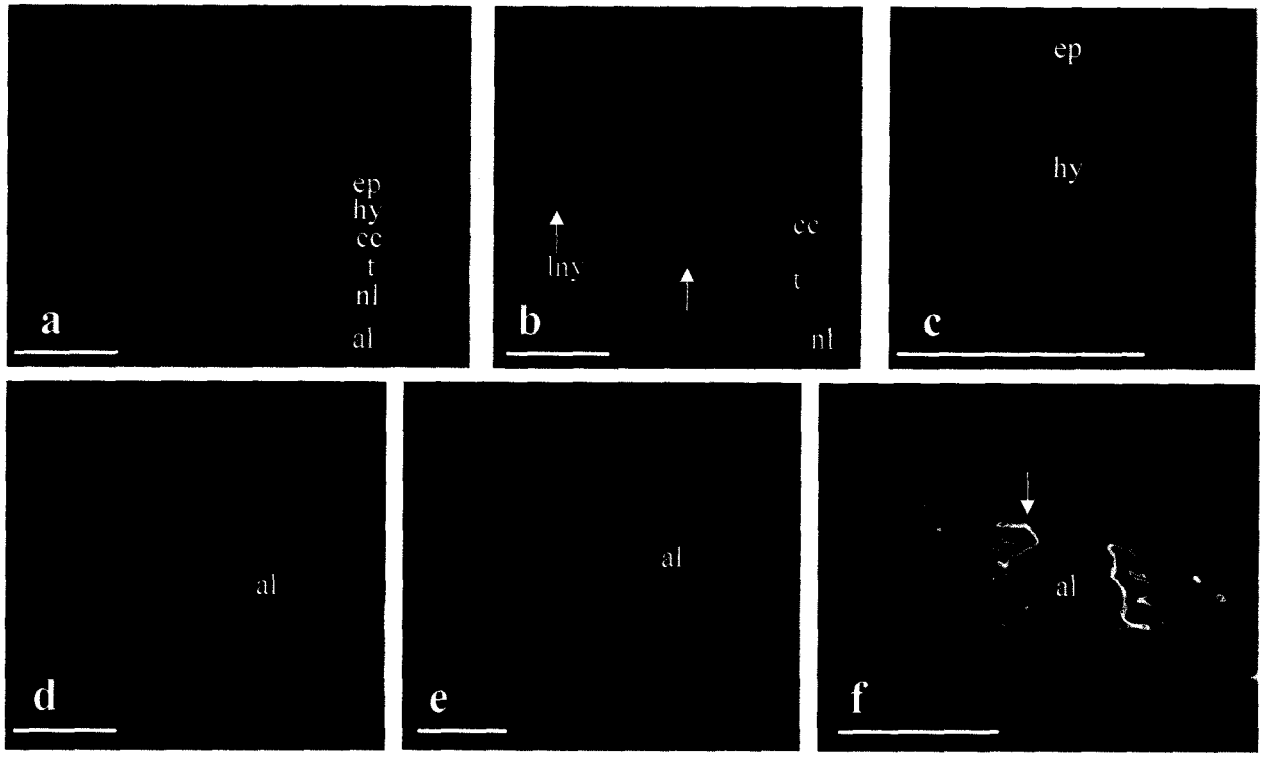

Bran samples treated with XYL 11-INAC for 24 h (WB in **a,** IB in **b,** OB in e and AL in **d)** or with XYL11-WT for 15 min (AL in e) and 30 min (AL in f) were examined by microscopy using the UV-induced autofluorescence of cell wall-linked phenol compounds. In **a,** all bran tissues, except the testa, display blue fluorescence. Fluorescence intensity in IB **(b)** is similar to that seen in **a.** Arrows indicate the location of the nucellar lysate, nly. OB (c) displays a less intense blue florescence compared to the previous layers and d, in which tell walls were particularly fluorescent. Compared to **d, e** shows that a 15-min treatment with XYL11-WT led to the loss of cell-wall autofluorescence. Of the original aleurone layer, only the median part of the periclinal walls remains fluorescent. Red arrows indicate the apparent bidirectional progression of the active enzyme. The micrograph of AL after a 30 min treatment with XYL 11-WT (f) shows a marked alteration of cell-wall integrity and the loss of anticlinal and periclinal aleurone-wall fluorescence. Only a thin layer that is directly in contact with the cytoplasm remains fluorescent. al = aleurone layer; nly = nucellar lysate; n1 = nucellar layer; t = testa; cc = cross cell; hy = hypodermis; ep = epidermis. Scale bars = 40 µm.

Figure 6 – Micrographs of XYL 11-WT and XYL 11-1NAC immunolabelling on bran sections visualized by LM (epipolarisation) or EM.

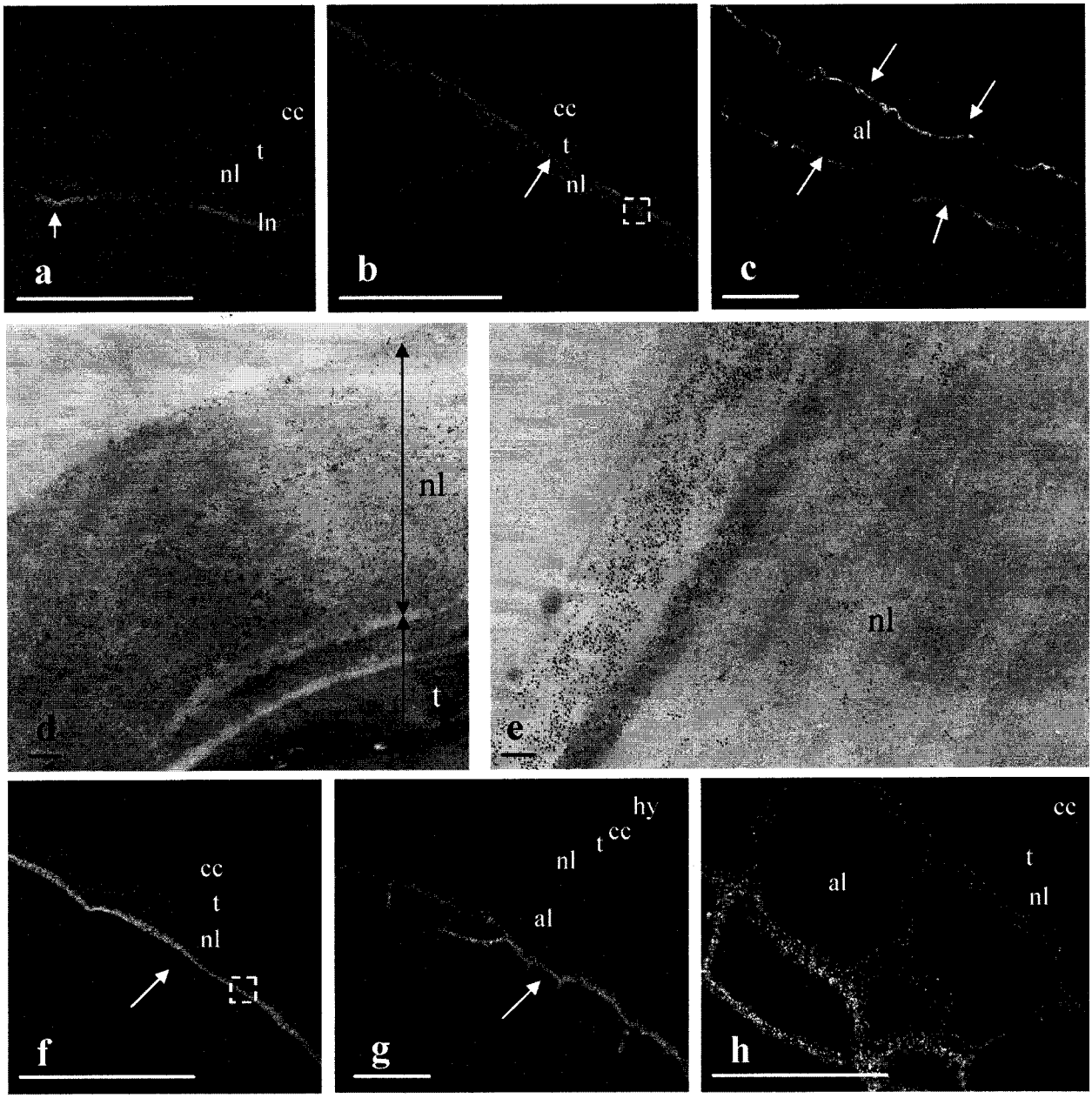

In **a,** IB subjected to a 30-min treatment with XYL11-WT was over-exposed in order to visualise unlabelled tissues. A wave of gold-silver enhanced particles, visualised as bright white spots, are visible at the nucellar lysate (white arrow). In **b,** after a 75-min XYL11-WT treatment, the labelling had progressed into the partially degraded nucellar layer up to the testa (not distinguishable). In c, after a 75-min treatment with XYL11-INAC, AL was labelled at the two periclinal surfaces. Electron microscopie observation **(d** and e) provide a detailed examination of the nucellar layer alter 75-min treatment with XYL11-WT and XYL11-INAC respectively. In **d,** XYL11-WT location is preferentially localised near to the testa. Little

labelling can be observed in the aleurone. XYL11-INAC distribution mirrors that of XYL11-WT (e), with intense labelling in the aleurone and in the vicinity of the aleurone-nl interface. In f (75-min treatment of IB), XYL11-1NAC labelling (white arrow) is similar to that of IB treated with XYL11-WT for 30 min (a), but differs radically with that of 1B treated with XYL 11-WT for 75 min (b). Pictures **g** and **h** are observations of WB following 75 min and 24 h treatment with XYL 11-INAC respectively. Alter 75 min (g), the XYL 11-INAC labelling is restricted to the AL anticlinal walls which are in contact with the starchy endosperm (white arrow). ln **h,** labelling is still strong in titis area, but is also now weakly detected throughout the aleurone cell-walls. al = aleurone layer; nly = nucellar lysate; nl = nucellar layer; t = testa; cc = cross cell; hy = hypodermis. Scale bars = 40 µm in **a, b, c, f, g, h** and 0.2 µm in **d, e.**

Figure 7 — Combined visualisation of XYL11-INAC immunolabelling and blue autofluorescence of the residual cell-walls of aleurone and starchy endosperm after 24 h incubation.

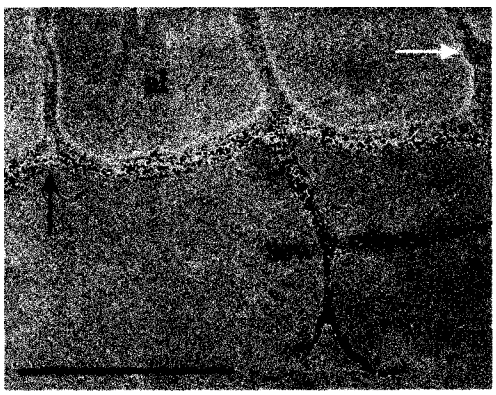

The aleurone cell-walls display apparent structural integrity and a strong blue UV-induced fluorescence. Intensive XYL11-INAC immunolabelling occurred in periclinal aleurone cell-walls facing endosperm (black arrow), and markedly declined across the anticlinal walls (white arrow). Notably, the infrequent occurrence of residual wall starchy endosperm was accompanied by intense XYL 11-1NAC immunolabelling. al = aleurone layer; sew = starchy endosperm wall. Scale bars = 40 µm.

Figure 8 — Micrographs showing immunolabelling of poorly substituted arabinoxylan in bran sections visualized by LM (epipolarisation).

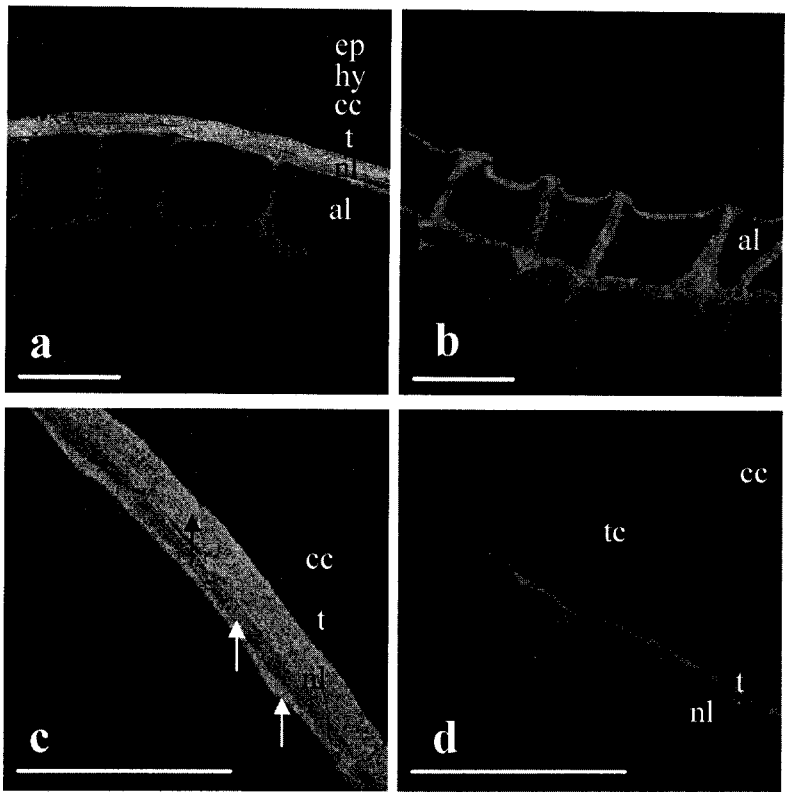

In **a,** labelling of (1—*4)-(3-unsubstituted xylan in WB treated for 24 h with XYL11-INAC was heterogeneous. Intense labelling can be observed throughout the nucellar layer and to a lower extent in the aleurone cell wall. Similarly, after 75-min XYL11-INAC treatment, AL **(b)** displays intensive labelling in the vicinity of the anticlinal-periclinal junction, whereas in IB (c) the nucellar layer is the only labelled structure. Micro heterogeneity of labelling was revealed by the differential labelling of three layers (arrows). With regard to the immunocytochemical controls, labelling of 75-min treated IB obtained using pre-immune (1—*4)-(3-unsubstituted xylan sera is shown in picture **d.** No significant labelling can be observed. al = aleurone layer; n1= nucellar layer; t = testa; tc = tube cell; cc = cross cell; hy = hypodermis; ep = epidermis. Scale bars = 40 μm.

Les sons constituent approximativement 15 à 20% de la masse du grain de blé, proportion variable selon le type de mouture appliqué au grain et selon la quantité d'amidon résiduel contenue dans les sons. A l'exception notable d'une couche cellulaire, la couche à aleurone, l'ensemble des cellules des sons sont vidées de leur contenu cellulaire; la masse des sons est donc majoritairement liée aux parois cellulaires. A raison de 30 à 40% de la masse des sons faiblement amidonnés, les arabinoxylanes sont les composants majoritaires des sons. Les produits plus ou moins complexes attendus de leur dégradation au sein des parois représentent un potentiel exploitable dans divers domaines (Ebringerovâ et Hromâdkovâ 1999). Dans ce contexte, nous avons centré nos recherches sur l'action d'endoxylanases thermostables particulièrement adaptées aux applications biotechnologiques et déjà utilisées par ailleurs (Zeikus et al. 1991, Beg et al. 2001). Récemment, les travaux de Benamrouche-Stitou (2002) ont montré que 50% des arabinoxylanes des sons de blé étaient solubilisés sous l'action d'une endoxylanase thermostable appartenant à la famille 11 des glycosyles hydrolases (xylanase GH11). Cette dégradation concerne les arabinoxylanes faiblement substitués principalement rencontrés dans les couches aleuronique et nucellaire. A l'inverse, les arabinoxylanes résistants proviennent des autres tissus du son (péricarpe) et présentent un taux de substitution élevé (rapport Arabinose/Xylose). Globalement, de faibles quantités en enzymes permettent de libérer des oligoarabinoxylanes associés à des acides hydroxycinnamiques (Lequart et al. 1999). Compte tenu de l'efficacité partielle de l'endoxylanase (proche des 50% de rendement), nous avons tenté de préciser dans cette étude les facteurs potentiellement limitant l'hydrolyse *in situ* des AX du son.

-Les arabinoxylanes du son sont-ils tous des substrats acceptables pour la xylanase?

Les arabinoxylanes retrouvés dans les tissus résiduels (testa, péricarpe) et non solubilisés par l'action de la xylanase ont un rapport moyen Arabinose/Xylose élevé (Benamrouche et al. 2002), valeurs proches de celles obtenues par Brillouet et Joseleau (1987). Il est en effet admis que la présence de nombreux groupes ramifiants (acides uroniques mais surtout arabinose) n'est pas favorable à l'action d'une endoxylanase de la famille 11 (Debeire et al. 1990, Biely et al. 1997).

-Le transfert de la xylanase du milieu réactionnel vers les arabinoxylanes pariétaux est t-il effectif dans l'ensemble des couches du son?

Les couches hydrophobes contenues dans les sons (testa, cutines) encadrent les tissus dits résistants à l'enzyme. De ce fait, on peut s'interroger sur l'incidence de la relative imperméabilité à l'eau de ces structures dans l'accession des enzymes aux cellules.

-La réticulation des composés pariétaux peut-elle limiter la progression de la xylanase dans le réseau?

Au niveau ultrastructural, les parois n'autorisent pas un passage uniforme des molécules de taille identique (Chesson et al. 1997). Les arabinoxylanes sensibles à la xylanase seraient ainsi ¡mbriqués dans des parois autorisant un passage facilité des enzymes en comparaison des parois où sont rencontrés les AX résistants. En particulier, la réticulation covalente des composés pariétaux via les acides hydroxycinnamiques (dimèrisation), ou encore l'association non covalente des xylanes avec la cellulose participerait à une certaine densification du réseau. A cet égard, les dimères d'acide férulique et la cellulose sont préférentiellement distribués dans le péricarpe, résistant à la xylanase. La taille de l'enzyme pourrait alors être un facteur déterminant à sa progression dans la paroi.

Certains composés pariétaux tels que les lignines sont susceptibles d'interagir avec les enzymes de manière non spécifique et par conséquent de limiter la dégradation des parois. De plus, l'ensemble des interactions établies par les substituants de la chaîne principale de xylose pourrait générer localement des contraintes stériques et/ou physicochimiques susceptibles d'entraver la liaison enzyme substrat. Ces considérations nous ont conduits à évaluer l'action de l'enzyme en présence de substrats distincts.

Relations entre variabilité biochimique des sons industriels - dégradabilité à la xylanase

La diversité génétique et éco-physiologique rencontrée chez les sons de blé dur *(Triticum durum,* Lempereur et al. 1997,1998) pourrait également concerner les variétés de blés tendres *(Triticum aestivum)* et se traduire par une dégradabilité variable à l'action de l'endoxylanase. Le traitement statistique des caractéristiques chimiques de 11 types de sons issus de variétés pures révèle une variation significative des teneurs en protéine, acides hydroxycinnamiques et polysaccharides. Cette variabilité des sons est cependant fortement liée à la teneur en amidon. Afin de s'affranchir de ce facteur et de l'interaction des inhibiteurs thermosensibles des xylanases (Rouau et Surget 1998) contenus dans les céréales (Goesaert et al. 2004), un désamidonnage à l'eau suivi d'un traitement thermique à sec ont été appliqués. A l'issue de ces traitements, les sons conservent une diversité structurale significative, toutefois la participation respective des facteurs éco-physiologiques et génétiques n'a pas pu être déterminée compte tenu de l'origine industrielle des sons.

L'action de la xylanase nous permet de distinguer deux familles d'arabinoxylanes. Une première que l'on nomme "sensible" car solubilisée des sons, et caractérisée par un rapport

moyen Arabinose/Xylose faible, la seconde nommée "resistante" qui correspond aux arabinoxylanes non solubilisés, ayant un rapport moyen Arabinose/Xylose élevé.

Les rendements de solubilisation des arabinoxylanes restent du même ordre de grandeur que les taux de dégradation rapportés pour un son désamidonné (Benamrouche-Stitou 2002), mais présentent toutefois des différences significatives selon les sons. La mise en relation de la susceptibilité à l'endoxylanase (de la famille 11) et la variabilité chimique des sons a été étudiée au regard des limitations potentielles rencontrées par l'enzyme. La teneur initiale en arabinoxylane n'a pas d'incidence marquée sur leur taux de dégradation, par contre le ratio Arabinose/Xylose des arabinoxylanes résiduels est négativement corrélé à l'efficacité de l'enzyme. Les substituants arabinoses de la chaîne principale sont donc une barrière à l'action de la xylanase, en accord avec les modalités de cette enzyme. Cependant, des corrélations fortes existent également entre les quantités d'arabinose et d'acides hydroxycinnamiques des sons. Si l'acide férulique est majoritairement estérifié par l'arabinose des arabinoxylanes, la xylanase est capable d'en solubiliser une grande partie sous forme de féruloyl-oligosaccharides (Lequart et al. 1999). La gêne occasionnée par cet acide phénolique refléterait en fait la présence du groupement arabinose qui le porte. En revanche, sa capacité à se dimériser est responsable de nombreuses connections inter polymères (Hatfield et al. 1999). Les trois principaux dimères (5,5'; 8-0-4'; 8,5') étant retrouvés en intégralité dans le son résiduel, leur teneur est négativement corrélée à la solubilisation des arabinoxylanes par l'endoxylanase. Ces agents réticulant de type diférulique constituent donc une limitation à l'action de la xylanase, qui s'ajoute à l'effet des substituants arabinose. Une dégradation moindre des arabinoxylanes pourrait dans ce cas résulter d'une densification accrue du réseau pariétal comportant les arabinoxylanes résiduels. Il aurait été intéressant de disposer d'un plus grand nombre d'échantillons et de variétés de sons. En particulier cette étude aurait pu être élargie à d'autres variétés de blé (blé dur ou variétés moins courantes), qui pourraient présenter des particularités de composition biochimique plus importantes.

Au delà de l'effet des substituants, les sons présentent une grande diversité chimique, et la participation de composés tels les lignines et les structures riches en polyesters ne sont pas à exclure pour expliquer la susceptibilité variable des sons.

Relations entre mise en place des parois – dégradabilité des arabinoxylanes à la xylanase

A travers la maturation des parois, nous avons essayé de révéler les événements déterminants de l'apparition des barrières limitant l'action de la xylanase. La dégradabilité des

arabinoxylanes d'enveloppes isolées manuellement à partir de grains prélevés à différents stades de maturation a été appréhendée en présence de cette même endoxylanase (famille 11 des GH). Des conditions en excès d'enzymes ont été retenues afin de pallier les interférences liées aux éventuels inhibiteurs des xylanases (Benamrouche-stitou 2002). Les cibles de cette étude sont principalement les arabinoxylanes, les acides phénoliques et leur type de liaison, les lignines mais aussi les polyesters. La présence des composés biochimiques ne préjugeant pas de leur organisation ni de leur localisation, l'approche microscopique (topochimie et ¡mmunomarquage des xylanases) avait pour objectif de préciser localement les cibles de l'enzyme.

Les ratios Arabinose/Xylose des enveloppes et des sons résiduels sont constants, l'ensemble suggérant que les arabinoxylanes sont définitivement mis en place dans les parois quel que soit le stade d'étude que nous avons considéré. De même la localisation tissulaire de la xylanase est identique (uniquement aleurone et couche nucellaire) dans tous les stades.

Les teneurs en composés phénoliques des enveloppes externes varient largement au cours de la maturation. La quantité d'acide férulique estérifié diminue avec la maturation, alors qu'augmente sa co-solubilisation par l'enzyme. Ce résultat confirme les conclusions précédentes, l'acide férulique n'est pas directement impliqué dans la résistance des arabinoxylanes résiduels à l'enzyme.

Les proportions en acides sinapique et p-coumarique co-solubilisés avec les arabinoxylanes sont similaires aux différents stades de maturité, les variations de leurs teneurs dans les enveloppes au cours du temps n'influencent pas de façon mesurable l'action de l'enzyme. Comme pour l'acide férulique, ces produits qui participent également au métabolisme général du grain ne semblent pas influencer directement l'impact de la xylanase sur les arabinoxylanes.

Les dimères d'acides féruliques sont eux aussi présents depuis le stade le plus jeune, où l'ensemble des structures du son est visible, jusqu'à la maturité physiologique des enveloppes (sons) mais en revanche leurs teneurs restent stables (5,5'; 8-0-4'; 8,5'). La pré-consolidation de paroi immature par des dimères d'acides hydroxycinnamiques avant la déposition de lignine a récemment été proposée (Obel et al. 2002).

Compte tenu des difficultés liées à la quantification des lignines dans des échantillons très peu lignifiés comme le son mature (environ 4%), la méthode de thioacidolyse a été retenue afin de libérer spécifiquement les monolignols liés par des liaisons aryl-alkyl éther au sein de la fraction lignine «non-condensée». Cette fraction des lignines n'est pas ou très faiblement entraînée du fait de l'action enzymatique dans la phase soluble. Contrairement aux dimères

phénoliques, les lignines non condensées sont décelées au deuxième stade de maturation retenu. Les caractéristiques structurales des parois sont alors proches du stade mature. Absente au tout premier stade retenu de formation du grain, l'incrustation ultérieure des lignines dans les enveloppes ne se traduit pas par une diminution mesurable de la dégradabilité des sons à la xylanase. La faible lignification contribuerait à densifier et à rendre hydrophobe le réseau pariétal de certaines couches cellulaires des sons (péricarpe), mais ne renforcerait que des barrières déjà suffisamment efficaces à l'action de la xylanase.

L'implication d'une potentielle barrière tissulaire a été envisagée à travers l'analyse des principaux polyesters des sons, essentiellement rattachés à la testa et aux couches cuticulaires dans les sons matures. Les polyesters montrent une variation qualitative et quantitative au cours du développement du grain. Les observations microscopiques suggèrent une mise en place précoce des structures cutinisées. Toutefois les composés dosés portent sur la globalité des sons en maturation et ne proviennent pas uniquement de ces structures. Une étude plus spécifique portant sur les couches micro disséquées en maturation par analyse chimique et coloration cytochimique serait envisageable pour localiser et préciser la nature des polyesters dans les enveloppes.

Relations entre nature des substrats — efficacité enzymatique

L'objectif était d'évaluer la contribution du ratio Arabinose/Xylose dans la dégradation des arabinoxylanes. Pour cela deux xylanases de familles différentes (GH10 et GH11) ont été testées pour leur efficacité à dégrader les arabinoxylanes. Ce choix repose sur la différence de leurs modes d'actions, la xylanase de la famille 1l (XYL11) nécessitant au moins trois résidus xylose consécutifs non substitués pour couper les arabinoxylanes, alors que la xylanase de la famille 10 (XYL10) peut agir prés d'un substituant de la chaîne principale. Sur le son, la XYL10 libère deux fois moins d'arabinoxylanes que la XYL11. Pour de nombreuses enzymes, et notamment celles dites accessoires des rendements inferieurs aux valeurs théoriquement attendues sont parfois obtenues. Dans le cas des xylanases, ce constat peut en partie s'expliquer par l'intervention de la longueur des chaînes d'arabinoxylanes (Li et al. 2000) et l'état physique du substrat, soluble ou insoluble (Bartolomé et al. 1995, Connerton et al. 1999, Courtin et Delcour 2001, Vardakou et al. 2003). Nous avons étudié l'influence du ratio Arabinose/Xylose des arabinoxylanes en solution sur ces deux enzymes. A l'inverse de ce qui est obtenu sur les sons, la XYL10 est deux fois plus efficace que la XYL11 sur une gamme de substrats solubles. Principalement testée sur des fractions extraites de son enrichies en arabinoxylanes, la XYL10 peut agir sur des substrats dont les rapports Arabinose/Xylose

sont plus élevés. L'effet de la XYL10 illustre l'importance de la physicochimie du substrat sur l'efficacité des enzymes. Néanmoins, l'efficacité relativement faible sur un substrat insoluble et complexe résulterait d'une barrière liée au réseau pariétal. La XYL10 proche de 40 kDa, soit approximativement le double de la XYL11, pourrait être limitée par un plus grand encombrement volumique, conduisant à une moins bonne accessibilité aux substrats.

Dans le cas de la XYL 11, une observation plaide également pour une contribution de la maille pariétale sur une certaine résistance du substrat des sons. L'extraction par la potasse du son résiduel après action de la XYL11 conduit à l'obtention d'une petite fraction d'arabinoxylanes qui s'est averée dégradable en solution par la même enzyme. Si ces arabinoxylanes sont inaccessibles à l'action de l'enzyme dans les parois, les interconnections du réseau pariétal seraient prépondérantes dans la limitation de la dégradation. Néanmoins cette fraction représente une proportion relativement faible par rapport aux arabinoxylanes du son.

L'action combinée des deux xylanases n'augmente pas significativement le rendement de dégradation des arabinoxylanes, la XYL10 agirait préférentiellement sur les produits solubilisés des parois des sons par la XYL11. Par ailleurs, le recoupement des analyses des produits libérés suggère que la combinaison des deux enzymes altère la même population d'arabinoxylane que la XYL11 individuellement. Les deux xylanases doivent rencontrer des limitations de niveaux similaires, au delà de la plus faible efficacité de la XYL10 sur un substrat de nature insoluble et complexe. Parmi ces limitations communes, pressenties au niveau du réseau pariétal, les dimères d'acides féruliques ont été considérés.

La XYL10, à l'instar de la XYL11, ne semble pas en mesure de solubiliser les dimères d'acides féruliques (5,5'; 8-0-4'; 8,5'). Celle ci co-solubilise une quantité globale d'acides hydroxycinnamiques moins importante que la XYL11, probablement en raison de sa moindre efficacité sur le son. L'interprétation des actions comparées des enzymes suggère l'existence de micro domaines (Faulds et al. 2003) au sein des parois sensibles aux enzymes, et/ou d'une hétérogénéité dans la concentration des composés phénoliques à l'intérieur des parois (Piot et al. 2000, Rhodes et al. 2002). Ces possibles sites de résistance sont globalisés par des caractéristiques chimiques, cependant la progression pas à pas de la dégradation suivie par des techniques de microscopie pourrait mettre en relief les micro domaines.

Relations entre distribution — accessibilité des substrats

Seule la localisation de la xylanase la plus performante en terme de dégradation des arabinoxylanes des parois du son a été étudiées. La XYL11 agit de façon progressive et unilatérale. Pénétrant uniquement dans les sons par l'interface milieu exterieur-paroi

anticlinale de l'aleurone, face albumen amylacé, elle progresse au travers des parois anticlinales aleuroniques jusqu'à la couche nucellaire, et finalement traverse cette structure pour parvenir jusqu'à la testa où se termine sa progression. Aucun marquage de l'enzyme n'est visible dans les structures où les arabinoxylanes sont a priori résistants.

En parallèle à la localisation de l'enzyme, nous avons utilisé des anticorps reconnaissant les substrats préférentiellement dégradés par la xylanase. Ces anticorps marquent les arabinoxylanes faiblement substitués (Guillon et al. 2004) dans le cas du son. Leur localisation est uniquement aleuronique et particulièrement intense dans la couche nucellaire, corroborant les résultats obtenus par analyse chimique des couches constitutives des sons (Benamrouche et al. 2002). Les arabinoxylanes de parois aleurones sont plus substitués que ceux de la couche nucellaire, mais néanmoins plus faiblement que dans le péricarpe.

Une relation nette unit la dégradation des arabinoxylanes faiblement substitués de l'aleurone et du nucelle et la progression de l'enzyme. La disparition des arabinoxylanes entraîne localement une désorganisation et un relâchement de l'édifice pariétal. Cette perte de cohésion pariétale parait être le pré-requis de la progression de la xylanase. L'incapacité de l'enzyme à agir sur les AX des couches résistantes pourrait alors être rattachée à une absence de progression dans la trame pariétale en raison:

-d'une fréquence élevée de ramifications portées par les arabinoxylanes, l'enzyme est inapte à dégrader ces AX hautement substitués

-et/ou d'une progression ralentie par le réseau pariétal (la porosité ou le volume accessible et les interactions).

L'apport de la biologie moléculaire a été décisif pour visualiser l'impact de la dégradation des arabinoxylanes sur la progression de l'enzyme dans les parois. Une xylanase mutante «inactive» possédant les mêmes caractéristiques (structure, affinité) que la XYL11 sauvage, à l'exception notable de l'activité catalytique, ne se fixe pas sur les structures récalcitrantes. Par contre, la perte de son activité catalytique ralentirait fortement sa pénétration dans les parois aleurones et nucellaires. Le relâchement du réseau pariétal résultant de la dégradation des arabinoxylanes dans ces parois permet la progression rapide de la xylanase.

Dans le cas des structures où la xylanase n'est pas retrouvée, et où conjointement les arabinoxylanes ne sont pas altérés, les parois des tissus résistants ne permettraient que la diffusion de molécules de plus petite taille que dans le reste du son (Chesson et al. 1997). Les agents principaux interconnectant les composés des sons, les dimères d'acides hydroxycinnamiques, sont retrouvés en plus grande quantité dans le péricarpe (Antoine et al.

2003). Or, dans l'aleurone et la couche nucellaire, le volume de la XYL11 (20 kDa) de la semble déjà un obstacle. Bien qu'en faible quantité dans la couche à aleurone les dimères pourraient jouer un rôle similaire à ce qui est attendu dans le péricarpe. Ils ne sont pas ou très faiblement solubilisés par la xylanase. A l'intérieur des structures désorganisées par la XYL11, un certain nombre de zones, jonctions cellulaires et couche interne de la paroi aleuronique, présentent une micro hétérogénéité révélée par leur relative résistance à de nombreuses enzymes. Les jonctions periclinale-anticlinale sont connues pour être riches en composés phénoliques (Piot et al. 2000). En plus des acides hydroxycinnamiques, la révélation des polysaccharides (PATAg) indique la persistance de structures réactives au sein des jonctions et de la paroi interne de l'aleurone. En particulier, des études supposent déjà que la résistance locale de cette structure à de nombreuses enzymes serait liée à la complexité des liaisons établies entre ses constituants (Taiz and Jones 1970, Rhodes and Stone 2002). La fluorescence persistante dans la paroi interne suggère que les dimères phénoliques de l'aleurone seraient préférentiellement localisés dans cette structure. Dans une certaine mesure celle ci présenterait un réseau d'une complexité comparable à celui du péricarpe. Des investigations complémentaires concernant la nature de cette couche apporterait sans doute des renseignements sur les causes de son apparente résistance à des nombreuses enzymes.

Le péricarpe peut être schématiquement considéré comme un bloc recouvert de cuticule. Ces couches riches en polyesters d'épaisseurs variables sont présumées imperméables à l'enzyme. Par microdissection, l'ouverture du péricarpe conduit à deux nouvelles faces non cutinisées ouvertes sur l'extérieur. Nous n'avons pas obtenu d'éléments en faveur d'une présence de l'enzyme sur ces couches épluchées. La couche cuticulaire recouvrant l'épiderme du péricarpe n'est pas la cause du non marquage de la xylanase à l'intérieur du péricarpe. Dans le cas de tissus sensibles, l'enzyme est capable de pénétrer bilatéralement dans les parois aleurones lorsque cette couche est isolée. Par contre l'enzyme pénètre unilatéralement dans la couche nucellaire liée à la testa, par la face normalement en contact avec la couche à aleurone. La testa, ou tout du moins un élément qui la compose empêche donc le passage de l'enzyme vers les couches nucellaire et aleurones.

La résistance d'environ 50% des arabinoxylanes pour la xylanase apparaît donc principalement liée à une fréquence élevée de leurs ramifications mais aussi à leur imbrication dans les parois.

La dégradation des arabinoxylanes des sons de blé tendre par une xylanase de la famille 11 est soumise à des limitations nombreuses bien que d'importance variable. En premier lieu, le taux de substitution des arabinoxylanes influence largement l'efficacité de l'enzyme. Le rapport Arabinose/Xylose des sons résiduels, incluant les arabinoxylanes résistants à l'action enzymatique, est proche de la valeur maximale des substrats pour lesquels la xylanase est active. L'utilisation d'une xylanase théoriquement plus efficace (XYL10) sur les zones fortement substituées par l'arabinose n'a pas amélioré le rendement de dégradation qui se situe autour de 50%. A l'inverse, avec un rendement de 25%, il semble que la masse moléculaire élevée (double de la XYL11) et des contraintes physicochimiques propres à cette enzyme ne soient pas favorables à son utilisation sur des substrats complexes. En effet, l'influence du réseau pariétal, notamment à travers ses interconnections inter polymères, est un deuxième paramètre déterminant de l'efficacité enzymatique. Dans les parois du son, les interactions susceptibles de gêner ou d'entraver complètement la pénétration et la progression des xylanases reposeraient en grande partie sur l'action réticulante des acides phénoliques, en particulier les dimères d'acides féruliques. Certaines hypothèses concernant la localisation préférentielle et l'arrangement de ces molécules au sein des structures récalcitrantes à l'enzyme devraient être précisées. Dans ce but, le développement d'outils pertinents pour des approches immunocytochimiques et microspectroscopiques permettrait de mieux appréhender l'implication des interactions intrapariétales dans l'action enzymatique. De même, la contribution de l'architecture pariétale dans la restriction à l'accès des enzymes au substrat pourrait être approfondie par l'étude du comportement de sondes protéiques dont les compétences seraient modulées par l'ingénierie moléculaire. Parallèlement, l'utilisation de sondes spécifiques marquées est envisageable pour cibler *in muros* la distribution locale des constituants pariétaux. Par exemple, des enzymes tronquées (carbohydrate binding module etc...) permettraient de révéler des substrats accessibles.

Afin de contourner les diverses limitations du substrat à l'efficacité enzymatique, la mise en oeuvre d'une xylanase plus performante pourrait être envisagée. Cette enzyme, de petite taille, serait capable de couper les arabinoxylanes à proximité des nombreux substituants. Une telle approche pourrait se développer grâce aux apports de la biologie moléculaire mais suppose toutefois une connaissance parfaite de l'ensemble des caractéristiques requises pour une protéine enzymatique idéale.

Une autre alternative repose sur l'utilisation combinée de xylanase et d'enzymes accessoires de spécificités différentes. Les essais réalisés dans ce sens restent néanmoins peu prometteurs, le rendement de solubilisation n'augmente pas sensiblement. Dans ce cas, la taille des

enzymes limiterait leur accès aux substrats au sein de la paroi, les enzymes accessoires ont en effet dans leur grande majorité une masse moléculaire supérieure à 20 kDa. D'autre part, leur efficacité catalytique reste le principal facteur restrictif, ces enzymes sont généralement peu actives sur des polymères. Dans le cadre de la bioconversion sélective des arabinoxylanes des sons, le développement d'enzymes accessoires pourrait par exemple viser la sélection et/ou l'amélioration de feruloyl estérases capables de couper les dimères d'acides féruliques dans un environnement complexe, ou encore d'une arabinofuranosidase capable de rompre les liaisons reliant l'arabinose à un xylose disubstitué.

Parallèlement à une action potentielle sur les performances enzymatiques, il serait certainement avantageux de combiner des traitements physicochimiques à une action enzymatique dans l'optique d'une valorisation rationnelle des sons. En particulier, compte tenu des fortes limitations existant au niveau de la dégradation du péricarpe par la xylanase, une déstructuration non enzymatique contrôlée des parois réfractaires contribuerait à l'ouverture du réseau pariétal et serait susceptible de faciliter l'action ultérieure d'outils enzymatiques sélectionnés.

Quelle que soit la démarche retenue, les voies de transformation des sons devront également prendre en considération la diversité naturelle et industrielle de ces co-produits pour une valorisation efficace et maîtrisée.

Adams EL, Kroon PA, Williamson G, Gilbert HJ, Morris VJ 2004 Inactiveted enzymes as probes of the structure of arabinoxylans as observed by atomic force microscopy. Carbohyd. Res. 339: 579-590.

Akin DE 1995 Microspectrophotometric characterization of aromatic constituents in cell walls of hard and soft wheats. J. Sci. Food Agric. 68: 207-214.

Aman P 1993 Composition and structure of cell wall polysaccharides in forage. In Forage cell wall structure and digestibility Jung HJG, Buxton DR, Hatfield RD Ralph J (eds) pp 183-199.

Aman P, Nordkvist E 1983 Chemical composition and in vitro degrability of botanical fractions of cereal straw. J. Agr. Eng. Res. 13: 61-67.

Andreasen MF, Christensen LP, Meyer AS, Ansen 2000 Content of phenolic acids and ferulic acid dehydrodimers in 17 rye (Secale cereal) varieties. J. Agric. Food Chem. 48: 2837-2842.

Andreasen MF, Kroon PA, Williamson G, Garcia-Conesa MT 2001 Esterase activity able to hydrolyse dietary antioxydant hydroxycinnamates is distributed along the intestine of mammals. J. Agric. Food Chem. 49: 5679-5684.

Antoine C, Lullien-Pellerin V, Abecassis J, Rouau X 2002 Intérêt nutritionnel de la couche à aleurone du grain de blé. Sciences des aliments 22: 545-556.

Antoine C 2003 Bases physico-chimiques et structurales de l'aptitude au fractionnement des enveloppes du grain de blé tendre *(Triticum aestivum L.)*. Thèse de doctorat, Ecole Nationale Supérieure Agronomique de Montpellier, Montpellier, France.

Antoine C, Peyron S, Mabille F, Lapierre C, Bouchet B, Abecassis J, Rouau X 2003 Individual contribution of grain outer layers and their cell wall structure to the mechanical properties of wheat bran. J. Agric. Food Chem. 51: 2026-2033.

Arnason JT, Gale J, Conilh de beyssac B, Sen A, Miller SS, Philogene BJR, Lambert JDH, Fulcher RG, Serratos A, Mihlm J 1992 Role of phenolics in resistance of maize grain to the stored grain insects, *Prostephanus truncatus* (horn) and *Sitophilus zeamais* (motch). J. Stored Prod. Res. 28: 119-126.

Aspinall GO 1959 Structural chemistry of the hemicelluloses; Adv carbohdr Chem 14: 429-468.

Atkins EDT 1992 Three-dimensional structure, interactions and properties of xylans. In Xylans and Xylanases Visser, J, Beldman, G, Kusters-van Someren, M. A, and Voragen, A.G.J., (eds). Elsevier Science Publishers, pp 39-50.

Bacic A, Harris PJ, Stone BA 1988 Structure and function of the plant cell wall. In The Biochemistry of Plant (eds), Academic Press, Cambridge, pp 297-371.

Bacic A, Stone BA 198la Isolation and ultrastructure of aleurone cell wall from wheat and barley. Aust. J. Plant. Physiol. 8: 453-474.

Bacic A, Stone BA 1981b Chemistry and organization of aleurone cell wall components from wheat and barley. Aust. J. Plant. Physiol. 8: 475-495.

Bacon JSD, Gordon AH, Morris EJ, Farmer VC 1975 Acetyl groups in cell-wall preparations from higher plants. Biochem J 149: 485-487.

Barlow EWR, Lee JW, Munns R, Smart MG 1980 Water relations of the developing wheat grain. Aust. J. Plant. Physiol. 7: 519-529.

Bartolomé B, Faulds CB, Kroon PA, Waldron K, Gilbert HJ, Hazlewood G, Williamson G 1997 An *Aspergillus niger* esterase (ferulic acid esterase III) and a recombinant *Pseudomonas fluorescens* subsp. cellulosa esterase (Xy1D) release a 5-5' ferulic dehydrodimer (diferulic acid) from barley and wheat cell walls. Appl. Environ. Microbiol. 63: 208-212.

Bartolomé B, Faulds CB, Tuohy M, Hazlewood GP, Gilbert HJ, Williamson G 1995 Influence of different xylanases on the activity of ferulic acid esterase on wheat bran. Biotechnol. Appl. Biochem. 22: 65-73.

Beaugrand J, Chambat G, Wong V, Goubet F, Rémond C, Paës G, Benamrouche S, Debeire P, O'Donohue M, Chabbert B 2004 Impact and efficiency of GH10 and GH11 thermostable endoxylanases on wheat bran and alkali-extractable arabinoxylans. Carbohyd. Res. Submitted.

Beaugrand J, Crônier D, Debeire P, Chabbert B 2004 Arabinoxylan and hydroxycinnamate content of wheat bran in relation to endoxylanase susceptibility. J. Cereal Sci. In press.

Beaugrand J, Reis D, Guillon F, Debeire P, Chabbert B 2004 Xylanase-mediated hydrolysis of wheat bran. Evidence for subcellular heterogeneity of cell walls. Int. J. Plant Sci. In press.

Beg QK, Kapoor M, Mahajan L, Hoondal GS 2001 Microbial xylanases and their industrial applications: a review. Appl. Microbiol. Biotechnol. 56: 326-338.

Benamrouche S, Crônier D, Debeire P, Chabbert B 2002 A chemical and histological study on the effect of (1--*4)-(3-endo-xylanase treatment on wheat bran. J. Cereal Sci. 36: 253-260.

Benamrouche-Stitou 2002 Biochimie et histologie de la dégradation enzymatique du son de blé par une endoxylanase. Thèse de doctorat de l'Université de Reims Champagne-Ardenne, Reims, France.

Biely P 1985 Microbial xylanolytic systems. Trends Biotechnology 3: 286-290.

Biely P, Kratky Z, Vrsanska M 1981 Substrate binding site of endo-1,4-béta-xylanase of yeast Cryptococcus albidus. Eur. J. Biochem. 119: 559-564.

Biely P, Vrsanska M, Tenkanen M, Kluepfel D 1997 Endo-(3-1,4-xylanase families: differences in catalytic properties. J. Biotechnol. 57: 151-166.

Bily AC, Reid LM, Taylor JH, Johnston D, Malouin C, Burt AJ, Bakan B, Regnault-Roger C, Pauls KP, Arnason JT, Philogène BJR 2003 Dehydrodimers of ferulic acid in maize grain pericarp and aleurone: resistance to *Fusarium graminearum*. Phytopathology 93: 712-719.

Black GW, Hazlewood GP, Millward-Sadler J, LauiriebJl 1995 A molecular xylanase containing a novel catalytic xylan-specific binding domain. Biochem. Journal 307: 191-195.

Blum DL, Li XL, Chen H, Ljungdahl LG 1999 Characterization of an acetyl xylan esterase from the anaerobic fungus *Orpinomyces sp.* strain PC-2. Appl. Environ. Microbiol. 65(9): 3990-3995.

Bourne Y, Henrissat B 2001 Glycoside hydrolases and glycosyltransferases: families and functional modules. Curr. Opin. Struct. Biol. 11: 593-600.

Bradbury D, MacMasters MM, Cull IM 1956 Structure of the mature wheat kernel.11. Microscopic structure of pericarp, seed coat, and other coverings of the endosperm and germ of hard red winter wheat. Cereal Chem. 33: 342-360.

Bray MR, Johnson PE, Gilkes NR, McIntosh LP, Kilbern DG, Warren RA 1996 Probing the role of tryptophane residues in a cellulose-binding domain by chemical modification. Protein Sci. 5: 2311-2318.

Bray MR, Clarke AJ 1992 Action pattern of xylo-oligosaccharide hydrolysis by *Schizophyllum* commune xylanase A. Eur. J. Biochem. 204: 191-196.

Breannan Y, Callen WN, Christoffersen L, Dupree P, Goubet F, Healey S, Hernândez M, Keller M, Li K, Palackal N, Sittenfeld A, Tamayo G, Wells S, Hazlewood GP, Mathur EJ, Short JM, Robertson DE, Steer BA 2004 Unusual microbial from insect guts. Appl. Environ. Microbiol. In press.

Briarty LG, Hugues CE, Evers AD 1979 The developing endosperm of wheat. A stereological analysis. Ann. Bot. 44: 641-658.

Brillouet JM, Mercier C 1981 Fractionation of wheat bran carbohydrates. J. Sci. Food Agric. 32: 243-251.

Brillouet JM, Joseleau JP, Utille JP, Lelievre D 1982 Isolation, purification, and characterization of a complex heteroxylan from industrial wheat bran. J. Agric. Food Chem. 30: 488-495.

Brillouet JM, Joseleau JP 1987 Investigation of the structure of a heteroxylan from the outer pericarp (beeswing bran) of wheat kernel. Carbohyd. Res. 159: 109-126.

Buchert T, Tenkanen M, Kantelinen A, Viikari L 1994 Application of xylanases in the pulp and paper industry. Bioresource Technol. 50: 65-72.

Bunzel M, Ralph J, Kim H, Lu F, Ralph SA, Marita JM, Hatfield RD, Steinhart H 2003 Sinapate dehydrodimers and sinapate-ferulate heterodimers in cereal dietary fiber. J. Agric. Food Chem. 51: 1427-1434.

Carpita NC, Salularse D, Montezinos D, Delmer DP 1979 Determination of the pore size of cell walls of living plant cells. Science 205: 1144-1147.

Carpita NC, DN Gibeaut 1993 Structural models of primary cell walls in flowering plants: consistency of molecular structure with the physical properties of the walls during growth. Plant J. 3: 1-30.

Chabbert B, Crônier D, Beaugrand J, Benamrouche S, Debeire P 2001 Structural and tissular heterogeneity of cell wall in wheat bran layers. In "9th International cell wall meeting" 2-7 september 2001, Toulouse pp 117.

Chanliaud E, Saulnier L, Thibault J-F 1995 Alkaline extraction and characterisation of heteroxylans from maize bran. J. Cereal Sci. 21: 195-203.

Chanzy H 1990 Aspects of cellulose structure. In Cellulose source and exploitation Kennedy JF, Pillips GO, Williams PA (eds) Ellis Horwood Limited, New York.: pp 3-12.

Chesson A, Gordon AH, Lomax JA 1983 Substituent groups linked by alkali-labile bonds to arabinose and xylose residues of legume, grass and cereal straw walls and their fate during digestion by rumen microorganisms. J. Sci. Food Agric. 34: 1330-1340.

Chesson A 1988 Lignin-polysaccharide complexes of the plant cell wall and their effect on microbial degradation in the rumen. Anim. Feed Sci. Technol. 21: 219-228.

Chesson A, Forsberg CW, Grenet E 1995 Improving the digestion of plant cell walls and fibrous feeds. In Recent development in the nutrition of herbivores, INRA (eds), Paris pp 249-277.

Chesson A, Gardner PT, Wood TJ 1997 Cell wall porosity and available surface area of wheat straw and wheat grain fractions. J. Sci. Food Agr. 75: 289-295

Christakopoulos P, Katapodis P, Kalogeris E, Kekos D, Macris BJ, Stamatis H, Skaltsa H 2003 Antimicrobial activity of acidic xylo-oligosaccharides produced by family 10 and 11 endoxylanases. Int. J. Biol. Macromol. 31: 171-175.

Clarke JH, Rixon JE, Ciruela A, Gilbert HJ, Hazlewood GP 1997 Family-10 and family-11 xylanases differ in their capacity to enhance the bleachability of hardwood and softwood paper pulps. Appl. Microbiol. Biotechnol. 48: 177-183.

Cleemput G, Booij C, Hessing M, Gruppen H, Delcour JA 1997 Solubilisation and changes in molecular weight distribution of arabinoxylans and protein in wheat flours during bread-making, and the effects of endogenous arabinoxylan hydrolysing enzymes. J. Cereal Sci. 26: 55-66.

Cochrane MP, Duffus CM 1979 Morphology and ultrastructure of immature cereal grains in relation to transport. Ann. Bot. 44: 67-72.

Connerton I, Cummings N, Harris GW, Debeire P, Breton C 1999 A single domain thermophilic xylanase can bind insoluble xylan: evidence for surface aromatic clusters. Biochem. Biophys. Acta 1433: 110-121.

Coughlan MP 1992 Towards and understanding of the mechanism of action of main chain cleaving xylanases. In Xylans and xylanases Visser J (eds), Elsevier, Amsterdam.

Courtin CM, Delcour JA 2001 Relative activity of endoxylanases towards water-extractable and water-unextractable arabinoxylan. J. Cereal Sci. 33: 301-312.

Cui W, Wood PJ, Blackwell B, Nikiforuk J 2000 Physicochemical properties and structural characterization by two-dimensional NMR spectroscopy of wheat (3-D-glucan. Comparison with other cereal [3-D-glucans. Carbohydr. Polym. 41: 249-258.

Daniel G, Nilsson T, Pettersson B 1989 Intra- and extracellular localization of lignin peroxidase during the degradation of solid wood and wood fragments by *Phanerochaete chrysosporium* by using transmission electron microscopy and immuno-gold labeling. Appl. Environ. Microbiol. 54: 871-881.

Davies GJ, Henrissat B 1995 Structures and mechanisms of glycosyl hydrolases. Structure 3: 853-859.

Debeche T, Cummings N, Connerton I, Debeire P, O'Donohue M 2000 Genetic and biochemical charactherization of a highly thermostable a-L-arabinofuranosidase from *Thermobacillus xylanilyticus.* Appl. Environ. Microbiol. 66: 1734-1736.

Debeire P, Priem B, Strecker G, Vignon M 1990 Purification and properties of an endo-1,4-13-xylanase excreted by a hydrolytic thermophilic anaerobe, *Clostridium thermolacticum*. A proposai for its action mechanism on larchwood 4-0-methylglucuronoxylan. Eur. J. Biochem. 187: 573-580.

Debeire-Gosselin M, Loonis M, Samain E, Debeire P 1992 Purification and properties of 22 kDa endoxylanase excreted by a new strain of thermophilic Bacillus. In Xylans and Xylanases, Visser, J, Beldman G, Kusters-van Someren MA, Voragen AGJ Elsevier Science Publishers pp 463-466.

Debyser W, Derdelinckx G, Delcour JA 1997 Arabinoxylan solubilization and inhibition of the barley malt xylanolytic system by wheat during mashing whith wheat whole meal adjuncts: evidence fora new class of enzyme inhibitors in wheat. J. Am. Soc. Brew. Chem. 55: 153-156.

Debyser W, Peumans WJ, van Damme EJM, Delcour JA 1999 Triticum aestivum xylanase inhibitor (TAXI), a new class of enzyme inhibitor affecting breadmaking performance. J. Cereal Sci. 30: 39-43.

Dekker RFH, Richards GN 1976 Hemicellulases: their occurrence, purification, properties and mode of action. Advances in Carbohydrate Chemistry and Biochemistry 32: 277-352.

Delcour JA, Van Win H, Grobet PJ 1999 Distribution and structural variation of arabinoxylanes in common wheat mill streams. J. Agric. Food Chem. 47: 271-275.

Dervilly G, Saulnier L, Roger P, Thibault J-F 2000 Isolation of homogeneous fractions from wheat water-soluble arabinoxylans. Influence of the structure on their macromolecular characteristics. J. Agric. Food Chem. 48: 270-278.

Dervilly-Pinel G 2001 Etude des relations entre la structure et les propriétés physicochimiques des arabinoxylanes hydro-solubles de l'albumen de blé. Thèse de doctorat, ENSIA, Université de Paris VII, Paris VI et INA-PG, France.

Dervilly-Pinel G, Tran V, Saulnier L 2004 Investigation of the distribution of arabinose residues on the xylan backbone of water-soluble arabinoxylans from wheat flour. Carbohyd. Polym. 55: 171-177.

Deshpande V, Hinge J, Rao M 1990 Chemical modification of xylanases : Evidence for essential tryptophan and cysteine residues at the active site. Biochim. Biophys. Acta 1041: 172-177.

Dey PM, Brison K 1984 Plant cell wall. Advances in Carbohydrate Chemistry and Biochemistry 42: 265-294.

Duffus CM, Rosie R 1973 Some enzyme activities associated with the chlorophyll containing layers of the immature barley pericarp. Planta 114: 219-226.

Du Pont MS, Selvendran RR 1987 Hemicellulosic polymers from cell walls of beeswing wheat bran : Part I, polymers solubilised by alcali at 2 °. Carbohyd. Research 163: 99-113.

Dupont FM, Altenbach SB 2003 Molecular and biochemical impacts of environmental factors on wheat grain development and protein synthesis. J. Cereal Sci. 38: 133-146.

Durand R, Rascle C, Fevre M 1996 Molecular characterization of Xyn 3, a member of the endoxylanase multigene family of the rumen anaerobic fungus *Neocallimastix frontalis.* Curr. Genet. 30: 531-540.

Ebringerovâ A, Hromâdkovâ Z 1999 Xylans of industrial and biomedical importance. Biotechnol. Genet. Eng. Rev. 16: 325-341.

Engels FM 1989 Some properties of cell watt layers determining ruminant digestion. In Chesson A, Orskov ER (eds) Physico-chemical characterization of plant residues for industrial and feed use. Appl. Sci. Publ., London.: pp 80-87.

Erikson Ô, Goring AI 1980 Structural studies on the chemical bonds between lignins and carbohydrates in spruce wood. Wood Science Technology 14: 267-279.

Evers AD, Reed M 1988 Some novel observations by scanning electron microscopy on the seed coat and nucellar layer of the mature wheat grain. Cereal Chem. 65: 81-85.

Evers AD, Blakeney AB, O'Brien L 1999 Cereal structure and composition. Aust. J. Agr. Res. 50: 629-650.

Evers T, Millar S 2002 Cereal grain structure and development: some implication for quality. J. Cereal Sci. 36: 261-284.

Faulds CB, Zanichelli D, Crepin VF, Connerton IF, Juge N, Bhat MK, Waldron KW 2003 Specificity of feruloyl esterases for water-extractable and water-unextractable feruloylated polysaccharides: influence of xylanase. J. Cereal Sci. 38: 281-288.

Ferreira LMA, Durrant AJ, Hall J, Hazlewood GP, Gilbert HJ 1990 Spatial separation of protein domains is not necessary for catalytic activity or substrate binding in a xylanase. Biochemistry Journal 269: 261-264.

Fierens E, Rombouts S, Gebruers K, Courtin CM, Goesaert H, Brijs K, Volckaert G, Van Campenhout S, Delcour, JA 2004 TL-XI, a novel type of xylanase inhibitor from wheat (Triticum aestivum) belonging to the thaumatin family. Biochemical Journal, soumis pour publication.

Figueroa-Espinoza MC, Morel MH, Surget A, Rouau X 1999 Oxidative cross-linking arabinoxylans by manganese peroxidase. Comparaison with laccase and horseradish peroxidase. Effect of cysteine and tyrosine on gelation. Sci. Food Agr. 79: 460-463.

Fincher GB, Stone BA 1986 Cell walls and their components in cereal grain technology. In Advances in Cereal Sciences, Pomeranz Y (eds), AACC: St Paul; MN, Vol 8 pp 207-295.

Fisher DB 2000 Long-distance transport. In B Buchanan, Gruissem W, Jones R (eds). Biochemistry and Molecular Biology of Plants, American Society of Plant Physiologist, spp 748-758.

Frederick MM, Kiang CH, Frederick JR, Reilly PJ 1981 Purification and characterization of a xylobiose and xylose producing endoxylanase from *Aspergillus Piger.* Carbohyd. Research 97: 87-103.

Frederix SA, Courtin C, Delcour JA 2003 Impact of xylanases with different substrate selectivity on gluten-starch separation of wheat flour. J. Agric. Food Chem. 51: 7338-7345.

Fry SC 1979 Phenolic components of the primary cell wall and their possible role in the hormonal regulation of growth. Planta 146: 343-351.

Fujimoto Z, Kaneko S, Kuno A, Kobayashi H, Kusakabe I, Mizuno H 2004 Crystal structures of decorated xylooligosaccharides bound to a family 10 xylanase from *Streptomyces olivaceoviridis E-*86. J. Biol. Chem. 279: 9606-9614.

Fulcher RG, TP O'Brien, JW Lee 1972 Studies on the aleurone layer, conventional and fluorescence microscopy of the cell watt with emphasis on phenol-carbohydrate complexes in wheat. Aust. J. Biol. Sci. 25: 23-34.

Fulcher RG, Wong SI 1980 Inside Cereals — a fluorescence microchemical view. In cereals for food and beverages, Inglett GE, Munck L (eds) New York, Academic Press pp 1-26.

Garcia-Conesa MT, Plumb GW, Waldron KW, Ralph J, Williamson G 1997 Ferulic acid dehydrodimers from wheat bran: isolation, purification and antioxidant properties of 8-0-4-diferulic acid. Redox Report 3: 319-323.

Gebruers K, Brijs K, Courtin CM, Fierens K, Goesaert H, Rabijns A, Raedschelders G, Robben J, Sansen S, S, rensen JF, Van Campenhout S, Delcour JA 2004 Properties of TAXI-type endoxylanase inhibitors. Biochem. Biophys. Acta 1696: 213-221.

Geissmann H, Neukom 1973 A note on ferulic acid as a constituent of the water insoluble pentosans of wheat flour. Cereal Chem. 50: 414-416.

Gilkes NR, Henrissat B, Kilburn DG, Miller RC, Warren RAJ 1991 Domains in béta 1,4 glycanases : Sequence conservation, function and enzyme families. Microbiol. Rev. 55: 303-315.

Goesaert H, Elliot G, Kroon PA, Gebruers K, Courtin CM, Robben J, Delcour JA, Juge N 2004 Occurence of proteinaceous endoxylanase inhibitors in cereals. Biochem. Biophys. Acta 1696: 193-202.

Goubet F, Jackson P, Deery MJ, Dupree P 2002 Polysaccharide analysis using carbohydrate gel electrophoresis: a method to study plant cell wall polysaccharides and polysaccharide hydrolases. Anal. Biochem. 300: 53-68.

Grabber JH, Hatfield RD, Ralph J 1998 Diferulate cross-links impedes the enzymatic degradation of non-Iignified maize walls. Sci.Food Agr. 77: 193-200.

Grabber JH, Ralph J, Hatfield RD 1998 Ferulate cross-links limit the enzymatic degradation of synthetically Iignified primary walls of maize. J. Agric. Food Chem. 46: 2609-2614.

Grethlein GE 1985 The effect of pore size distribution on the rate of enzymatic hydrolysis of cellulosic substrates. Biotechnology 3: 155-160.

Greve LC, Labavitch JM, Hungate RE 1984 Alpha-L-arabinofuranosidase from *Ruminococcus allus:* purification and possible role in hydrolysis of alfalfa cell wall. Appl. Environ. Microbiol. 47(5): 1135-1140.

Gruppen H, Hamer RJ, Voragen AGJ 1993 Water unextractable cell wall material from wheat flour. III. A structural model for arabinoxylans. J. Cereal Sci. 18: 129-143.

Gubler F, AE Ashford, JV Jacobsen 1987 The release of a-amylase through gibberellin-treated barley aleurone cell walls. Planta 172: 155-161.

Guillon F, Chevalier T, Ordaz Ortiz JJ, Quillien L, Utille JP, Bouchet B, Devaux MF, Saulnier L 2002 A xylan polyclonal antibody and its use in immunocytochemical location of poorly substituted arabinoxylans in wheat grain', 3`[a] European symposium Enzymes in Grain processing, September 25-27, Louvain, Belgium.

Guillon F, Tranquet O, Quillien L, Utille JP, Ordaz Ortiz JJ, Saulnier L 2004 Generation of polyclonal and monoclonal antibodies against arabinoxylans and their use for immunocytochemical localization of arabinoxylans in cell walls of the wheat grain endosperm. J. Cereal Sci. In press.

Hakomori S 1964 Rapid permethylation of glycolipids and polysaccharides catalysed by methylsulfinyl carbanion in dimethylsulfoxide. J. Biochem. 55: 205-208.

Hamm M, Debeire P, Monties B, Chabbert B 2002 Changes in the cell wall network during the thermal dehydration of alfalfa stems. J. Agric. Food Chem. 50: 1897-1903.

Harlan HV 1920 Daily development of kernels of hannchen barley from flowering to maturity at Aberdeen, Idaho. J. Agr. Res. 9: 393-430.

Harris PJ, Hartley RD 1976 Detection of bound ferulic acid in cell walls of the Gramineae by ultraviolet fluorescence microscopy. Nature 259: 508-510.

Harris GH, Pickersgill RW, Conneron I, Debeire P, Touzel JP, Breton C, Pérez S 1997 Structural basis on the properties of an industrially relevant thermophilic xylanase. Protein. Struct. Funct. Genet. 29: 77-86.

Hartley RD 1972 p-coumaric and ferulic acid components of cell walls of ryegrass and their relationships with lignin and digestibility. J. Sci. Food Agric. 23: 1347-1354.

Hartley RD, Jones EC 1977 Phenolic components and degradability of cell walls of grass and legume species. Phytochemistry 16: 1531-1534.

Hartley RD, Morrisson WH, Himmelsbach DS, Borneman WS 1990 Cross-linking of cell wall phenolic arabinoxylans in graminaceous plants. Phytochemistry 29: 3705-3709.

Hatfield RD 1993 Cell wall polysaccharide interactions and biodegradability. In Forage Cell Wall Structure and Digestibility Jung HG, Buxton DR, Hatfield RD, Ralph J (eds), American Society of Agronomy, Crop Science Society of America, soil Science Society of America, madison, pp 285-314.

Hatfield RD, Ralph J, Grabber JH 1999 Cell wall cross-linking by ferulates in grasses. J. Sci. Food Agric. 79: 403-407.

Hegde SS, Kumar AR, Ganesh KN, Swaminathan CP, Khan MI 1998 Thermodynamics of ligand (substrate/end product) binding to endoxylanase from *Chainia sp.* (NCL-82-5-1): isothermal calorimetry and fluorescence titration studies. Biochim. Biophys. Acta 1388: 93-100.

Hengtrakul P, Lorenz K, Mathias M 1991 Alkylresorcinol homologs in cereals grains. J. Food Compos. Anal. 4: 52-57.

Henrissat B, Claeyssens M, Tomme P, Lemesle L, Mornon JP 1989 Cellulase families revealed by hydrophobic cluster analysis. Gene 81: 83-95.

Henrissat B 1991 A classification of glycosyl hydrolases based on amino acid sequence similarities. Biochem. J. 280: 309-316.

Henrissat B, Callebaut I, Fabrega S, Lehn P, Mornon JP, Davies GJ 1995 Conserved catalytic machinery and the prediction of a common fold for several families of glycosyl hydrolases. Proc. Nat. Acad. Sci. USA 92: 7090-7094.

Henrissat B, Bairoch A 1996 Updating the sequence based classification of glycosyl hydrolases. Biochem. J. 316: 695-696.

Henrissat B, G Davies G 1997 Structural and sequence-based classification of glycoside hydrolases. Curr. Opin. Struct. Biol. 7: 637-644.

Hernanz D, Muiez V, Sancho AI, Faulds CB, Williamson G, Bartolomé B, Gémez-Cordovés C 2001 Hydroxycinnamic acids and ferulic acid dehydrodimers in barley and processed barley. J. Agr. Food Chem. XX: 4884-4888.

Hildèn L, Daniel G, Johansson G. 2003 Use of a fluorescent, carbohydrate-binding module from *Phanerochaete chrysosporium* Ce17D for studying wood cell wall ultrastructure. Bitchnol Lett 25: 553-558.

Hinton JJC 1955 Resistance of the testa to entry of water into wheat kernel. Cereal Chemistry 32: 296-306.

Hrmova M, Biely P, Vrsanska M 1986 Specificity of cellulase and béta-xylanase induction in *Trichoderma reesei* QM 9414. Arch. Microbiol. 144: 307-311.

Iiyama K, Lam TBT, Stone BA 1994 Covalent cross-links in the cell wall. Plant Physiology 104, 315-320.

Iiyama K, TBT Lam, BA Stone 1990 Phenolic acid bridges between polysaccharides and lignin in wheat internodes. Phytochemistry 29:733-737.

Irwin D, Jung ED, Wilson DB 1994 Characterization and sequence of a *Thermomonospora fusca* xylanase. Apll. Environ. Microbiol. 60: 763-770.

Ishii T 1991 Acetylation at O-2 of arabinofuranose residues in feruloylated arabinoxylans from bamboo shoot cell-walls. Phytochem. 30: 2317-2320.

Izydorczyk MS, Biliaderis CG, Bushuk W 1990 Oxidative gelation studies of water-soluble pentosans from wheat. J. Cereal Sci. 11: 153-169.

Izydorczyk MS, MacGregor AW 2000 Evidence of intermolecular interactions of (3-glucans and arabinoxylans. Carbohydr. Polym. 41: 417-420.

Johnson DG, Silva MC, Mac Kenzie CR, Schneider H, Fontana JD 1989 Microbial degradation of hemicellulosic materials. Appl. Biochem. Biotech. 20/21: 245-258.

Juge N, Payan F, Williamson G 2004 XIP-I, a xylanase inhibitor protein from wheat: a novel protein function. Biochimica et Biophysica Acta 1696: 203-211.

Jung HJG, Sahlu T 1986 Depression of cellulose digestion by esterified cinnamic acids. Journal of Science Food Agricultural 37: 659-665.

Jung HJG, Jorgensen MA, Linn JG, Engels FM 2000 Impact of accessibility and chemical composition on cell wall polysaccharide degradability of maize and lucerne stems. J. Sci. Food Agric. 80: 419-427.

Kabel M 2002 Characterisation of complex xylo-oligosaccharides from xylan by-products. Thèse de doctorat. Wageningen University, Wageningen, The Netherlands.

Kaji A 1984 L(arabinosidases). Advances in Carbohydrate Chemistry Biochemistry 42: 383-394.

Kanda T, Amano Y, Nisizawa K 1985 Purification and properties of two endo-1,4-béta-xylanases from Irpex lacteus (Polyporus tulipiferae). J. Biochem. 98: 1545-1554.

Keskar SS, Srinivasan MC, Deshpande VV 1989 Chemical modification of a xylanase from a thermotolerant Streptomyces. Evidence for essential tryptophan and cysteine residues at the active site. Biochem. J. 261: 49-55.

Khasin A, Alchanti I, Shoham Y 1993 Purification and characterization of a thermostable xylanase from Bacillus stearothermophilus T-6. Appl. Environ. Microbiol. 59: 1725-1730.

Kidby DK, Davidson DJ 1973 A convenient ferricyanide estimation of reducing sugars in the nanomole range. Anal. Biochem. 55: 321-325.

Kim JC, Mullan BP, Simmins PH, Pluske JR 2003 Variation in the chemical composition of wheats grown in western Australia as influenced by variety, growing region, season, and post-harvest storage. Aust. J. Agr. Res. 54: 541-550.

Ko EP, Akatsuka H, Moriyama H, Shinmyo A, Haya Y, Katsube Y, Urabe I, Okada H 1992 Site-directed mutagenesis at aspartate and glutamate residues of xylanase from *Bacillus pumilus.* Biochem. J. 288: 117-121.

Kolattukudy P 1980 Biopolyester membranes of plants: cutin and suberin. Science 208: 990-999.

Kolattukudy PE 1981 Structure, biosynthesis, and biodegradation of cutin and suberin. Plant Physiology 32: 539-567.

Kolattukudy PE 2001 Polyesters in higher plants. Advances in Biochemical Engineering and Biotechnology 71: 1-49.

Koshland DE 1953 Stereochemistry and the mechanism of enzymatic reactions. Biol. Rev. 28: 416-436.

Kozubek A 1985 Isolation of 5-n-alkyl-, 5-n-alkenyl-, and 5-n-alkdienyl-homologs of alk(en)ylresorcinols from rye grains. Acta Aliment. Polon. 9: 185-198.

Kozubek A, Tyman JHP 1995 Greal grain resorcinolic lipids : mono and dienoic homologues are present in rye grains. Chem. Phys. Lipids 78: 29-35.

Lam TBT, Iiyama K, Stone BA 1990 Primary and secondary walls of grasses and other forage plants: taxonomic and structural consideration, In Microbial and Plant Opportunities to improve Lignocellulose Utilization by Ruminants, Akin DE, Ljundahl MG, Wilson RJ, Harris PJ (eds) Elsevier, New-York pp 43-69.

Lam TBT, Iiyama K, Stone BA 1992 Changes in phenolic acids from internodes walls of wheat and phalaris during maturation. Phytochemistry 31: 2655-2658.

Lam TBT, Iiyama K, Stone BA 1992 Cinnamic acid bridges between cell wall polymers in wheat and phalaris internodes. Phytochemistry 31: 1179-1183.

Lam TBT, Iiyama K, Stone BA 2003. Hot alkali-labile linkages in the walls of the forage grass *Phalaris aquatica* and *Lolium perenne* and their relation to in vitro wall digestibility. Phytochemistry 64: 603-607.

Lapierre C, Monties B, Rolando R 1986 Thioacidolysis of poplar lignins: identification of monomeric syringyl products and caracterizationet of guaiacyl-syringyl rich fractions. Holzforschung 40: 113-119.

Lee YH, Fan LT 1982 Kinetics studies of enzymatic hydrolysis of insoluble cellulose : analysis of initial rates. Biotechnol. Bioeng. 24: 2383-2406.

Lempereur I 1997 Bases physico-chimiques du fractionnement et de la fragmentation du grain de blé dur *(Triticum durum* Desf.) par voie sèche. Thèse de doctorat, Université des Sciences et Techniques de Montpellier, Montpellier, France.

Lempereur I, Rouau X, Abecassis J 1997 Genetic and agronomie variation in arabinoxylan and ferulic acid contents of durum wheat *(Triticum durum* L) grain and its milling fractions. J. Cereal Sci. 25: 1-8.

Lempereur I, Rouau X, Abecassis J 1997 Arabinoxylan and ferulic acid variations in durum wheat *(Triticum durum* desf.) grain and distribution in mill streams. J. Cereal Sci. 25: 103-110.

Lempereur I, Surget A, Rouau X 1998 Variability in dehydrodiferulic acid composition of durum wheat *(Triticum durum)* and distribution in milling fractions. J. Cereal Sci. 28: 251-258.

Lequart C 1999 Déstructuration des parois végétales lignifiées par une endoxylanase et un complexe abiotique MnO_2/oxalate — Application à la paille de blé. Thèse de doctorat de l'Université de Reims Champagne-Ardenne, Reims, France.

Lequart C, Nuzillard JM, Kurek B, Debeire P 1999 Hydrolysis of wheat bran and straw by an endoxylanase : production and structural characterization of cinnamoyl-oligosaccharides. Carbohyd. Res. 319: 102-111.

Li K, Azadi P, Collins R, Tolan J, Kim JS, Eriksson KE 2000 Relationships between activities of xylanases and xylan structures. Enzyme Microb. Technol. 27: 89-94.

Mac Kenzie CR, Bilous D 1988 Ferulic acid esterase activity from *Schzophyllum* commune. Appl. Environ. Microbiol. 54: 1170-1173.

Mac Masters MM, Hinton JJC, Bradbury D 1978 Microscopic structure and composition of the wheat kernel. In Wheat Chemistry and technology; Pomeranz, Y, (Eds) Pullman, Washington State University pp 51-113.

Maes C, Delcour JA 2002 Structural characterisation of water-extractable and water-unextractable arabinoxylans in wheat bran. J. Cereal Sci. 35: 315-326.

Maes C, Vangeneugden B, Delcour JA 2004 Relative activity of two endoxylanases towards water-unextractable arabinoxylans in wheat bran. J. Cereal Sci. 39: 181-186.

Marlow E, Lane D 1988 Adsorption to remove nonspecific binding. In Antibodies: A laboratory manual, Cold Spring Harbor Laboratory Press, New York pp 632-633.

Matzke K, Riederer M 1990 The composition of the cutin of the caryopses and leaves of Triticum aestivum L. Planta 182: 461-466.

McCallum JA, Walker JRL 1991 Phenolic biosynthesis during grain development in wheat *(Triticum aestivum* L.) III. Changes in hydroxycinnamic acids during grain development. J. Cereal Sci. 13: 161-177.

McCann MC, Roberts K 1994 Changes in cell wall architecture during cell elongation. J. Exp. Bot. 45: 1683-1691.

McCann MC, Wells B, Roberts K 1990 Direct visualisation of cross-links in the primary cell wall. J. Cell Sci. 96: 323-334.

McCleary BV, Matheson NK 1983 Action patterns and substrate-binding requirements of béta-D-mannanase with mannosaccharides and mannan-type polysaccharides. Carbohyd. Res. 119: 191-219.

McKeehen JD, Busch RH, Fulcher RG 1999 Evaluation of wheat *(Triticum aestivum* L.) phenolic acids during grain development and their contribution to Fusarium resistance. J. Agric. Food Chem. 47: 1476-1482.

McLauchlan WR, Garcia-Conesa MT, Williamson G, Roza M, Ravestein P, Maat J 1999 A novel class of protein from wheat which inhibits xylanases. Biochem. J. 338: 441-446.

McMasters MM, Hinton JJC, Bradbury D 1971 Microscopic structure and composition of the wheat kernel. In Wheat: Chemistry and Technology, Pomeranz Y. (eds) American Association of Cereal Chemist, St Paul, MN. pp 51-113.

Meagher MM, Tao BY, Chow JM, Reilly PJ 1988 Kinetics and subsite mapping of D-xylobiose and D-xylose producingAspergillus *P iger* endo-(1-4)-béta-D-xylanase. Carbohyd. Res. 173: 273-283.

Meikle PJ, Hoogenraad NJ, Bonig I, Clarke AE, Stone BA 1994 A (1–*3,1–4)-(3-glucan-specific monoclonal antibody and its use in the quantification and immunocytochemical location of (1–X3,1--*4)-(3-glucans. The Plant Journal 5 (1):1-9.

Migné C, Prensier G, Grenet E 1994 Immunogold labeling of xylans and arabinoxylans in the plant cell walls of maize stem. Biol. Cell. 81:267-276.

Miyamoto T, Everson E 1958 Biochemical and physiological studies of wheat seed pigmentation. Agronomical Journal 50: 733-734.

Monties B 1980 Les lignines in "Les polymères végétaux, polymères pariétaux et alimentaires non azotés" Costes C, Monties B (eds) Gauthier Villars, Paris pp 123-155.

Morrison IN, Kuo J, O'Brien TP 1975 Histochemistry and fine structure of developing wheat aleurone cells. Planta 123: 105-116.

Morrison WH, Hartley RD, Himmelsbach DS 1992 Synthesis of substituted truxillic acids from p-coumaric and ferulic acids: Simulation of photodimerisation in plant cell walls. J. Agr. Food Chem. 40: 766-771.

Nienartowicz B, Kozubec A 1993 Antioxidant activity of cereal bran resorcinolic lipids. Pol. J. Food Nutr. Sci. 2: 51-60.

Obel N, Porchia AC, Scheller HV 2002 Dynamic changes in cell wall polysaccharides during wheat seedling development. Phytochemistry 60: 603-610.

ONeil M, Albersheim P, Darvill A 1990 The pectic polysaccharides of primary cell walls. In Methods in Biochemistry Dey CL, Harbone JB (eds), Carbohydrates. Academiv Press Publication.

Palackal N, Brennan Y, Callen WN, Dupree P, Frey G, Goubet F, Hazlewood GP, Healey S, Kang YE, Kretz KA, Lee E, Tan X, Tomlinson GL, Verruto J, Wong VWK, Mathur EJ, Short JM, Robertson DE, Steer BA 2004 An evolutionary route to xylanase process fitness. Protein Sci. 13: 494-503.

Panbangred W, Shinmyo A, Kinoshita S, Okada H 1983 Purification and properties of endoxylanase produced by *Bacillus pumilus.* Agric. Biol. Chem. 47: 957-963.

Pell G, Taylors EJ, Gloster TM, Turkenburgs JP, Fontes CMGA, Ferreira LMA, Nagy T, Clark SJ, Davies GJ, Gilbert H 2004 The mechanisms by which family 10 glycoside hydrolases bind decorated substrates. J. Biol. Chem. 279: 9597-9605.

Pellerin P, M Gosselin, JP Lepoutre, E Samain, P Debeire 1991 Enzymatic production of oligosaccharides from corncob xylan. Enzyme Microb. Technol. 13: 617-621.

Percival J 1921 The wheat plant. In Duckworth and Co. London: 129-143.

Peyron S 2002 Bases physico-chimiques et structurales de l'aptitude au fractionnement du grain de blé dur *(Triticum durum* Desf.). Thèse de doctorat, Ecole Nationale Supérieure Agronomique de Montpellier, Montpellier, France.

Peyron, S, Chaurand M, Rouau X, Abecassis J 2002 Relationship between bran mechanical properties and milling behaviour of durum wheat *(Triticum durum* Desf.). Influence of tissue thickness and cell wall structure. J. Cereal Sci. 36: 377-386.

Peyron S, Abecassis J, Autran JC, Rouau X 2002 Influence of UV exposure on the phenolic acid content, the mechanical properties of the bran and the milling behaviour of durum wheat *(Triticum durum* desf.). Cereal Chem. 79: 726-731.

Piot 0 2000 Characterisation par microspectrométrie Raman des espèces moléculaires responsables de la cohésion des grains de blé tendre. Thèse de doctorat, Université de Reims Champagne-Ardenne, pp 194.

Piot O, Autran JC, Manfait M 2000 Spatial distribution of protein and phenolic constituents in wheat grain as probed by confocal raman microspectroscopy. J. Cereal Sci. 32: 57-71.

Pomeranz Y 1982 Chemical composition of kernel structures. In Wheat: chemistry and technology, Pomeranz Y(eds), American Association of Cereal Chemists, St Paul, MN. pp 97-110.

Pomeranz Y 1987. Cereal Crops – general. In Modern cereal science and technology Pomeranz Y (eds), VCH Publishers, Inc, New York pp 14-23.

Poutanen K 1988 An alpha-L-arabinosidase of *Trichoderma reesei.* J. Biotechnol. 7: 271-282.

Poutanen K 1988 Characterization of xylanolytic enzymes for potential applications. Technical Research Centre of Finlind. Publications 47. Espoo.

Poutanen K, Puis J 1989 The xylanolytic enzyme system of *Trichoderma reesei.* In Cell Wall Polymers, Biogenesis and Biodegradation. N. G. Lewis NG, Paice MG (eds). ACS Symposium N399, Amer Chem Soc, Washington pp 630-640.

Prade RA 1996 Xylanases: from biology to biotechnology. Biotechnol. Genet. Eng. Rev. 13: 101-131.

Pussayanawin V, Wetzel DL, Fulcher RG 1998. Fluorescence detection and mesurement of ferulic acid in wheat milling fractions by microscopy and HPLC. J. Agr. Food Chem. 36: 515-520.

Radley M 1976 The development of wheat grains in relation to endogenous growth substances. J. Exp. Bot. 27: 1009-1021.

Ralph J, Quideau S, Grabber JH, Hatfield RD 1994 Identification and synthesis of new ferulic dehydrodimers present in grass cell walls. Journal of Chemical Society 1: 3485-3498.

Ralph J, Grabber JH, Hatfield RD 1995 lignin-ferulates cross-links in grasses: active incorporation of ferulate polysaccharide esters into ryegrass lignins. Carbohyd. Polym. 275: 167-178.

Raynal-Ioualalen R 1996 Procédé de fractionnement des sons de blé. Extraction et étude des propriétés fonctionnelles des arabinoxylanes. Thèse de doctorat, Institut National Polytechnique de Toulouse, Toulouse, France.

Reese ET 1977 Degradation of polyméric carbohydrates by microbial enzymes. Rec. Adv. Phytochem. 11: 311-367.

Regnault-Roger C, Pauls KP, Arnason JT, Philogène BJR 2003 Dehydrodimers of ferulic acid in maize grain pericarp and aleurone: resistance to *Fusarium graminearum*. Phytopathology 93: 712-719.

Régnier T 1994 Les composés phénoliques du blé dur *(Triticum turgidum* L. var. *durum):* variations au cours du développement et de la maturation du grain. Relations avec l'apparition de la moucheture. Thèse de Doctorat, Université Montpellier II, France.

Régnier T, Macheix JJ 1996 Changes in wall-bound phenolic acids, phenylalanine and tyrosine ammonia-lyases, and peroxidases in developing durum wheat grains *(Triticum turgidum* L. var. *durum).* J. Agric. Food Chem. 44, 1727-1730.

Reilly PJ 1981 Xylanase : Stucture and function. In Trends in the biology of fermentations for fuels and chemicals. Plenum Press, New York. 14: 111-129.

Reis D, Vian B, Roland JC 1993 Cellulose-glucuronoxylans and plant cell wall structure. Micron 25: 171-187.

Rémond-Zilliox C 1996 Etude des mécanismes de dégradation enzymatique des parois végétales. Application à l'hydrolyse de la paille de blé par une endoxylanase purifiée. Thèse de doctorat, Université de Reims Champagne-Ardenne, Reims, France.

Rémond-Zilliox C, Debeire P, Reis D, Vian B 1997 Immunolocalization of a purified xylanase during hydrolysis of wheat straw stems. Int. J, Plant Sci. 158(6): 769-777.

Rhodes DI, Stone BA 2002 Proteins in walls of wheat aleurone cells. J. Cereal Sci. 36: 83-101.

Rhodes DI, Sadek M, Stone BA 2002 Hydroxycinnamic acids in walls of wheat aleurone cells. J. Cereal Sci. 36: 67-81.

Ricard J 1987 Dynamics of mufti-enzyme reactions, cell growth and perception of ionic signais from external milieu. J Theor. Biol. 128: 253-278.

Riederer M, Schônherg J 1986 Quantitative gas chromatographic analysis of methyl esters of hydroxy acids derived from plant cutin. J. Chromat. 360: 151-161.

Ring SG, Selvendran RR 1980 Isolation and analysis of cell wall material from beeswing wheat bran *(Triticum aestivum).* Phytochemistry 19: 1723-1730.

Rouau X, Surget A 1998 Evidence for the presence of a pentosanase inhibitor in wheat flours. J. Cereal Sci. 28: 63-70.

Rouau X, Cheynier V, Surget A, Gloux D, Barron C, Meudec E, Louis-Montero J, Criton M 2003 A dehydrotrimer of ferulic acid from maize bran. Phytochemistry 63: 899-903.

Roy S, Watada AE, Wergin WP 1997 Characterisation of the cell wall microdomain surrounding plasmodesmata in apple fruit. Plant Physiology 114:539-547.

Saadi A, Lempereur I, Sharonov S, Autran JC, Manfait M 1998 Spatial distribution of phenolic materials in durum wheat grain as probed by confocal fluorescence spectral imaging. J. Cereal Sci. 28: 107-114.

Samain E, Debeire P, Debeire-Gosselin M, Touzel J-P 1991 Xylanase, souches de Bacillus productrices de xylanases et leurs utilisations. Patent FR-9101191.

Samain E, Touzel J-P, Brodel B, Debeire P 1992 Isolation of a thermophilic bacterium producing high levels of xylanase. In Visser J, Beldman G, Kusters- van Someren MA, Voragen AGJ (eds) Xylans and Xylanases. Elsevier Science Publishers BV, Amsterdam, pp 467-470.

Sarkanen KV 1971 Lignin precursors and their polymerization. In Lignin: Occurence, formation, structure and reactions, Sarkanen KV, Ludwig CH (eds), Wiley-Interscience, New York pp 95-163.

Sarwardeker JS, Sloneker JH, Jeanes A 1965 Quantitative determination of monosaccharides as their alditol acetates by gas liquid chromatography. Anal. Chem. 37: 1602-1604.

Saulnier L, Marot C, Chanliaud E, Thibault JF 1995 Cell wall polysaccharide interactions in maize bran. Carbohyd. Polym. 26: 279-287.

Saulnier L, Crépeau MJ, Lahaye M, Thibault JF, Garcia-Conesa MT, Kroon PA, Williamson G 1999 Isolation and structural determination of two 5,5'-diferuloyl oligosaccharides indicate that maize heteroxylans are covalently cross linked by oxidatively coupled ferulates. Carbohyd. Res. 320: 82-92.

Scalbert A, Monties B, Lallemand J-Y, Guittet E, Rolando C 1985 Ether linkage between phenolic acids and lignin fractions from wheat straw. Phytochemistry 24: 1359-1362.

Schooneveld-Bergmans MEF, Beldman G, Voragen AGJ 1997 Extraction and partial characterization of feruloylated glucuronoarabinoxylans from wheat bran. Carbohyd. Polym. 35: 39-47.

Schooneveld-Bergmans MEF, Beldman G, Voragen AGJ 1999 Structural features of (Glucurono)arabinoxylans extracted from wheat bran by barium hydroxide. J. Cereal Sci. 29: 63-75.

Schooneveld-Bergmans MEF, Dignum MJW, Grabber JH, Beldman G, Voragen AGJ 1999 Studies on the oxidative cross-linking of feruloylated arabinoxylans from wheat flour and wheat bran. Carbohyd. Polym. 38: 309-317.

Schreiber L, Hartmann K, Skrabs M, Zeier J 1999 Apoplastic barriers in roots: chemical composition of endodermal and hypodermal cell walls. J. Exp. Bot. 50: 1267-1280.

Schwarz PB, Kunerth WH, Youngs VL 1988 The distribution of lignin and other fiber components within hard red spring wheat bran. Cereal Chem. 65: 59-64.

Schwarz PB, Youngs VL, Shelton DR 1989 Isolation and characterization of lignin from hard red spring wheat bran. Cereal Chem. 66: 289-295.

Shetlar M, Rankin G, Lyman J, France W 1947 Investigation of the proximate chemical composition of the separate bran layers of wheat. Cereal Chemistry 24: 111-122.

Shetlar MR 1948 Chemical study of the mature wheat kernel by means of the microscope. Cereal Chem. 25: 99-110.

Shiiba K, Yamada H, Hara H, Okada K, Nagao S 1993 Purification and characterization of two arabinoxylans from wheat bran. American Association of Cereal Chemists 70(2): 209-214.

Simpson HD, Haufler UR, Daniel RM 1991 An extremely thermostable xylanase from the thermophilic eubacterium Thermotoga. Biochemistry Journal 277: 413-417.

Simpson DJ, Fincher GB, Huang AHC, Cameron-Mills V 2003 Structure and function of cereal and related higher plant (1—4)-f3-xylan endohydrolases. J. Cereal Sci. 37: 111-127.

Smith MM, Hartley RD 1983 Occurrence and nature of ferulic acid substitution of cell wall polysaccharides in graminace plants. Carbohyd. Res. 118: 65-80.

Srebotnik E, Messner K, Foisner R 1988 Penetrability of white rot-degraded pine wood by the lignin peroxydase of Phanerochaete chrysosporium. Appl. Environ. Microbiol. 54: 2608-2614.

Stenvert NL, K Kingswood 1976 An autoradiographic demonstration of the penetration of water into wheat during tempering. Cereal Chem. 53: 141-149.

Struski DGJ, Kozubec A 1992 Cereal grain alkylresorcinols protect lipids against ferrous ions-induced peroxidation. Z. Naturforsch. 46: 47-50.

Sun R, Lawther JM, Banks WB 1997 A tentative chemical structure of wheat straw lignin. Ind. Crops Prods. 6: 1-8.

Sunna A, Antranikian G 1997 Xylanolytic enzymes from fungi and bacteria. Crit. Rev. Biotechnol. 17: 39-67.

Suzuki K, Kitamura S, Kato Y, Itoh T 2000 Highly Substituted glucuronoarabinoxylans (hsGAXs) and low-branched xylans show a distinct localization pattern in the tissues of *Zea mays* L. Plant Cell Physiol. 41(8): 948-959.

Taiz L, Jones RL 1970 Gibberelic acid, (3-1,3-glucanase and the cell walls of barley aleurone layers. Planta 92: 73-84.

Taiz L, Jones RL 1973 Plasmodesmata and an associated cell wall component in barley aleurone tissue. Amer. J. Bot. 60(1): 67-75.

Tanaka M, Ikesaka M, Matsuno R 1988 Effect of pore size in substrate and diffusion of enzyme on hydrolysis of cellulosic materials with cellulases. Biotechnol. Bioeng. 32: 698-706.

Tenkanen M, Schuseil J, Poutanen K 1991 Production, purification and characterization of an esterase liberating phenolic acids from lignocellulosics. J. Biotechnol. 18: 69-84.

Terashima N, Fukushima K, He L-F, Takabe K 1993 Comprehensive model of the lignified plant cell wall. In Forage cell wall structure and digestibility, Jung HG, Buxton DR, Hatfield RD, Ralph J (Eds) ASA, CSSA, SSSA: Madison, WI, pp. 247-270.

Tervil-Wilo A, Parkkonen T, Morgan A, Hopeakoski-Nurminen M, Poutanen K, Heikkinen P, Autio K 1996 In vitro digestion of wheat microstructure with xylanase and cellulase from *Trichoderma reesei.* J. Cereal Sci. 24: 215-225.

Thiéry JP 1967 Mise en évidence des polysaccharides sur coupes fines en microscopie électronique. Journal de Microscopie 6: 987-1018.

Thimm JC, Burritt DJ, Ducker WA, Melton LD 2000 Celery (Apium graveolens L.) parenchyma cell walls examined by atomic force microscopy: effect of dehydration on cellulose microfibrils. Planta 212: 25-32.

Tôrrônen A, Mach RL, Messner R, Gonzalez R, Kalkkianen N, Harkki A, Kubicek CP 1992 The two major xylanases from *Trichoderma reesei :* Characterization of both enzymes and genes. Bio/Technology 10: 1461-1465.

Tôrrônen A, Harkki A, Rouvinen J 1994 Three-dimensional structure of endo-1,4-(3-xylanase II from *Trichoderma reesei:* two conformational states in the active site. Embo J. 13: 2493-2501.

Tôrrônen A, Rouvinen J 1995 Structural comparison of two major endo-1,4-xylanases from *Trichoderma reesei.* Biochemistry 34: 847-856.

Tottman DR, Makepeace RJ 1979 An explanation of the decimal code for the growth stages of cereals, with illustrations. Ann. Appl. Biol. 93: 221-234.

Vardakou M, Katapodis P, Samiotaki M, Kekos D, Panayotou G, Christakopoulos P 2003 Mode of action of family 10 and 11 endoxylanases on water-unextractable arabinoxylan. Int. J. Biol. Macromol. 33: 129-134.

Verdeal K, Lorenz K 1977 Alkylresorcinols in wheat, rye, and triticale. Cereal Chem. 54: 475-483.

Viëtor RJ, Angelino SAGF, Voragen AGJ 1992 Structural features of arabinoxylanes from barley and malt cell wall material. J. Cereal Sci. 15: 213-222.

Wakarchuk WW, Robert L, Campbell RL, Sung WL, Davoodi J, Yaguchi M 1994 Mutational and crystallographic analyses of the active site residues of the *Bacillus circulans* xylanase. Prot. Sci. 3: 467-475.

Waldron KW, Smith AC, Parr AJ, Ng A, Parker ML 1997 New approaches to understanding and controlling cell separation in relation to fruit and vegetable texture. Trends Food Sci. Technol. 8: 213-221

White BA, Mackie RI, Doerner KC 1993 Enzymatic hydrolysis of forage cell walls. In Forage cell wall structure and digestibility Jung HJG, Buxton DR, Hatfield RD, Ralph J (eds) pp 455-484.

Wilkie KCB 1979 The hemicelluloses of grasses and cereals. Advances in Carbohydrate chemistry and Biochemistry 36: 215-264.

Willats WG, Steele-King CG, Mc Carney L, Orfila C, Marcus SE, Knox JP 2000 Making and using antibody probes to study plant cell walls. Plant Physiol. Biochem. 38: 27-36.

Wong KKY, Tan LUL, Saddler JN, Yaguchi M 1986 Purification of a third distinct xylanase from the xylanolytic system of *Trichoderma harzianum*. Can. J. Microbiol. 32: 570-574.

Wong KKY, Tan LUL, Saddler IN 1988 Multiplicity of (3(1,4) xylanase in microorganisms: functions and applications. Microbiology Review 52: 305-317.

Wood TM, Mc Crae SI 1986 Studies of two low-molecular-weight endo-(1,4)-béta-D-xylanases constitutively synthetised by the cellulolytic fungus *Trichoderma koningii*. Carbohyd. Res. 148: 321-330.

Zeier J, Schreiber L 1998 Comparative investigation of primary and tertiary endodermal cell walls isolated from the roots of five monocotyledoneous species: chemical composition in relation to fine structure. Planta 206: 349-361.

Zeikus JG, Lee C, Lee Y-E, Saha BC 1991 Thermostable saccharidases: new sources, uses and biodesigns. In Leatham GF, Himmel ME. (eds), Enzymes in Biomass Conversion, Am Chem Soc, Washington DC pp. 36-51.

Zilliox C, Debeire P 1998 Hydrolysis of wheat straw by a thermostable endoxylanase : Adsorption and kinetic studies. Enzyme Microb. Technol. 22: 58-63.

Zinbo M, Timell TE 1965 The degree of branching of hardwood xylans. Svensk Papperstidn. 68: 647-662.

Bases cytologiques et moléculaires de la dégradation enzymatique du son de blé tendre

Le son de blé est un co-produit de l'agriculture abondant pour lequel la valorisation des arabinoxylanes (AX) par une endoxylanase est envisagée. En effet, le son de blé tendre *(Triticum aestivum)* désamidonné est riche en AX, environ 40%, et comprend des couches cellulaires d'origine distinctes: le péricarpe, la testa, la couche nucellaire, et la couche à aleurone. Cette complexité tissulaire et cellulaire se traduit par une grande hétérogénéité pariétale. Afin de mieux comprendre dans quelle mesure l'hétérogénéité histologique, cellulaire et pariétale entraîne des limitations dans l'accessibilité et l'action de l'enzyme, nous avons développé une stratégie basée sur la caractérisation chimique et la visualisation *in situ* de l'action de l'enzyme. Des sons industriels désamidonnés dont les teneurs en polysaccharides, protéines, acides hydroxycinnamiques (HCA) et diféruliques (DiFA), et le ratios A/X présentent des taux distincts de dégradation par la xylanase. En particulier, la proportion en DiFA des sons de blé résiduels à l'action xylanolytique est négativement corrélée avec les taux de solubilisation des AX, suggérant que les caractéristiques des AX et leurs interactions au sein des parois sont des facteurs limitants. L'importance du ratio A/X et de l'état physique du substrat a été abordée par une étude comparative sur deux xylanases thermostables. Les valeurs des paramètres cinétiques indiquent que malgré son aptitude à dégrader des substrats très substitués, la xylanase de la famille 10 est moins efficace que celle de la famille 11 pour solubiliser les AX insolubles du son. Les résultats concernant la dégradation enzymatique d'enveloppes de grains prélevés à divers stades de maturation suggèrent que la présence d'acides féruliques et le faible dépôt de lignine dans les enveloppes n'altèrent pas l'efficacité de l'enzyme. Comme pour les enveloppes issues de grain matures, l'aleurone et la couche nucellaire sont fortement dégradés alors que le péricarpe reste intact quel que soit le stade de maturité. L'immunolocalisation d'une xylanase (famille 11) sauvage ou sa forme mutante inactive, et d'AX faiblement substitués a été réalisée sur du son ou sur ses couches individualisées. Sur le son, la xylanase active est d'abord retrouvée dans les parois de l'aleurone côté albumen amylacé, puis progresse unilatéralement au travers de l'aleurone et au final dégrade la couche nucellaire. Des micro domaines résistants sont toutefois apparents. A l'opposé, la présence de xylanase n'est pas observée dans le péricarpe et la testa, pour lesquels aucun marquage des AX non substitués n'a été détecté. En plus de la barrière physique représentée par les couches cuticulaires, le réseau pariétal peut également limiter à la fois la pénétration et la diffusion de l'enzyme. En l'occurrence, la pénétration de la xylanase est facilitée par la dégradation des arabinoxylanes dans les parois sensibles à son action.

Mots clefs: son de blé *(Triticum aestivum)*, xylanases, arabinoxylanes, acides phénoliques, parois cellulaires, accessibilité, sonde

Cytological and molecular aspects of soft wheat bran enzymatic degradation

Wheat bran is an abundant agricultural by-product for which xylanase upgrading of arabinoxylans (AX) is of interest. Indeed, starch-depleted wheat bran *(Triticum aestivum)* is rich in AX (about 40%) and includes botanically distinct layers: the pericarp, the testa, the nucellar layer and the aleurone layer, resulting in a mixture of chemically heterogeneous cell-walls. To better understand the way by which the chemical heterogeneity of the bran cells, the cell-wall network and the tissular organization hamper both accessibility and enzyme action, we have devised a strategy based on chemical analysis and *in situ* visualisation of the xylanase action. Industrial destarched wheat brans display significant variations in carbohydrate, A/X ratio, protein, hydroxycinnamic acid (HCA) and diferulic acid (DiFA) contents and differed in their susceptibility to xylanase. Notably the total DiFA in enzyme-depleted bran was negatively correlated with the amount of soluble AX, suggesting that both structural feature of AX and cross-linking were limiting factors. The impact of the A/X ratio and the physical state of the substrate was further studied while comparing two thermostable xylanases. In spite of its ability to disrupt highly substituted AX, the xylanase from family 10 is less efficient than the family 11 xylanase for AX solubilisation from the insoluble wheat bran in respect to their kinetic parameters. Examination of the enzymatic degradation of the external layers isolated from maturing wheat grain suggests that the slight lignin deposition and ferulic accumulation would not significantly alter enzyme efficiency. As for mature wheat bran, aleurone and nucellar layers were mostly degraded whereas pericarp stayed intact at all stages of maturation. Immunocytochemical localization of both feebly substituted arabinoxylans and xylanase family 11 (active and engineered inactive forms) was performed using wheat bran and micro-dissected layers. In wheat bran, the active xylanase was confined to the AL cell walls close to the endosperm, and then progressed unilaterally throughout the AL and finally attack the nucellar layer; some resistant micro domains were also evidenced. In contrast, no enzyme was observed in the pericarp and the testa that did not show any labeling with the non-substituted AX antiserum. Apart from the physical barriers provided by the cuticle layers, the cell wall network would also restrict enzyme penetration and diffusion. Thereby, xylanase penetration was facilitated by the concomitant depletion of arabinoxylans in enzyme-sensitive cell walls.

Keywords: wheat bran *(Triticum aestivum)*, xylanases, arabinoxylans, phenolic acids, cell wall, accessibility, probe